Initial Stages of Soil and Clay Minerals Formation

Case study: Morteratsch Proglacial Area

(SE Switzerland)

Dissertation

zur

Erlangung der naturwissenschaftlichen Doktorwürde

(Dr. sc. nat.)

vorgelegt der

Mathematisch-naturwissenschaftlichen Fakultät

der

Universität Zürich

von

Christian Mavris

aus

Italien

Promotionskomitee

Prof. Dr. Wilfried Haeberli (Vorsitz)

Prof. Dr. Markus Egli (Leitung der Dissertation)

Dr. Michael Plötze

Zurich, 2012

"He who controls the present, controls the past. He who controls the past, controls the future."

George Orwell

Part A: Synopsis

Part B: Manuscripts

Manuscript IV:

Weathering and mineralogical evolution in a high Alpine soil chronosequence: a combined approach using SEM-EDX, cathodoluminescence and Nomarski DIC microscopy.

Christian Mavris, Jens Götze, Michael Plötze, Markus Egli

(Sedimentary Geology; DOI 10.1016/j.sedgeo.2012.04.008)

Acknowledgements

This research was supported by the Swiss National Foundation (SNF), project grant n. 200021-117568. Also, a substantial contribution for the stay at TU Bergakademie Freiberg (Germany) came from SIMP (Società Italiana di Mineralogia e Petrologia) through the fellowship granted in 2009.

The present work is the result of the contribution of many, and I am deeply indebted to each one of them. Namely, I want to thank:

- Prof. Markus Egli, for his commitment to work and for the pleasant atmosphere created during working time. His passion for this project was never hindering brainstorming and additional ideas, which gave me the chance to test my own hypotheses and theories. I am indebted to him, I learned a lot from this experience.
- Prof. Wilfried Haeberli, for the representation of the faculty and his helpful suggestions and comments.
- Dr. Michael Plötze, for the practical approach to the resolution of mineralogical problems (XRD and Rietveld analysis, but also simple brainstorming) and for the involvement in the ClayLab (ETH) activities.
- Prof. Aldo Mirabella, for the fruitful suggestions concerning clay mineralogy
- Prof. Jens Götze, for the introduction to CL and NDICM and for the great time at TU Bergakademie Freiberg.
- Dr. Filippo Favilli, for the invaluable help in both field and lab (AAS), and for the great time together.
- Dr. Eileen Eckmeier, for the German version of the summary

(zusammenfassung) and for the great time together.

- Daniele Giaccai (Istituto Sperimentale per lo Studio e la Difesa del Suolo, ISSDS, Firenze), for his help in the lab (XRD, OM density separation) and for the great time together.
- Bruno Kägi (lab technician, Department of Geography, University of Zurich), for his invaluable support and suggestions during endless hours in the lab.
- The Geography Graduate School – and especially Ross Purves - for the very useful courses and for the financial support which allowed me to follow a very important summer school.
- Pamela Alean Kirkpatrick, lecturer of the Project Management course (in the framework of the Geography Graduate School) for the very useful advices concerning time and risk management.
- Rudy Tschernich, for suggesting me to make a PhD in Mineralogy. A priceless suggestion, which changed my life forever.
- The Mindat.org staff, and especially Jolyon Ralph and the Board, for the constant brainstorming activity - since the year 2000 - and constructive exchange of ideas regarding the new frontiers of mineralogy, at any possible level.

A special 'thanks' goes to my family, my friends and everyone else who supported me during this project, from personal to professional level.

Summary

Weathering of rocks is fundamental for pedogenesis and landscape evolution. It represents the main source of inorganic nutrients for plant growth, and therefore the basis for life. A major interest in chemical and physical denudation of rocks is also due to its potential to affect the local up to global cycle of elements.

Alpine and cryic environment show a high sensitivity to climate changes. Previous investigations in Alpine areas indicated that weathering and mineral formation and transformation processes should theoretically be very fast at the beginning of soil formation. Understanding the processes on a small scale is of major importance and provides the answers which can be used - as a basis for numerical modelling - to other proglacial areas dominated by acidic moraines.

The study of soil chronosequences is an important tool to derive weathering rates and the consequent formation or transformation of soil minerals. Weathering rates of young soils (age < 1000 years) seem to be two to three orders of magnitude higher than in 'old' soils (c. 10 000 years). However, very little is known on how fast such processes really are.

The present project investigated soils developing in a proglacial area within a 0 – 150 years time span. Selected case study is the Morteratsch proglacial forefield (Upper Engadine, Switzerland. Since the LIA the Morteratsch glacier, like all Alpine glaciers, continuously retreated leaving fresh sediments to weathering. Compared to other glaciers, however, its retreat was constant and not interrupted by readvancements (i.e. Damma glacier).

The aim of this study is to understand soil formation processes involved in the very first 150 yr of sediment exposure. The combination of pedology, (soil) mineralogy and water chemistry was the innovative, multidisciplinary approach proved successful in answering our research question.

The morainic sediments derive from the abrasive action of the glacier on the granitoid bedrock (Lower Austroalpine Bernina Nappe). Progressively decreasing pH and grain size were measured at increasing age of moraine exposure. As a consequence to exposure, pedogenesis was observed as continuously occurring. Its development was more advanced on north-facing sites. Biotite and epidote significantly decreased with time. Calcite – occasionally observed as disseminated veinlets in local rocks – was confirmed in both mineralogy and water chemistry, and it was quickly leached as a function of soil formation. The study of the clay fraction (< 2 μm), the fraction 2 – 32 μm, and the fine earth (< 2 mm) regarding (clay) mineralogy gave important insights about chemical and structural transformations. Special emphasis was hereby given to the weathering of mica (biotite and muscovite) and amphibole. These phases were progressively (and quickly) transforming into hydroxy-interlayer vermiculite (HIV), vermiculite and smectite-like phases. The presence of the latter, widely accepted in literature as a proxy for soil formation, was confirmed to be time-dependent in Morteratsch. The formation of clay minerals was effectively measurable only in the clay fraction, therefore confirming the link between surface reactivity and grain size. When specific phases did not show a remarkable weathering trend, the combined application of cathodoluminescence, Nomarski DIC microscopy and scanning electron microscope (SEM) proved to be a helpful tool. This is the first time that such a combined technique was applied to soil science and mineral weathering. Even notoriously resistant minerals – i.e. quartz - underwent weathering steps at the bond scale, much before chemical leaching was involved. The same was observed for plagioclase, alkali feldspar and apatite, whose alteration patterns could be observed and described. Element mass balances of soil fine earth fraction showed no significant trend, confirming that mineral dissolution is at the very early stages.

The study of mineral weathering processes in high Alpine areas lead is a complex subject due to the broad amount of variables involved in an open system such as soil. However, the combination of several techniques was proved to be a successful tool in decoding those processes, approaching the research question from different sides. This multiple approach, quite innovative in the field of soil formation, open a pathway for the study of several proglacial areas and similar climatic settings with granitoid bedrock. With a broader statistical study, a more precise quantification can be performed, from clay mineral formation to single mineral weathering, to elemental loss and nutrient availability.

Zusammenfassung

Die Verwitterung des Ausgangsgesteins ist grundlegend für die Bildung von Böden und für die Entwicklung einer Landschaft. Sie bildet die Hauptquelle mineralischer Nährstoffe für das Pflanzenwachstum und ist daher die Basis des Lebens. Von bedeutendem Interesse sind auch die Effekte der physischen und chemischen Verwitterung des Gesteins auf die lokalen bis globalen Stoffkreisläufe.

Alpine Gebiete und die Kryosphäre reagieren hochsensibel auf Klimaänderungen. Frühere Untersuchungen im Alpenraum zeigten, dass die Verwitterung sowie die Mineralneubildung und –umformung zu Beginn der Bodenbildung theoretisch sehr schnell ablaufen sollten. Das Verständnis der Prozesse auf kleiner Skalenebene ist von grosser Bedeutung und vermittelt die Grundlagen, welche als Basis für eine numerische Modellierung auch auf andere Gletschervorfelder mit silikatischem bzw. saurem Moränenmaterial anwendbar sind.

Verwitterungsraten junger Böden (< 1000 Jahre alt) schienen zwei- bis dreifach höher zu sein als in „alten“ Böden (ca. 10 000 Jahre alt). Unklar war jedoch bislang, wie schnell diese Prozesse tatsächlich ablaufen.

Im Rahmen der vorliegenden Arbeit wurden Böden untersucht, die sich innerhalb einer Zeitspanne von 0 bis 150 Jahren im Vorfeld eines Gletschers bildeten. Das ausgewählte Fallbeispiel ist das Vorfeld des Morteratschgletschers (Oberengadin, Schweiz). Nach der Kleinen Eiszeit zog sich der Morteratschgletscher, so wie alle alpinen Gletscher, zurück und hinterliess frisches Material zur Verwitterung. Im Gegensatz zu anderen Gletschern verlief der Rückzug jedoch kontinuierlich und wurde nicht durch Wiedervorstösse unterbrochen, wie z.B. beim Dammagletscher.

Das Ziel dieser Studie ist, die Prozesse der Bodenbildung innerhalb der ersten 150 Jahre der Sedimentverwitterung zu verstehen. Mit der Kombination der Disziplinen Bodenkunde, Bodenmineralogie und Wasserchemie wurde ein innovativer und

multidisziplinärer Ansatz gewählt, mit welchem unsere Fragestellungen erfolgreich beantwortet werden konnten.

Die Moränensedimente stammen von den abrasiven Gletscherbewegungen auf den unterliegenden Graniten (unterostalpine Bernina-Decke). Mit zunehmendem Alter der freiliegenden Sedimente nahmen pH und Korngrösse progressiv ab, und es wurde, als Folge der Expositionsdauer, eine kontinuierliche Bodenbildung beobachtet, die an den nordexponierten Hängen stärker ausgeprägt war. Biotit und Epidot nahmen im Verlauf der Zeit signifikant ab. Calcit, welches gelegentlich in disseminierten Calcitäderchen im anstehenden Gestein vorkommt, konnte sowohl in der Bodenmineralogie als auch im Wasser nachgewiesen werden, es wurde im Verlauf der Bodenbildung schnell aus dem Boden gelöst. Die Untersuchung der Tonfraktion (< 2 μm), der Fraktion 2 – 32 μm und der Feinerde (< 2 mm) führte zu wichtigen Erkenntnissen über chemische und strukturelle Umwandlungen der (Ton)minerale, inbesondere im Hinblick auf die Verwitterung von Glimmer (Biotit und Muskovit) und Amphibol. Diese wurden zunehmend (und schnell) in HIV (Hydroxy-Interlayered Vermiculite), Vermikulit und smektitartige Phasen umgewandelt. Die Präsenz von Smektiten, ein allgemein anerkannter Proxy für die Bodenbildung, war in Morteratsch abhängig von dem Expositionsalter. Die Bildung von Tonmineralen war effektiv nur in der Tonfraktion messbar, was den Zusammenhang zwischen Oberflächenreaktion und Partikelgrösse bestätigte. Bei Phasen, welche keinen sichtbaren Verwitterungstrend zeigten, war die kombinierte Anwendung der Kathodolumineszenz, der Nomarski-DIK-Mikroskopie und der Rasterelektronenmikroskopie (REM) hilfreich. Zum ersten Mal wurde die Kombination dieser Methoden für Fragestellungen der Bodenkunde und Mineralverwitterung angewendet. Sogar bei besonders resistenten Mineralen, d.h. Quarz, zeigten sich Verwitterungserscheinungen auf der Skala der chemischen

Bindungen im Kristallgitter, lange bevor die chemische Verwitterung einsetzte. Für Plagioklas, Alkalifeldspat und Apatit wurden diese Verwitterungsmuster ebenfalls beobachtet und beschrieben. Die Massenbilanzen der Elemente in der Feinerdefraktion zeigten keinen signifikanten Trend, somit befindet sich die Mineralverwitterung noch in einem sehr frühen Stadium.

Die Untersuchung der Prozesse der Mineralverwitterung in alpinen Gebieten ist ein komplexes Thema, da in einem offenem System wie dem Boden viele Variablen involviert sind. Die Kombination verschiedener Techniken aber konnte diese Prozesse erfolgreich aufschlüsseln, da die Fragestellung von verschiedenen Seiten angegangen wurde. Der multiple, in der Pedogenese innovative Ansatz eröffnet die Möglichkeit, weitere Gletschervorfelder mit ähnlichen geologischen und klimatischen Voraussetzungen zu untersuchen. Eine breitere statistische Untersuchung würde eine präzisere Quantifizierung ermöglichen: von der Tonmineralneubildung zur Verwitterung einzelner Minerale, zur Auswaschung einzelner Elemente und zur Nährstoffverfügbarkeit.

List of abbreviations

AAS = Atomic Absorption Spectrometry

CF = clay fraction (< 2 μm)

CL = cathodoluminescence

FEF = fine earth fraction (< 2 mm)

HIS = hydroxy-interlayered smectite

HIV = hydroxy-interlayered vermiculite

IS = inherited smectite

IV = inherited vermiculite

LIA = Little Ice Age

Micro-DRIFT = Diffuse Reflectance Infrared Fourier Transform (for solid finite samples, no powder)

Nano-SIMS = Secondary Ion Mass Spectrometer for solid samples

NDICM = Nomarski Differential Interference Contrast Microscopy

OM = organic matter

SEM = scanning electron microscope

SF = silt fraction (in this study, 32-2 μm)

SOC = soil organic carbon

$^{87}Sr/^{86}Sr$ = Sr isotopic ratio

Part A: Synopsis

1. Introduction

1.1 Global warming and climate change: glaciers and proglacial areas as environmental monitors

The point of view of a human being is based on his average lifetime expectation (<100 yr). This (limited) perception of space/time leads to a close-to-immobile view of events, considering a geologic time scale as the chronicles of events too far from us to (directly) influence our lives. Important earthquakes, formation and dismantlement of entire orogenic chains, appearance and extinction of forms of life, are events which occurred very often since Earth's genesis. Along with them, important cycles of temperature fluctuations occurred in the past, as well. The latter influenced the life patterns of flora and fauna, and thus remarkably contributed to shape the landscape accordingly.

For the individuals and the broad community in general, the interest towards global warming and climate change begins as soon as the direct impact on our lives is observed. Drought, flooding, and natural-related local disasters – i.e. debris flows - are only few among the possible events which have reached us all on various degrees and scales. The labile borders of an exclusively scientific pattern for climate change have been bypassed since few decades. Therefore, the study of climate fluctuations (and related events through time) may represent a good compromise between human and geologic time scale. It can help us understand short- and long- term processes.

Due to a broad variety of studies on Holocene moraines, we are able to trace past climatic variations. Many investigations - i.e. pedological (e.g.: Gamper, 1985) and palynological studies (e.g.: Burga, 1993) – took place in the Swiss Alps. Those studies proved that the Alps witnessed frequent temperature variations, and thus confirmed ice cap oscillations through time.

1. Introduction

From c. 5000 B.P. (maximum glacial retreat) to the LIA (comprised between the 14th and mid 19th century; Ivy-Ochs et al., 2008a) a cooling period occurred. Radiocarbon measurements (^{14}C) date back to c. 5000 B.P. a frequent succession of rather short soil development phases and phases of increasing geomorphological activity – i.e. solifluction (Gamper, 1985). Glaciers in the Alps attained their LIA maximum extents in the 14th, 17th, and 19th centuries, with most reaching their greatest LIA extent in the final 1850/1860 AD advance (Ivy-Ochs et al., 2008b).

Continuous atmospheric warming implies glacier vanishing rates much higher than historical and Holocene variability ranges. Compared to the past millennia, modern times proved that complex systems are far from conditions of dynamic equilibrium. When observed, the individual components involved in climate change process show a very high variability (i.e. snow: days to seasons, glaciers: years to decades, forest: decades to centuries, soil: centuries to millennia).

Glaciers are an excellent example of early monitoring of ice masses. Systematic glacier observations were initiated in this densely populated high-mountain region. Some glaciers (i.e. Unteraar Glacier, Switzerland, by Agassiz' group; Haeberli, 2008) were monitored since the middle of the 19th century already in the means of glacial stands, local temperatures and precipitations. Specific cases (i.e. Mont Blanc, Glacier Bay) captured the interest of specialists as extraordinary events to be documented and analyzed (Haeberli, 2008).

With the (progressive) increase of the global temperature, the melting of ice masses became inexorable. In the Alps, the decrease of total glacier-covered surface area was roughly estimated from 4500 km^2 (c. 1850) to slightly more than 2900 km^2 (1970s), when systematic glacier inventories were compiled in all Alpine countries (Haeberli et al., 2011). The corresponding area loss rate of about 10 to 15 km^2 per year sharply increased after 1985 to about 40 to 45 km^2 per year, when the total glacier surface

area was reduced to slightly more than 2000 km^2 in 2003. That year is considered an exemplary date for exceptional glacial melt. Satellite images from the Landsat Thematic Mapper (TM) collected on that year allowed the compilation of a new, uniform and synchronous glacier inventory for the entire European Alps (Paul et al., submitted).

Dry summers - like 2003 - remarkably lower the albedo of glacial surfaces (Paul et al. 2005, Oerlemans et al. 2009). Also, they contribute to increase disintegration, collapse and subglacial cavity formation, as well as the development of numerous new lakes. Those features increase the rate of ice vanishing (Paul et al., 2007). The studies performed on those comprehensive datasets help settling the fundaments for the IPCC scenarios for potential global changes – temperature and precipitations – until the year 2100.

Ice- and frost-dominated regions - such as polar and high Alpine environment - are among the most sensitive areas in the means of climate changes (i.e. Hall et al., 2002; Föllmi et al., 2009a,b). World glacier monitoring comprehends a set of investigations on complex (physical) processes, ranging from shear stress to area coverage, ice volume fluctuations, albedo and runoff quantification. Modern age global warming leads to the melting of perennial snow and glaciers in cold areas, thus contributing to model ice cap extension and properties. Nowadays, the World Glacier Monitoring Service (WGMS) collects the quantitative documentation of recent, ongoing and possible future glacier changes (Haeberli et al., 2011). Over more than a century of idealistic and patient work also provided an especially rich documentation (Haeberli 2008).

Glacial retreat offers an ideal open-air setting for the study of initial weathering processes. While the Holocene climatic oscillations can be studied only on old

sediments and features, actual glacial fluctuations can be measured and witnessed in real time.

The study of the processes occurring since melting of the ice involves several aspects. The implications can be various and mostly related to environmental queries (i.e. slope stabilization, landslides, soil formation, vegetation and forest development) but also linked to a perspective economic exploitation of the areas (i.e. tourism resorts, Alpine lakes and artificial water reservoirs, cattles).

The quantification of the actual changes in the landscape are important for understanding what occurred in the past and to attempt to foresee what could occur in the near future. Moreover, the study of the dynamic equilibrium ruling those processes is of basic importance for a comprehensive vision of the abiotic:biotic (in this case, rock:life) transition pattern and timing in a transforming cryic environment.

1.2 From 'bare rock' to soil: sediment weathering and implications for landscape evolution in high Alpine regions

High Alpine mountains are gigantic silent guardians who have witnessed a broad range of climatic and landscape transformations through time. Across millennia, glaciers formed, retreated, disappeared and then appeared again with a broad variety of fluctuations. The alternate persistence of those ice masses and their activity shaped the landscapes. Contrarily to popular belief, in fact, glaciers are active masses featuring a highly abrasive action. The friction on the ice:bedrock interface results in the detachment of rock material under the shape of detrital masses of varying grain size. Detached rock material is progressively embedded into the ice mass. Thawing of the ice in the originally frost-sustained sediments leads to the collapse of the latter, and consequently to its mobilization. The subglacial sediment is transported, abraded and then accumulated under the form of moraines. Conceptually, the glacial areas can

be divided in two parts: unexposed (subglacial environment) and exposed portion (proglacial area) (Fig. 1).

Low-temperature geochemical reactions are often too unclear or little to be detected, and in general their interpretation is rarely directly contextualized in the framework of mineral weathering and soil formation. Only a handful of studies deal with specific elemental losses from parental sediment in recently exposed proglacial areas, thus leaving insight for primary mineral dissolution (e.g.: Föllmi et al., 2009a, b). Despite several environmental studies consider mineral weathering as a remarkable contribution to the chemistry of the watershed (e.g.: Erel et al., 2004; Oliva et al., 2004), no studies have ever been carried out on primary mineral dissolution (and consequent quantification) within a 0-150 yr time span. The contribution of (altering) mineralogy to pedogenesis at the early stage of alterations must be understood at the bond scale.

Recently deglaciated terrain, in which vegetation is not established, might be expected to share some characteristics of the subglacial environment (Anderson et al., 2000). The bed of the glacier is likely to be out of contact with the atmosphere (Raiswell and Thomas, 1984; Tranter et al., 1993), resulting in high pH in runoff and low silicate weathering rates (Anderson et al., 2000). The investigation of glacial runoff is a useful indicator of the chemical processing occurring under the glaciers. The runoff from glacier-covered basins tends to carry relatively high calcium and potassium loads, regardless of bedrock (Anderson et al., 1997). Carbonate dissolution and sulphide oxidation dominate the solute flux from many glacial basins (Brown et al., 1994; Sharp et al., 1995; Tranter et al., 1997). Moreover, relatively high potassium concentrations in glacial runoff (commonly resulting in K/Na ratios in excess of 1.0) probably derive from leaching of interlayer cations from biotite (Anderson et al., 2000).

Fig. 1. Morteratsch glacier, Upper Engadine, Switzerland. The images represent the glacial position in 1985 (upper) and in 2002 (lower). It is evident the difference in the vegetation development. (source: http://www.swisseduc.ch/glaciers/morteratsch/vegetation/index-en.html?id=5).

The glacial water fluxes detected underneath the glacier form an intricate watershed. However, the deciphering of the contributions of this network is quite complex. An example is reported by Tranter et al. (2002). They carried out sampling of glacial water through boreholes scattered along the surface of the Haut Glacier d'Arolla (Switzerland). The glacier is developed on a granitoid bedrock. The investigations proved that different kind of waters might occur in the subglacial environment, reflecting a variety of microenvironmental conditions. The observed reactions are shown in Table 1. Waters having long residence time are testified by the high

rock:water ratios, which promote the formation of secondary reaction products, such as clays, which depleted Si from till (Tranter et al., 2002). Also the promotion of the exchange of Fe^{3+} for Fe^{2+} and Ca^{2+} on silicates is observed, along with the increase of the HCO_3^- : SO_4^{2-} ratio. A water with lower residence time, and thus with a higher circulation rate, shows an opposite character. The high pH of these waters favours relatively high rates of Si dissolution, and therefore relatively high Si concentrations are found. The formation of secondary weathering products, such as clays, is likely to be hindered by the relatively short residence time of water in these environments (Tranter et al., 2002).

Different types of water, most probably derived by the mixing of the above mentioned, were also detected and labelled as third group (at varying proportions, according to precipitation input and flux intensity) due to the intermediate chemical character of the samples. Bulk runoff composition was proved to be quite similar to the last two water types. Tranter et al. (2002) also suggested that the microbial activity on subglacial chemical weathering could be of high relevance, due to their influence in changing the local environment into anoxic, and thus promoting mineral alteration and elemental depletion.

When the glacial sediment is uncovered, it starts experiencing a much higher weathering rate compared to what is observed in the subglacial environment. Open air settings are highly oxidising, and the settlement of different microbial populations is enhanced. Moreover, freshly exposed sediments tend to receive eolian material – i.e. pollen, organic matter, loess – that may enhance weathering to various degrees. As soon as exposure is involved, chemical – and partially, physical – alteration takes place.

Physical and chemical weathering are intimately linked to each other. Physical weathering processes expose fresh rock and surface to chemical weathering, whereas

chemical weathering reduces the strength of rock, making it susceptible to physical breakdown (Anderson et al., 2002). The process of physical weathering does not change the chemical and mineralogical composition of the original rock (Favilli, 2010). Chemical weathering reduces the strength of rock and includes the partial dissolution of bedrock by superficial fluids (i.e. organic acids produced by the plants) and removal of soluble ions in dissolution (Anderson et al., 2002; von Blackenburg, 2005).

It is commonly considered that cold regions, being 'cold', might inhibit temperature-driven chemical reactions. This is indeed the case of some regions, where weathering reactions are kinetically very slow or almost non-occurring. Chemical reactions are freeze-thaw - and thus, temperature – dependent (*Manuscript IV*). According to Egli et al. (2006), also moisture availability plays a major role in the weathering process. During freeze-thaw cycles, large volumes of dilute meltwaters and fine-grained sediments are put in contact with each other (Föllmi et al., 2009a,b; Arn et al., 2003).

Knowledge about weathering rates and mineral transformation processes is fundamental in analyzing the release of nutrients to ecosystems during primary succession (*Manuscript I*). The delicate balance kept in this fragile environment can be studied with several approaches, ranging from water chemistry to soil mineralogy (*Manuscript IV*).

In general, rock weathering involves several processes, such as dissolution of primary mineral phases, deposition of authigenic minerals, ionic exchange and sorption (Salvioli et al. 2001). In the case of Alpine soils, Lång (2000) defines weathering effects as an integrated result of the conditions that have existed since deglaciation.

We can compare soils to an open-air archive of encoded informations. Ranging from elemental leaching to mineral transformation and organic matter development, all data can be retrieved and decoded.

Table 1. Principal geochemical weathering reactions in subglacial environments. Modified after Tranter et al., 2002.

Carbonation

Feldspar surfaces

$CaAl_2Si_2O_8(s) + 2CO_2(aq) + 2H_2O(l) \Leftrightarrow Ca^{2+}(aq) + 2HCO_3^-(aq) + H_2Al_2Si_2O_8(s)$

(Ca-rich feldspar) (weathered feldspar surface)

Carbonate

$Ca_{1-x}(Mg_x)CO_3(s) + CO_2(aq) + H_2O(l) \Leftrightarrow (1-x)Ca^{2+}(aq) + xMg^{2+}(aq) + 2HCO_3^-(aq)$

(Mg)calcite

Hydrolisis

Carbonate

$Ca_{1-x}(Mg_x)CO_3(s) + H_2O(l) \Leftrightarrow (1-x)Ca^{2+}(aq) + xMg^{2+}(aq) + HCO_3^-(aq) + OH^-(aq)$

Feldspar

$KAlSi_3O_8(s) + H_2O(l) \Leftrightarrow HAlSi_3O_8 + K^+(aq) + OH^-(aq)$

Silica

$SiO_2(s) + 2H_2O(l) \Leftrightarrow H_4SiO_4(aq)$

Pyroxene

$Mg_2Si_2O_6(s) + 6H_2O(l) \Leftrightarrow 2Mg^{2+}(aq) + 4OH^-(aq) + 2H_4SiO_4(aq)$

Oxidation

Organic carbon

$C_{org}(s) + O_2(aq) + H_2O(l) \Leftrightarrow CO_2(aq) + H_2O(l) \Leftrightarrow H^+(aq) + HCO_3^-(aq)$

Sulphide oxidation coupled to carbonate dissolution

$4FeS_2(s) + 16Ca_{1-x}(Mg_x)CO_3(s) + 15O_2(aq) + 14H_2O(l) \Leftrightarrow 16(1-x)Ca^{2+}(aq) + 16xMg^{2+}(aq) + 16HCO_3^-(aq) + 8SO_4^{2-}(aq) + 4Fe(OH)_3(s)$

Sulphide oxidation coupled to feldspar dissolution

$4FeS_2(s) + 16Na_{1-x}K_xAlSi_3O_8(s)(s) + 15O_2(aq) + 86H_2O(l) \Leftrightarrow 16(1-x)Na^+(aq) + 16xK^+(aq) + 8SO_4^{2-}(aq) + 4Al_4Si_4O_{10}(OH)_8(s) + 32H_4SiO_4(aq) + 4Fe(OH)_3(s)$

Sulphide (by oxygen)

$FeS_2(s) + 14Fe^{3+}(aq) + 8H_2O(l) \Leftrightarrow 15Fe^{2+}(aq) + 2SO_4^{2-}(aq) + 16H^+(aq)$ (12)

$14Fe^{2+}(aq) + 7/2\ O_2(aq) + 14H^+(aq) \Leftrightarrow 14Fe^{3+}(aq) + 7H_2O(l)$ (13)

$FeS_2(s) + 7/2\ O_2(aq) + H_2O(l) \Leftrightarrow Fe^{2+}(aq) + 2SO_4^{2-}(aq) + 2H^+(aq)$ (14)

Sulphide (by ferric ions)

$FeS_2(s) + 14Fe^{3+}(aq) + 8H_2O(l) + 16CaCO_3(s) \Leftrightarrow 15Fe^{2+}(aq) + 16Ca^{2+}(aq) + 2SO_4^{2-}(aq) + 16HCO_3^-(aq)$

Sulphide (by FeIII coupled to carbonate dissolution as SO_4^{2-}: HCO_3^- ratios of 1 : 1) (in equivalents)

$FeS_2(s) + 14Fe(OH)_3(s) + 4CaCO_3(s) \Leftrightarrow 15Fe(OH)_2(s) + 4Ca^{2+}(aq) + 2SO_4^{2-}(aq) + 4HCO_3^-(aq) + 4H_2O(l)$

$FeS_2(s) + 14Fe^{3+}$ - silicate(s) $+ 38H_2O(l) + 4CaCO_3(s) \Leftrightarrow 15Fe(OH)_2(s) + 14H_3$ - silicate $+ 4Ca^{2+}(aq) + 2SO_4^{2-}(aq) + 4HCO_3^-(aq)$

Sulphide (by FeIII coupled to carbonate dissolution as SO_4^{2-} : HCO_3^- ratios of 1 : 4) (in equivalents)

$FeS_2(s) + Fe_{14}^{III}$ - silicate(s) $+ 8H_2O(l) + 16CaCO_3(s) \Leftrightarrow Fe_{15}^{II}Ca_6$ - silicate(s) $+ 10Ca^{2+}(aq) + 2SO_4^{2-}(aq) + 16HCO_3^-(aq)$

Formation of kaolinite from K-feldspar

$4KAlSi_3O_8(s) + 22H_2O(l) \Leftrightarrow 4K^+(aq) + 4OH^-(aq) + Al_4Si_4O_{10}(OH)_8(s) + 8H_4SiO_4(aq)$

Dissolution of gypsum

$CaSO_4 \cdot 2H_2O(s) \Leftrightarrow Ca^{2+}(aq) + SO_4^{2-}(aq) + 2H_2O(l)$

Soil is the interface between weathering rock (i.e. moraines) and the atmosphere. It can be defined as the first direct link between abiotic (minerals) and biotic (microbes, plants) domain. The establishment of life, starting by microbial populations and pioneer plants, occurs as soon as nutrients become available. Colonisation by

vegetation contributes to the chemical and physical weathering of the surfaces and to the stabilisation of the slopes (Matthews, 1992). In general, the more the weathering occurs, the more nutrients are available, and thus plants and trees may develop and settle in the newly forming soils.

During weathering and soil formation, parent mineral tends to decompose and lose major cations as a function of solar energy on Earth's surface, which is mainly manifested through atmospheric and soil-temperature variations (Righi and Meunier, 1995). Along with a broad variety of parameters - i.e. rock composition, biota and soil organic matter, weathering time, topography – temperature and water availability lead to transformation processes in the weathering column. Since most climates are seasonal, the rate of chemical and biological activity will vary during the year. Nevertheless, the main effect of temperature on soils is to influence the rates of reactions, given its importance on most pedogenic parameters (Righi and Meunier, 1995).

Soil forming processes are the latest stage of the landscape adaptation. Understanding the processes behind pedogenesis is useful in interpreting climatic changes and temperature fluctuations occurred in the past. Because the past is the key to the future, in a second step they might eventually substantially contribute to assess paths of climate change in cold regions.

However, despite the importance of global warming and climate change (and their direct impact on the Earth's surface), not much is known about the very initial stages of soil and secondary (clay) mineral formation since proglacial areas are ice-freed and fresh granitoid sediment are exposed.

1.3 Mineralogy as a decoder for weathering

Bedrock composition plays a key role in landscape adaptation to global climate cycles. The variety of existing rocks allows a high degree of soil evolution scenarios, when set in the broader framework of climate-driven weathering. Each rock formation and lithotype hosts a specific elemental concentration, which is distributed through the typical mineralogy, thus defining the rock itself.

Mineralogy is the base for local chemical processes in geomorphic processes. Mineral phases show features (habitus, lattice arrangement, paragenesis) which perfectly reflect the settings occurring during their formation. The empirical equation for mineral genetic conditions can be expressed as *f*(temperature, pressure, pH, redox potential, chemistry, …) of the forming environment. When a rock is exposed to the atmosphere, minerals undergo different conditions, and therefore become unstable. After contact with dilute waters at the earth's surface they tend to dissolve or transform into minerals that are more stable there (Saether and de Caritat, 1997). The same authors define weathering as a general term for this transformation, including the physical and chemical breakdown of the primary rock, and the accumulation of secondary products as soils.

Materials released during weathering are removed from the system either by leaching water or react in the system to form a variety of crystalline and amorphous products like clay minerals and hydrous oxides of iron and aluminium (Nettleton and Brasher, 1983).

During the leaching process, rock grains interact with runoff and, in general, with circulating waters. The pH of those waters represents a source of protons which may alter the equilibrium conditions (stability domain) of the individual minerals. Therefore, according to the crystallographic and chemical features of each phase, the alteration of the lattice will occur (e.g.: Oliva et al., 2003; 2004).

An important factor in the water-sediment interplay is the grain size of the till. As a general rule, the finer the grain size, the higher the available surface. The link between physical and chemical weathering is dependent on the available leached surface since the exposure of the sediment. When this is coupled with the high reactivity surface of freshly exposed grains, the weathering potential of glacial till becomes remarkable.

The first reaction in the crystal lattice of a mineral between protons and the grain – catalysed by runoff, organic acids and microbial activity – is the destabilisation of the balance of the electric charges. This process weakens the structural bonds, therefore rearranging the original framework and promoting ionic dispersion. The loss of structure-modifier ions in the lattice causes major transformation. The element position can be replaced by ion(s) circulating in the leaching solution, therefore partially modifying the original crystal structure compensating the missing charges. However, the balance of the electric charges cannot restore the precursor's lattice arrangement. These transformations usually occur on preferential areas – i.e. outer surface, cleavage or mechanically-derived cracks - where water can easily penetrate, circulate, or simply interact with the grain surfaces. During mineral weathering, water has a double role. It is, in fact, simultaneously the carrier of protons (triggering electronic destabilization of bonds) and of leached elements from the lattice structure.

Key insights into weathering can be obtained by investigating the runoff and waters circulating in the study basin. The use of molar ratios for major cations, such as Ca/Na (e.g.: Gaillardet et al. 1999; Blum et al. 2002; Oliva et al., 2004) and K/Na (e.g.: Anderson et al., 2000) was already used in previous studies for estimating the main mineral weathering occurring in early sediments and proglacial areas. In this respect, the work from Gaillardet et al. (1999) pointed out the importance to define the silicatic (and non-silicatic, as well) end-members with Ca/Na and Mg/Na values

derived by sediments. Large cations (Ca, Mg, Na, K) are bond to the crystal lattice with less energy compared to smaller atoms (Si, Al), and thus their leaching will be related to their atomic properties. The abundance of these elements in the runoff draws a weathering pattern for the glacial till. The waters, in fact, clearly reflect the composition of the weathering mineralogy.

The element mass balance during pedogenesis, when compared to the mineralogical composition of the parent material, delineates the weathering stage and indicates the relative age of the soils (cf., Egli and Fitze, 2000; Egli et al., 2001a; 2003; 2004; 2006; Favilli, 2010).

The elements leached from primary minerals lead to the precipitation of amorphous and/or (weakly) crystallized compounds. The precipitation of solid compounds - which are mainly Si-, Al- and Fe-oxy-hydroxides - from the circulating solution may occur immediately after leaching due to the quick formation of weak bonds. However, they are mostly detectable after a relatively high degree of weathering (few hundreds of years of pedogenesis). The formation of those compounds is hypothesised to be linked to the availability of fine material. The high reactivity surface of fine particles (mostly SF and CF) is likely to promote the precipitation of these phases.

In soils, secondary minerals formed in the corroded zones of primary ones can originate from two different processes: precipitation from solution enriched in dissolved components (nucleation and growth) – typical for oxy-hydroxides - and transformation of the parent crystal lattice by diffusion – typical for phyllosilicate alteration (Righi and Meunier, 1995). The detection of secondary phases (well, weakly crystallized, amorphous, organic bound) is usually performed with the selective extraction of Si, Al and Fe with specific treatments (i.e. dithionite, oxalate and Na-pyrophosphate).

Low-temperature geochemical reactions are often too unclear or little to be detected,

and in general their interpretation is rarely directly contextualized in the framework of mineral weathering and soil formation. Only a handful of studies deal with specific elemental losses from parental sediment in recently exposed proglacial areas, thus leaving insight for primary mineral dissolution (e.g.: Föllmi et al., 2009a, b). Despite several environmental studies which consider mineral weathering as a remarkable contribution to the chemistry of the watershed (e.g.: Erel et al., 2004; Oliva et al., 2004), no studies have ever been carried out on primary mineral dissolution (and consequent quantification) within a 0-150 yr time span.

1.3.1 Clay mineralogy

Along with oxy-hydroxides (either amorphous or crystallized), clay minerals are the most common weathering products of rock-forming minerals, generally phyllosilicates (Fig. 2, 3). When first studied, clay minerals were defined on the basis of their crystal size. They were determined as the minerals whose particle diameters were < 2 μm, hence the name of the CF grain size (Velde, 1995).

The topsoil usually represents the oldest exposed horizon in a soil column, and thus hosts the highest amount of clay minerals in the entire profile. Quantitative and qualitative description of soil secondary minerals gives crucial insight on pedogenic processes. This is the case of Alpine soils and, in general, soils developed in cryic settings. Studies on Italian and Swiss Alpine soils (e.g.: Egli et al., 2001a,b; 2003; 2006; Mirabella and Egli, 2003) have demonstrated that the amount of weathering end-products (i.e. smectite and vermiculite) can be directly linked to the age of the topsoil. Turpault et al. (2008) pointed out that clay minerals record the changes of environmental conditions at very small spatial and temporal scales within already three months. Part of the vermiculite collapsed due to K fixation in the surface layer (promoted by proton activity due to organic matter), aluminium precipitated on the

external surfaces of particles or in the vermiculite interlayers, and its degree of hydroxylation decreased in the subsurface layers (Turpault et al., 2008).

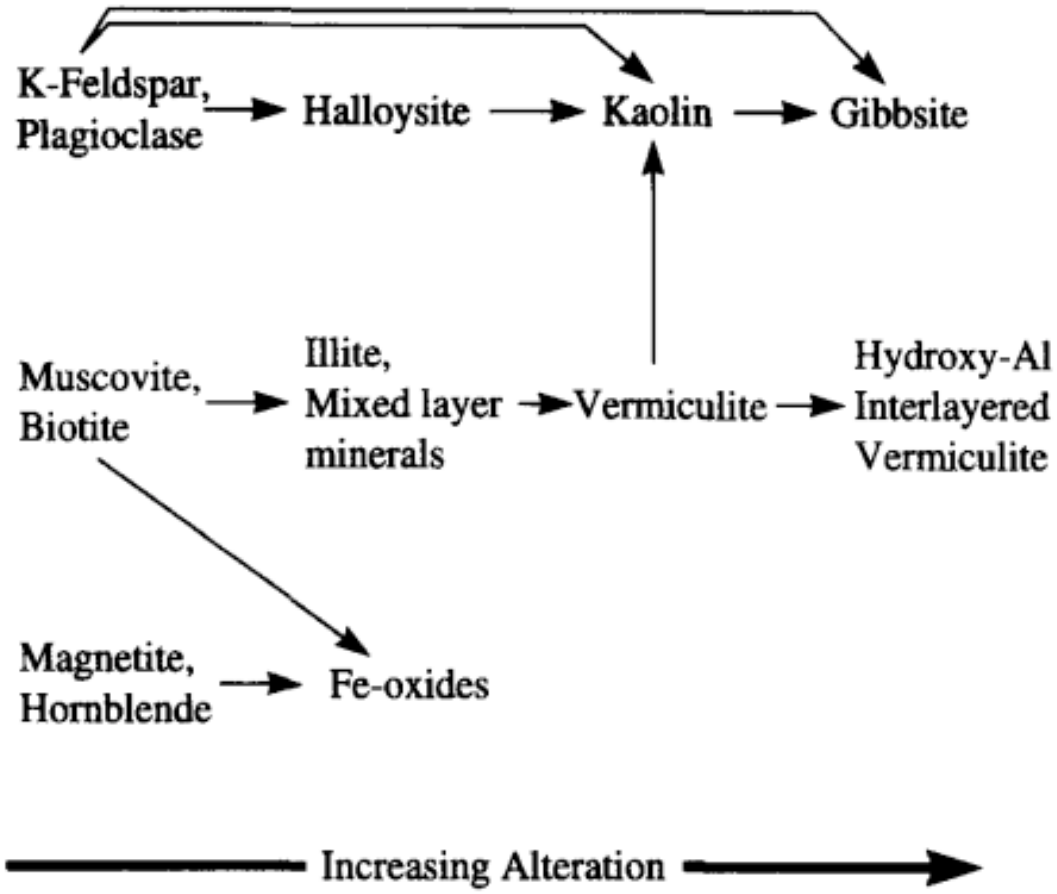

Fig. 2. Simplified weathering sequence of the main granite minerals during soil formation. From Dahlgren et al. (1997).

Clay mineralogy can be certainly considered as a marker for sediment weathering in the broader domain of geomorphology and landscape adaptation. With respect to chemical weathering, several studies have shown that smectitic components can be taken as an indicator of weathering intensity in Alpine soils and cold regions (*Manuscript IV*). The greatest changes in soil chemistry of Alpine soils – high Alpine environment - on granitic till occur within the first 3000 – 4000 years of soil development (Egli et al., 2001). Mineral weathering is generally driven by a significant decrease of primary phyllosilicates (i.e. chlorite and micas) and lead to the formation of smectite and regularly and irregularly interstratified mica-smectite

phases (*Manuscript IV*).

Given the composition of the parent material and climatic pedogenic settings, it is – in theory – possible to hypothesize a time and spatial distribution of secondary clay phases. The degree to which constraints are relevant into the pedogenic equation varies from case to case, making therefore unlikely the possibility to obtain a unique correlation valid for different settings. Even at similar climatic settings, a small change in the parental composition triggers a different weathering rate, and thus clay production will not be the same. Temperature and water availability are the basic pawns in the rock:water interplay, and therefore there is a strict connection to climate change and global warming. The retreat of ice caps, leading to the exposure of fresh sediments, allows the circulation of waters in an oxidizing, open-air system.

Despite the importance of secondary clay phases during incipient pedogenesis, no studies were ever carried out on the formation rates at the very early stages of granitoid sediment since deglaciation.

Moreover, the direct connection between soil development and (clay) mineralogy has been rarely performed in recently exposed proglacial chronosequences.

According to IPCC scenarios (2010), the increase of global temperatures foreseen until the year 2100 will lead to an increase of the mean annual temperature ranging between 2 and 4 degrees circa. Assuming no drastic fluctuations within this time span, a model considering temperature-related soil formations should also include these variations.

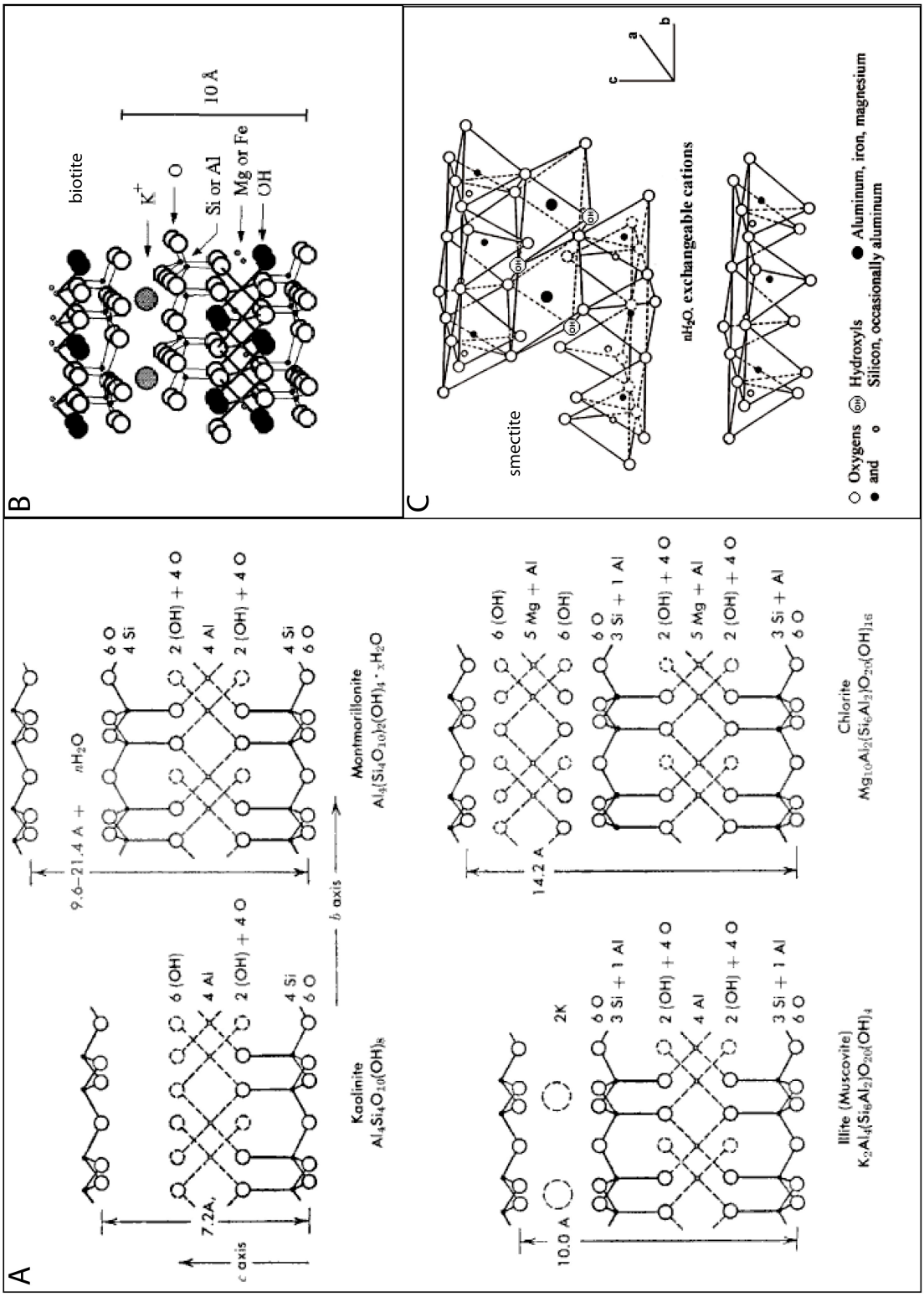

Fig. 3. Idealized crystal structures for various interstratified minerals: A) Kaolinite, montmorillonite, illite, chlorite (Source: http://www.seafriends.org.nz/enviro/soil/rocktbl1.htm) B) Mica. An octahedral layer of cations (Fe, Mg, and Al) lies between two layers of tetrahedral Si and Al. The interlayer K ion compensates for the negative charge on the 2: 1 -sheet caused by isomorphous substitution of octahedral and/or tetrahedral ions. From Malmström et al., 1997. C) Schematic diagram of the structure of smectites. From Valenzuela Diaz et al., 2001.

1.4 $^{87}Sr/^{86}Sr$ as environmental tracer

Diadochic substitutions in mineral phases are known to occur quite often due to elemental affinity. They can be observed, with varying concentrations, from trace elements (inclusions) to major components (enrichments, or solid solution members). Sr is an alkaline earth metal, which usually occurs in minor amounts in various rock-forming phases. However, it can be rarely found as individual phase, as well (i.e. strontianite, $SrCO_3$). Sr shows a high affinity with Ca and Mg, which often substitutes them in the lattice structures without significantly altering the mineral framework. Acting as an analogue of Ca, natural strontium isotopes are undeniably powerful tools, as tracers of nutrient sources of forest stands and as monitors of weathering processes in soils and catchments (Drouet et al., 2007).

Regardless the bedrock, $^{87}Sr/^{86}Sr$ is an effective chemical tracer of solute sources. Ranging from atmospheric inputs to weathering and soil formation, the $^{87}Sr/^{86}Sr$ of labile[1] Sr in soil provides information about the source of cations within the profile. Its uses in the weathering systems proved to be very fruitful (e.g.: Graustein and Armstrong, 1983; Åberg et al., 1989; Gosz and Moore, 1989; Krishnaswami et al., 1992, Miller et al., 1993; Negrel et al., 1993; Blum et al., 1994; 2002; Capo et al., 1994, Quade et al., 1995, Galy et al., 1999; Negrel and Roy, 1999; Oliva et al., 2004). The soil-vegetation system requires the determination of the isotopic composition of the soil parent material, of local rain and dust, and of groundwater and surface waters that come in contact with the soil (Capo et al., 1998). Soil parent materials often have distinct Sr isotopic signatures. Once the isotopic compositions of the sources of strontium to the soil–atmosphere–biosphere system are known, $^{87}Sr/^{86}Sr$ ratios in soil, precipitation, dust, and vegetation can track the geochemical cycling of Sr within and

[1] the sum of cations present in the soil solution and of 'exchangeable' cations adsorbed on mineral and organic soil colloids (Drouet et al., 2007)

between components (Capo et al., 1998).

The Sr isotopic composition of different soil pools – i.e. bulk and labile soil fraction, HCl extracts simulating weathering, soil solution – was described by Drouet et al. (2007). This was applied in conjunction with physico-chemical investigations and a mineralogical assessment method. The coupling of these methods highlighted several weathering processes along a fully developed soil column. The main mineralogical changes were mostly the dissolution of carbonates and Ca-plagioclase (parent material) and the weathering of the K-bearing minerals (i.e. incongruent weathering processes of K-feldspar in the topsoil). The preferential leaching of radiogenic Sr was also observed. Drouet et al., (2007) concluded that $^{87}Sr/^{86}Sr$ of the exchangeable pool can be used as a record of the integrated soil processes over the age of the soil and not a signature of present-day weathering. This approach would provide clear implications on long-term applications.

Despite the wide range of the $^{87}Sr/^{86}Sr$ tracing method during weathering processes, only few studies applied it to a high Alpine environment soil chronosequence (e.g.: Bullen et al., 1997; Blum and Erel, 1997; Anderson et al., 2000; Jacobson et al., 2002). Moreover, no studies have been carried out in the Alpine chronosequences. This approach would unravel pedogenic – and in general, weathering – processes featured on freshly exposed sediments.

1.5 Optical and spectroscopic microscopy in soil science

In order to improve the study of weathering-linked processes, Lång (2000) suggests a combined approach with diverse petrographic analyses to a limited number of key minerals and fractions.

The advantages of a combined study of soil mineralogy with optical and spectroscopic mineralogical investigations must be taken into account. In this framework, the combined use of SEM-EDX, CL and NDICM can indeed reveal a wide range of information.

SEM-EDX has been extensively applied to soil mineralogy in the last decades and will not be discussed. The application of both CL and NDICM in the broader domain of geosciences, however, is rather uncommon.

Transmitted-light CL microscopy is a technique applied to building materials (e.g.: Michalski et al., 2002; Götze and Siedel, 2007; Götze, 2009), archaeology (e.g.: Lapuente et al., 2000; Götze and Siedel, 2004) and geosciences (e.g.: Götze et al., 2000; Richter et al., 2003; Götze et al., 2004). Most materials show distinct luminescence properties that allow a rapid identification of phase distribution and transformation.

NDICM is an optical-based technique developed by G. Nomarski and first documented by Nomarski and Weill (1951) and Nomarski (1955). It allows the observation of micromorphological features in natural materials and/or metal alloys, and it has been routinely applied in reflected light microscopy to metallurgy and petrographic research (e.g.: Anderson, 1983; Pearce et al., 1987; 1990; Keevil and Walker, 1992). The varying resistance of different phases to grinding and polishing results in a microtopography (in the order of 0.2-1 μm), which is thrown into a sharp relief by the equipment, allowing a better resolution of micro-textures (Götze, 2009). NDICM has never been applied to soil mineralogy.

The combination of CL and NDICM can give quite important insights about the correlation between chemistry and crystal arrangements of the investigate samples (ie. point defects, cationic changes, etc.). Despite the relative straightforward preparation of the samples and the high amount of information that can be retrieved by the combination of both techniques, their application is rare (e.g.: Götze and Seidel, 2004; 2007). Griffin (2000) reports the combined application of SEM-EDX and CL as a successful imaging tool for the recognition of internal structures in a diverse range of materials, with case study quartz.

Despite it is widely accepted that changes occur at the bond scale when elements are leached, no studies were ever performed on the direct observation of the structural variations and bond breakdown of the individual primary phases during early soil formation.

2. Objectives

The present investigation focused on the mineralogical transformation processes involving silicatic morainic sediments since deglaciation (0 yr) to early soil formation stages (c. 150 yr). The choice of the Morteratsch proglacial forefield as case study will be extensively explained in Chapter 3.

The research question of this project was:

"What is the weathering trend of granitoid till in a high Alpine environment across a time span of 0-150 yr since its first exposure?".

A wide range of investigation techniques – from pedology to water chemistry, isotope geology, and traditional mineralogy – was used during this project. The idea behind this multidisciplinary method was to 'embrace' the problem by most possible sides and with a variety of known methods.

Manuscript I consisted in a first preliminary screening of the general features of the soils and waters, ranging from mineralogy to isotopic tracers. The research questions were:

a. Do silicatic sediments show high weathering rates?
b. How is the bulk mineralogy (FEF) varying in the investigated topsoils?
c. What is the role of disseminated calcite in the water and soil chemistry?
d. Can we relate the presence of the main cations (ie. Ca, Na, K, etc.) in the water catchments to the progressive leaching of specific mineral phases?
e. Is it possible to detect the weathering pattern of primary minerals with an isotopic tracer (in this case, Sr)?

The next step consisted in the investigation of the CF and partially of the SF. The reactivity surface of this grain size is suitable to prove a higher degree of changes in the mineralogy, with special focus on the phyllosilicates. The finer the grain size, the

higher the surface reactivity – and thus, the weathering during soil formation.

At this stage, several questions rose up (*Manuscript II*):

a. What is the weathering trend of inherited and pedogenic phyllosilicates as a function of time?
b. Is it possible to distinguish between geologically (inherited) and newly formed (pedogenic) phyllosilicates in the investigated fractions?
c. What is the weathering pattern in the CF and the SF?
d. Is there any link between soil formation rates and grain size?
e. Can smectite (and other newly formed clay phases) be quantified in the topsoils of the chronosequence?

Smectite acts as proxy for soil formation, therefore its content in topsoils is a reliable diagnostic tool for the degree of Podzolization. In *Manuscript II* the increase of pedogenic smectite as a result of primary phyllosilicate weathering was pointed out. Therefore, in *Manuscript III* a set of 35 samples for the Morteratsch proglacial area was considered, and the content of expandable clay phases was estimated and smectite quantified per each sample. The investigation was coupled with the use of an existing vegetation map (Burga et al., 2010). The key questions aimed to be answered were:

a. How does local topography – i.e. convexity, concavity, exposure - influence smectite formation across the forefield?
b. Does smectite reflect local mineral heterogeneities of parent material?
c. What is the link between soil moisture and smectite formation rates?
d. Is there any direct relationship between humus development and primary phyllosilicate weathering – and thus, transformation into smectite?

As a consequence to the findings of *Manuscript I* (and partially of *Manuscript II* and *III*), an investigation of the structural features of the bulk mineralogy (FEF) was carried out. The combined application of several method (CL, NDICM, SEM) was performed in order to shade light to the weathering behavior of the observed mineral fraction. Structural arrangements and transformations, preferential weathering patterns, and elemental depletion (for both abundant and trace REE, when possible) for the observed soil mineral phases within a time span of 0-150 yr were investigated. The research questions were (*Manuscript IV*):

a. Which phases are showing a clear micromorphological dissolution pattern as a function of exposure time?
b. Is elemental dissolution already observable via SEM-EDX at early pedogenic stages? If yes, can it be linked to the formation of secondary phases (ie. clay minerals)?
c. Can the weathering trend for the bulk mineralogy traced back, given the structural and trace elements variations?

3. General settings

3.1 Geography and climatic settings

The Morteratsch proglacial area (Fig. 3) is located in the Upper Engadine, a high valley (mean altitude c. 1700m) located in SE Switzerland. Soils and water catchments used in this research were collected within this forefield. Outer border of the proglacial area is the 1850s moraine, which represents the maximum glacial advancement during modern age (ie. Little Ice Age; Ivy-Ochs et al., 2008a,b). A broad literature on geomorphology, pedology and pioneer plant biology of the area is available (Burga, 1999; Egli et al., 2006; Burga et al., 2010).

The actual length of the investigated forefield is approx. 3 km, and has an area of 1.8 km^2. The valley where it is located runs N–S. The altitude ranges from 1900 m asl to about 2150 m asl (Fig. 4).

Alpine glaciers have fluctuated during the last 10 000 yr near the borders of the moraines formed in the year 1850. Several investigations indicate more or less similar climatic (±1–1.5 °C) and hydrologic conditions within that period (e.g.: Patzelt, 1977; Maisch, 1992; Magny, 1992; Burga and Perret, 1998).

The regional climate of the Upper Engadine is moderately continental with high temperature amplitude (Kneisel, 2003). The precipitations in Upper Engadine tend to be scarce in the North area (80 cm/yr; Fig. 5), and steadily increase moving South (Bernina group), reaching values up to 160-200 cm/yr (Konzelmann et al., 1992). Low clouds and occasional thunderstorms occur during the summer season (GISALP Project; Haeberli et al., 2007).

During winter - and by night, as well - an intense cooling air is often observed (Gensler, 1978). West and north winds in the Upper Engadine generally contribute with low rainfall, while the main precipitation events are related to southern winds, especially during winter.

Fig. 3. Morteratsch glacier front in june 2008. Noteworthy, the initial collapse of the roof of the subglacial cave. Photo: C. Mavris, 2008.

The latter also have been of crucial importance in building the snow cover (Gensler, 1978). During the summer season, wind from Maloja plays a major role. On sunny days, it usually starts around noon as a result of the rising temperatures, and it is later on replaced by moist air coming from the Bregaglia Valley. When blowing, it can exceed 40km/h, with noticeably cooling influences. The Maloja stream, as the name suggests, blows from the Maloja Pass. It forms a narrow band of clouds and winds along the side slopes down the valley. It is formed by condensation of moist air from the Bregaglia or the Po Valley and it usually represents a harbinger of bad weather (Gerig, 1978). In the Morteratsch proglacial area, a weather station is located at Chamanna da Boval CAS hut (Swiss coordinates: 791020/143670; elevation: 2540 m a.s.l.), on the side of the glacier (year 1850).

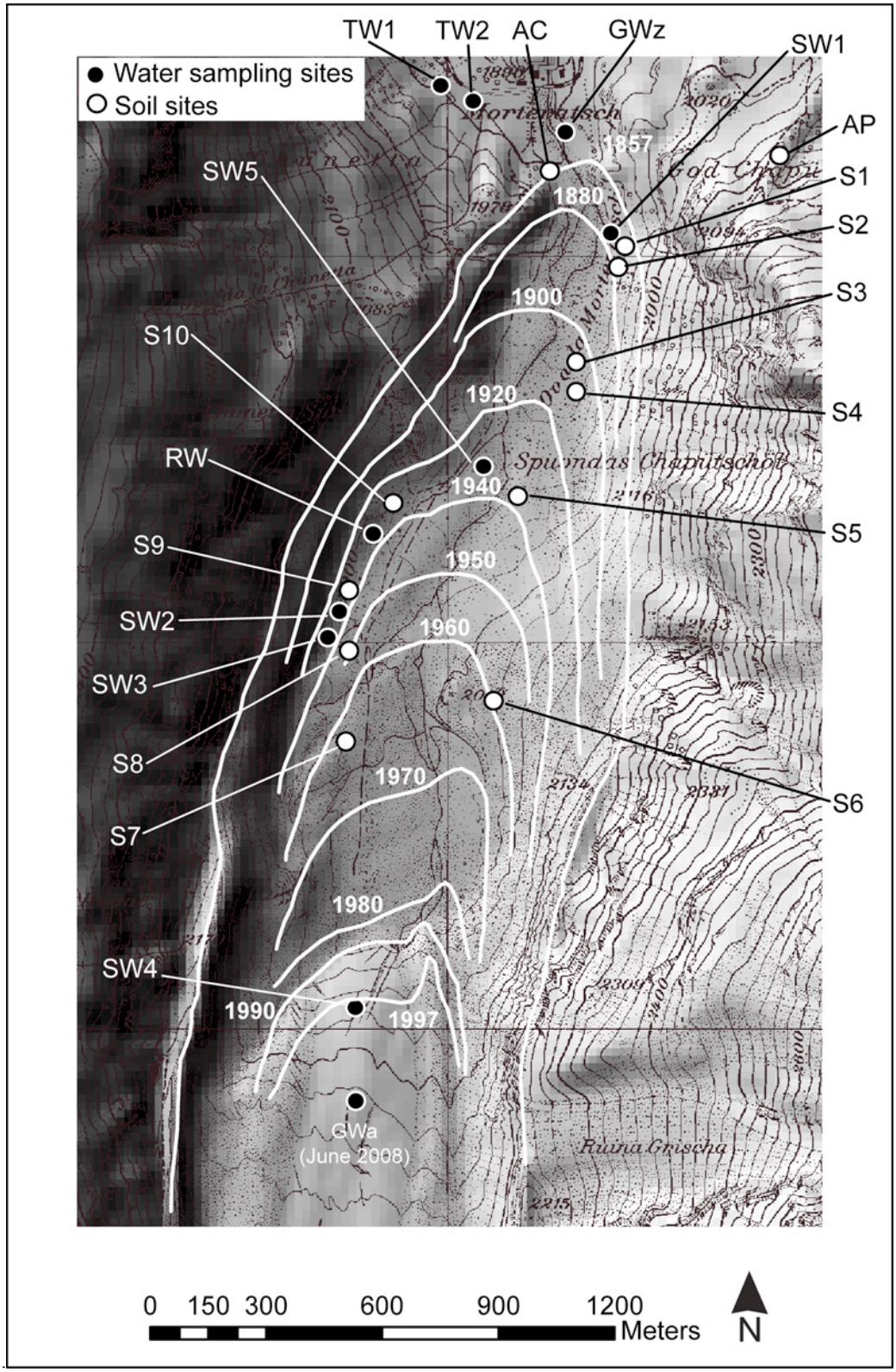

Fig. 4. Sampling sites in the Morteratsch proglacial area. Isochrones of related glacial margins from Burga (1999).

Nemec et al. (2009) reconstructed the mass loss of Vadret da Morteratsch - between 1865 and 2005 - with a two-dimensional energy-balance model (Oerlemans, 2001). This was found to be approximately 46 m w.e. The cumulative specific mass balance over this period shows an almost continuous mass loss, with short periods of mass gain around 1920, 1935 and 1980 (Nemec et al., 2009). After 1980 a trend towards a more negative mass balance is found. The decreasing specific mass balance is mainly associated with increasing summer temperature (Nemec et al., 2009).

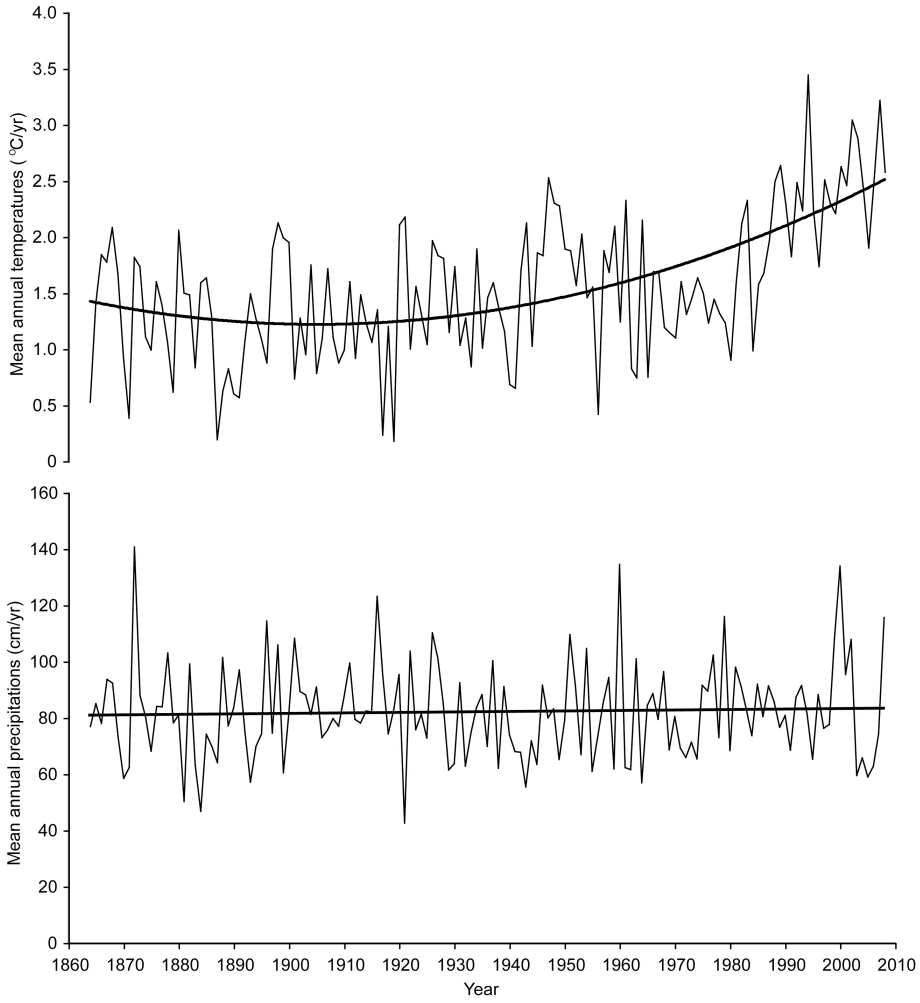

Fig. 5. Annual temperatures (upper plot) and precipitations (lower plot) at Sils-Maria, Upper Engadine, with trendlines. (data source: Federal Office of Meteorology and Climatology, MeteoSwiss)

Climate studies proved that cold glacial wind (katabatic flow; Hoinkes, 1954; Kuhn, 1987; Van der Broeke, 1997) generally blows from South, with a mean annual temperature is c. 0 °C, but with a high variability (up to ±10 °C; Oerlemans, 2010).

Energy balance on the Morteratsch glacier (Klok et al., 2002) report that below 3100 m a.s.l. the annual surface heat flux is positive. Above this altitude, the value is approx zero, implying that there is no melting and the snow/ice pack does not gain or lose heat on an annual basis (Klok et al., 2002) The mass balance and the radiation are strictly related. Solar radiation (sum of the net shortwave and longwave) is maximum at the end of the glacial tongue, where also albedo reorts minimum values. In this area, the mass balance reaches its minimum for the glacier (down to -6000 mm w.e.), thus indicating a strong decrease of the original glacial mass and a remarkable melting trend (Klok et al., 2002).

3.2 Geology

The Morteratsch proglacial area is set in the Lower Austroalpine Bernina Nappe, mainly constituted of plutonic rocks, such as granodiorites and diorites, syenites and alkali-granites (Fig. 6). These units were metamorphosed during the High Alpine orogenic event (Oligocene–Eocene) to the 'greenschists' facies (Trommsdorff and Dietrich, 1999). Due to the metamorphism, Na–Ca-amphiboles have been formed in the granite and granodiorite (Büchi, 1994).

In most observed granitoid rocks of the glacial forefield, the 'saussuritization' phenomenon is observed. Thereby, primary rock-forming plagioclase was partially transformed into minerals including epidote, albite, sericite, zoisite, zeolites and calcite (*Manuscript I*) (Fig. 7). Additional rock types (i.e. gabbro, limestone) are also reported in literature as sporadically occurring. Due to the glacial mixing and transport of these materials, the soil parent material can be considered as relatively homogeneous (*Manuscript I*). This feature fulfils the precondition for the 'chronosequence' (Jenny, 1980), which is among the basic '*conditio sine qua non'* of the present investigation.

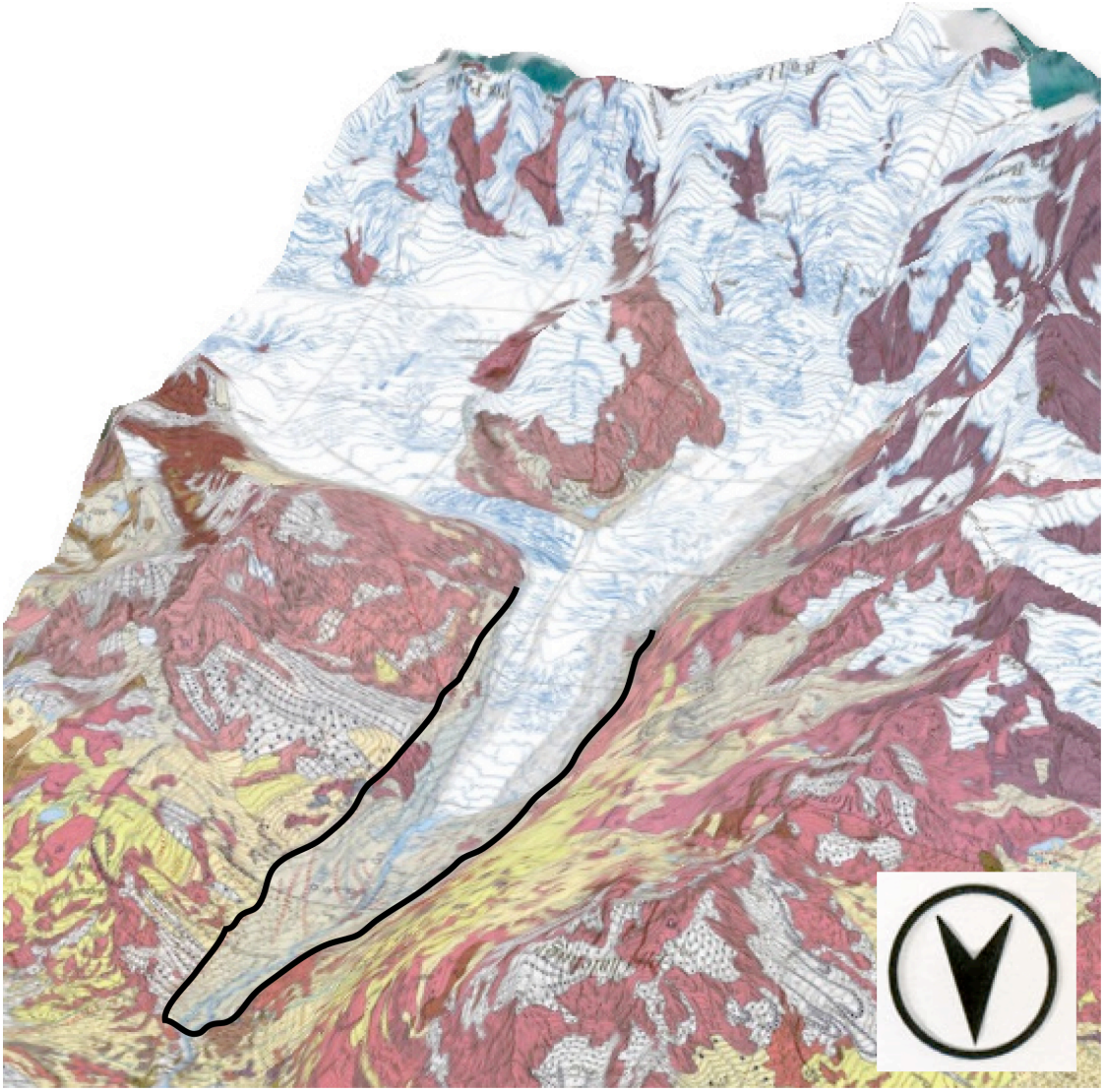

Fig. 6. Oblique view of the Morteratsch proglacial area. The outer moraine (black line) represents the limit of the LIA maximum (c. 150 yr ago). In red-purple, alkali feldspar granite and syenite, and locally gneiss. In yellow, quaternary moraine sediments. Geological Atlas of Switzerland (GA25), sheets nr. 118/1277 "Bernina" (2005) and nr. 119/1257 "St. Moritz" (2005) (pixelmaps ©swisstopo), visualized with the GOOGLE Earth Terrain model (grafic provided by Max Maisch, 2011).

Fig. 7. Typical granitoid block (max size up to 40 cm) with epidote covered side after ‘saussuritization’. Photo: C. Mavris, 2008.

3.3 Vegetation

The vegetation cover of the Morteratsch proglacial area has been studied by Burga (1999) and Burga et al. (2010). The first flowering plants invading young deglaciated surfaces are scattered individuals of mostly sterile *Epilobium fleischeri* and *Linaria alpina* that appear after about 7 years. *Epilobietum fleischeri* community has a higher cover-abundance after c. 27 years (Fig. 8). First plants of the community *Oxyrietum digynae* appear after c. 12 years and disappear after c. 27 years. The establishment of *Larici-Pinetum cembrae* forests takes place after about 77 years (Burga, 1999) on sites where the soil has been more intensely developed (*Manuscript I*).

Primary plant succession of the pro-glacial area of Morteratsch with its predominantly siliceous parent material starts with the pioneer plant communities *Oxyrietum digynae*

Fig. 8. Epilobium fleischeri grown on silicatic glacial till. Field of view: approx. 40 cm. Photo: C. Mavris, 2009.

and *Epilobietum fleischeri* and ends with the larch-Swiss stone pine forest after substantially more than 150 years (Burga et al., 2010). The first plants, i.e. *Epilobium fleischeri, Oxyria digyna, Linaria alpina*, *Saxifraga aizoides*, *Rumex scutatus*, appear about 7 years after deglaciation and reach greater cover-abundance values after about 27 years. The first species of the short-living *Oxyrietum digynae* appears approx. 10 years after deglaciation and disappears approx. 30 years later. The first small larch trees, the first shrubs of willows and green alder and the first dwarf-shrubs (e.g.: the rust-leaved alpenrose) are found on areas that have been ice-free for about 12 to 15 years. The establishment of *Larici-Pinetum cembrae* takes place after about 77 years. Surprisingly, lichens such as *Stereocaulon* cf. *dactylophyllum* need about 15 – 20 years to establish the first populations, and 150 years are definitely not sufficient for the establishment of a larch-Swiss stone pine stand (Burga et al., 2010).

3.4 Soils and organic matter

Parent material is silica-rich (acidic) glacial till, shaped and accumulated as moraines. Soils in the proglacial area are weakly developed and have a maximum age of 150 years. Forested areas outside the glacier stage of 1857 are characterised by Podzols having an age of 10,000 years or more (Burga et al., 2010). The dominant soil units in the proglacial area are Endoskeletic Fluvisols, Skeletic or Lithic Leptosols, Humi-skeletic Leptosols, including some sites with Ranker (Fig. 9; 10) (FAO, 1998), that have a weak B horizon and Dystric and Gleyic Cambisols (endoskeletic) (Egli et al., 2011).

Some sites, however, do not have a soil. The young soils that are close to the glacier showed almost no morphologic signs of chemical weathering and alteration products. They were usually characterised by a very thin and often discontinuous humus layer. The oldest soils (150 years) often had a spatially continuous humus layer (O or A

horizon) and some signs of weathering-product formation (formation of Fe- and Al-oxyhydroxides, start of clay mineral formation/transformation) and, thus, a weakly pronounced B horizon (Egli et al., 2011).

Fig. 9. Typical Ranker from the investigated proglacial area. Photo: M. Egli.

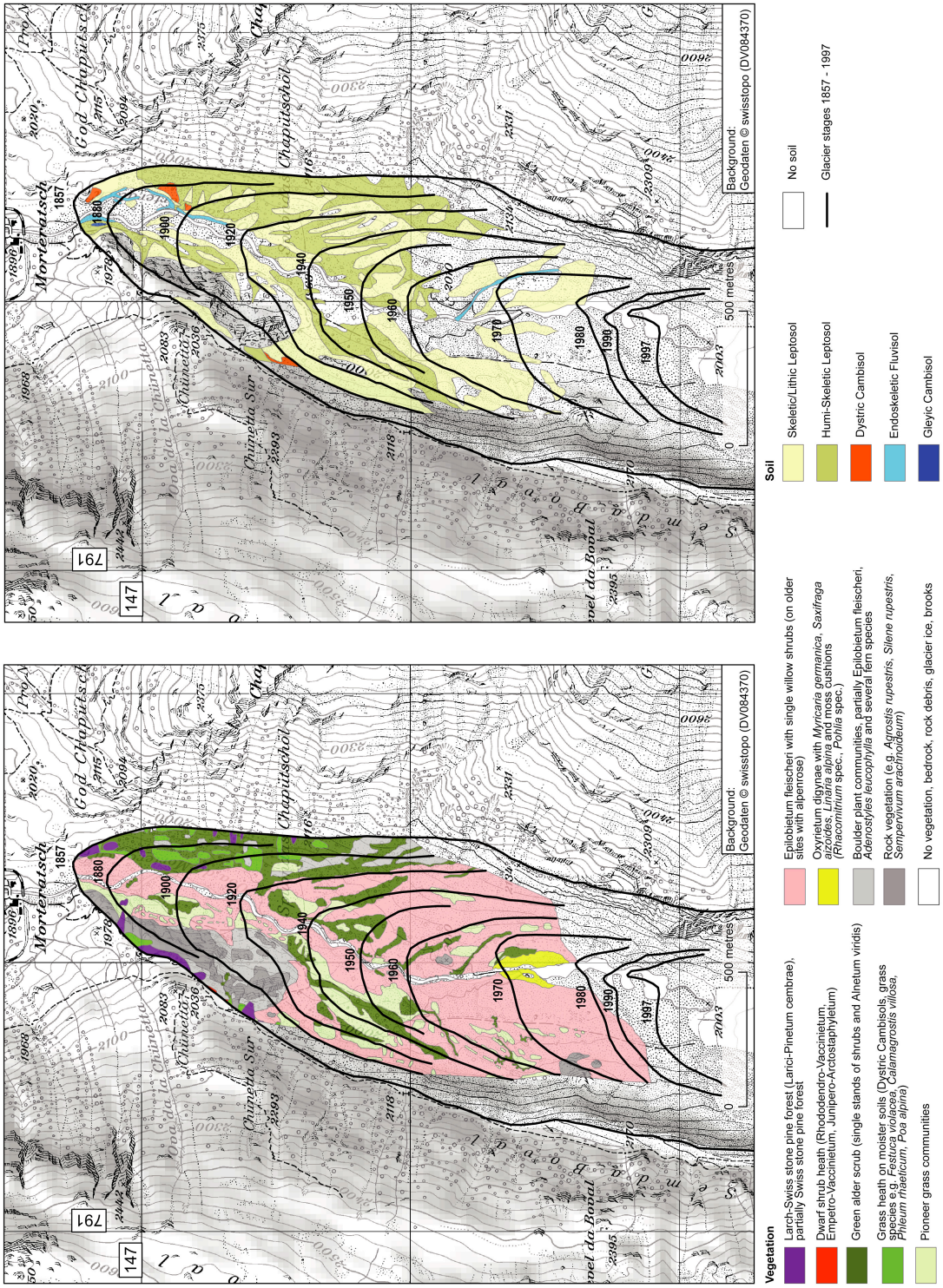

Fig. 10. Digital vegetation (left) and soil map (right) of the proglacial area (*Manuscript III*).

3.5 Soil temperature and moisture

Soil temperature has been measured with iButton digital thermometers. They were installed in the topsoil (0-10cm) of the proglacial area and the local temperatures were automatically collected in situ for one year round, every hour (Fig. 11). The temperature values show a remarkable discrepancy when sites with low and high vegetation cover are compared (Fig. 12). The higher exposure of fresh sediments to solar radiation contributes to a higher thermal conductivity. This could certainly represent an accelerating factor during the weathering of primary mineral phases, thus weakening the crystal lattice structure and promoting elemental loss.

When a higher vegetation cover is established, a shelter is provided to both topsoil and snow cover, thus contributing to its temperature decrease. Moreover, the role of organic matter – in more developed soils – appears to be remarkable for the thermal insulation of the layers which lay underneath the topsoil.

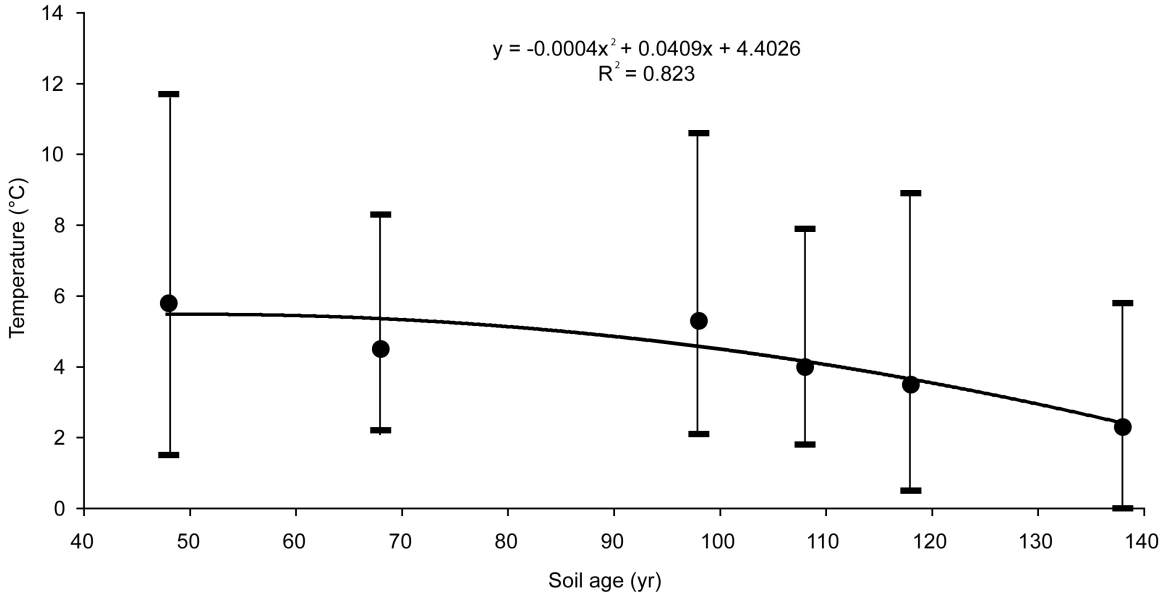

Fig. 11. Mean annual temperature distribution as a function of soil age.

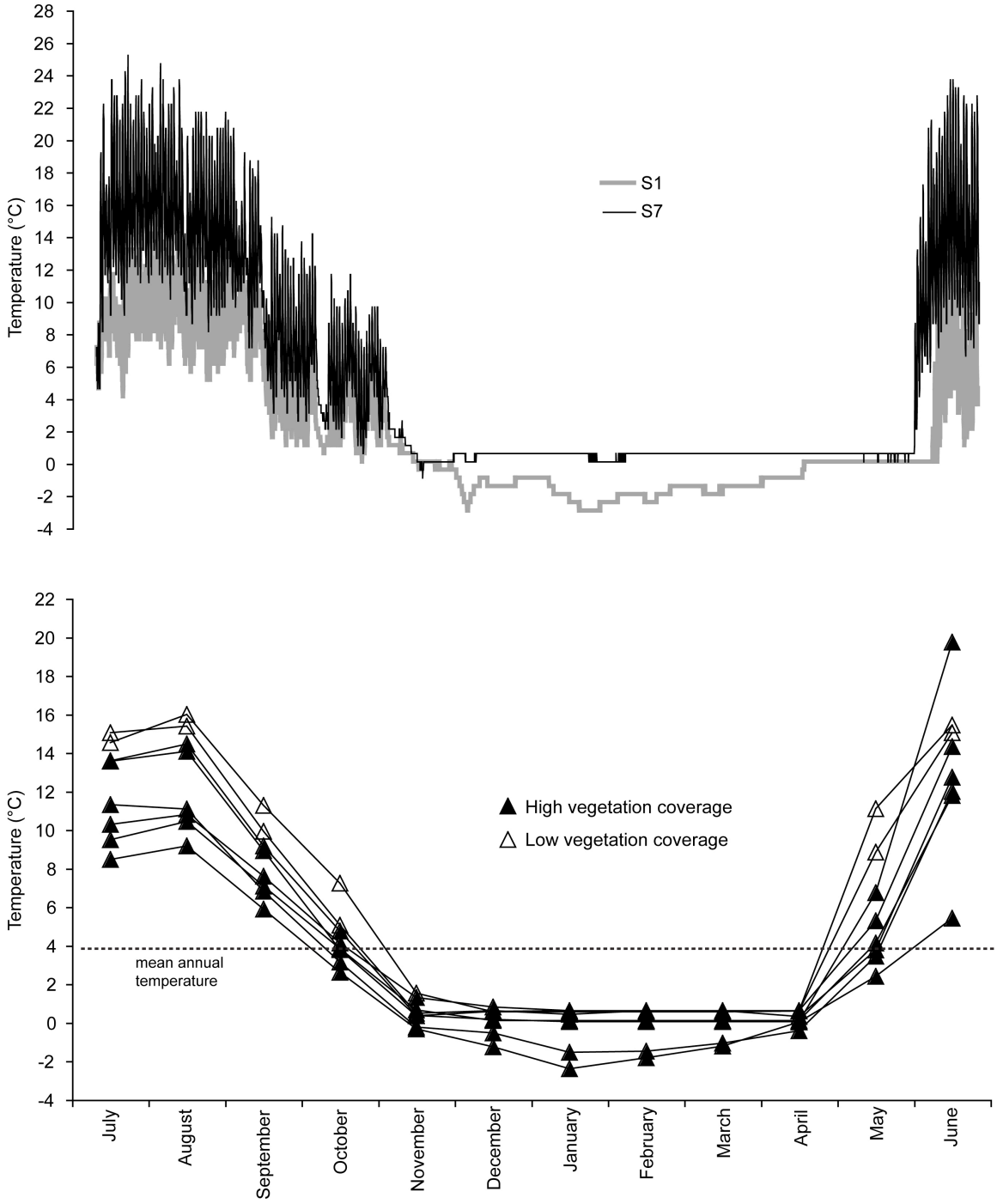

Fig. 12. Topsoil temperatures collected in the topsoils (0-10 cm) of the Morteratsch forefield. Upper figure: comparison between a site with well-established vegetation cover (S1 = 138 yr; young forest) and a poorly covered site (S7 = 48 yr; bushes and shrubs). Lower figure: monthly mean temperatures per sites.

Important insights derive also from the grain size of the soils, which influence the soil water properties as well. Both water content and pore water tension of the soil show a

weak tendency - although not significant. Water content slightly increases, while pore water tension slightly decreases along the chronosequence (Fig. 13).

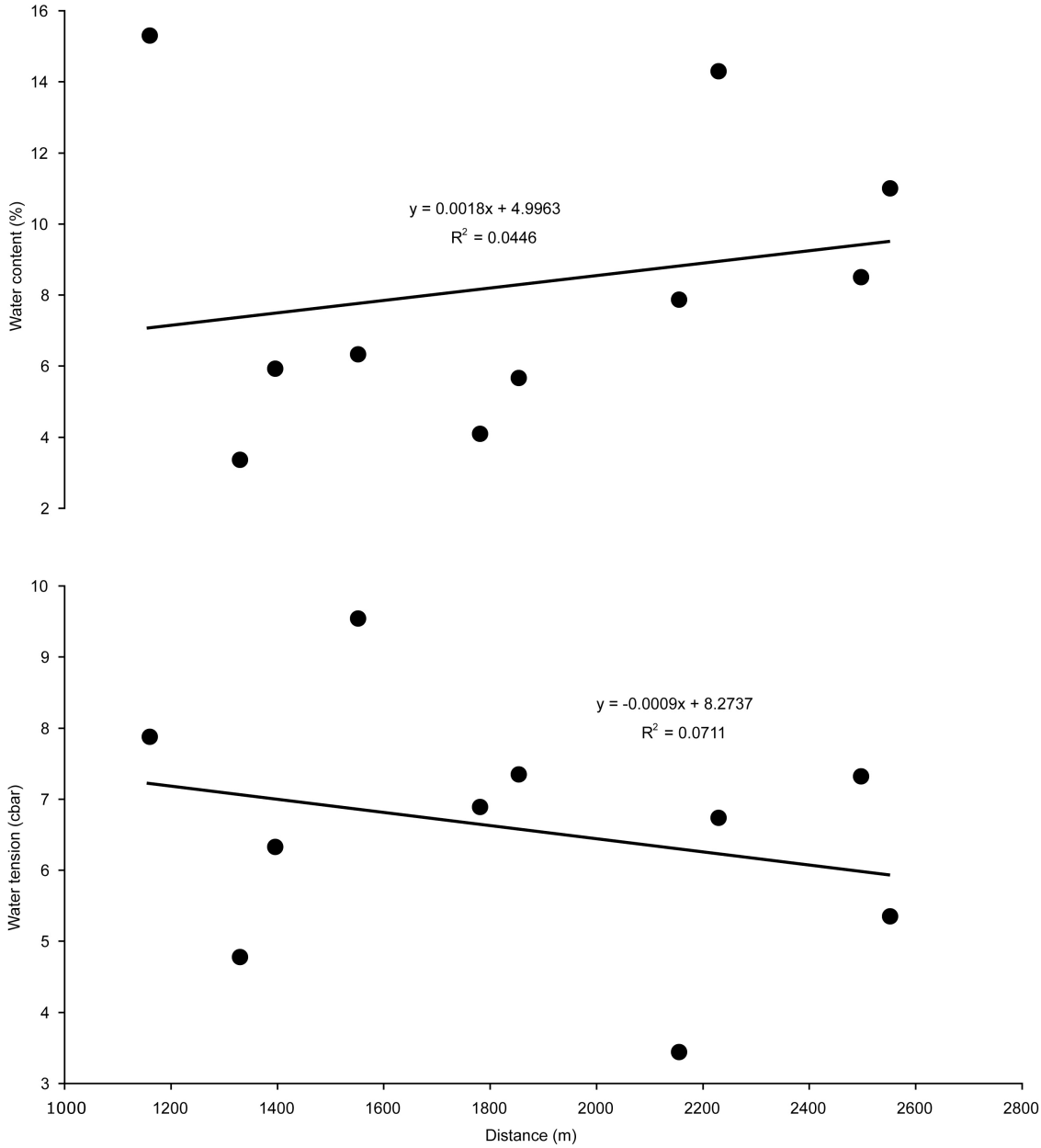

Fig. 13. Water content (upper figure) and pore water tension (lower figure) of the topsoils as a function of distance from the glacier front.

When old and young sites are compared, pore water pressure and soil water content confirmed their behavior as a function of grain size (Fig. 14). Despite the variable skeleton content, the soils of the proglacial area can be classified as sandy soils, which is typical for soils with water content up to 10% and pore water pressure up to 200

hPa. This is consistent with what observed after laboratory grain size measurements (*Manuscript I*). During those measurements, no direct link between soil properties and precipitations was taken into account.

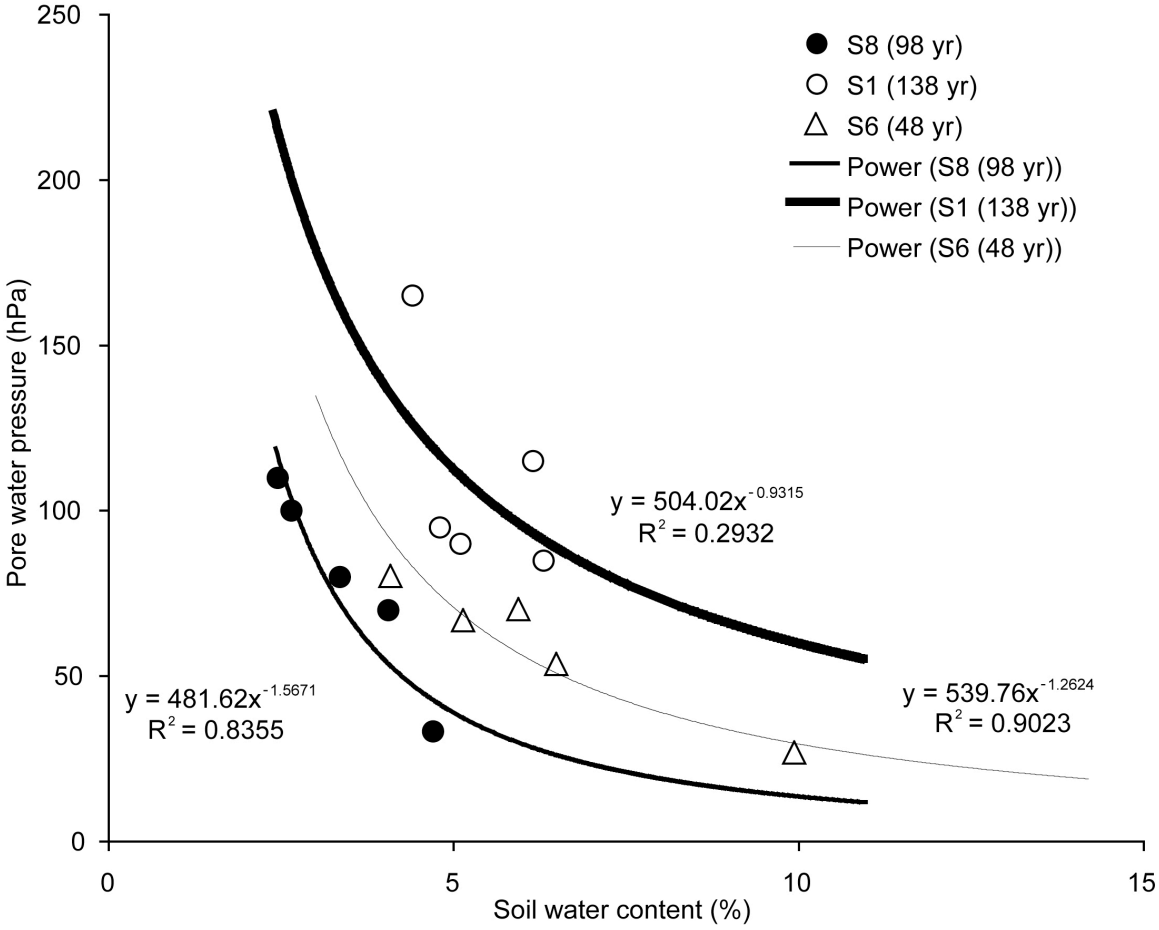

Fig. 14. Soil water content vs pore water pressure for three topsoils of the proglacial area Morteratsch.

4. Results

Soil mineralogy was confirmed as a reliable tool to detect climate changes as a function of time. Mineral weathering was proved to be very fast in the first decades of sediment exposure. Since deglaciation occurred, soils continuously formed and were settled by plant species, which reflected the degree of pedogenesis, therefore providing an uninterrupted evolutional timeline. This leads to the formation of Leptosols within less than 150 yr. A brief summary of the most important results is listed.

In the investigated chronosequence biotite, calcite and epidote weather rather quickly (<100 yr pedogenesis). Major cations (Ca in epidote, and Fe and – partially – K in biotite) are partially leached and decrease in content in the oldest topsoils. Ca depletion was confirmed with spectroscopic methods and due to its content in the runoff, decreasing and increasing as a function of the chronosequence, respectively. Elemental loss is a remarkable evidence of mineral weathering in this Alpine case study.

→ The combination of IR spectroscopy (DRIFT), diffractometry (PXRD) and water chemical concentrations (AAS, IC) give remarkable insight on the weathering of phases, even if they are present as minor components in the parent material (i.e. calcite). Furthermore, the use of Ca/Na molar ratio can help detecting the dissolution rates of Ca-bearing phases (i.e. calcite, apatite, epidote) compared to Na-bearing phases (i.e. plagioclase) (*Manuscript I*).

The study of a highly weathering phase (i.e. biotite, calcite) required also the use of $^{87}Sr/^{86}Sr$ as tracer in the proglacial runoff. As a comparison, water sites were sampled also outside the proglacial area.

→ $^{87}Sr/^{86}Sr$ confirmed the early weathering of biotite within the proglacial area. Therefore, it is suitable for investigations in cryic environments, set on silicatic bedrock (*Manuscript I*).

The investigation of finer grain size (CF) allowed the clear detection of clay minerals (mainly smectite and vermiculite), with an estimation of the latter. Measurements in the low angle (2-15° 2Theta) and d_{060} range (58-64° 2Theta) confirmed the progressive increase of dioctahedral phyllosilicates, with a strong loss of trioctahedral phases due to weathering agents.

→ Clay phases increased up to c. 10% within the chronosequence, confirming the active role of fine fresh surfaces during weathering. As stated by Egli et al. (2001a,b; 2003) and Mirabella et al. (2005), CF of freshly exposed sediments feature a high reactivity surface, therefore are keen to show major differences during transformation processes. Remarkable was the detection of traces of kaolinite in the parent material (geologically inherited) and in the oldest topsoil (pedogenic), confirming an incipient dissolution process for primary minerals in early soils, i.e. K-feldspar (*Manuscript II*).

Treatment with C18 and secondary peak splitting procedure allowed the detection of individual peak contributions. Low- and high-charged phases were detected and labelled.

→ Specific peaks were addressed to precursor phases (i.e. biotite, hornblende) due to specific layer charges, when already described in literature. Plagioclase could not be precisely attributed as source phase, and its position remains only hypothetic (*Manuscript II*).

Primary, rock forming phyllosilicates (mica, chlorite) degrade and lose major cations as a function of weathering, therefore leaving room to pedogenic clay phases. Among those, smectite was proved to appear in the topsoils (*Manuscript II*). The presence of this phase depends on the degree of weathering of the precursor phases, but also on a broad variety of factors (i.e. moisture, gran size, vegetation coverage).

→ Smectite forms across the proglacial area following a distinct trend. When related to soil formation and vegetation development, the scatter is quite high, but the amount of smectite in the topsoils is increasing as a function of pedogenesis. Local topography – inclination, concavity or convexity and (north- and south-) exposure – strongly influence the formation rates of smectite, showing highest values in protected areas, where erosion is limited or sediment accumulation is not occurring. The presence of expandable pedogenic clay phases is also linked to the grain size, which provides a high reactivity surface. Moreover, smectite showed highest concentrations where the soil was more moist and vegetation was established since longer time. Those sites were proved to have a finer grain size than others (sandy loam). Although the factor vegetation cannot be considered as a fully independent one, it had a significant effect on the clay minerals assemblage. Higher contents of smectite were related to green alder stands and grass heath where moister soils (having in most cases also a finer texture) could be encountered (*Manuscript III*).

The investigation of selected FEF grains proved that elemental dissolution occurs as a function of time. Surface micromorphology becomes gradually smoother and more etched, even on quartz grains. In thin section, the elemental composition is strongly changing mostly for biotite, progressively impoverished with exposure due to its platy structure and high surface availability. Moreover, the investigation of rock forming silicates like K-feldspar, plagioclase and quartz (structurally defined ‘tectosilicates’)

upset the common belief that those phases tend to weather only under strongly acidic pH, and thus in more developed soils. Also apatite – present in too little amount to be detected with PXRD – was detected and measured in both parent material and oldest topsoil, showing a remarkable weathering trend as a function of time. Its detection confirms its active role as source of inorganic P – and Ca, as well – in the forming soils.

→ The use of CL spectra, combined to NDICM and SEM-EDX, provided evidences of the quick degradation rates of the structural bonds due to proton contributions by runoff and – in a second step – organic acids and soil pH. Noteworthy the comparison of the CL spectra of each phase along the chronosequence. It was quite fruitful in this project due to a relative semiquantitative approach of rock forming mineral weathering. The applications of this method, however, could be a new approach for the detection of individual mineral weathering changes - at the bond scale - as a *f*(T, pH, …) (*Manuscript IV*).

→ Chemical transformations are occurring as related to individual phases, ranging from weak to resistant to weathering and elemental leaching. The lack of significant changes in the overall chemistry (parent material and soils > 100 yr) proved that we are still in the range of the very early stages of pedogenesis (*Manuscript I, II, III, IV*).

5. Conclusions and implications

5.1 Mineralogy

With the present research, a new boundary has been crossed. In *Manuscript I* it was demonstrated that epidote and biotite remarkably decreased in quantity as a function of sediment exposure (XRD, and DRIFT for biotite) due to their relatively weak lattice structure. The crystal framework of primary minerals opens and releases structure-forming elements. Structural changes can be underlined by the combination of SEM-EDX, NDICM, and CL. When elemental depletion is occurring at the major element scale (structure modifiers), SEM-EDX suffices. However, in early soil formation the combination with optical (NDICM) and spectroscopic techniques (CL) can certainly provide remarkable insight on the changes at the bond level. Moreover, the comparison of the CL spectra in different stages of sediment exposure, can provide key insight on the nutrients involved in soil formation (*Manuscript IV*). The application of this combined technique opens a brand new branch and perspective in soil mineralogical studies. A high amount of investigations on weathering parent material can help establishing a correlation between the relative intensity of the different spectral bands and the relative quantification of the depleted elements.

Secondary mineralogy can also be used as proxy for weathering. When the initial concentration of clay phases is known, it is possible to predict the pedogenic-related phases forming in the new soils (*Manuscript II, III*). Thus, the reverse approach is also possible. When the exposure speed of specific sediment – in this case, granitoid – is known, along with the climatic and microtopographic settings are known as well, it is possible to hypothesize the approximate age since the first exposure. Therefore, the quantification of clay mineralogy can provide very good insight about the age of the soil and its developing stage during the pedogenic process.

5.2 Water

Water chemical composition reflects the weathering stages of exposed rocks. As extensively discussed in *Manuscript I*, Ca/Na ratio is varying as a function of the exposure age of the leached moraines. However, water flows through different paths as a function of a broad variety of factors, often involving parent rocks with diverse ages. Chemical leaching by runoff and water composition cannot be clearly seen as a precise age indicator. They can be quite useful in understanding cationic mixing occurring throughout the catchments, and thus can indicate the main leached mineral phases along the runoff path and the relative alteration stage in the study area.

$^{87}Sr/^{86}Sr$ is a reliable tool to track chemical weathering of individual mineral phases. When combined to cationic ratios (i.e. Ca/Sr, Ca/Mg), it is possible to recognize whether the solution is closer to the rock or the runoff domain (*Manuscript I*). The tracked trend can give insights about the weathering rate of primary minerals as a function of time.

5.3 Geochronology

The combined investigation of soils and leaching waters provides basic insight on the processes involved during early pedogenesis (*Manuscript I, II, III, IV*). Mineralogy and (water) geochemistry can indeed reveal what occurs within the first decades of sediment exposure. A higher amount of samples would allow to hypothesize the weathering rates for specific mineral phases, and thus to approach a more precise quantification of nutrients involved in the pedogenic processes. In a second step, it would be possible to consider mineral:mineral or element:element ratios as a key indicator for weathering and soil formation rates.

The coupling of different techniques is a successful method to unravel incipient pedogenic processes. Soil mineralogy in (paleo)climatic reconstructions is

acknowledged since several decades as a fruitful approach. According to Singer (1980), clay mineral formation is directly related to climatic parameters. Also the use of water chemistry gives quite good insights about weathering and recent soils' formation, as already reported in several studies (e.g.: Hinkley, 1996; White et al., 1996; Anderson et al., 2000; Burkins et al., 2000, Anderson, 2007). When combined, different analytical approaches reveal the (recent) changes occurred at the sediment scale. However, given a similar climate regime and bedrock composition, the combination of those techniques can help predicting the formation and spatial distribution of soils. Therefore, the present study represents a solid basis for the modeling of high Alpine landscape evolution as a function of global warming and climate change. Its application can be extended to progressively exposed sediments in cryic environment worldwide.

6. Perspectives

The carried out project answered the majority of the initially stated research questions. It was proved that the combination of different techniques in the broad context of incipient mineral weathering and soil formation is indeed a successful approach leading to remarkable results.

However, as an expected consequence, several unanswered points remain, along with new interesting queries that came out.

In order to provide comprehensive insight to the field and cover a big part of the knowledge gap, it is highly suggested to follow a few directions. For that purpose, some investigations and projects are hereby suggested.

What are the transformations – at structural and bond-level – occurring in mica within the first 50 yr of pedogenesis?

Mineralogical results suggest a high weathering for primary rock-forming silicates (i.e. biotite; *Manuscript I*). However, XRD, DRIFT and the combination of CL, NDICM and SEM-EDX could not help detecting in detail what is happening during the first five decades of sediment exposure and weathering. Relevant insight came from the elemental concentrations in the runoff, but no structural modifications could be detected in the early soil phases.

Lab experiments conducted on natural material in controlled conditions revealed the initial stages revealed the alteration mechanisms of biotite and muscovite in strongly oxidizing conditions (Murakami et al., 2003). Dissolution rate at the edge of the crystallites is larger by two orders of magnitude than at the basal surface, therefore producing Fe-oxides (i.e. hematite) within a very short time span (Turpault and Trotignon, 1994). Dissolution experiments revealed that a higher Mg content in

biotite facilitates the formation of vermiculite, at least in the early stage. Because vermiculite dissolves at a much slower rate than biotite, Mg-rich biotite dissolves at a slower rate than Fe-rich biotite (Murakami et al., 2003). Malmström et al. (1996) had already observed this behavior for both biotite and chlorite in near-neutral pH region, estimating a turn-over time (10^1-10^2 yr) for molecular oxygen and a time scale (10 months) to develop characteristic Fe^{2+} concentrations for a granitic groundwater.

Malmström and Banwart (1997) attempted to model the hypothetical dissolution behavior of biotite at different pH conditions, with basic assumptions a constantly wetted surface for the investigated phase, and a congruent dissolution. Given those parameters, they found out that the stoichiometric dissolution of biotite (T = 25 °C, pH = 7) would take place within 50 yr. However, this is an ideal approach, because phyllosilicates feature incongruent dissolution (Turpault and Trotignon, 1994; Murakami et al., 2003). Therefore, the modelization of dissolution mechanisms must take into account different parameters and discard the possibility of constant supply of water. This is the case of Morteratsch biotite, where the initial (chemical) weathering of the latter is observed only within 150 yr of exposure, therefore providing insight for stoichiometrically slow dissolution (i.e. formation of secondary clay phases; *Manuscript I, II, III, IV*).

Based on those studies, HRTEM investigations on Morteratsch material could reveal the transformations of the individual layers, with the transition from trioctahedral to dioctahedral structure (mica). Moreover, with Nano-SIMS[2] it would be possible to map the elemental leaching of main cations from the individual crystallites. Eventually, the detection of the bond breaking and changes could be detected with Micro-DRIFT.

This approach would allow an investigation of soil formation based on the progressive incongruent dissolution rates of micas detectable in Morteratsch moraine sediments – and thus, in an open-air environment.

[2] this analytical technique focuses on areas down to 50 nm size (i.e. for Cs) while maintaining extremely high sensitivity at High Mass Resolution

Fractionation and variation of multiple stable isotope as a f(weathering, exposure time) within the proglacial area Morteratsch?

Sr is a known proxy for weathering in natural environment. Preliminary evaluations (*Manuscript I*) have revealed that the main weathering phases are weak-structured silicates (mainly biotite and epidote). However, Sr is not the only known tracer for weathering processes. Several isotopic ratios could be taken into account.

$\delta^{18}O$

Long-term geological processes (i.e. ore mineralizations, old rock formations) feature very often $\delta^{18}O$ measurements in order to show the occurring genetic conditions. However, very few studies take into account short-term processes like soil formation (e.g.: Schaub et al., 2009; Lawrence and Taylor, 1972) or rock weathering in general.

$\delta^{7}Li$

Fractionation of $\delta^{7}Li$ during continental weathering processes demonstrated its reliability in tracing environmental (paleo)conditions. This is given by the combined process of dissolution of primary phases and the surface sorption by secondary (mostly clay) phases. Rock surfaces are isotopically light (^{6}Li) compared to the inner, unexposed portion (Pristiner and Henderson, 2003). The same authors report the method as used on volcanic rocks. However, the presence of lithium is high in granites and especially in pegmatite rocks, which occur throughout the proglacial area of Morteratsch.

$^{234}U/^{238}U$ and $^{230}Th/^{238}U$

The use of U and Th in rock weathering is also documented as a method to assess the formation age of a saprolite (e.g.: Mathieu et al., 1995). Granites feature high concentrations of U and Th. Weathering is responsible for the opening of the system, and therefore $^{234}U/^{238}U$ and $^{230}Th/^{238}U$ isotopic ratios are in radioactive disequilibrium (Mathieu et al., 1995).

$\delta^{30}Si$

Silicon isotopes can also be useful in the study of weathering in different environmental settings. Basile-Doelsch (2006) describes the occurrence in nature of two silicon pools exist: Si_I (contained in igneous rocks of the continental and oceanic crust) and Si_{II} (Si that leaves Si_I by weathering). The Si_{II} pool includes both dissolved Si (as silicilic acid, $Si(OH)_4$, in continental and seawaters) and Si-bearing phases (formed by geochemical or biochemical precipitation of Si in various terrestrial and marine environments). The distribution of Si in these pools may have changed during the geological times as well as during climatic cycles (Basile-Doelsch, 2006). Despite the remarkable implications and insight that can be retrieved from such investigations, the $\delta^{30}Si$ technique counts only a handful of studies (e.g.: De La Rocha, 2002; Cardinal et al., 2003). The study of Si isotopic variations should permit to better constraint the Si cycle during its transfer through the vegetation biomass and through the soils, with implications at the weathering scale (Basile-Doelsch, 2006).

$\delta^{56}Fe$

Mobilization of Fe under oxidizing conditions can occur by the formation of Fe^{3+} colloids, solubilization of Fe^{3+} by organic complexation, and local reduction of Fe^{3+} to Fe^{2+} (Fantle and DePaolo, 2004). Limited available datasets suggest that exchangeable Fe in soils and sediments, and aqueous Fe in rivers, groundwater, and sediment pore waters can be isotopically fractionated relative to igneous rocks (Brantley et al., 2001; Bullen et al., 2001). Reduction, complexation with organic ligands, and inorganic speciation of Fe have been shown to affect the isotopic composition of Fe (Fantle and DePaolo, 2004). The reduced or complexed phase can have $\delta^{56}Fe$ as much as 1.3x lower than the source Fe (Beard et al, 1999; Brantley et al., 2001). Aqueous solutions at equilibrium (22 °C) contain Fe^{3+} that has $\delta^{56}Fe$ values that are 3x higher than that of Fe^{2+} (Welch et al., 2003). Mobile Fe^{2+} and

complexed Fe^{3+} in weathering environments can be considerably lighter than the material from which they are derived (Fantle and DePaolo, 2004). The extent of isotope fractionation and the degree of mobility are intricately related to the oxidation state, pH, and both the activity and Fe-affinity of complexing ligands. Processes within soils produce both isotopically light and heavy Fe (Fantle and DePaolo, 2004). Biological processes, such as the growth of surface vegetation and synthesis of organic ligands, produce a source of isotopically light, relatively mobile Fe within the soil that can be transported to streams via soil pore waters. Local reductive dissolution of oxide coatings in water saturated horizons, while subject to seasonal and annual fluctuations, can also contribute isotopically light Fe to the mobile phase (Fantle and DePaolo, 2004).

$\delta^{44}Ca$

Calcium isotope data have been used in the last decades to reconstruct palaeoenvironmental conditions related to P_{CO2} (e.g.: Schmitt et al., 2003). In the framework of weathering and soil formation processes, *$\delta^{44}Ca$* was used in the proglacial area of Damma, Central Switzerland (Hindshaw et al., 2011). Measurements on both rocks and soils did not show any variations at the early stages of pedogenesis. The only Ca pool which was strongly fractionated from bulk rock was vegetation, which exhibited an enrichment of light Ca isotopes (Hindshaw et al., 2011). The authors conclude that significant Ca isotope fractionation between bulk rock and the dissolved flux of Ca is likely to only occur where the Ca biogeochemical cycle is dominated by secondary processes such as biological cycling, adsorption and secondary mineral precipitation (Hindshaw et al., 2011).

With batch experiments in controlled conditions (i.e. user-defined t, pH, known initial composition of water and mineralogy) it would be possible to measure the changes in

both aqueous solution and the mineralogy, and to compare them with the measurements of catchments.

This would substantially improve the knowledge on the weathering processes involved in the very first stages (i.e. up to 24 weeks) of sediment exposure. Furthermore, the comparison with field data (i.e. Morteratsch, Damma, Arolla) could validate the combined use of both isotopic tracers during soil formation and mineral dissolution processes.

The idea behind this approach is to confirm the reliability of the above mentioned isotopic ratios as tracers of mineral weathering within a – geologically – short time span. Given the presence of all those elements in the granitoid material of Morteratsch proglacial area, the use of those techniques should be taken into account. If the hypothesis will be confirmed, a new perspective on mineral weathering mechanisms will be opened, providing a solid base for a new weathering model based on runoff and watersheds, starting with cryic environmental settings.

7. References

Åberg, G., Jacks, G., Hamilton, P.J., 1989. Weathering rates and $^{87}Sr/^{86}Sr$ ratios: An isotopic approach. Journal of Hydrology 109, 65–78.

Anderson, S.P., Drever, J. I., Humphrey, N. F., 1997. Chemical weathering in glacial environments. Geology 25**,** 399–402.

Anderson, S.P., Drever, J.I., Frost, C.D., Holden, P., 2000. Chemical weathering in the foreland of a retreating glacier. Geochimica et Cosmochimica Acta, 64, 1173-1189.

Anderson, S.P., Dietrich, W.E., Brimhall, Jr. G.H., 2002. Weathering profiles, mass-balance analysis, and rates of solute loss: Linkages between weathering and erosion in a small, steep catchment. Bulletin of the Geological Society of America 114, 1143-1158.

Anderson, S.P., 2007. Biogeochemistry of Glacial Landscape Systems. Annual Reviews of Earth and Planetary Sciences35, 375-399.

Arn, K., Hosein, R., Föllmi, K.B., Steinmann, P., Aubert, D., Kramers, J., 2003. Strontium isotope systematics in two glaciated crystalline catchments: Rhone and Oberaar glaciers (Swiss Alps). Swiss Bulletin of Mineralogy and Petrology 83, 273-283.

Basile-Doelsch, I., 2006. Si stable isotopes in the Earth's surface: A review. Journal of Geochemical Exploration 88, 252-256.

Brantley, S.L., Liermann, L., Bullen, T.D., 2001. Fractionation of Fe isotopes by soil microbes and organic acids. Geology 29, 6, 535-538.

Bullen, T., White, A., Blum, A., Harden, J., Schulz, M., 1997. Chemical weathering of a soil chronosequence on granitoid alluvium: II. Mineralogic and isotopic constraints on the behavior of strontium. Geochimica et Cosmochimica Acta 61, 2, 291-306.

7. References

Bullen, T.D., White, A.F., Childs, C.W., Vivit, D.V., Schulz, M.S., 2001. Demonstration of significant abiotic iron isotope fractionation in nature. Geology 29, 8, 699-702.

Beard, B.L., Johnson, C.M., Cox, L., Sun, H., Nealson, K.H., Aguilar, C., 1999. Iron isotope biosignatures. Science 285, 5435, 1889-1892.

Blum, J. D., Erel, Y., Brown, K., 1994. $^{87}Sr/^{86}Sr$ ratios of Sierra Nevada stream waters: Implications for relative mineral weathering rates. Geochimica et Cosmochimica Acta 58**,** 5019–5025.

Blum, J.D., Erel, Y., 1997. Rb-Sr isotope systematics of a granitic soil chronosequence: The importance of biotite weathering. Geochimica et Cosmochimica Acta 61, 15, 3193-3204.

Blum J. D., Klaue A., Nezat C. A., Driscoll C. T., Johnson C. E., Siccama T. G., Eagar C., Fahey T. J., and Likens G. E., 2002. Mycorrhizal weathering of apatite as an important calcium source in base poor forest ecosystems. Nature 417**,** 729–731.

Brown, G.H., Sharp, M.J., Tranter, M., Gurnell, A.M., Nienow, P.W., 1994. The impact of post–mixing chemical reactions on the major ion chemistry of bulk meltwaters draining the Haut Glacier d'Arolla, Valais, Switzerland. Hydrological Processes 8, 465–480.

Burga, C., 1993. Swiss alpine paleoclimate during the Holocene: pollen analytical evidence and general features. In: Frenzel, B. (Ed.), Solifluction and climatic variation in the Holocene. Palaeoclimate Research, ESF Project "European Palaeoclimate and Man 6", Strasbourg, vol. 11, pp. 11–21.

Burkins, D.L., Blum, J.D., Brown, K., Reynolds, R.C., Erel, Y., 2000. Chemistry and mineralogy of a granitic, glacial soil chronosequence, Sierra Nevada Mountains, California. Chemical Geology 162, 1, 1-14.

7. References

Büchi, H., 1994. Der variskische Magmatismus in der östlichen Bernina (Graubünden, Schweiz). Schweizerische Mineralogische und Petrographische Mitteilungen 74, 359–371.

Burga, C., 1999. Vegetation development on the glacier forefield Morteratsch (Switzerland). Applied Vegetation Science 2, 17-24.

Burga, C., Perret, R., 1998. Vegetation und Klima der Schweiz seit dem jüngeren Eiszeitalter. Ott Verlag, Thun.

Burga, C., Krüsi, B., Egli, M., Wernli, M., Elsener, S., Ziefle, M., Fischer, T., Mavris, C., 2010. Plant succession and soil development on the foreland of the Morteratsch glacier (Pontresina, Switzerland): Straight forward or chaotic? Flora 205, 561-576.

Capo, R.C., Chadwick, O.A., Hendricks, D.M., 1994. Constraining atmospheric inputs and in situ weathering in soils developed along a climate gradient using Sr isotopes. 8th Int. Conference Geochronological and Cosmochronological Isotopic Geology U.S. Geological Survey Circular 1107, 47.

Capo, R.C., Steward, B.W., Chadwick, O.A., 1998. Strontium isotopes as tracers of ecosystem processes: theory and methods. Geoderma 82, 197-225.

Cardinal, D., Alleman, L., De Jong, J., Ziegler, K., Andrè, L., 2003. Isotopic composition of silicon measured by multicollector plasma source mass spectrometry in dry plasma mode. Journal of Analytical Atomic Spectrometry 18, 213-218.

Dahlgren, R.A., Boettinger, J.L., Huntington, G.L., Amundson, R.G., 1997. Soil development along an elevational transect in the Sierra Nevada, California. Geoderma 78, 3-4, 207-236.

De La Rocha, C.L., 2002. Measurement of silicon stable isotope natural abundances via multicollector inductively coupled plasma spectrometry. Geochemical and Geophysical Geosystems 3.

Drouet, T., Herbauts, J., Gruber, W., Demaiffe, D., 2007. Natural strontium isotope composition as a tracer of weathering patterns and of exchangeable calcium sources in acid leached soils developed on loess of central Belgium. European Journal of Soil Science 58, 302-319.

Egli, M., Fitze, P., 2000. Formulation of pedologic mass balance based on immobile elements: a revision. Soil Science 165, 437-443.

Egli, M., Mirabella, A., Fitze, P. 2001a. Weathering and evolution of soils formed on granitic, glacial deposits: results from chronosequences of Swiss alpine environments. Catena 45, 19-47.

Egli, M., Mirabella, A., Fitze, P., 2001b. Clay mineral formation in soils of two different chronosequences in the Swiss Alps. Geoderma 104, 145-175.

Egli, M., Mirabella, A., Fitze, P., 2003. Formation rates of smectites derived from two Holocene chronosequences in the Swiss Alps. Geoderma 117, 81-98.

Egli, M., Mirabella, A., Mancabelli, A., Sartori, G., 2004. Weathering of soils in Alpine areas as influenced by climate and parent material. Clays and Clay Minerals 22, 287-303.

Egli, M., Wernli, M., Kneisel, C., Haeberli, W., 2006. Melting Glaciers and Soil Development in the Proglacial Area Morteratsch (Swiss Alps): I. Soil Type Chronosequence. Arctic, Antarctic, and Alpine Research 38, 499-509.

Egli, M., Mavris, C., Mirabella, A., Giaccai, D., 2010. Soil organic matter formation along a chronosequence in the Morteratsch proglacial area (Upper Engadine, Switzerland). Catena 82, 61-69.

Fantle, M.S., DePaolo, D.J., 2004. Iron isotopic fractionation during continental weathering. Earth and Planetary Science Letters 228, 547-562.

Favilli, F., 2010. Soil and Alpine Landscape Evolution since the Lateglacial and Early/Mid Holocene in Val di Sole (Trentino, Italy). PhD thesis, University of

Zurich, Switzerland.

Föllmi, K.B., Arn, K., Hosein, R., Adatte, T., Steinmann, P., 2009a. Biogeochemical weathering in sedimentary chronosequences of the Rhône and Oberaar Glaciers (Swiss Alps): rates and mechanisms of biotite weathering. Geoderma 151, 270-281.

Föllmi, K.B., Hosein, R., Arn, K., Steinmann, P., 2009b. Weathering and the mobility of phosphorus in the catchments and foefields of the Rhône and Oberaar glaciers, central Switzerland: Implications for the global phosphorus cycle on glacial-interglacial timescales. Geochimica et Cosmochimica Acta 73, 2252-2282.

Gaillardet, J., Dupre, B., Louvat, P., Allegre, C. J., 1999. Global silicate weathering and CO2 consumption rates deduces from the chemistry of large rivers. Chemical Geology 159**,** 3–30.

Galy A., France-Lanord C., Derry L. A., 1999. The strontium isotopic budget of Himalayan Rivers in Nepal and Bangladesh. Geochimica et Cosmochimica Acta 63**,** 1905–1925.

Gamper, M.W., 1985. Morphochronologische Untersuchungen an Solifluktionszungen, Moränen und Schwemmkegeln in der Schweizer Alpen. Eine Gleiderung mit Hilfe der ^{14}C-Altersbestimmung fossiler Böden. Thesis, Physische Geographie 17, pp. 1-117.

Gensler, G., 1978. Das Klima von Graubünden. Ein Beitrag zur Regionalklimatologie der Schweiz. Habilitationsschrift, Zürich.

Gerig, M., 1978. Der Malojawind: Ein Sonderfall unter der Talwinden, Bündner Zeitung.

Götze, J., Krbetschek, M.R., Habermann D., Wolf, D., 2000. High-resolution cathodoluminescence studies of feldspar minerals. In: Pagel, M., Barbin, V., Blanc

P., Ohnenstetter, D. (Eds.), Cathodoluminescence in Geosciences, Springer, Berlin, pp. 245–270.

Götze, J., Plötze, M., Greupner, T., Hallbauer, D. K., Bray, C. J., 2004. Trace element incorporation into quartz: A combined study by ICP-MS, electron spin resonance, cathodoluminescence, capillary ion analysis, and gas chromatography. Geochimica et Cosmochimica Acta 68, 18, 3741-3759.

Götze J, Siedel H., 2004. Microscopic scale characterization of ancient building sandstones from Saxony (Germany). Material Characterization 53, 209–22.

Götze J, Siedel H., 2007. A complex investigation of building sandstones from Saxony (Germany). Material Characterization 58, 1082–94.

Götze, J., 2009. Application of Nomarski DIC and cathodoluminescence (CL) microscopy to building material. Material Characterization 60, 594-602.

Gosz, J.R., Moore, D.I., 1989. Strontium isotope studies of atmospheric inputs to forested watersheds in New Mexico. Biogeochemistry 8, 115–134.

Graustein, W.C., Armstrong, R.L., 1983. The use of strontium-87 / strontium-86 ratios to measure transport into forested watersheds. Science 219, 289–292.

Griffin, B.J., 2000. Charge Contrast Imaging of Material Growth and Defects in Environmental Scanning Electron Microscopy – Linked Electron Emission and Cathodoluminescence. Scanning 22, 234-242.

Haeberli, W., 2008. Changing views of changing glaciers. In: Orlove, B., Wiegandt, E. and B. H. Luckman (eds.): Darkening Peaks - Glacial Retreat, Science and Society. University of California Press, 23–32.

Haeberli, W., Paul, F., Zemp, M., 2011. Vanishing Glaciers in the European Alps. International Workshop 'The Fate of Mountain Glaciers in the Anthropocene', Academia Pontificia, Vatican.

Haeberli, W., Keller, F., Krüsi, B., Egli, M., Rothenbühler, C., Meilwes, J., Gruber,

S., 2007. GISALP – Raum-zeitliche Informationen über schnelle Klimaänderungen in hochalpinen Umweltsystemen als strategisches Werkzeug. Forschungsbericht NFP 48, Universität Zürich.

Hall, K., Thorn, C.E., Matsuoka, N., Prick, A., 2002. Weathering in cold regions: some thoughts and perspectives. Progress in Physical Geography 26, 577-603.

Hindshaw, R.S., Reynolds, B.C., Wiederhold, J.G., 2011. Calcium isotopes in a proglacial weathering environment: Damma glacier, Switzerland. Geochimica et Cosmochimica Acta 75, 106-118.

Hinkley, T.K., 1996. Preferential weathering of potassium feldspars in mature soils. In: Basu, A., Hart, S. (Eds.), Earth Processes: Reading the Isotopic Code, Vol. 95. Geophysical Monograph, American Geophysical Union.

Hoinkes, H., 1954. Beiträge zur Kettnis des Gletscherwindes. Archiv für Meteorologie, Geophysik und Bioklimatologie B6, 36-53.

Ivy-Ochs, S., Kerschner, H., Maisch, M., Christi, M., Kubik, P.W., Schlüchter, C., 2008a. Latest Pleistocene and Holocene glacier variations in the European Alps. Quaternary Science Reviews 28, 21-22, 2137-2149.

Ivy-Ochs, S., Kerschner, H., Reuther, A., Preusser, F., Heine, K., Maisch, M., Kubik, P.W., Schlüchter, C., 2008b. Chronology of the last glacial cycle in the European Alps. Journal of Quaternary Science 23, 6-7, 559-573.

Jacobson, A. D., Blum, J. D., Chamberlain, C. P., Poage, M. A., Sloan, V. F., 2002. Ca/Sr and Sr isotope systematics of a Himalayan glacial chronosequence: Carbonate versus silicate weathering rates as a function of landscape surface age. Geochimica et Cosmochimica Acta 66**,** 13–37.

Jenny, H., 1980. The soil resource. Springer, New York.

Keevil, C.W., Walker J., 1992. Nomarski DIC microscopy and image analysis of biofilms. Binary Computational Microbiology 4, 93–95.

Klok, E.J. (Lisette), Oerlemans, J., 2002. Model study of the spatial distribution of the energy and mass balance of Morteratschgletscher, Switzerland. Journal of Glaciology 48, 168.

Kneisel, C., 2003. Electrical resistivity tomography as a tool for geomorphological investigations – some case studies. In: Schrott, L., Hoerdt, A., Dikau, R. (Eds.), Geophysical methods in geomorphology. Zeitschrift für Geomorphologie Supplementband 132, 37-49.

Konzelmann, T., Wehren, B., Weingartner, R., 1992. Hydrologischer Atlas der Schweiz (H.A.De.S.). In: Folder 1, Chapter 2.1(2). Ed.: Landeshydrologie, Bundesamt für Wasser und Geologie. June 1992, ISBN 3-9520262-0-4.

Krishnaswami, J., Trivedi, J. R., Sarin, M. M., Ramesh, R., Sharma, K. K., 1992. Strontium isotopes and rubidium in the Ganga-Bramaputra river system: Weathering in the Himalaya, fluxes to the Bay of Bengal and contributions to the evolution of oceanic $^{87}Sr/^{86}Sr$. Earth Planetary Sciences Letters 109**,** 243–253.

Kuhn, M., 1987. Micro-meteorological conditions for snow melt. Journal of Glaciology 33, 24-26.

Lång, L.O., 2000. Heavy mineral weathering under acidic soil conditions. Applied Geochemistry 15, 415-423.

Lapuente, M.P., Turi, B., Blanc, P., 2000. Marbles from Roman Hispania: stable isotope and cathodoluminescence characterization. Applied Geochemistry 15, 1469–93.

Lawrence, J.R., Taylor, H.P.Jr., 1972. Hydrogen and oxygen isotope systematics in weathering profiles. Geochimica et Coscmochimica Acta 36, 1377-1393.

Magny, M., 1992. Holocene lake-level fluctuations in Jura and the northern subalpine ranges, France. Regional pattern and climatic implications. Boreas 21, 319–334.

Maisch, M., 1992. Die Gletscher Graubündens: Rekonstruktion und Auswertung der

Gletscher und deren Veränderung sit dem Hochstand von 1850 im Gebiet der östlichen Schweizer Alpen (Bündnerland und angrenzende Regionen). Schriftenreihe Physische Geographie, vol. 32. Universität Zürich-Irchel, Switzerland.

Malmström, M., Banwart, S., Lewenhagen, J., Duro, L., Bruno, J., 1996. The dissolution of biotite and chlorite at 25 °C in the near-neutral pH region. Journal of Contaminant Hydrology 21, 201-213.

Malmström, M., Banwart, S., 1997. Biotite dissolution at 25 °C: The pH dependence of dissolution rate and stoichiometry. Geochimica et Cosmochimica Acta 61, 14, 2779-2799.

Mathieu, D., Bernat, M., Nahon, D., 1995. Short-lived U and Th isotope distribution in a tropical laterite derived from granite (Pitinga river basin, Amazonia, Brasil): Application to assessment of weathering rate. Earth and Planetary Science Letters 136, 703-714.

Matthews, J.A., 1992. The Ecology of Recently Deglaciated Terrain: A Geo-ecological Approach to Glacier Foreland and Primary Succession. Cambridge University Press, Cambridge.

Michalski, S.T., Götze, J., Siedel, H., Magnus, M., Heimann, R.B., 2002. Investigations into provenance and properties of ancient building sandstones of the Zittau/Görlitz region (Upper Lusatia, Eastern Saxony, Germany). In: Siegesmund, S., Vollbrecht, A., Weiss, T., (Eds.), Natural stone, weathering phenomena, conservation strategies and case studies. Special Publications, vol. 205. London: Geological Society; 2002, pp. 281–295.

Miller, E.K., Blum, J.D., Friedland, A.J., 1993. Determination of soil exchangeable-cation loss and weathering rates using Sr isotopes. Nature 362, 438–441.

Mirabella, A., Egli, M., 2003. Structural transformations of clay minerals in soils of a climosequence in an Italian Alpine environment. Clays and Clay Minerals 51, 3, 264-278.

Murakami, T., Utsunomiya, S., Yokohama, T., Kasama, T., 2003. Biotite dissolution processes and mechanisms in the laboratory and in nature: Early stage weathering environment and vermiculitization. American Mineralogist 88, 377-386.

Negrel, P., Allegre, C. J., Dupre, B., Lewin, E., 1993. Erosion sources determined by inversion of major and trace element ratios and Sr isotopic ratios in river water. The Congo basin case. Earth Planetary Science Letters 120**,** 59–76.

Negrel, P., Roy, S., 1998. Chemistry of rainwater in the massif central (France): A strontium isotope and major element study. Applied Geochemistry 13**,** 941–952.

Nemec, J., Huybrechts, P., Rybak, O., Oerlemans, J., 2009. Reconstruction of the annual balance of Vadret da Morteratsch, Switzerland, since 1865. Annals of Glaciology 50, 126-134.

Nettleton, W.D., Brasher, B.R., 1983. Correlation of Clay Minerals and Properties of Soils in the Western United States. Soil Science Society of America Journal 47, 5, 1032-1036.

Nomarski, G., Weill, A.R., 1951. Sur l'observation des figures de croissance des cristaux par les methods interférentielles à deux ondes. Société française de Minéralogie et de Cristallographie Bulletin 77, 840–868.

Nomarski, G., 1955. Microinterféromètre differentiell a ondes polarisées. Journal de Le Physique et Le Radium 16, 9–13.

Oerlemans, J., 2001. Glaciers and climate change. Lisse, etc., A.A. Balkema, Leiden, The Netherlands.

Oerlemans, J., Giessen, R.H., van den Broeke, M.R., 2009. Retreating alpine glaciers: increased melt rates due to accumulation of dust (Vadret da Morteratsch, Switzerland). Journal of Glaciology 55, 192, 729–736.

Oerlemans, J., 2010. The Microclimate of Valley Glaciers. Igitur, Utrecht Publishing and Archiving Services, Universiteitsbibliotheek Utrecht.

Oliva, P., Viers, J., Dupré, B., 2003. Chemical weathering in granitic environments. Chemical Geology 2002, 225-256.

Oliva, P., Duprè, B., Martin, F., Viers, J., 2004. The role of trace minerals in chemical weathering in a high-elevation granitic watershed (Estibère, France): Chemical and mineralogical evidence. Geochimica et Cosmochimica Acta 68, 10, 2223-2244.

Patzelt, G., 1977. Der zeitliche Ablauf und das Ausmass postglazialer Klimaschwankungen in den Alpen. In: Frenzel, B. (Ed.), Dendrochronologie und postglaziale Klimaschwankungen in Europa:Wiesbaden, Erdwissenschaftliche Forschung, vol. 13, pp. 248–259.

Paul, F., Machguth, H., and Kääb, A. (2005): On the impact of glacier albedo under conditions of extreme glacier melt: the summer of 2003 in the Alps. EARSeL eProceedings **4**, 2, 139–149.

Paul, F., Frey, H., LeBris, R. (submitted): A new glacier inventory for the European Alps from Landsat TM scenes of 2003: challenges and results. Annals of Glaciology.

Paul, F., Kääb, A. and Haeberli, W. (2007): Recent glacier changes in the Alps observed from satellite: Consequences for future monitoring strategies. Global and Planetary Change, 56 (1/2), 111-122.

Pearce, T.H., Russell, J.K., Wolfson, I., 1987. Laser-interference and Nomarski interference imaging of zoning profiles in plagioclase phenocrysts from the May 18, 1980, eruption of Mount St. Helens, Washington. American Mineralogist 72,

1131–1143.

Pearce, T.H., Kolisnik, A.M., 1990. Observations of plagioclase zoning using interference imaging. Earth Science Reviews 29, 9–26.

Pristiner, J.S., Henderson, G.M., 2003. Lithium-isotope fractionation during continental weathering processes. Earth and Planetary Science Letters, 214, 327-339.

Quade, J., Chivas, A.R., McCulloch, M.T., 1995. Strontium and carbon isotope tracers and the origins of soil carbonate in South Australia and Victoria. Palaeogeography, Palaeoclimatology, Palaeoecology 113, 103–117.

Raiswell R. and Thomas A. G. (1984) Solute acquisition in glacial melt waters. I. Fjallsjökull (south-east Iceland): Bulk melt waters with closed-system characteristics. Journal of Glaciology 30**,** 35–43.

Richter, D.K., Götte, T., Götze, J., Neuser R.D., 2003. Progress in application of cathodoluminescence (CL) in sedimentary petrology. Mineralogy and Petrology 79, 127-166.

Righi, D., Meunier, A., 1995. Origin of Clays by Rock Weathering and Soil Formation. In: Velde, B. Origin and Mineralogy of Clays: Clay and the environment. Eds.: Springer Verlag.

Velde, B., 1995. Origin and Mineralogy of Clays: Clay and the environment. Eds.: Springer Verlag.

Salvioli-Mariani, E., Toscani, L., Venturelli, G., 2001. Weathering of granodiorite and micaschists, and soil pollution at Mt. Mottarone (northern Italy). Mineralogical Magazine 65, 3, 409-419.

Saether, O.M., de Caritat, P., 1997. Geochemical Process, Weathering and Groundwater Recharge in Catchments. Eds.: Saether, O.M., de Caritat, P. A.A. Balkema, Rotterdam.

Schaub, M., Seth, B., Alewell, C., 2009. Determination of $\delta^{18}O$ in soils: measuring conditions and a potential application. Rapid Communications in Mass Spectrometry 23, 313-318.

Schmitt, A.D., Chabaux, F., Stille, P., 2003. The calcium riverine and hydrothermal isotopic fluxes and the oceanic calcium balance. Earth and Planetary Science Letters 213, 503-518.

Sharp, M., Tranter, M., Brown, G. H., Skidmore, M., 1995. Rates of chemical denudation and CO2 drawdown in a glacier-covered alpine catchment. Geology 23**,** 61–64.

Singer, A., 2000. The paleoclimatic interpretation of clay minerals in soils and weathering profiles. Earth-Science reviews 15, 4, 303-326.

Tranter, M., Brown, G., Raiswell, R., Sharp, M., Gurnell, A., 1993. A conceptual model of solute acquisition by Alpine glacial meltwaters. Journal of Glaciology 39**,** 573–581.

Tranter, M., Sharp, M. J., Brown, G. H., Willis, I. C., Hubbard, B. P., Nielsen, M. K., Smart, C. C., Gordon, S., Tulley M., Lamb, H. R., 1997. Variability in the chemical composition of in situ subglacial meltwaters. Hydrological Processes 11**,** 59–77.

Tranter, M., Sharp, M.J., Lamb, H.R., Brown, G.H., Hubbard, B.P., Willis, I.C., 2002. Geochemical weathering at the bed of Haut Glacier d'Arolla, Switzerland – a new model. Hydrological Processes 16, 959-993.

Valenzuela Diaz, F.R., de Souza Santos, P., 2001. Studies on the acidic activation of Brazilian smectitic clays. Quimica Nova 24, 3, 345-353.

Van der Broeke, M.R., 1997. Structure and diurnal variation of the atmospheric boundary layer over a mid-latitude glacier in summer. Boundary-Layer Meteorology 83, 183-205.

Velde, B., 1995. Origin and Mineralogy of Clays: Clay and the environment. Springer Verlag.

Trommsdorff, V., Dietrich, V., 1999. Grundzüge der Erdwissenschaften. Auflage, Zürich, Switzerland. vdf-Verlag, 6.

Turpault, M.P., Trotignon, L., 1994. The dissolution of biotite single crystals in dilute HNO_3 at 24 °C — Evidence of an anisotropic corrosion process of micas in acidic solutions. Geochimica et Cosmochimica Acta 58, 2761–2775.

Turpault, M.-P., Righi, D., Utèrano, C., 2008. Clay minerals: Precise markers of the spatial and temporal variability of the biogeochemical soil environment. Geoderma 147, 108-115.

von Blackenburg, F., 2005. The control mechanisms of erosion and weathering at basin scale from cosmogenic nuclides in river sediments. Earth and Planetary Science Letters 242, 224-239.

Welch, S.A., Beard, B.L., Johnson, C.M., Braterman, P.S., 2003. Kinetic and equilibrium Fe isotope fractionation between aqueous Fe(II) and Fe(III), Geochimica et Cosmochimica Acta 67, 22, 4231-4250.

White, A.F., Blum, A.E., Schultz, M.S., Bullen, T.D., Harden, J.W., Peterson, M.L., 1996. Chemical weathering rates of a soil chronosequence on granitic alluvium: I. Quantification of mineralogic and surface area changes and calculation of primary silicate reaction rates. Geochimica et Cosmochimica Acta 60, 2533-2550.

8. Curriculum vitae Christian Mavris

Personal data:

born in Naples, Italy (8th May 1983).

Educational background:

- High School Diploma (Matura) at the Italian School of Athens, Greece (2000)
- MSc in Mineralogy (24th March 2006) at the University of Parma, Italy. Grade: 104/110. Title of the thesis: "Melanophlogite from Case Montanini: mineralogical and crystallographic characterization".

Publications:

- Mario Tribaudino, Andrea Artoni, **Christian Mavris**, Danilo Bersani, Pier Paolo Lottici, and Daniele Belletti (2008). Single-crystal X-ray and Raman investigation on melanophlogite from Varano Marchesi (Parma, Italy). American Mineralogist 93, 88-94.
- **Christian Mavris**, Markus Egli, Michael Plötze, Joel D. Blum, Aldo Mirabella, Daniele Giaccai, Wilfried Haeberli (2010). Initial stages of weathering and soil formation in the Morteratsch proglacial area (Upper Engadine, Switzerland). Geoderma, 155, 359-371.
- Egli, M., **Mavris, C**., Mirabella, A., Giaccai, D., Haeberli, W. (2010) Soil organic matter formation along a chronosequence in the Morteratsch proglacial area (Upper Engadine, Switzerland). Catena 82, 61-69.
- Burga, C.A., Krüsi, B., Egli, M., Wernli, M., Elsener, S., Ziefle, M., Fischer, T., **Mavris, C** (2010). Plant succession and soil development on the foreland of the Morteratsch glacier (Pontresina, Switzerland): straight forward or chaotic?**.** Flora 205, 561-576.
- Egli, M., Wernli, M., Bruga, C., Kneisel, C., **Mavris, C.**, Valboa, G., Mirabella, A., Plötze, M., Haeberli, W. (2011). Fast but temporally scattered smectite-formation in the proglacial area Morteratsch: an evaluation using GIS. Geoderma 164, 11-21.
- **Mavris, C.**, Plötze, M., Mirabella, A., Giaccai, D., Valboa, G., Egli, M. (2011). Clay mineral evolution along a soil chronosequence in an Alpine proglacial area. Geoderma 165, 106-117.
- **Mavris, C.**, Götze, J., Plötze, M., Egli, M. (2012). Weathering and mineralogical evolution in a high Alpine soil chronosequence: a combined approach using SEM-EDX, cathodoluminescence and Nomarski DIC microscopy. Sedimentary Geology (DOI 10.1016/j.sedgeo.2012.04.008).

Congresses and conferences:

- "Initial stages of soil and clay minerals formation - Case study: Morteratsch proglacial area (SE Switzerland)" 14th International Clay Conference, Castellaneta Mare, Taranto, Italy, 14-20 June 2009 (oral presentation)
- "Initial stages of soil and clay minerals formation - Case study: Morteratsch proglacial

area (SE Switzerland)" International Geochronology Summerschool, Anzonico, Val Leventina, Ticino, Switzerland, 31.08 - 4.09.2009 (oral presentation)

- "Initial stages of soil and clay minerals formation - Case study: Morteratsch proglacial area (SE Switzerland)" Swiss Geosciences Meeting, Neuchatel, Switzerland, 20-21 November 2009 (oral presentation)
- "Initial pedogenesis in a recently exposed Alpine proglacial area - Case study: Morteratsch glacier (SE Switzerland)" - IMA 2010, Budapest, Hungary, 21-27 August 2010 (oral presentation)

Summer schools:

- International Geochronology Summerschool "Dating Anthropogenic and Natural Changes in a Fragile Alpine Environment". Anzonico, Val Leventina, Ticino, Switzerland, 31.08 - 4.09.2009

Acta from congresses:

- Tribaudino Mario, Bersani Danilo, Artoni Andrea, **Mavris Christian**: New X-ray and Raman data on melanophlogite, a clathrate phase of silica - Geoitalia 2007, Sixth Italian Forum for Earth Sciences - Rimini, 12-14 September 2007
- **Christian Mavris**, Markus Egli, Michael Plötze, Joel D. Blum, Wilfried Haeberli: Initial stages of soil and clay minerals formation in the Morteratsch proglacial area (Upper Engadine, Switzerland). 14th International Clay Conference, Castellaneta Mare, Italy, 14-20 June 2009
- **Christian Mavris**, Markus Egli, Michael Plötze, Wilfried Haeberli: Initial pedogenesis in a recently exposed Alpine proglacial area (Case study: Morteratsch proglacial area, Switzerland). 20th IMA Conference, Budapest, Hungary, 21-27 August 2010.

Awards and fellowships:

- Fellowship from the Italian Society for Mineralogy and Petrology (SIMP) in the framework of the PhD project "Initial stages of soil and clay minerals formation" – Awarded during the annual meeting of the Society in Rimini, 10th September 2009

Interviews:

- 21 April 2010: live radio interview on BBC show at Athens International Radio 104.4 (Athens, Greece).
  Topic: Island volcanic ash cloud and its implications

Invited talks and seminars:

- 30 November 2010: "Granitoid mineral weathering across a chronosequence in a high Alpine environment: a multiple approach - Case study: the Morteratsch proglacial area (SE Switzerland)" – GGG seminar, invited by Prof. Jörn H. Kruhl, Technische Universität München, German

- "Melanophlogite: a weird phase of silica?" – 1st International Mindat.org Conference, 10-17 July 2011, Lwowek Slaski, Poland
- "Soil mineralogy: a proxy for climate change – A case study from the Swiss Alps" - 1st International Mindat.org Conference, 10-17 July 2011, Lwowek Slaski, Poland

Other experiences

- Convener at Goldschmidt 2011, Session: The Geochemistry of Landscape Evolution: Linkages between Regolith Formation, Erosion, and Chemical Fluxes (14-19 August 2011).
- March 2010 - present: manager of MinDat.org.

Part B: Manuscripts

Geoderma 155 (2010) 359–371

Contents lists available at ScienceDirect

Geoderma

journal homepage: www.elsevier.com/locate/geoderma

Initial stages of weathering and soil formation in the Morteratsch proglacial area (Upper Engadine, Switzerland)

Christian Mavris [a], Markus Egli [a,*], Michael Plötze [b], Joel D. Blum [c], Aldo Mirabella [d], Daniele Giaccai [d], Wilfried Haeberli [a]

[a] Department of Geography, University of Zurich, Zurich, 8057, Switzerland
[b] ETH Zurich, Institute for Geotechnical Engineering, Zurich, 8093, Switzerland
[c] Department of Geological Sciences, University of Michigan, Ann Arbor, MI 48109, USA
[d] Istituto Sperimentale per lo Studio e la Difesa del Suolo, Centro di ricerca per l'Agrobiologia e la Pedologia, Piazza D'Azeglio 30, 50121 Firenze, Italy

ARTICLE INFO

Article history:
Received 18 May 2009
Received in revised form 22 December 2009
Accepted 23 December 2009
Available online 18 January 2010

Keywords:
Chemical weathering
Proglacial area
Sr isotopes
Soil mineralogy
Water chemistry

ABSTRACT

Investigations in Alpine soils indicate that mineral weathering is much faster in 'young' soils (<1000 yr) than in 'old' soils (~10,000 yr). However, little is known about the initial stages of weathering and soil formation, i.e. during the first decades of soil genesis. In this study we investigated rock-forming minerals weathering at very early stages of soil formation. Due to the continuous retreat of the Morteratsch glacier (Upper Engadine, Swiss Alps), the proglacial area offers a full time sequence from 0 to 150 yr old surfaces. A low slope and the absence of glacier which might have interrupted soil formation processes, contributed to the choice of the Morteratsch proglacial valley for this case study. The area is well documented regarding vegetation and soils. The tectonic unit is the Bernina-crystalline, which is mainly constituted of granitoid rocks. Consequently, the glacial till has an acidic character. Mineralogical measurements were carried out on the soil fraction <2 mm using XRD and DRIFT for qualitative and quantitative phase analysis. In addition, chemical analyses of the stream water from the main channel, tributaries and of rainwater were performed with a special focus on Ca/Sr and Sr isotope ratios ($^{87}Sr/^{86}Sr$). Furthermore, the accumulation of organic matter within the time sequence and physical soil properties were measured. Decreasing grain size with time shows active physical weathering processes. Soil organic matter has been accumulated during 150 yr at very high rates. Special emphasis has been given to chemical weathering and to the formation and transformation mechanisms of minerals. Of special interest were biotite, chlorite, epidote, plagioclase and calcite. Biotite has been continuously transformed into illite-like components. Within 150 yr, the concentration of epidote significantly decreased. The high Ca/Sr as well as $^{87}Sr/^{86}Sr$ ratios in the stream and spring waters confirmed that Ca bearing minerals are weathering and transforming at very high rates in the proglacial area. Also in cryic, ice-free environments, chemical weathering rates are high leading to the formation and transformation of minerals. Disseminated calcite in granitoid rocks, not confined to sedimentary carbonate rocks, also plays a role in subglacial environments. It is, however, not known for how long such an influence is significant and measurable. The high Ca/Na and Ca/Sr ratio in the stream and tributary waters showed that calcite contributes to the supply of soluble Ca, although the ion activity product calculations clearly demonstrated that the waters were undersaturated with respect to this mineral.

1. Introduction

Glaciers and periods of glaciation may have a significant impact on global weathering, changing the interplay between physical and chemical weathering processes by putting large volumes of dilute meltwaters and fine-grained sediment in contact with each other. Glaciers are significant agents of physical erosion; for example, the mechanical denudation of glaciated valleys in Alaska and Norway is an order of magnitude greater than that in equivalent non-glaciated basins (Hallet et al., 1996). Knowledge about weathering rates and mineral transformation processes is fundamental in analysing the release of nutrients to ecosystems during primary succession. Mountainous ecosystems are, for several reasons, likely to be especially responsive to changing environmental conditions such as global warming, acid deposition and atmospheric nutrient inputs (Theurillat et al., 1998; Arn, 2002; Hosein et al., 2004). Parent material lithology determines the physical and mineralogical nature and, thus, the reactivity of the weathering column. Dissolution of most primary rock-forming minerals is limited by slow kinetics of reactions at the mineral–water interfaces. Dissolution rates depends on extrinsic

* Corresponding author. Tel.: +41 44 635 51 14; fax: +41 44 635 68 48.
E-mail address: markus.egli@geo.uzh.ch (M. Egli).

0016-7061/$ – see front matter © 2010 Elsevier B.V. All rights reserved.
doi:10.1016/j.geoderma.2009.12.019

factors (T, pH, Eh, and exudates from microbes and plant roots) and on intrinsic factors (mineral surface properties and the presence of weathering products). Acidity and the availability of (organic) ligands promote the dissolution reactions of primary minerals and govern the transformation into secondary minerals. Erosion provides materials with an easily weatherable surface and consequently influences one main intrinsic factor. Chemical weathering and physical erosion are coupled to the degree that mineral weathering rates depend on the availability of fresh mineral surfaces with high reactivity (White et al., 1999a; Jacobson and Blum, 2003; Riebe et al., 2004).

Weathering is kinetically limited in regions having young surfaces (West et al., 2005). Proglacial areas in Alpine regions belong to this category. Silicate weathering depends on the kinetic rate of mineral dissolution, the supply of material (e.g. by erosion) and the time available for reaction. Additionally, the weathering rate of a mineral or rock decreases with the time (West et al., 2005) that the mineral spends in the weathering environment. Silicate weathering and transformation reactions should, consequently, be most intense in the initial stages of soil formation.

The rates of reactions and their dependencies on environmental factors (such as climate) are of fundamental interest to understanding the soil system and its interaction with surrounding environmental conditions. In this context, the influence of climate is of growing interest with respect to landscape and soil evolution because of observed and predicted global climate changes. Due to climate warming, additional areas will become ice-free and subject to weathering and soil formation. Proglacial environments are important for the understanding of global CO_2 cycling on glacial/interglacial timescales as they made up a significant amount of the global land surface during the Quaternary due to the advance and retreat of glaciers and ice sheets (Gibbs and Kump, 1994). The proglacial area is a potential zone of high geochemical reactivity due to the availability of freshly ground reactive material (subglacially derived), high water to rock ratios and contact times, high permeability and a constant supply of dilute waters (meltwaters and rain/snowmelt) percolating through the deposits. There is, however, not an equivocal agreement about the rates of reaction in proglacial areas. Anderson et al. (2000) concluded from their measurements that silicate weathering is not enhanced in proglacial areas and suggest that silicate weathering reactions may be important only after vegetation cover is established. However, high silicate weathering rates have been measured in proglacial areas in the Alps (Arn, 2002; Hosein et al., 2004) and the Rocky Mountains (Taylor and Blum, 1995). Proglacial weathering intensities depend mainly on the lithology (e.g. highly reactive minerals like carbonates and sulphates vs. crystalline rocks), the development of organic matter (Conen et al., 2007), the rate of supply of fresh rock material to the proglacial zone, the age of exposure and the character of the proglacial hydrological drainage system.

There exist only few measurements of the very early stages of weathering or soil formation (with ages of 0–150 yr). The proglacial areas in the Alps are in most cases defined as the area between the present-day glacier and the distinct moraines deposited in the 1850s. The most evident soil changes in the Alps will occur in proglacial areas where already-existing young soils will continuously develop and new soils will form due to glacier retreat (Egli et al., 2006). The aim of our research was, therefore, to study the weathering mechanisms of silicate, glacial parent material within a time span of 0–150 yr. The rates can be obtained from time sequences when the different glacial states and their ages are precisely known. The study of soil chronosequences is an important tool to derive short- to long-term weathering rates and the consequent formation or transformation of soil minerals (e.g. Egli et al., 2003). Studies of soil chronosequences require that soils can be differentiated on the single variable 'time' if the other factors (climate, parent material, organisms, and topography) affecting soil development are subordinate or relatively constant (Jenny, 1980).

2. Materials and methods

2.1. Study area

The soils studied lie within the proglacial area of the Morteratsch glacier in the Upper Engadine (Switzerland) (Fig. 1). The border of the proglacial area is given by distinct moraines deposited in the 1850s during the 'Little Ice Age' (Fig. 2). The actual length of this proglacial area is approx. 2 km and has an area of 1.8 km^2. The proglacial area is in a valley that runs N–S. The altitude ranges from 1900 m asl to about 2150 m asl (Table 1). Alpine glaciers have fluctuated during the last 10,000 yr near the borders of the moraines formed in the year 1850 indicating more or less similar climatic (±1–1.5 °C) and hydrologic conditions within that period (e.g. Patzelt, 1977; Maisch, 1992; Magny, 1992; Burga and Perret, 1998). The vegetation cover of the Morteratsch proglacial area has been studied by Burga (1999). The first flowering plants invading young deglaciated surfaces are scattered individuals of mostly sterile *Epilobium fleischeri* and *Linaria alpina* that appear after about 7 years. *Epilobietum fleischeri* community has a higher cover-abundance after c. 27 years. First plants of the community *Oxyrietum digynae* appear after c. 12 years and disappear after c. 27 years. The establishment of Larici-Pinetum cembrae forests takes place after about 77 years (Burga, 1999) on sites where the soil has been more intensely developed.

The tectonic units are the Bernina- and Stretta-crystalline, mainly constituted of granitoid rocks (Table 1); consequently, the glacial till has a silica rich character. These units were metamorphosed during the High Alpine orogenic event (Oligocene–Eocene) to the 'greenschists' facies (Trommsdorff and Dietrich, 1999). Due to the metamorphism, Na–Ca-amphiboles have been formed in the granite and granodiorite (Büchi, 1994). Typically, the saussuritization phaenomenon is found: with primary rock-forming plagioclase partially transformed into minerals including epidote, albite, sericite, zoisite, zeolites and calcite. Due to the glacial mixing and transport of these materials, the soil parent material can be considered as relatively homogeneous.

2.2. Soil sampling

Soil samples were collected from 21 soil pits distributed over the whole proglacial area (Fig. 2). 11 of these sites (S1–S10 and A) were selected for a more detailed chemical and mineralogical characterisation. This procedure resulted in the collection of a soil chronosequence of surfaces ranging from 0–150 yr old. Furthermore, 2 additional soil profiles were excavated in vicinity to the proglacial area Morteratsch on known older moraines having an age of 1300 yr (Dystric Cambisol, Egli et al., 2003) and 11,500 yr (Albic Podzol). Soil profiles were excavated down to the C horizon (Table 2). For each horizon, approximately 1–2 kg of material was collected. Soil bulk density was measured with a soil core sampler with a known specific volume or by excavated holes with a volume of about 500–2000 ml that were backfilled with a measurable volume of quartz sand.

2.2.1. Soil chemistry and physics

Total organic C and N contents of the soil and parent material were measured with a C/H/N analyzer (Elementar Vario EL).

The soil organic carbon (SOC) stock was calculated according to the following equation:

$$SOC_{stock} = \sum_{i}^{dz} C_i d_i \rho_i (1-RM) \quad (1)$$

where SOC_{stock} denotes the org. C abundance (kg/m^2), C the organic C concentration (kg/t), d_i the thickness of layer i (m), ρ = soil density (t/m^3) and RM the mass proportion of rock fragments. Soil pH (in 0.01 M $CaCl_2$) was determined on air-dried fine earth samples

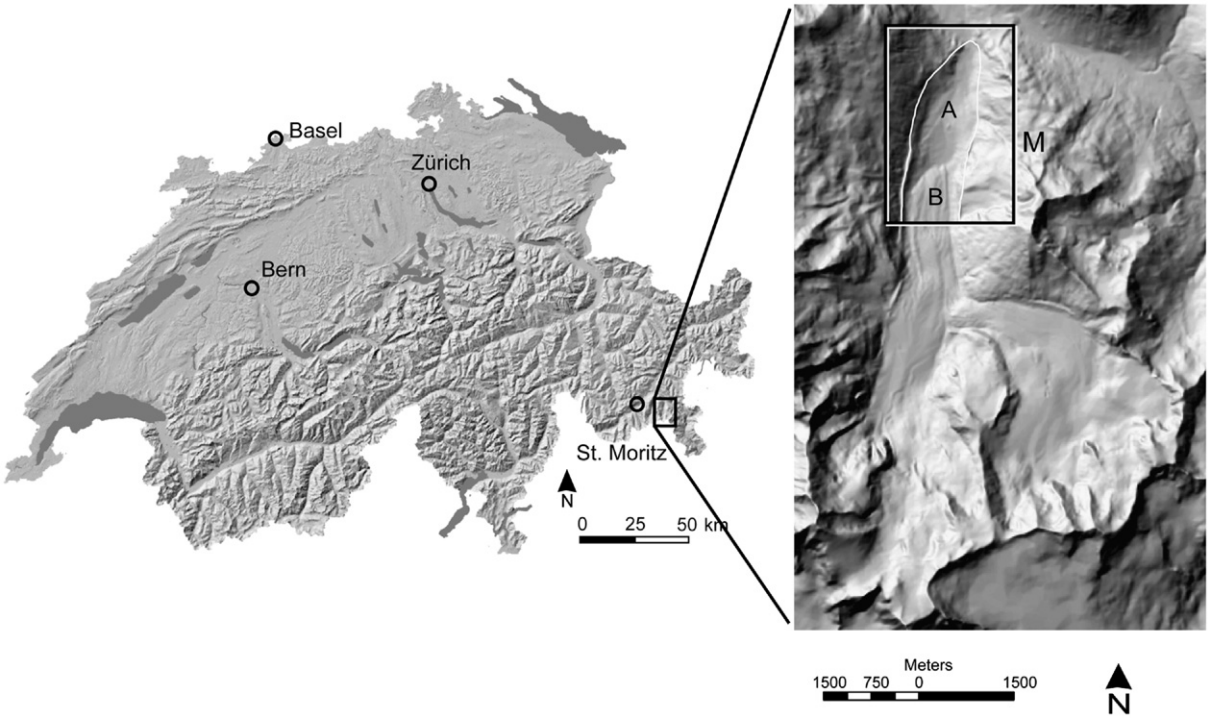

Fig. 1. Location of the Morteratsch proglacial area (Engadine, SE Switzerland). M = investigation area (see Fig. 2), A = proglacial area, B = Morteratsch glacier.

using a soil:solution ratio of 1:2.5. Element pools in the bulk parent material (Ca, Mg, K, Na, Fe, Al, Mn, Si and Ti) were analysed using AAS after total dissolution (using a mixture of HF, HCl, HNO_3, and H_3BO_3).

The particle size distribution was determined on some selected soil samples. After a pre-treatment of the samples with H_2O_2 (3%), particle size distribution of the soils was measured by a combined method consisting of sieving the coarser particles (32–2000 µm) and the measurement of the finer particles (<32 µm) by means of an X-ray-sedimentometer (SediGraph 5100). The weight proportion of soil skeleton was determined by sieving the bulk soil material (2 mm sieve).

2.3. Mineralogy

The mineralogical composition of samples from 7 selected sites (of the monitored sites S1–S10 and having all a different age between 0–150 yr) was determined using X-ray diffraction analysis on randomly oriented specimens of the <2 mm size fraction. X-ray measurements were made using a Bragg–Brentano diffractometer (BRUKER AXS D8, CuKα with theta compensating slits and graphite monochromator) in the range of 4–80°2Θ with a step width of 0.02°2Θ and a counting time of 5 s. For XRD analysis, the bulk material was milled 5 min in ethanol with a McCrone micronising mill. After milling, the obtained powder (<20 µm) was dried at 60 °C and then mixed with zincite as an internal standard for the determination of the amorphous content (Srodon et al., 2001). A special frontloading preparation was carried out to hold the preferred orientation as low as possible in randomly oriented specimens (Kleeberg et al., 2008). The measurement of texture specimens (smear slides) enables better identification of clay minerals based on their basal reflexes and their positions after different treatments. The intercalation of ethylene glycol causes a typical shift of the (00 l) reflexes in the XRD pattern of expandable clay minerals. The qualitative phase composition was determined on the basis of the peak position and the relative intensities of the mineral phases were identified in comparison to the ICDD data base. The analysis was carried out with the software package DIFFRACplus (Bruker AXS). The quantitative mineralogical composition of the inorganic part of the material was determined using Rietveld analysis (program AutoQuan, GE SEIFERT) of XRD patterns of randomly oriented specimens (Bergmann and Kleeberg, 1998; Ufer et al., 2008).

Typical mineral spectra (in the OH stretching region from 4000–2000 cm^{-1} and in the OH-bending and M–O region from 900–400 cm^{-1}) were measured using DRIFT (Diffuse Reflection Infrared Fourier Transform; Bruker, Tensor 27). Spectra were recorded from 4000 to 250 cm^{-1}. The individual spectra were first normalised (min–max method; using the software OPUS 6) and then compared to each other.

2.4. Water sampling

Three different types of water were considered: spring or tributary water (SW), precipitation (RW) and glacial stream water (GWa–z) (Fig. 2).

Water was collected during the summer period of 2008 (June–September), 1–2 times per month. All sampling bottles were acid washed (HNO_3 1 M) and rinsed with double distilled water to prevent contamination. The precipitation water collectors were placed in installed PVC tubes in the field to protect them from sunshine.

In addition, two streams outside the proglacial area (TW) were sampled to compare waters from young and older surfaces. The surface outside the proglacial area has a much older age (10,000–15 000 yr; Fitze, 1982) than the proglacial area (maximum age = 150 yr) (Fig. 2).

All water samples were filtered with 0.45 µm pre-cleaned millipore filters to eliminate suspended particles and stored in the dark at 4 °C.

2.5. Water chemistry

Electric conductivity, pH, HCO_3^- and temperature were measured directly in the field. Water-pH was measured using a field pH-meter Metrohm E 604, conductivity with a microprocessor conductivity meter (LF320) with the standard conductivity cell (TetraCon 325) and HCO_3^- was determined by titration (using HCl).

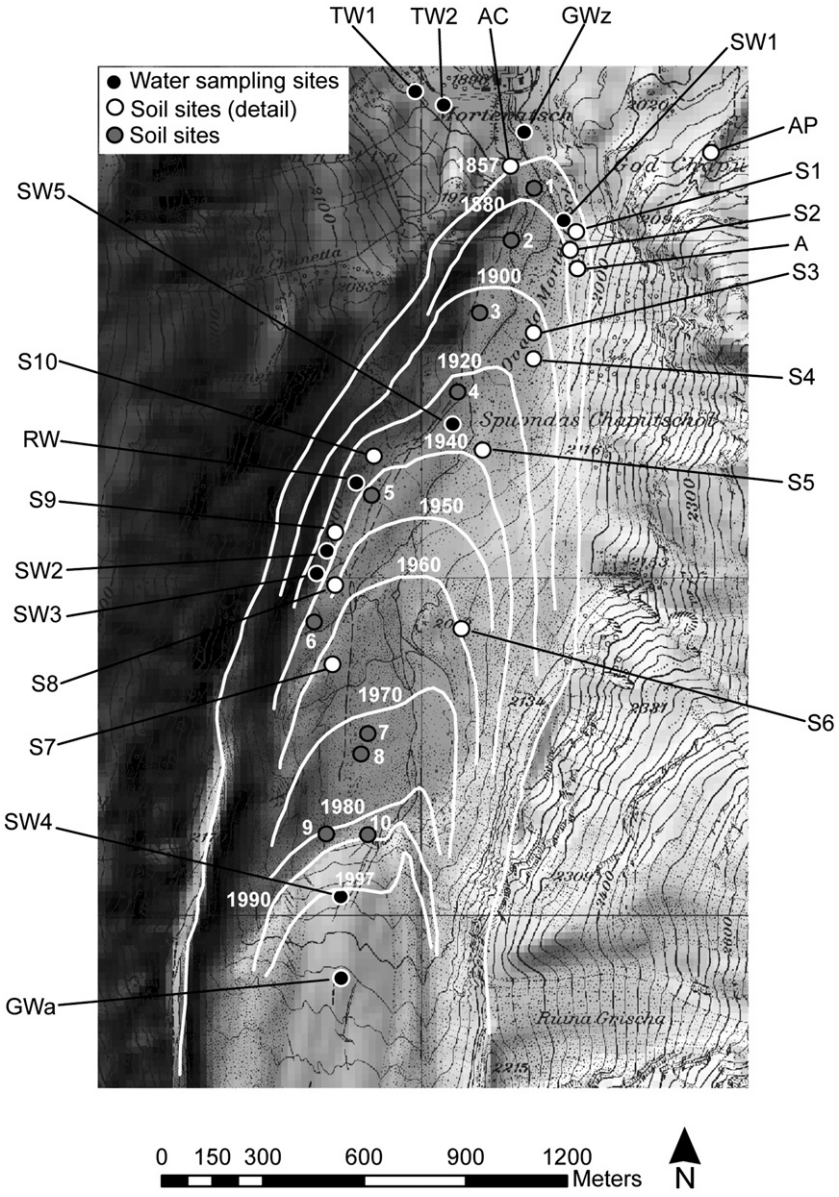

Fig. 2. Sampling sites within and outside the proglacial area of Morteratsch. with SW = spring waters, TW = brooks, GWa–z = glacial stream, RW = rainwater, S = monitored soil sites (where A = Humic Leptosol, 140 yr), AC = Acid Cambisol (1300 yr; border or the proglacial area), AP = Albic Podzol (11,500 yr; outside the proglacial area). The sites S1–S10, A, AC and AP were investigated more in detail (soil chemistry and mineralogy). The retreat phases of the glacier (isochrones) are according to Burga (1999).

Ca, Mg, K, Na and Sr were analysed with AAS (Perkin Elmer Atomic Absorption Spectrometer) using graphite furnace for the Sr measurements. The anions Cl^-, NO_3^- and SO_4^{2-} were analysed with an ion chromatograph Metrohm 733 IC Separation Centre.

In addition, some samples were analysed for Al, Ba, Fe, P, Si, Sr using inductively coupled plasma optical emission spectrometry (ICP-OES; PE 3300DV). Strontium isotope ratios were determined on aliquots of Sr separated from each sample using cation exchange chromatography with a thermal ionization mass spectrometer (TIMS, MAT-262,). A detailed description of methods of chemical separation and isotope ratio measurement of Sr can be found in Dasch et al. (2006). Briefly, between 100 and 200 isotope ratios were measured for each sample, yielding a mean $^{87}Sr/^{86}Sr$ ratio with an analytical uncertainty of less than ± 0.000020 ($\pm 2\sigma$). Repeated measurements of NBS-987 during the period of analysis resulted in a mean $^{87}Sr/^{86}Sr$ value of 0.710237 ± 0.000025 ($\pm 2\sigma$).

Table 1
General features of the Morteratsch proglacial area.

Latitude	46°26′N
Longitude	9°56′E
Elevation at glacier front	2117 m asl
Elevation at proglacial area front	1900 m asl
Main orientation	North
Geology	Granite and granodiorite
Mean annual temperature	0.5 °C
Mean annual precipitation	1100–1300 mm
Mean slope	<10°

3. Results

3.1. Physical and chemical soil properties

Soils were only weakly developed and soil types within the proglacial were predominantly Leptosols (Table 2). The soils had a high proportion of soil skeleton that could be up to 70% of the mass. These are typical values for Alpine soils on debris or morainic substratum (Egli et al., 2001).

Table 2
Physical and chemical properties of the monitored soil sites.

Site/soil (FAO, 1998)	Soil age (yr)	Horizons	Depth (cm)	Bulk density (g/cm^3)	Skeleton (wt.%)	Sand (g/kg)	Silt (g/kg)	Clay (g/kg)	pH ($CaCl_2$)	Org. C (g/kg)	Org. N (g/kg)
S1/Humi-Skeletic	138	O	0–6	0.2	41	n.m.*	n.m.	n.m.	4.60	321.10	12.22
Leptosol		A	6–9	1.6	50	777	184	39	4.80	6.18	0.32
		BC	9–14	1.6	53	830	158	12	4.70	3.69	0.22
		C	14–30	1.8	40	757	222	21	4.60	2.80	0.12
S2/Humi-Skeletic	128	A	0–10	1.4	64	754	204	42	4.85	13.76	0.76
Leptosol		AC	10–40	1.5	68	695	272	33	4.90	4.79	0.26
S3/Humi-Skeletic	108	A	0–3	1.1	54	667	265	68	5.10	28.10	1.58
Leptosol		AC	3–15	1.7	70	677	281	42	4.50	3.89	0.23
S4/Humi-Skeletic	98	A	0–1	0.8	55	n.m.	n.m.	n.m.	5.30	56.01	3.10
Leptosol		AC	1–5	1.7	51	939	61	15	5.20	4.24	0.25
		C	5–30	1.6	70	931	57	12	5.20	1.76	0.08
S5/Humi-Skeletic	68	A1	0–1	0.8	7	n.m.	n.m.	n.m.	4.85	40.25	1.34
Leptosol		A2	1–4	1.5	1	530	432	38	4.55	5.01	0.22
		C1	4–9	1.4	36	573	387	40	4.65	2.53	0.15
		C2	9–20	1.8	64	570	372	58	4.60	3.65	0.21
S6/Skeletic	48	A	0–2.5	1.6	64	n.m.	n.m.	n.m.	4.80	37.47	1.69
Leptosol		C	2.5–25	1.7	68	852	129	19	5.00	2.10	0.13
S7/Skeletic	48	A	0–4	1.4	26	n.m.	n.m.	n.m.	6.10	60.24	5.20
Leptosol		C1	4–11	1.6	37	823	146	31	5.20	2.82	0.22
		C2	11–34	2.0	67	747	211	42	5.10	3.65	0.28
S8/Skeletic	58	OA	0–12	1.0	63	n.m.	n.m.	n.m.	4.60	118.20	6.32
Leptosol		C	12–33	1.8	48	712	220	68	4.40	3.12	0.22
S9/Humi-Skeletic	73	O	0–3	0.5	44	n.m.	n.m.	n.m.	5.15	147.80	8.96
Leptosol		AC	3–10	1.5	65	785	175	40	4.40	4.81	0.30
		C	10–36	1.7	58	832	133	35	4.65	3.27	0.22
S10/Humi-Skeletic	78	A1	0–2	0.6	49	n.m.	n.m.	n.m.	4.70	53.40	2.73
Leptosol		A2	2–10	1.7	68	818	143	39	4.50	5.15	0.23
		AC	10–25	1.7	84	733	219	48	4.80	4.33	0.21
A/Humi-Skeletic Leptosol	140	A	0–7	1.4	65	770	190	40	5.20	34.30	2.50
		(B)A	7–25	1.9	59	780	190	30	5.10	3.70	0.30
		C	>25	1.9	64	780	190	30	5.40	2.50	0.20
1/Skeletic Fluvisol	140	(C)A1	0–2	1.0	11	550	360	90	4.80	16.40	0.60
		(C)A1	2–8	1.0	11	550	360	90	4.80	16.40	0.60
		2C	8–14	1.3	19	490	420	90	4.90	8.40	n.d.*
		3C	14–23		70	n.m.	n.m.	n.m.	4.90	8.40	n.d.
2/Humi-Skeletic Leptosol	120	A	0–3	1.5	40	754	204	42	5.50	176.10	7.60
		C	3–13	1.5	65	695	272	33	4.90	16.70	1.40
3/Skeletic Leptosol	100	A	0–2	1.5	40	667	265	68	n.m.	6.90	0.40
		C	2–26	1.5	70	677	281	42	5.00	1.70	n.d.
4/Skeletic Leptosol	80	A	0–2	1.1	15	n.m.	n.m.	n.m.	n.m.	5.20	0.37
		AC	2–6	1.5	70	850	120	30	4.50	5.20	0.37
		(B)C	6–8	1.5	75	850	120	30	4.50	5.20	0.37
		C	8–14	1.4	75	840	140	20	4.80	1.70	n.d.
5/Skeletic Leptosol	70	A	0–3		40	818	143	39	n.m.	n.m.	n.m.
		C	3–22	1.3	68	730	220	50	4.50	4.40	n.d.
6/Skeletic Leptosol	60	CA	0–12	1.5	55	850	130	20	5.10	6.00	0.46
7/Skeletic Leptosol	30	AC	0–6	1.5	53	920	60	20	5.20	1.90	0.14
		C	6–25	1.4	70	830	140	30	5.40	0.70	n.d.
8/Skeletic Leptosol	30	(A)C	0–15	1.6	66	820	170	10	5.70	2.00	0.14
9/Skeletic Leptosol	20	(A)C	0–18	1.8	77	n.m.	n.m.	n.m.	5.70	2.00	0.14
10/Lithic Leptosol	10	C	0–9	1.7	75	750	220	30	5.80	0.90	0.07

*n.m. = not measured, n.d. = not detectable.

Most soils were texturally a loamy sand or a sand and some were a sandy loam (Table 2).

In Table 3, the mean composition of the Morteratsch parent material is shown. In addition to the very young soils, an older site close to the proglacial area and one outside the proglacial area were sampled (Table 4). The site (c. 1300 yr old; Egli et al., 2003) close to the border of the proglacial area had a Dystric Cambisol and the other one (having an age of approximately 11,500 yr) an Albic Podzol. The Dystric Cambisol and Albic Podzol were characterised by very acid and strongly leached conditions (eluviation and illuviation of Fe and Al; Table 4). The soils in the proglacial varied in the pH range of 4.5–6 and are, thus, much less acidified than the old soils.

Although the weathering stage of the proglacial sites seemed to be low, a distinct time-trend of soil skeleton concentration, sand content (less significant) in the topsoil and abundance of soil organic carbon (SOC; whole profile) and nitrogen could be observed (Fig. 3). The soil skeleton and sand content steadily decreased with increasing age of

Table 3
Mineralogical composition of the fine earth fraction (<2 mm) of the parent material ($t=0$) and the most developed soil horizon (A horizon of a Humi-Skeletic Leptosol (Ranker), $t=138$ yr) within the proglacial area.

Minerals	Parent material ($t=0$) wt.%	A horizon ($t=138$ yr) wt.%
Quartz	29.1 (±0.8)	30.1 (±0.8)
Albite	27.0 (±1.3)	27.8 (±1.3)
Microcline	11.8 (±0.8)	12.0 (±1.0)
Muscovite	9.4 (±0.7)	10.5 (±0.8)
Epidote	8.0 (±0.7)	6.2 (±0.7)
Hornblende	5.5 (±0.6)	3.9 (±0.5)
Chlorite	1.8 (±0.7)	1.7 (±0.6)
Illite	1.4 (±0.6)	1.9 (±0.6)
Biotite	1.0 (±0.4)	0.7 (±0.5)
Calcite	0.2 (±0.3)	0.6 (±0.3)

Table 4
Geochemical characteristics (total analysis of the bulk material including soil skeleton (up to a diameter of 20 cm) and fine earth (<2 mm)) of three soils in the investigation area with a different age (see also Fig. 2).

Soil and age	Depth (cm)	Organic matter* (%)	pH ($CaCl_2$)	Al_2O_3 (%)	SiO_2 (%)	TiO_2 (%)	CaO (%)	MgO (%)	K_2O (%)	Na_2O (%)	Fe_2O_3 (%)	MnO_2 (%)
Albic Podzol (11,500 yr)												
(AP)	0–5	26.49	3.3	7.67	47.99	0.41	0.29	0.30	2.96	1.53	1.19	0.015
	5–10	2.00	3.3	10.91	74.22	0.47	0.10	0.32	4.43	2.60	1.58	0.012
	15–25	0.70	4.4	13.01	73.37	0.46	0.24	0.35	4.65	2.87	2.05	0.027
	40–60	0.13	4.7	12.60	74.80	0.46	0.32	0.40	4.43	2.86	1.93	0.035
	70–80	0.00	4.9	12.03	75.16	0.44	0.15	0.30	4.61	2.95	1.57	0.029
	110–120	0.00	4.9	13.29	74.66	0.43	0.42	0.45	4.60	2.99	1.88	0.033
Dystric Cambisol (1300 yr)												
(AC)	0–10	9.94	3.6	11.27	68.90	0.50	0.11	0.20	4.42	1.28	2.02	0.012
	15–20	2.04	3.7	10.07	77.51	0.41	0.04	0.14	4.74	1.55	1.97	0.011
	35–40	1.19	3.9	12.66	74.75	0.37	0.05	0.12	5.28	2.09	2.83	0.011
Humic Leptosol (138 yr)												
(A)	0–7	2.13	5.2	13.98	68.03	1.09	1.63	1.26	3.61	3.16	3.70	0.067
	10–25	0.26	5.1	14.15	69.28	1.14	1.96	1.20	3.37	3.35	3.72	0.065
	25–30	0.16	5.4	13.97	69.95	1.13	1.81	1.31	3.57	3.20	3.99	0.080

*Organic matter = org. C × 1.72.

surface exposure. Physical weathering was, therefore, a significant process in the proglacial area. The clay content also increased, although less significantly ($p = 0.11$). The rather high scatter of the data with time shows that not only time is the factor controlling the amount of clays in the soils. The micro-topography (concavity) and the composition of the glacial till (glacier sediment transport) exerted also their influence. Furthermore, a net increase within 150 yr could be identified for the abundance of SOC and nitrogen. A period of only 100–150 yr of soil evolution led to an accumulation of about 1–5.5 kg SOC/m^2 (stored in the fine earth fraction). It is noteworthy that the relationship is not linear. The logarithmic function tends to an asymptotic value.

The time dependent sequence of the pH ($CaCl_2$) could be best described by a potential function. The relationship between time and pH was highly significant (Fig. 3). As soon as the parent material had been exposed to weathering, a rapid acidification started which led to a pH reduction from an initial value of about 5.5 or 6.0 to about 4.5.

3.2. Mineralogy

In general, the parent material (<2 mm fraction) as well as the soils are dominated by quartz, mica (biotite and muscovite), Na-plagioclase, K-feldspar, hornblende and epidote (Table 3). Minor phases were illite and chlorite and traces of calcite. The measured mineral contents are typical for a dioritic–granitic parent material.

The quantitative phase analysis was done for the monitoring sites. In Fig. 4, time dependent trends for biotite, epidote and illite are shown. For biotite and epidote a small, but significant, decrease could be detected while the illite content slightly increases within the time span of 150 yr.

Calcite as an important possible source of Ca was detected in very low amounts (<1%; near or below detection limit using XRD) and no significant time-trend could be measured. Fig. 5 shows the DRIFT spectra of the parent material and the most weathered soil horizon in the proglacial area. The peaks at 845, 2630 and 2868 cm^{-1} could be attributed to traces of calcite in the parent material and in the topsoil. The peaks at 727 and 2522 cm^{-1} could indicate some traces of dolomite. Various regions in the IR spectrum contain OH vibrational information. In the OH-bending region, the bands associated with hydroxyl groups can be discriminated from each other, and band assignment is straightforward. Furthermore, this region is not affected by the presence of residual water molecules (Vantelon et al., 2001). The signals in the region 600–850 cm^{-1} were, however, generally weak and differences should consequently not be over-interpreted. Quartz was recognised by the peaks near 780 and 800 cm^{-1}. The band near 790 cm^{-1} could be attributed to δFeMgOH (Farmer, 1974; Goodman et al., 1976). The band at 750 cm^{-1} corresponds to mica and chlorite and seems to decrease slightly with time.

3.3. Water chemistry

The dominant cation in the spring and stream waters (more than 50% of the positively charged equivalents) was Ca^{2+} (typical values were in the range of 1–6 $mmol_c/dm^3$). Na^+ was present in concentrations of 0.2–2.2 $mmol_c/dm^3$. The other cations (Mg^{2+}, K^+, Sr^{2+}) were measured in lower concentrations. HCO_3^- and SO_4^{2-} dominated the anions. Cl^- and NO_3^- were present in concentrations <0.1 $mmol_c/dm^3$. The mean concentrations of Ca, Na or Mg in the rainwater were however 10 to 20 times lower than in the spring or stream waters. The spring and stream waters had an average Ca concentration of about 10^{-4} mol/dm^3 while rainwater had only $7 \cdot 10^{-6}$ mol/dm^3.

The $^{87}Sr/^{86}Sr$ ratio of the measured water samples are reported in Fig. 6. The $^{87}Sr/^{86}Sr$ ratios for the rivers and spring waters inside the proglacial area were in the range of 0.74–0.76 and consequently slightly higher than outside the proglacial area (range 0.73–0.74). The ratios for rainwater were near 0.71 which is close to values reported in literature (Blum et al, 2002; Oliva et al., 2004; Keller et al., 2007). Rainwater and melting of ice seem to influence the stream water chemistry. The $^{87}Sr/^{86}Sr$ ratio of the rainwater (near 0.71) is quite similar to the glacial stream at the glacier front (near 0.72). The $^{87}Sr/^{86}Sr$ ratio increases with increasing distance from the glacier front (up to about 0.753 at the end of the proglacial area). The spring waters within the proglacial area better reflect weathering processes because they are less influenced by melting ice. The spring waters usually had an $^{87}Sr/^{86}Sr$ ratio between 0.740 and 0.755 which was distinctly higher than the one measured for the stream water at the end of the proglacial area. The $^{87}Sr/^{86}Sr$ ratios inside and outside the proglacial area exhibit rather high values which are characteristic of biotite and potassium-feldspar (Blum and Erel, 1997; White et al., 2005). The Ca/Sr ratios were in the range of 400–600 (Fig. 6) and near the glacier front slightly higher (about 800). The Ca/Sr ratios were roughly near the Ca-silicate phase range. A ratio of 400–600 is, however, high for pure Ca-silicates which suggests a strong contribution from calcite and/or apatite and consequently a preferential weathering. This is supported by data from Büchi (1994) who measured a mean Ca/Sr-ratio of around 300 (±60) in the rocks of the region (granite, garnodiorite).

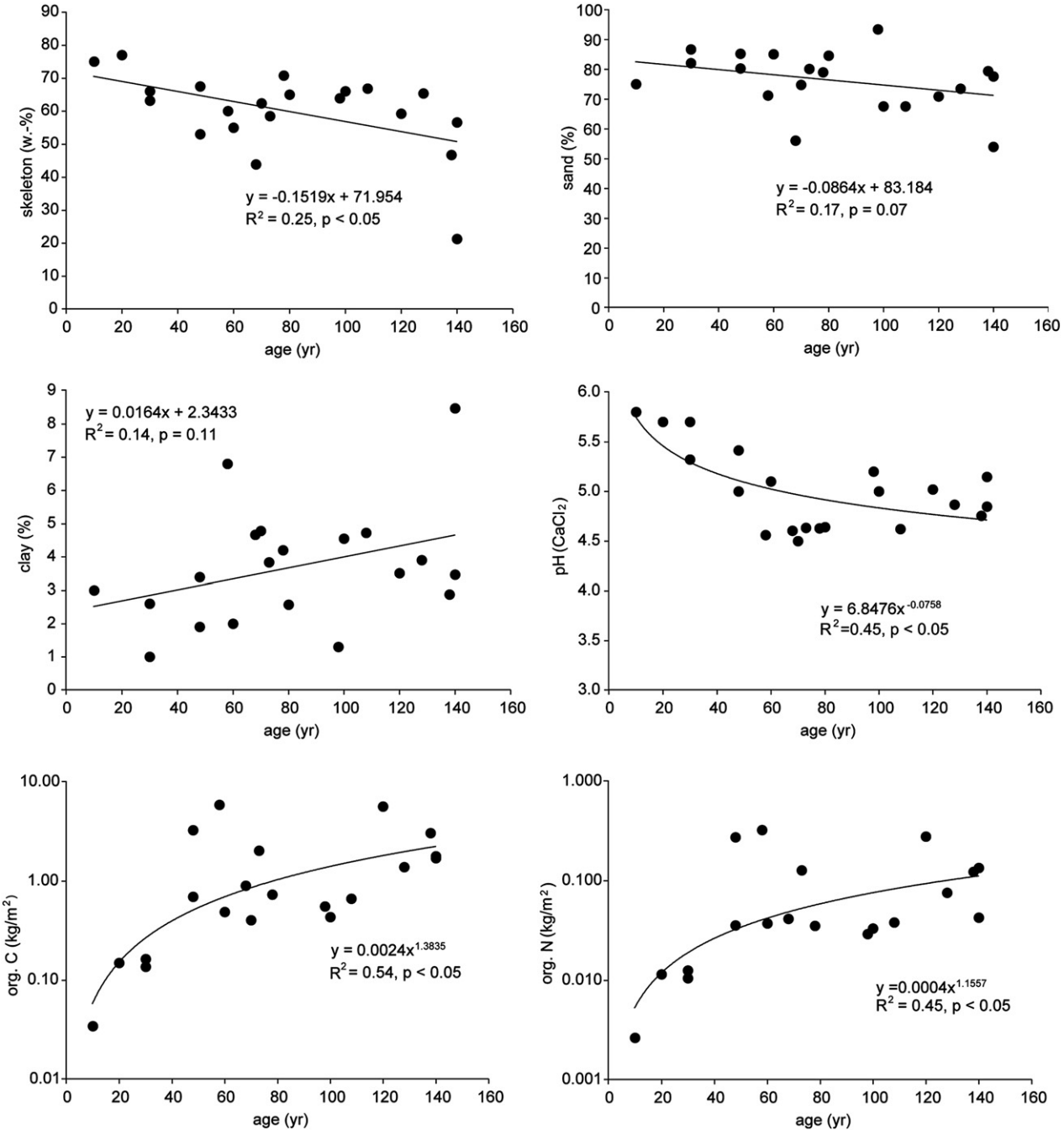

Fig. 3. Soil physical and chemical properties within the proglacial area as a function of time. Soil skeleton (fraction>2 mm), sand and clay content and pH refer to the topsoil (uppermost 15 cm). Organic C and N are given as stocks (kg/m^2).

Molar Ca/Na ratios of the water samples were very high for the samples close to the glacier tongue (Fig. 7). These ratio seems to decrease with increasing distance to the glacier and approaches relatively quickly the value of the parent material (Ca/Na = 0.62; Fig. 7). A Ca/Na ratio of 0.62 is typical for granitic material and agrees well with the values measured for rocks in the surrounding area (around 0.5 for granites and granodiorites; Büchi, 1994).

4. Discussion

4.1. Physical and chemical soil properties

A distinct decrease of the soil skeleton and, less significantly, of the sand fraction was measured within the short period of only 150 yr, indicating that physical weathering (freeze–thaw weathering) proceeds rather quickly. Due to the increasing vegetation cover with age of surface exposure and higher plant productivity, more organic carbon is transferred into the soils as they develop (Fig. 3). Already after 150 yr of soil formation, the soil organic matter stocks reached around 1–5.5 kg/m^2, which is a quite considerable amount. The calculation of the SOC stocks is bound to some uncertainties (see Perruchoud et al., 2000; Goidts et al., 2009 for a detailed discussion). In our case, the SOC stocks (on a site-specific and consequently local level) might be underestimated due to the neglect of SOC in the soil skeleton fraction. Organic C concentrations in the soil skeleton fraction were, however, available for the sites S1–S10. The concentration of organic C in the soil skeleton fraction is low (data not shown). Although the soil skeleton fraction makes up to about 80% of

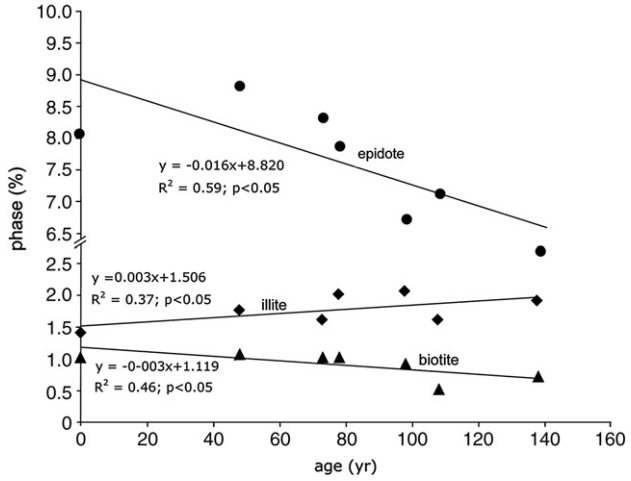

Fig. 4. Mineral phases in the fine earth as a function of time.

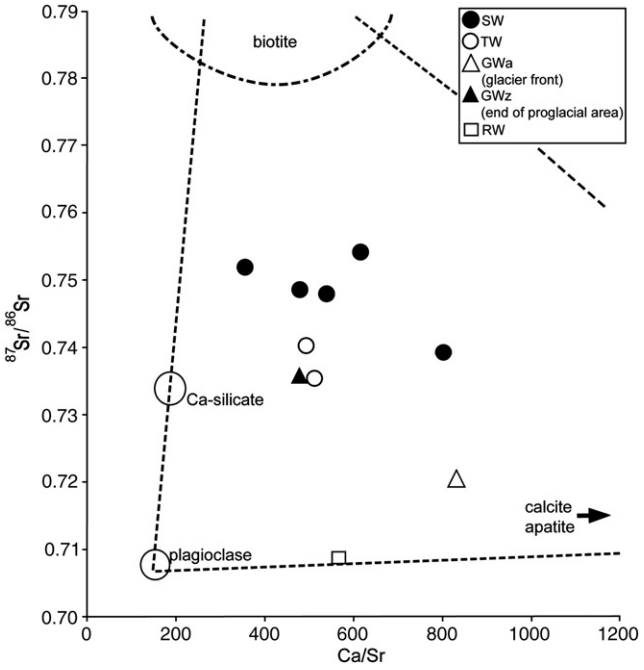

Fig. 6. Ca/Sr vs. $^{87}Sr/^{86}Sr$ molar ratios of waters sampled in different catchments. Typical ranges for biotite (Oliva et al., 2004; White et al., 2005), Ca-silicate (Blum et al., 2002), plagioclase (White et al., 2005), calcite (White et al., 2005), apatite (Blum et al., 2002; Nezat et al., 2007) and precipitation (Keller et al., 2007) are also given.

the mass, only very little C is stored in this fraction. The relative error due to the omission of SOC in the soil skeleton fraction could be estimated to 13.7%. The increase in organic matter stocks correlates with the vegetation type and cover. In Alpine environments, soils developed on silicate parent material have up to more than 40 kg organic C/m^2; with frequent values between 15 and 25 kg C/m^2 (Hitz, 2002; Egli et al., 2008). Mean annual rates of organic C accumulation during 150 yr of soil development are consequently in the range of 7–36 g C/m^2/yr. These values were even higher than rates reported from other Holocene soil chronosequences. Egli et al. (2001) reported accumulation rates of 6.7–9 g C/m^2/yr for a 400 yr sequence and 2–4 g C/m^2/yr for Podzols which had an age of about 11,000 yr in the Swiss Alps. Lichter (1998) reported accumulation rates of 9 g C/m^2/yr for a chronosequence developed on coastal dunes in Michigan, USA. Usually, organic matter accumulation in soils showed a non-linear trend tending to an asymptotic value.

It is known that pH may have a very strong spatial variability (e.g. Papritz and Flühler, 1991). Despite some spatial variability of the pH, a distinct decrease with time was observed. A sharp decrease of the pH at the beginning of soil formation is typical (see also Sauer et al., 2009). This sharp decrease is due to the low buffering capacity of young silicate with low ion exchange capacity.

4.2. Weathering processes indicated by mineral and water analysis

Also in granitic catchments, carbonate leaching is often seen as the major source of Ca (e.g. White et al., 1999a,b; Hosein et al., 2004). Carbonate dissolution is viewed as primarily being controlled by a combination of the influences of water supply and its consequent percolation within the soil, CO_2 production, temperature and surface properties of the carbonates (Stumm and Morgan, 1996). For interactions among calcite, dolomite and the soil solution, the saturation state

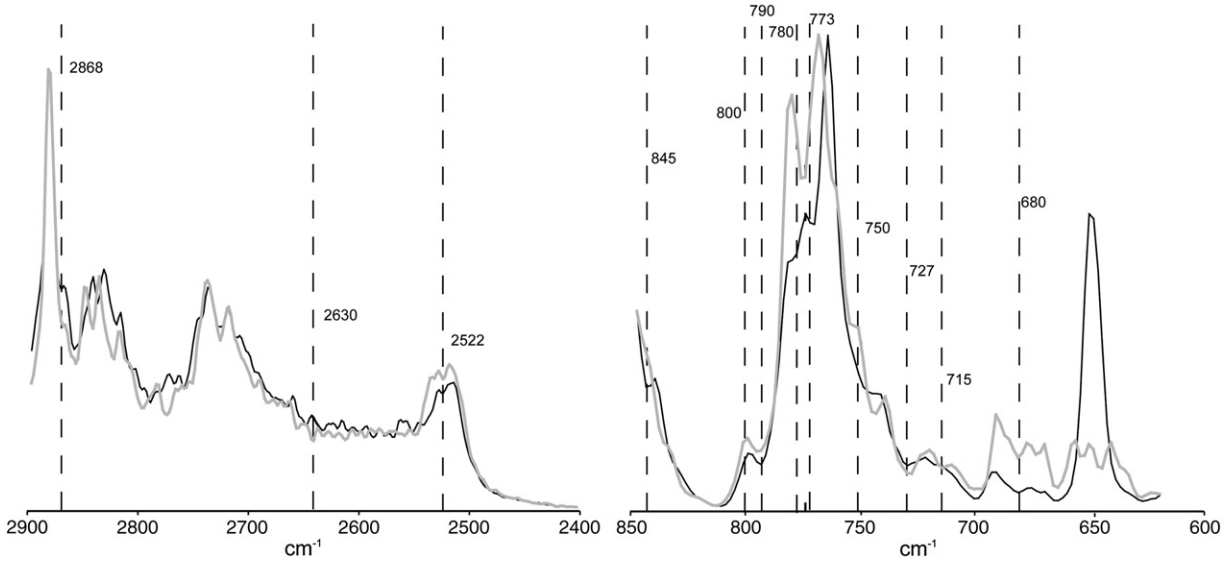

Fig. 5. Comparison of DRIFT spectra in the OH-bending and M–O region (2900 to 2400 cm^{-1} and 850 to 600 cm^{-1}). The parent material ($t=0$) is given by the black line and oldest topsoil ($t=138$ yr) by the grey line.

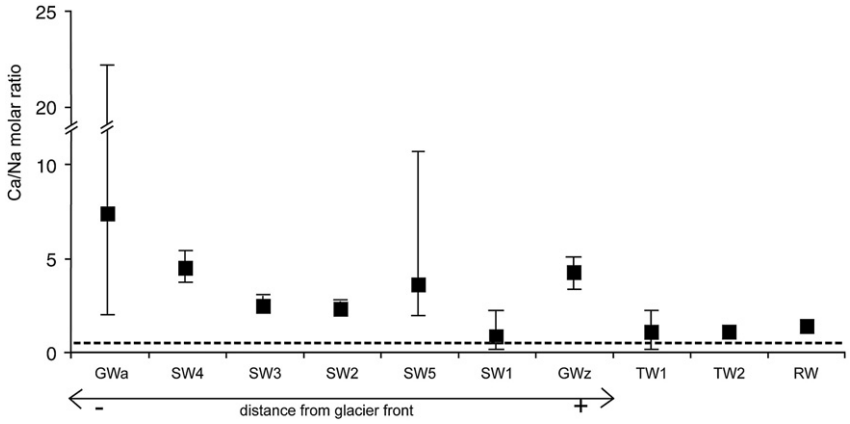

Fig. 7. Ca/Na molar ratio vs. age for water catchments inside (GW = glacial water (a = glacier front; z = end of proglacial area), SW = spring water) and outside (TW = brooks) the proglacial area. Mean, minimum and maximum values are given. Also precipitations (RW = rainwater) were considered, for comparison. The horizontal dashed line corresponds to Ca/Na = 0.62 (typical value for a granitic composition), calculated from the mean composition of the parent material.

of the solution ($\log SI_{\text{calcite, dolomite}}$) is determined using the following equation for calculating the degree of saturation:

$$\log SI_{\text{calcite,dolomite}} = \log \frac{Q_p}{K^T_{\text{calcite,dolomite}}} \quad (2)$$

where Q_p is the ion activity product of the solution and K is the thermodynamic solubility-product constant of the mineral phase of interest at the temperature T. A logSI value>0 suggests oversaturation and logSI<0 suggests undersaturation. The equilibrium constants were corrected for temperature. If $\Delta H_r°$ is not a function of the temperature, which normally is presumed in the temperature range of 0 °C to 35 °C, then a first approximation for the temperature dependency of the reaction constant follows the equation

$$\ln K_x(T) = \ln K_x(T°) + \frac{\Delta H_r^°}{R}\left[\frac{1}{T^°} - \frac{1}{T}\right] \quad (3)$$

where $T°$ is the standard temperature (298.15 K), T is the measured temperature of the water, $\Delta H_r°$ is the reaction enthalpy, and R is the universal gas constant.

The investigated waters (springs, glacial stream, and rivers outside the proglacial area) are strongly undersaturated with respect to calcite and dolomite (Table 5, Fig. 8). Usually, an equilibrium with carbonates is quickly established in waters and soils (Stumm and Morgan, 1996; Egli et al., 2008). Thus, the behaviour of Ca^{2+} and Mg^{2+} cannot be explained by only these two mineral phases. Carbonate phases contribute to the Ca and Mg solubility (see also Fig. 8), but are not the controlling solubility phases. These calculations suggest that the solubility of Ca and Mg is kinetically controlled by Ca- and Mg-bearing phases (silicates, phosphates and carbonates). The dissolution of apatite may represent a significant source of Ca (Blum et al., 2002). In addition, apatite is the main source for phosphorus, but following dissolution P is generally retained in Fe oxyhydroxides and organic matter. In the presence of biotite, the Fe in biotite may also lock up all of the P immediately (Nezat et al., 2007). Föllmi et al. (2009a) showed that with time organic- and iron-bound P almost completely replace detrital P. Apatite should easily be dissolved in surface waters due to its high dissolution rate compared to silicate minerals. The solubility of P was, however, low and concentrations in the range of 0.01–0.2 mg/l were measured. XRD and DRIFT measurements did not reveal the presence of apatite.

Many waters draining granitoid bedrock show Ca/Na ratios near 0.9. Gaillardet et al. (1999) assigned the Ca/Na ratio of <1 to silicate "end-members" (i.e. plagioclase) while values greater than 1 indicate the dissolution of disseminated calcite within granite (Oliva et al., 2004). This shows consequently that on the one hand the parent material does not weather congruently and on the other hand carbonates and also phosphates probably contribute to the weathering fluxes. The decreasing tendency of the Ca/Na ratio indicated that the release of Na became more significant with time and, consequently, also the contribution of plagioclase (or in general — silicate) weathering. The ternary plot (Fig. 9) indicates that the contribution of plagioclase and alkali-feldspar increased with increasing age.

Saussuritization leads to minerals that may act as a dominant source of Ca, both in soils and waters (White et al., 1999b; Hosein

Table 5
Characteristic reactions with respect to the carbonate system.

Reaction	log$K$[a] (25°C)	$\Delta H_r°$ (kJ/mol)
$CaCO_3 + 2H^+ = CO_2(g) + H_2O + Ca^{2+}$	9.80	−14.76
$0.5CaMg(CO_3)_2 + 2H^+ = 0.5Ca^{2+} + 0.5\ Mg^{2+} + H_2O + CO_2(g)$	9.62	−21.90
$CO_2(g) + H_2O = H_2CO_3$	−1.47	−20.77
$H_2CO_3 = H^+ + HCO_3^-$	−6.35	7.6

[a] Stumm and Morgan (1996).

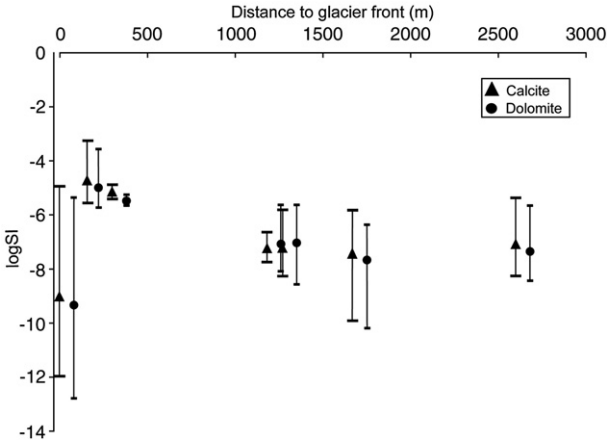

Fig. 8. Saturation state of the solution (logSI) with respect to calcite and dolomite and as a function of distance from the glacier front.

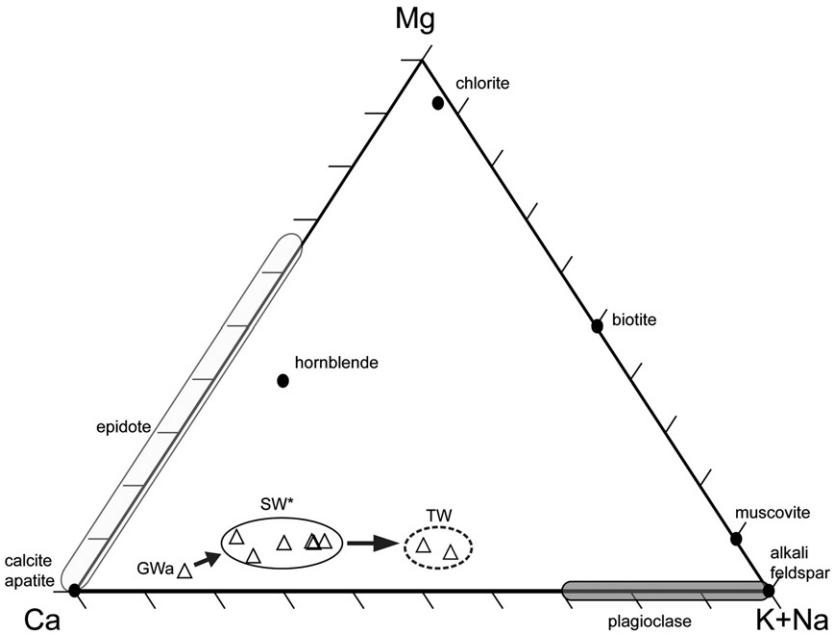

Fig. 9. Chemical composition of the sampled waters plotted in a ternary diagram (molar ratios). GWa is the glacial water at the glacier front ($t=0$); the SW* domain includes water samples within the proglacial area (surface age <150 yr) and meteoric water; TW are brooks outside the proglacial area (surface age around 11,000 years). The mineralogical compositions are from Nezat et al. (2007), except for epidote (Armbruster et al., 2006).

et al., 2004). Secondary calcite veins are not unusual in granitic rocks of the Morteratsch proglacial area. They most probably replace calcic cores in primary plagioclases (see White et al., 1999b). The dissolution reaction for calcite is:

$$CaCO_3 + CO_2 + H_2O = Ca^{2+} + 2HCO_3^- \quad (4)$$

and for plagioclase:

$$Ca_xNa_{(1-x)}Al_{(1+x)}Si_{(3-x)}O_8 + (1+x)CO_2 + (2+2x)H_2O = xCa^{2+} + (1-x)Na^+ + (3-x)SiO_2 + (1+x)HCO_3^- + (1+x)Al(OH)_3 \quad (5)$$

where x is the Ca-rich component (White et al., 1999b). According to Gaillardet et al. (1999), elemental depletion can be better interpreted by considering both the Ca/Na and the Mg/Na ratio (Fig. 10).

The total contents of major ions in soils within, at the border and outside of the proglacial are given in Table 4. The ages of the soils vary considerably (from 150 to 11,500 yr). The Ca/Na ratio decreased with the age of the soils with values of about 0.3 for young soils and 0.01–0.1 for old soils. The molar Mg/Na ratios in old soils were between 0.07 and 0.15 and in the young soil near 0.26. Similarly, the Ca/Na and Mg/Na ratio of the spring waters, rivers and glacial stream decreased with surface age. The ratios were, however, generally higher than in the soils (Fig. 10). These observations are in agreement with the findings of Gaillardet et al. (1999). Calcium was preferentially mobilised with respect to Na. This finally lead to higher ratios in the spring waters, rivers and the glacial stream (with Ca/Na>1) than in the soil bulk soil material where this ratio was much lower than 1 (see also Oliva et al. 2004) and the material was depleted in Ca.

Besides the Ca/Na or the Mg/Na ratios, Sr isotopes are a useful tracer of water–rock interactions (Arn et al., 2003; Négrel, 2006). The primary sources of Sr in groundwater are from atmospheric contributions (precipitation and "red dust"), Sr-bearing minerals (i.e. carbonates and silicates) and from anthropogenic input. Due to

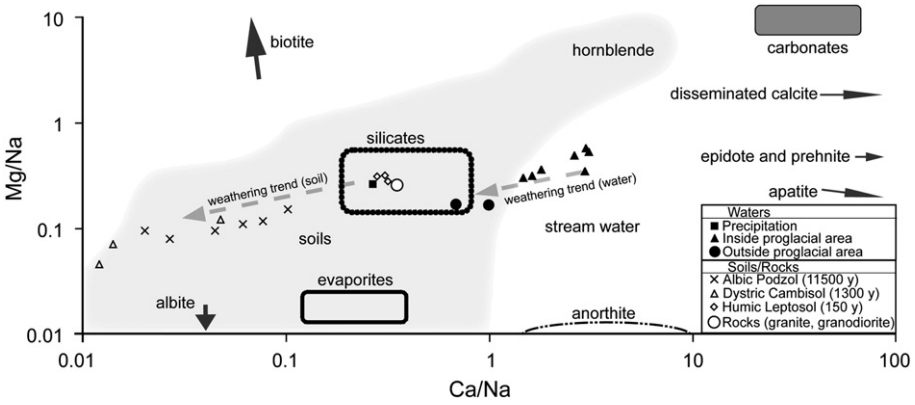

Fig. 10. Ca/Na vs. Mg/Na molar ratios for waters, soils and rocks (mean value of granite and granodiorite of the investigation area and surroundings; taken from Büchi, 1994), related to various literature data connected to chemical weathering in granitic environment. Soil and stream water domains are plotted after Oliva et al. (2004). Evaporite, siliceous and carbonate rock types domains are taken from Gaillardet et al. (1999). The bright-grey area represents the granitic rock domain (Oliva et al., 2004, and references therein). Biotite, epidote, zoisite, apatite and plagioclase are taken from Oliva et al. (2004). Hornblende data is from April et al. (1986) and disseminated calcite data is from White et al. (1999b).

the location of the catchments in a high Alpine environment, the latter was considered to be negligible.

The $^{87}Sr/^{86}Sr$ ratios for the waters are reported in Fig. 6. In and outside the proglacial area, the waters have very high $^{87}Sr/^{86}Sr$ ratios, which is typical of the weathering of biotite from granitoid rocks (White et al., 2005; Négrel, 2006). Taylor et al. (2000) showed that biotite dissolves incongruently leading to a preferential release of ^{87}Sr (concentrated in the interlayer sites) during the first stages of dissolution, which shifts the $^{87}Sr/^{86}Sr$ ratios to higher values. Due to its perfect basal cleavage, the surfaces of biotite sheets are resistant to chemical weathering, and dissolution occurs preferentially at the edges of biotite grains (Turpault and Trotignon, 1994). Föllmi et al. (2009b) observed that the weathering rates of biotite (relative edge-surface area) are initially very high and sharply decrease with time. Spiegel et al. (2002) measured $^{87}Sr/^{86}Sr$ ratios in the range of 0.711–0.723 for epidote of the Austroalpine hinterland (Err–Bernina region). Consequently, epidote also contributes to weathering, especially in very young surfaces.

Mg is also continuously mobilised as hornblende (decreasing trend with time) and biotite weather (Fig. 10). When biotite transforms to vermiculite it can either release Mg or in some instances it actually retains Mg. Both laboratory and field studies of biotite weathering demonstrated that in general Fe^{2+} is oxidized to Fe^{3+}, Mg is partially retained in the vermiculite and interlayer K (as well as other trace interlayer cations including Rb and Sr) are released (e.g., Gilkes and Suddhiprakam, 1979; Acker and Bricker, 1992). Apparently, the elemental depletion in biotite involves Sr and Mg at the first stages and leads to a vermiculitization process in the interlayers. In a first step, illite was produced and detected in the <2 μm size fraction. There is a trend of decreasing $^{87}Sr/^{86}Sr$ ratios from waters draining young surfaces (within the proglacial area) to old surfaces (outside the proglacial area). The formation of vermiculites and smectites is very much advanced outside the proglacial area because the soils are much older (around 11,500 yr; Egli et al., 2003). No biotite was found anymore in the topsoils and only a low content in the subsoil.

The amount of biotite decreases with time while illite increases. Illite and hydrobiotite are the first weathering product of biotite alteration. Murakami et al. (2003) performed laboratory experiments and observed (using HRTEM) that within 56 days in batch experiments secondary minerals (vermiculite-like layers and hematite on the edges of the platelets) were already detected on biotite. The phase transition from biotite to illite (vermiculitization, as reported by Murakami et al., 2003) is a layer-by-layer transformation. The same authors also showed that weathering processes were faster with Mg-rich than with Fe-rich biotites, due to the fast depletion of Mg. Muscovite is the K–Al end-member of the muscovite–celadonite series (Tischendorf et al., 2007) and also large cations like Mg may be usually found in its crystal lattice (Murakami et al., 2003). The octahedral structure of the minerals is also different. The more resistant muscovite has a dioctahedral and the less resistant biotite a trioctahedral structure. It is known from experimental studies that parts of a previously trioctahedral structure (in this case the cation is $Fe^{2+}$and probably chlorite is involved) become dioctahedral (mostly Fe^{3+}; in this case Mg and Al are not involved) under oxidic (Dreher and Niederbudde, 2000a) as well as under nearly natural weathering conditions (Dreher, 1994). Biotite therefore weathers in a first step to illite (and hydrobiotite) and vermiculite and in a last step (i.e., Al^{3+} for Mg^{2+} substitution in the octahedron) to smectite (Egli et al., 2007).

The content of epidote, a Ca-rich sorosilicate, decreases with time, even more distinctly than biotite (Fig. 4). Rose (1991) and Kalinowski et al. (1998) also showed that zoisite and epidote weather faster than albite under the same experimental conditions. Also plagioclase usually weathers relatively fast (Sverdrup and Warfvinge, 1993; Oliva et al., 2004). In the proglacial area of Morteratsch, a decrease in the plagioclase content could, however, not be detected although Fig. 8 indicates a trend towards plagioclase. The content of hornblende decreased slightly with time (but less significant; $R^2 = 0.18$; $p < 0.1$). Hornblende, a Ca- and Mg-rich inosilicate, transforms with time, similarly to biotite, into smectite (Dreher and Niederbudde, 2000b). The beginning of such a process must also be assumed for the proglacial area Morteratsch (see also Egli et al., 2003).

5. Conclusion

The first stages of weathering (within 0–150 yr of exposure) were studied by analysing the soil mineralogy and the water chemistry inside and outside the proglacial area of the Morteratsch glacier. We obtained the following results:

- Due to physical weathering, the amount of coarse particles (diameter >2 mm) decreased by about 15% over the observed time span of 150 yr and the clay fraction increased (about 2.5%).
- The accumulation of soil organic matter was distinct. Depending on the vegetation cover, 1–5.5 kg C/m^2 was accumulated which corresponds to 7–36 g C/m^2/yr. These are high rates compared to the average accumulation in well-developed soils and it demonstrates the reactivity of young surfaces to changing environmental conditions.
- Weathering is also linked to acidification. A distinct decrease of the pH-value within 150 yr could be detected.
- The water and soil chemistry indicated significant losses of Ca and Mg. Disseminated calcite occurs in granitoid rocks and plays a role in this subglacial environments. It is, however, not known for how long such an influence is significant and measurable. Although carbonates were present in trace amounts, the saturation state (log*SI*) was strongly negative and consequently showed that carbonates did not predominantly control the concentration of Ca and Mg.
- The Ca/Na ratio of soils and waters showed a remarkable decreasing tendency with time and, consequently, a preferential leaching of Ca over Na.
- The content of epidote, a Ca-rich sorosilicate, decreased with time, even more distinctly than biotite. Epidote contributed significantly to the Ca fluxes.
- The first signs of a biotite transformation into illite could be detected (hydrobiotite formation). Biotite weathering was also supported by the $^{87}Sr/^{86}Sr$ analysis and the Ca/Sr-ratio in the waters (spring waters, rivers, glacial stream water). Water chemistry indicated, furthermore, that weathering of plagioclase had started.
- In addition, hornblende, a Ca- and Mg-rich inosilicate, seemed to decrease (although less significantly) and was involved in the first weathering mechanisms after the exposure of the surface.

Soils in the proglacial area have a very young age. Their reactivity was clear and within only 150 yr of soil development weathering trends could be measured. Immediately after deglaciation, physical and chemical weathering as well as mineral transformation started at high rates. These results highlight the importance of weathering processes of freshly exposed granitoid rocks in High Alpine environments, document a series of time dependent processes related to the weathering of rock-forming minerals and evidence that climate warming directly influences the biogeochmical cycles in cold, alpine areas.

Acknowledgements

This research was supported by the Swiss National Foundation (SNF), project grant no. 200021-117568. We would like to thank B. Kägi for the laboratory work and F. Favilli for the help in the field. We are, furthermore, indebted to K. Föllmi and an unknown reviewer for their helpful comments on an earlier version of the manuscript.

References

Acker, J.G., Bricker, O.P., 1992. The influence of pH on biotite dissolution and alteration kinetics at low temperature. Geochimica et Cosmochimica Acta 56, 3073–3092.

Anderson, S.P., Drever, J.I., Frost, C.D., Holden, P., 2000. Chemical weathering in the foreland of a retreating glacier. Geochimica et Cosmochimica Acta 64, 1173–1189.

April, R., Newton, R., Coles, L.T., 1986. Chemical weathering in two Adirondack watershed: past and present-day rates. Geological Society of America Bulletin 97, 1232–1238.

Armbruster, T., Bonazzi, P., Akasaka, M., Bermanec, V., Chopin, C., Gieré, R., Heuss-Assbichler, S., Liebscher, A., Menchetti, S., Pan, Y., Pasero, M., 2006. Recommended nomenclature of epidote-group minerals. European Journal of Mineralogy 18, 551–567.

Arn, K., 2002. Geochemical weathering in the sub- and proglacial zone of two glaciated crystalline catchments in the Swiss Alps (Oberaar- and Rhoneglacier). Ph.D. Thesis, University of Neuchâtel, Neuchâtel, Switzerland.

Arn, K., Hosein, R., Föllmi, K.B., Steinmann, P., Aubert, D., Kramers, J., 2003. Strontium isotope systematics in two glaciated crystalline catchments: Rhone and Oberaar glaciers (Swiss Alps). Swiss Bulletin of Mineralogy and Petrology 83, 273–283.

Bergmann, J., Kleeberg, R., 1998. Rietveld analysis of disordered layer silicates. Materials Science Forum 278–281, 300–305.

Blum, J.D., Erel, Y., 1997. Rb-Sr isotope systematics of a granitic soil chronosequence: the importance of biotite weathering. Geochimica et Cosmochimica Acta 61, 3193–3204.

Blum, J.D., Klaue, A., Nezat, C.A., Driscoll, C.T., Johnson, C.E., Siccama, T.G., Eagar, C., Fahey, T.J., Likens, G.E., 2002. Mycorrhizal weathering of apatite as an important calcium source in base-poor forest ecosystems. Nature 417, 729–731.

Büchi, H., 1994. Der variskische Magmatismus in der östlichen Bernina (Graubünden, Schweiz). Schweizerische Mineralogische und Petrographische Mitteilungen 74, 359–371.

Burga, C., 1999. Vegetation development on the glacier forefield Morteratsch (Switzerland). Applied Vegetation Science 2, 17–24.

Burga, C., Perret, R., 1998. Vegetation und Klima der Schweiz seit dem jüngeren Eiszeitalter. Ott Verlag, Thun.

Conen, F., Yakutin, M.V., Zumbrunn, T., Leifeld, J., 2007. Organic carbon and microbial biomass in two soil development chronosequences following glacial retreat. European Journal of Soil Science 58, 758–762.

Dasch, A.A., Blum, J.D., Eagar, C., Fahey, T.J., Driscoll, C.T., Siccama, T.G., 2006. The relative uptake of Ca and Sr into tree foliage using a whole-watershed calcium addition. Biogeochemistry 80, 21–40.

Dreher, P., 1994. Tonmineralbildung in Braunerden aus Amphibolit und Biotitgli-merschiefer sowie Untersuchungen zur Biotitumwandlung im Modellversuch. Ph. D. Thesis, Technical University of Munich.

Dreher, P., Niederbudde, E.-A., 2000a. Potassium release from micas and characterization of the alteration products. Clay Minerals 29, 77–86.

Dreher, P., Niederbudde, E.-A., 2000b. Characterization of expandable layer silicates in humic-ferralic cambisols (Umbrept) derived from biotite and hornblende. Journal of Plant Nutrition and Soil Science 163, 447–453.

Egli, M., Fitze, P., Mirabella, A., 2001. Weathering and evolution of soils formed on granitic, glacial deposits: results from chronosequence of Swiss alpine environments. Catena 45, 19–47.

Egli, M., Mirabella, A., Fitze, P., 2003. Formation rates of smectites derived from two Holocene chronosequences in the Swiss Alps. Geoderma 117, 81–98.

Egli, M., Wernli, M., Kneisel, C., Haeberli, W., 2006. Melting glaciers and soil development in the proglacial area Morteratsch (Swiss Alps): I. Soil type chronosequence. Arctic, Antarctic, and Alpine Research 38, 499–509.

Egli, M., Mirabella, A., Sartori, G., Giaccai, D., Zanelli, R., Plötze, M., 2007. Effect of slope aspect on transformation of clay minerals in Alpine soils. Clay Minerals 42, 375–401.

Egli, M., Merkli, C., Sartori, G., Mirabella, A., Plötze, M., 2008. Weathering, mineralogical evolution and soil organic matter along a Holocene soil toposequence on carbonate-rich materials. Geomorphology 97, 675–696.

FAO (Food and Agriculture Organization of the United Nations), 1998. World Reference Base for Soil Resources. World Soil Resources Reports, vol. 84. FAO, Rome.

Farmer, V.C., 1974. Layer silicates. In: Farmer, V.C. (Ed.), Infrared Spectra of Minerals. Monograph, vol. 4. Mineralogical Society, London, pp. 331–363.

Fitze, P.F., 1982. Zur Relativdatierung von Moränen aus der Sicht der Bodenentwicklung in den kristallinen Zentralalpen. Catena 9, 265–306.

Föllmi, K.B., Hosein, R., Arn, K., Steinmann, P., 2009a. Weathering and the mobility of phosphorus in the catchments and foefields of the Rhône and Oberaar glaciers, central Switzerland: implications for the global phosphorus cycle on glacial–interglacial timescales. Geochimica et Cosmochimica Acta 73, 2252–2282.

Föllmi, K.B., Arn, K., Hosein, R., Adatte, T., Steinmann, P., 2009b. Biogeochemical weathering in sedimentary chronosequences of the Rhône and Oberaar Glaciers (Swiss Alps): rates and mechanisms of biotite weathering. Geoderma 151, 270–281.

Gaillardet, J., Dupré, B., Louvat, P., Allègre, C.J., 1999. Global silicate weathering and CO_2 consumption rates deduced from the chemistry of large rivers. Chemical Geology 159, 3–30.

Gibbs, M.T., Kump, L.R., 1994. Global chemical erosion during the last glacial maximum and the present: sensitivity to changes in lithology and hydrology. Paleoceanography 9, 529–543.

Gilkes, R.J., Suddhiprakam, A., 1979. Magnetite alteration on deeply weathered ademellite. Journal of Soil Science 30, 357–361.

Goidts, E., van Wesemael, B., Crucifix, M., 2009. Magnitude and sources of uncertainties in soil organic carbon (SOC) stock assessments at various scales. European Journal of Soil Science 60, 723–739.

Goodman, B.A., Russel, J.D., Fraser, A.R., Woodhams, F.W.D., 1976. A Mössbauer and IR spectroscopic study of the structure of nontronite. Clays and Clay Minerals 24, 53–59.

Hallet, B., Hunter, L., Bogen, J., 1996. Rates of erosion and sediment evacuation by glaciers: a review of field data and their implications. Global and Planetary Change 12, 213–235.

Hitz, C., 2002. Inventur und Dynamik der organischen Substanz in Böden der alpinen Stufe. Schriftenreihe Physische Geographie, vol. 42. Universität Zürich.

Hosein, R., Arn, K., Steinmann, P., Adatte, T., Föllmi, K.B., 2004. Carbonate and silicate weathering in two presently glaciated, crystalline catchments in the Swiss Alps. Geochimica et Cosmochimica Acta 68, 1021–1033.

Jacobson, A.D., Blum, J.D., 2003. Relationship between mechanical erosion and CO_2 consumption in the New Zealand Southern Alps. Geology 31, 865–868.

Jenny, H., 1980. The soil resource. Origin and behavior. Ecological Studies, vol. 37. Springer-Verlag, New York.

Kalinowski, B.E., Faith-Ell, C., Schweda, P., 1998. Dissolution kinetics and alteration of epidote in acidic solution at 25 °C. Chemical Geology 151, 181–197.

Keller, K., Blum, J.D., Kling, G.W., 2007. Geochemistry of soils and streams on surfaces of varying ages in Arctic Alaska. Arctic, Antarctic and Alpine Research 39, 84–98.

Kleeberg, R., Monecke, T., Hillier, S., 2008. Preferred orientation of mineral grains in sample mounts for quantitative XRD measurements: how random are powder samples? Clays and Clay Minerals 56, 404–415.

Lichter, J., 1998. Rates of weathering and chemical depletion in soils across a chronosequence of Lake Michigan sand dunes. Geoderma 85, 255–282.

Magny, M., 1992. Holocene lake-level fluctuations in Jura and the northern subalpine ranges, France. Regional pattern and climatic implications. Boreas 21, 319–334.

Maisch, M., 1992. Die Gletscher Graubündens: Rekonstruktion und Auswertung der Gletscher und deren Veränderung sit dem Hochstand von 1850 im Gebiet der östlichen Schweizer Alpen (Bündnerland und angrenzende Regionen). Schriften-reihe Physische Geographie, vol. 32. Universität Zürich-Irchel, Switzerland.

Murakami, T., Satoshi, U., Yokohama, T., Kasama, T., 2003. Biotite dissolution processes and mechanisms in the laboratory and in nature: early stage weathering environment and vermiculitization. American Mineralogist 88, 377–386.

Négrel, P., 2006. Water–granite interaction: clues from strontium, neodymium and rare earth elements in soil and waters. Applied Geochemistry 21, 1432–1454.

Nezat, C.A., Blum, J.D., Yanai, R.D., Hamburg, S.P., 2007. A sequential extraction to determine the distribution of apatite in granitoid soil mineral pools with application to weathering at Hubbard Brook Experimental Forest, NH, USA. Applied Geochemistry 22, 2406–2421.

Oliva, P., Dupré, B., Martin, F., Viers, J., 2004. The role of trace minerals in chemical weathering in a high-elevation granitic watershed (Estibère, France): chemical and mineralogical evidence. Geochimica et Cosmochimica Acta 68, 2223–2244.

Papritz, A., Flühler, H., 1991. Räumliche Variabilität von bodenchemischen Grössen auf Transekten zwischen Bäumen (Beobachtungsfläche Lägern). In: Pankow, W. (Ed.), Belastung von Waldböden. : NFP, vol. 14. Verlag der Fachvereine, Zürich, pp. 125–136.

Patzelt, G., 1977. Der zeitliche Ablauf und das Ausmass postglazialer Kimaschwankungen in den Alpen. In: Frenzel, B. (Ed.), Dendrochronologie und postglaziale Klimaschwankungen in Europa: Wiesbaden, Erdwissenschaftliche Forschung, vol. 13, pp. 248–259.

Perruchoud, D., Walthert, L., Zimmermann, S., Lüscher, P., 2000. Contemporary carbon stocks of mineral forest soils in the Swiss Alps. Biogeochemistry 50, 111–136.

Riebe, C.S., Kirchner, J.W., Finkel, R.C., 2004. Erosional and climatic effects on long-term chemical weathering rates in granitic landscapes spanning diverse climate regimes. Earth and Planetary Science Letters 224, 547–562.

Rose, N.M., 1991. Dissolution rates of prehnite, epidote and albite. Geochimica et Cosmochimica Acta 55, 3273–3286.

Sauer, D., Schülli-Mauer, I., Sperstad, R., Sørensen, R., Stahr, K., 2009. Albeluvisol development with time in loamy marine sediments of southern Norway. Quaternary International 209, 31–43.

Spiegel, C., Siebel, W., Frisch, W., Berner, Z., 2002. Nd and Sr isotopic ratios and trace element geochemistry of epidote from the Swiss Molasse Basin as provenance inidicators: implications for the reconstruction of the exhumation history of the Central Alps. Chemical Geology 189, 231–250.

Srodon, J., Drits, V.A., McCarty, D.K., Hsieh, J.C.C., Eberl, D.D., 2001. Quantitative X-ray diffraction analysis of clay bearing rocks from random preparations. Clays and Clay Minerals 49, 514–528.

Stumm, W., Morgan, J.J., 1996. Aquatic Chemistry, Third edition. John Wiley and Sons, Inc., New York.

Sverdrup, H., Warfvinge, P., 1993. Calculating field weathering rates using a mechanistic geochemical model PROFILE. Journal of Applied Geochemistry 8, 273–283.

Taylor, A., Blum, J.D., 1995. Relation between soil age and silicate weathering rates determined from the chemical evolution of a glacial chronosequence. Geology 23, 979–982.

Taylor, A.S., Blum, J.D., Lasaga, A.C., MacInnis, I.N., 2000. Kinetics of dissolution and Sr release during biotite and phlogopite weathering. Geochimica et Cosmochimica Acta 64, 1191–1208.

Theurillat, J.P., Felber, F., Geissler, P., Gobat, J.M., Fierz, M., Fischlin, A., Küpfer, P., Schlüssel, A., Velluti, C., Zhao, G.-F., Williams, J., 1998. Sensitivity of plant and soil ecosystems of the Alps to climate change. In: Cebon, P., Dahinden, U., Davies, H.C., Imboden, D., Jaeger, C.C. (Eds.), Views from the Alps. MIT Press, Massachusetts, pp. 225–308.

Tischendorf, G., Förster, H.-J., Gottesmann, B., Rieder, M., 2007. True and brittle micas: composition and solid-solution series. Mineralogical Magazine 71, 285–320.

Trommsdorff, V., Dietrich, V., 1999. Grundzüge der Erdwissenschaften. Auflage, Zürich, Switzerland. vdf-Verlag, 6.

Turpault, M.P., Trotignon, L., 1994. The dissolution of biotite single crystals in dilute HNO_3 at 24 °C: evidence of an anisotropic corrosion process of micas in acidic solutions. Geochimica et Cosmochimica Acta 58, 2761–2775.

Ufer, K., Stanjek, H., Roth, G., Dohrmann, R., Kleeberg, R., Kaufhold, S., 2008. Quantitative phase analysis of bentonites with the Rietveld method. Clays and Clay Minerals 56, 272–282.

Vantelon, D., Pelletier, M., Michot, L.J., Barres, O., Thomas, F., 2001. Fe, Mg and Al distribution in the octahedral sheet of montmorillonites. An infrared study in the OH-bending region. Clay Minerals 36, 369–379.

West, A.J., Galy, A., Bickle, M., 2005. Tectonic and climatic controls on silicate weathering. Earth and Planetary Science Letters 235, 211–228.

White, A.F., Blum, A.E., Bullen, T.D., Vivit, D.V., Schulz, M., Fitzpatrick, J., 1999a. The effect of temperature on experimental and natural chemical weathering rates of granitoid rocks. Geochimica et Cosmochimica Acta 63, 3277–3291.

White, A.F., Bullen, T.D., Vivit, D.V., Schulz, M.S., Clow, D.W., 1999b. The role of disseminated calcite in the chemical weathering of granitoid rocks. Geochimica et Cosmochimica Acta 63, 1939–1953.

White, A.F., Schulz, M.S., Lowenstern, J.B., Vivit, D.V., Bullen, T.D., 2005. The ubiquitous nature of accessory calcite in granitoid rocks: implications for weathering, solute evolution, and petrogenesis. Geochimica et Cosmochimica Acta 69, 1455–1471.

Geoderma 165 (2011) 106–117

Contents lists available at ScienceDirect

Geoderma

journal homepage: www.elsevier.com/locate/geoderma

Clay mineral evolution along a soil chronosequence in an Alpine proglacial area

Christian Mavris [a], Michael Plötze [b], Aldo Mirabella [c], Daniele Giaccai [c], Giuseppe Valboa [c], Markus Egli [a,*]

[a] Department of Geography, University of Zurich, Zurich, 8057, Switzerland
[b] ETH Zurich, Institute for Geotechnical Engineering, Zurich, 8093, Switzerland
[c] Istituto Sperimentale per lo Studio e la Difesa del Suolo, Centro di ricerca per l'Agrobiologia e la Pedologia, Piazza D'Azeglio 30, 50121 Firenze, Italy

ARTICLE INFO

Article history:
Received 16 April 2011
Received in revised form 1 July 2011
Accepted 7 July 2011
Available online 6 August 2011

Keywords:
Proglacial area
Smectite
Mica
Clay minerals
Soil chronosequence
Alps

ABSTRACT

As a consequence of global warming, additional areas will become ice-free and subject to weathering and soil formation. The most evident soil changes in the Alps will occur in proglacial areas where young soils will continuously develop due to glacier retreat. Little is known about the initial stages of weathering and soil formation, i.e. during the first decades of soil genesis. In this study, we investigated clay minerals formation during a time span 0–150 years in the proglacial area of Morteratsch (Swiss Alps). The soils developed on granitic till and were Lithic Leptosols.

Mineralogical measurements of the clay (<2 μm) and fine silt fraction (2–32 μm) were carried out using XRD (X-ray Diffraction) and DRIFT (Diffuse Reflectance Infrared Fourier Transform). Fast formation and transformation mechanisms were measured in the clay fraction. The decreasing proportion of trioctahedral phases with time confirmed active chemical weathering. Since the start of soil formation, smectite was actively formed. Some smectite (low charge) and vermiculite (high charge) was however already present in the parent material. Main source of smectite formation was biotite, hornblende and probably plagioclase. Furthermore, irregularly and regularly interstratified clay minerals (mica–HIV or mica–vermiculite) were formed immediately after the start of moraine exposure to weathering. In addition, hydroxy-interlayered smectite (HIS) as a transitory weathering product from mica to smectite was detected. Furthermore, since the start of soil evolution, kaolinite was progressively formed. In the silt fraction, only little changes could be detected; i.e. some formation of an interstratified mica–HIV or mica–vermiculite phase.

The detected clay mineral formation and transformation mechanisms within this short time span confirmed the high reactivity of freshly exposed sediments, even in a cryic environment.

1. Introduction

Glaciers and periods of glaciation may have a significant impact on global weathering, changing the interplay between physical and chemical weathering processes, by putting large volumes of dilute meltwaters and fine-grained sediment in contact with each other (Arn et al., 2003; Föllmi et al., 2009a,b). Due to climate warming, additional areas will become ice-free and subject to weathering and soil formation. Proglacial environments are important for the understanding of global CO_2 cycling on glacial/interglacial timescales as they made up a significant amount of the global land surface during the Quaternary due to the advance and retreat of glaciers and ice sheets (Gibbs and Kump, 1994). As stated in several previous publications (see Dümig et al., 2011; Föllmi et al., 2009a,b; Hosein et al., 2004), the proglacial area is a potential zone of high geochemical reactivity with respect to weathering processes or organic matter accumulation. This issue is also shown by chronosequence studies. The derivation of soil chronosequence curves for main chemical elements in Alpine climates gave weathering rates (loss of mass per unit area) as a function of time. Weathering rates of young soils (age <1000 years) on silicatic parent material seem to be two to three orders of magnitude higher than in old soils (c. 12,000 years; Egli et al., 2001a). The most weathered soils in Alpine environments as well as subarctic environments are usually podzols (e.g. Gustafsson et al., 1995; Olsson and Melkerud, 2000). Also the rate of organic matter accumulation is at the beginning of soil formation much higher than in old and weathered soils (Conen et al., 2007; Egli et al., 2010; Jenny, 1980).

There is, however, not an equivocal agreement about the velocity of reaction in proglacial areas. Anderson et al. (2000) concluded from their measurements that silicate weathering is not enhanced in proglacial areas. According to them, silicate weathering reactions may be important only after vegetation cover is established. In contrast, Wadham et al. (2001), Hosein et al. (2004) and Egli et al. (2003) suggested that glacially derived material is subjected to enhanced chemical weathering (due to the dissolution of the most reactive phases such as sulphide oxidation and carbonate dissolution), starting immediately after deposition in the pro-glacial zone and subsequently continuing for thousands of years after glacier retreat. Föllmi et al.

* Corresponding author. Tel.: +41 44 635 51 14; fax: +41 44 635 68 48.
E-mail address: markus.egli@geo.uzh.ch (M. Egli).

0016-7061/$ – see front matter © 2011 Elsevier B.V. All rights reserved.
doi:10.1016/j.geoderma.2011.07.010

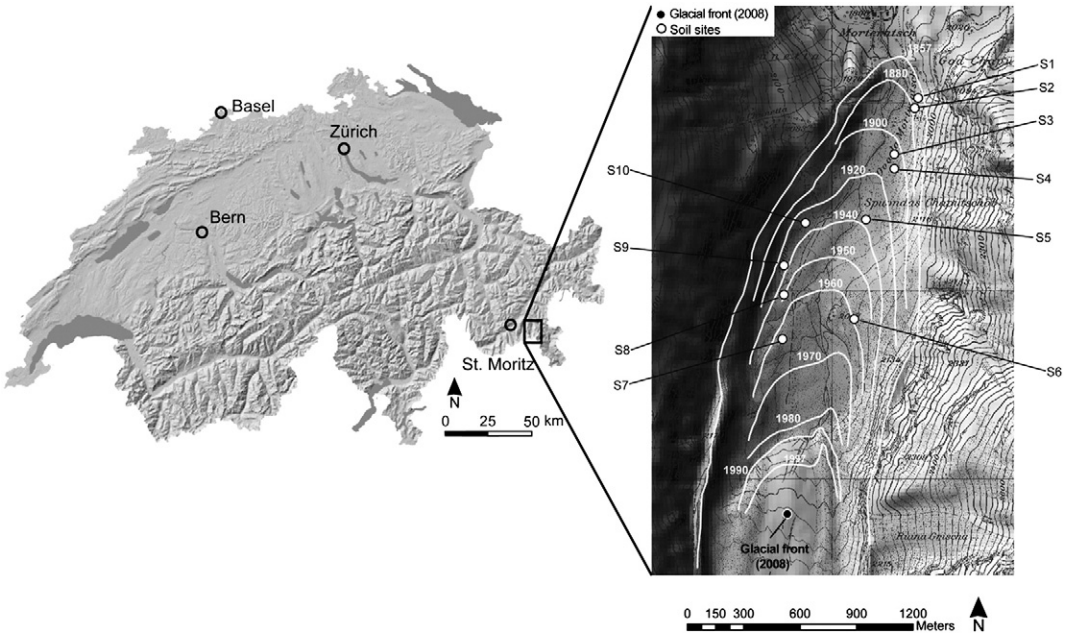

Fig. 1. Location of the Morteratsch proglacial area (SE Switzerland), with isochrones (after Burga, 1999) and monitored sites.

(2009a,b) measured higher biotite weathering rates in young soils (<100 years) of a proglacial area than in old soils (11,000 years).

Furthermore, two different kinds of soil production functions are discussed in literature (Humphreys and Wilkinson, 2007). Soil evolution and, consequently, weathering can be modelled using a humped or an exponential function. With a humped function, soil production and weathering is maximised at a certain soil depth or time (Anderson, 2002; Cox, 1980; Gilbert, 1877). In contrast to this approach, models using an exponential function are often applied (e.g. Egli et al., 2001a; Heimsath et al., 1997; Humphreys and Wilkinson, 2007; Wilkinson et al., 2005). According to these studies, production and weathering exponentially decreases with time. A challenge is now to test the applicability of the existing two soil production functions and as yet unknown forms to different kinds of situations.

A main gap in knowledge exists about the velocity of (clay) mineral transformations or formations in soils or material starting to be a soil in high alpine and arctic climate zones. According to Egli et al. (2003), Arn et al. (2003), Hosein et al. (2004) or Föllmi et al. (2009a), highest formation rates of clay minerals (especially smectite) or transformation rates of primary sheet silicates should be greatest at the very beginning of soil formation. There exist, however, almost no measurements for this stage of weathering or soil formation (with ages of 0–150 years) and especially related to clay mineralogical formations and transformations. The main goals of this study were consequently: i) can we detect changes in the clay mineralogy already after 150 years of soil formation in a cryic environment? ii) and if yes, can changes be attributed to specific formation and transformation processes? Consequently, we focused on the identification of clay mineral formation and transformation reaction mechanisms in a proglacial area having very young soils. Although mineral transformation reactions are often reported to be slow and almost undetectable in alpine and young areas, we hypothesised that also within a very short period of weathering changes in the clay mineralogy could be detected and assigned to transformation mechanisms. Based on this hypothesis, we want to demonstrate that alpine and cryic environments are highly reactive.

2. Study area

The proglacia area of Morteratsch is located in Upper Engadine, SE Switzerland (Fig. 1). The valley runs in N–S direction and the current length of the exposed area is approx. 3 km. The glacier is continuously retreating without re-advancements since the 1850s (end of the Little Ice Age; Burga, 1999) (Table 1). The moraine deposited in that period constitutes the outer border of the investigated area. The altitude of the investigated proglacial valley ranges from 1900 masl to approx 2150 masl, with no abrupt stacks and slopes along its main axis. The glacial till consists of granite and gneissic material (Table 1). The morainic material was produced through glacial transport within a small area of relatively homogeneous parent material.

Geologically, the proglacial area of Morteratsch is set in the Lower Austroalpine Bernina Nappe, which is mainly constituted by plutonic rock types, such as granodiorites and diorites, syenites and alkali-granites. Accessory rocks such as dolomites, gabbros and serpentines are also reported, but are rare (Büchi, 1987, 1994). These units underwent a 'Greenschists' facies metamorphic event during the High Alpine orogenesis event (Oligocene–Eocene; Trommsdorff and Dietrich, 1999). This event was the reason for a 'saussuritisation' process, which partially transformed primary rock forming plagioclases into albite, epidote, calcite and zeolites (D'Amico et al., 1998). Furthermore, Na–Ca–amphiboles formed as well (Büchi, 1994). The vegetation cover of the Morteratsch proglacial area has been studied by Burga (1999).

The first flowering plants colonising young deglaciated surfaces are scattered individuals of *Epilobium fleischeri* and *Linaria alpina* that appear after about 7 years. First plants of the community *Oxyrietum digynae* appear after c. 12 years and disappear after c. 27 years. The second most important community is the green alder community,

Table 1
General features of the Morteratsch proglacial area.

Latitude	46°26′N
Longitude	9°56′E
Elevation at glacier front	2117 masl
Elevation at pro-glacial area front	1900 masl
Main orientation	North
Geology	Granite and granodiorite (Bernina nappe, Stretta lithostratigraphic formation)
Mean annual temperature	0.5 °C
Mean annual precipitation	1100–1300 mm
Mean slope	<10°

which starts early and grows continuously in importance until it overtakes the *Epilobietum fleischeri* after about the 100 first years of succession (Burga et al., 2010). The establishment of *Larici-Pinetum cembrae* forests (open larch-Swiss stone pine forest) takes place after about 77 years (Burga, 1999) on sites where the soil is more intensely weathered. The following vegetation could be encountered at the individual sites: open larch-Swiss stone pine forest at the site S2 (Fig. 1; see also Table 2), green alder scrub at the sites S3, S4, S5, S8 and S9, *Epilobietum fleischeri* with single willow shrubs at site S6, pioneer grass communities at site S7 and S10. The soils are weakly developed and are mostly Lithic Leptosols (IUSS Working Group WRB, 2006).

Present climatic conditions for the Morteratsch site are approx. 0.5 °C mean annual temperature and approx. 1000–1300 mm mean annual precipitation (EDI, 1992).

3. Materials and methods

3.1. Soil sampling

10 topsoil (uppermost, mineral horizon) samples were collected across the proglacial area of Morteratsch (Fig. 1). The sites were chosen from an existing soil chronosequence ranging from 0 to 150 yr old soils (Table 2). Approximately 1–2 kg of material was collected per sample.

3.2. Typical soil characteristics

Soil pH was measured in 0.01 M $CaCl_2$ using a soil solution ratio of 1:2.5. The particle size distribution was determined on some selected soil samples. After a pre-treatment of the samples with H_2O_2 (3%), particle size distribution of the soils was measured by a combined method consisting of sieving the coarser particles (32–2000 μm) and the measurement of the finer particles (<32 μm) by means of an X-ray-sedimentometer (SediGraph 5100). The weight proportion of soil skeleton was determined by sieving the bulk soil material (2 mm sieve).

3.3. Fractionation of the clay (<2 μm) and fine silt fraction (2–32 μm)

The clay fraction (<2 μm) was collected from the parent material (averaged from the parent material of 6 monitored sites and one sample of freshly exposed subglacial sediment, collected at the glacier front) and 6 topsoils (that were representative for the selected chronosequence; sites S1, S3, S6, S7, S8, S10; see Table 2), i.e. the uppermost mineral horizon, and was analysed in detail. To separate the clay fraction (<2 μm), the fine earth samples (<2 mm) were pre-treated at room temperature with diluted and Na-acetate buffered (pH 5) H_2O_2 to remove organic matter. The clay fraction was obtained by dispersion with Calgon and sedimentation in water. Specimens were then Mg-saturated, washed free of chloride and freeze-dried.

The fine-silt fraction (<32 μm) was obtained after the extraction of the clays by wet sieving. This fraction was then Mg saturated ($MgCl_2$ 2M), washed free of chlorides and freeze-dried.

3.4. X-ray diffraction analyses of the clay fraction

Textured specimens, prepared by sedimentation on glass slides from a water suspension, were analysed using a 3-kW Rigaku D/MAX III C diffractometer, equipped with a horizontal goniometer and a graphite monochromator, using Cu-Kα radiation. Slides were step-scanned from 2 to 15°2θ with steps of 0.02°2θ and 2 s counting time. The measurements were carried out after the following treatments were performed: Mg-saturation, ethylene glycol solvation and K saturation, followed by heating for 2 h at 335 °C and 550 °C.

In a further step, the Na-citrate treatment (modified after Tamura, 1958) was performed to extract hydroxy-Al (or Fe) polymers from the interlayers of 2:1 clay minerals to check whether HIS (hydroxy-interlayered smectites) or HIV (hydroxy-interlayered vermiculites) were present. The citrate treatment enabled us to infer the presence of low-charged 2:1 clay minerals, whose expansion was hindered in the untreated state by interlayered polymers. After this treatment, HIS behaves like a 'normal' smectite when EG solvated. The Tamura

Table 2
Some properties of the monitored soil sites.

Site/Soil	Soil age (yr)	Horizons	Depth (cm)	Skeleton (wt.%)	Sand (g/kg)	Silt (g/kg)	Clay (g/kg)	pH ($CaCl_2$)
S1/Humi-Skeletic Leptosol	138	O	0–6	41	n.m.*	n.m.	n.m.	4.60
		A	6–9	50	777	184	39	4.80
		BC	9–14	53	830	158	12	4.70
		C	14–30	40	757	222	21	4.60
S2/Humi-Skeletic Leptosol	128	A	0–10	64	754	204	42	4.85
		AC	10–40	68	695	272	33	4.90
S3/Humi-Skeletic Leptosol	108	A	0–3	54	667	265	68	5.10
		AC	3–15	70	677	281	42	4.50
S4/Humi-Skeletic Leptosol	98	A	0–1	55	939	61	15	5.30
		AC	1–5	51	939	61	15	5.20
		C	5–30	70	931	57	12	5.20
S5/Humi-Skeletic Leptosol	68	A1	0–1	7	n.m.	n.m.	n.m.	4.85
		A2	1–4	1	530	432	38	4.55
		C1	4–9	36	573	387	40	4.65
		C2	9–20	64	570	372	58	4.60
S6/Skeletic Leptosol	48	A	0–2.5	64	n.m.	n.m.	n.m.	4.80
		C	2.5–25	68	852	129	19	5.00
S7/Skeletic Leptosol	48	A	0–4	26	n.m.	n.m.	n.m.	6.10
		C1	4–11	37	823	146	31	5.20
		C2	11–34	67	747	211	42	5.10
S8/Skeletic Leptosol	58	OA	0–12	63	n.m.	n.m.	n.m.	4.60
		C	12–33	48	712	220	68	4.40
S9/Humi-Skeletic Leptosol	73	O	0–3	44	n.m.	n.m.	n.m.	5.15
		AC	3–10	65	785	175	40	4.40
		C	10–36	58	832	133	35	4.65
S10/Humi-Skeletic Leptosol	78	A1	0–2	49	n.m.	n.m.	n.m.	4.70
		A2	2–10	68	818	143	39	4.50
		AC	10–25	84	733	219	48	4.80

* n.m. = not measured.

procedure (Tamura, 1958) was applied in a modified form in which a contact time of 24 h without extractant removal was obtained by heating the samples in an autoclave at 135 °C. After the Na-citrate procedure, the samples were Mg-saturated, ethylene glycol solvated and K saturated, followed by heating for 2 h at 335 °C and 550 °C. XRD patterns of the treated samples were then compared with those of the corresponding untreated samples.

The *d*(060) region of sheet silicates was studied on random mounts. The 58 to 64°2θ range was step-scanned with steps of 0.02°2θ at 10 s counting time using a Bragg–Brentano diffractometer (BRUKER AXS D8, CuKα with automatic θ compensating slits and graphite monochromator). For a better distinction of trioctahedral phases, the peak position at 0.182 nm, typical for quartz, was then compared to the one at 0.1542 nm, whose intensity is the same (Moore and Reynolds, 1997). Layer-charge estimation of smectites was performed using the long-chain alkylammonium ion C18 (and C12) according to the method proposed by Olis et al. (1990).

For the monolayer to bilayer transition, the following equation was used:

$$C18 : d(001) = 8.21 + 34.22\xi$$

with ξ = mean layer-charge and *d*-values given in Å.

For the bilayer to pseudotrimolecular layer transition, the equation is:

$$C18 : d(001) = 8.71 + 29.65\xi$$

3.5. X-ray diffraction analyses of the fine-silt fraction

The fine-silt fraction (32–2 μm) of the parent material (t = 0 yr) and the oldest topsoil (t = 138 yr) was chosen for an overview of the occurring mineralogical transformations The XRD measurements were carried out following the same procedure as for the clay fraction (except the citrate treatment).

3.6. XRD data evaluation

Digitised X-ray data were smoothed and corrected for Lorentz and polarization factors (Moore and Reynolds, 1997). Diffraction patterns were smoothed by a Fourier transform function and fitted by the Origin™ PFM programme using the Pearson VII algorithm. Background values were calculated by means of a non-linear function (polynomial 2nd order function Lanson, 1997).

The semi-quantitative estimation of phyllosilicate concentration was performed by the combination of the individual peak areas of the ethylene glycol solvated, the Mg-saturated, the K-saturated and the heated (335 °C and 550 °C) samples. On the basis of the obtained integrals, an estimate of clay minerals composition was performed. The sum of the areas between 2 and 15°2θ, which were attributed to HIV (hydroxy interlayered vermiculites), smectite, vermiculite, mica, chlorite and kaolinite, were normalised to 100%. The relative change of the areas, with respect to the treatments, enabled the above mineral phases to be distinguished. For the Mg-saturated and for the ethylene glycol solvation treatment, the area of the following peaks (d-spacings) had to be corrected by a weighting factor F: 1.6 nm with F = 0.453, 1.4 nm with F = 0.478, and 0.71 nm with F = 0.16 (Gjems, 1967; Laves and Jahn, 1972; Niederbudde and Kussmaul, 1978; Schwertmann and Niederbudde, 1993). This procedure allowed the estimation of the relative concentrations of sheet-silicates in the clay fraction. Although the (semi-)quantification of clay minerals in soils is bedevilled by manifold problems (Kahle et al., 2002), the applied and standardised (sample preparation, treatments, measurement and calculation) procedure enabled the assessment of the variability of clay mineral assemblage amongst the sites.

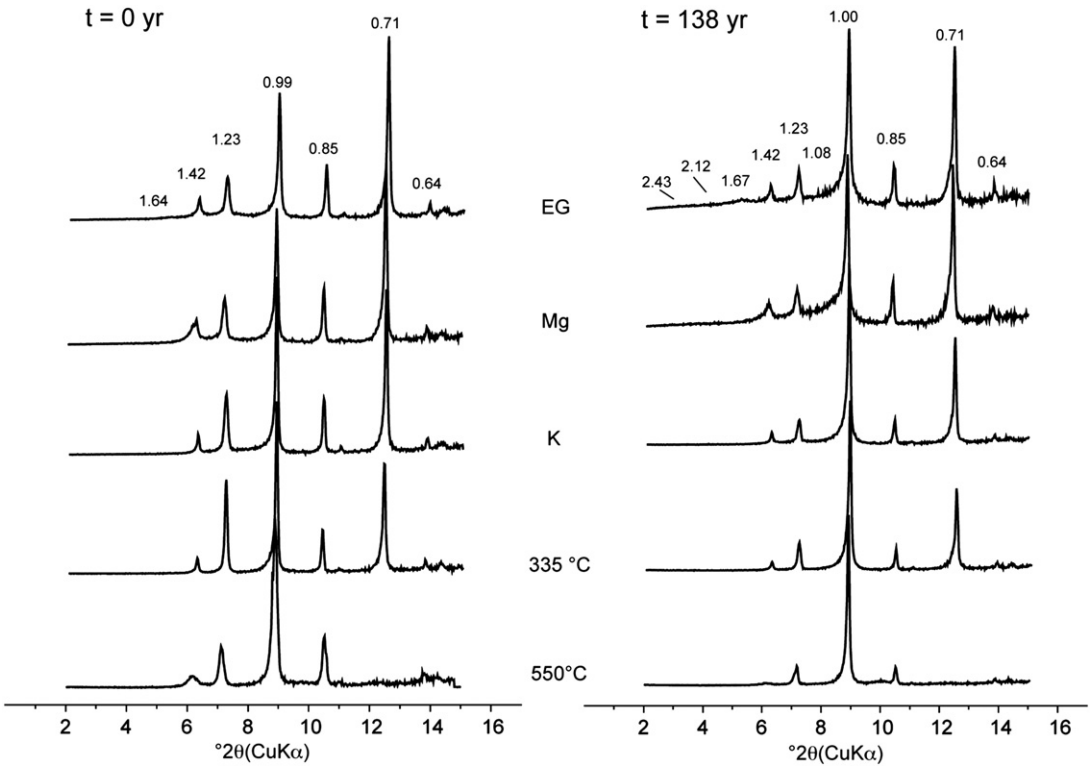

Fig. 2. XRD patterns of the parent material of site S1 (t = 0 year) and the oldest topsoil (t = 138 years, S1; see also Table 2). The XRD curves were smoothed and corrected for Lorentz and polarization factors. *d*-spacings are given in nm. EG = ethylene glycol solvation, Mg = Mg-saturation, K = K-saturation and corresponding heating treatments.

The same semi-quantitative approach was already successfully used in other mineralogical studies of Alpine soils (e.g., Egli et al., 2001b, 2003; Favilli et al., 2009).

3.7. Diffused Reflectance Infrared Fourier Transform (DRIFT)

When chlorite was found using XRD, the presence of kaolinite was checked with FT-IR (Brooker Optics, Tensor 27) analysis (OH-stretching bands near 3690 cm^{-1}). About 10 mg of clay material and 350 mg of KBr were homogenised in a mill using a fine ball-mill (Zr) for 45 s (frequency 25.0). Prior to measurement, the samples were dried in the oven at 70 °C. Spectra were recorded from 4000 to 250 cm^{-1}. The evaluation of FT-IR spectra was performed using OPUS 6 software.

4. Results

4.1. X-ray diffraction of clay fraction

In all samples, relatively sharp and clear peaks could be identified at 1.42, 1.23, 0.99, 0.85 and 0.71 nm (Fig. 2). Small peaks were detectable at 1.64 and 0.64 nm. Mg- and K-saturation and the subsequent heating treatments allowed the identification of chlorite (1.42 nm, after heating at 550 °C), some hydroxy-interlayered vermiculite (HIV) and interstratified mica–HIV having chloritic layers. According to Ezzaïm et al. (1999) and Turpault et al. (2008), the peaks persisting at 1.23 nm after heating at 550 °C can be attributed to chloritic layers in the mica–HIV phase. Already in the parent material (t = 0 yr; freshly exposed sediment), a small amount of smectite could be detected (1.64 nm following ethylene glycol solvation). The peaks at 0.64 nm and 0.85 nm could be attributed to plagioclase and amphibole, respectively. Some kaolinite was also identified by the peak at 0.71 nm, as confirmed by DRIFT (Fig. 3).

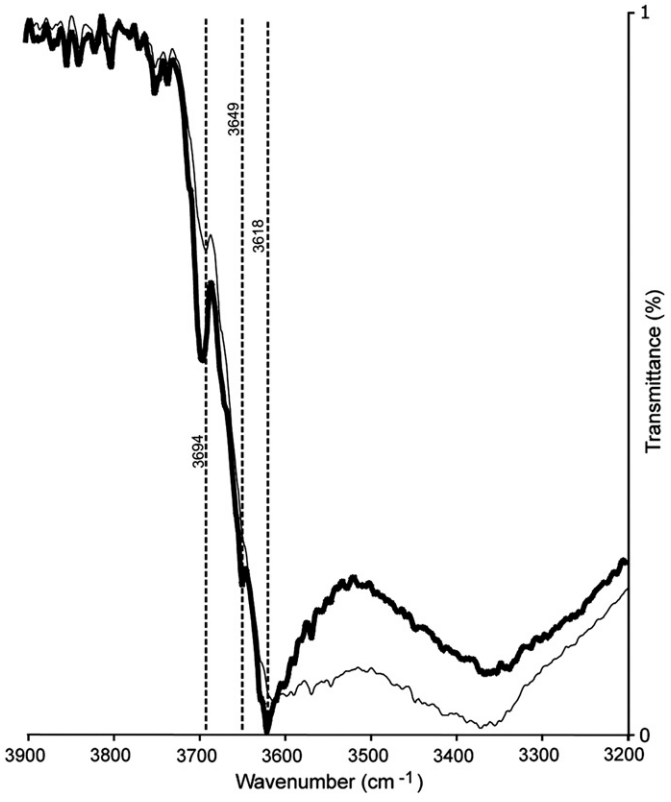

Fig. 3. Comparison of FT-IR spectra of clay fraction in the OH-stretching region (range 3200–3900 cm^{-1}) between t = 0 year (thin line; parent material of site S1) and t = 138 years (thick line; topsoil of S1).

In the sample having an age of 48 years, the same minerals described above were detected. Nonetheless, some smaller changes in the clay mineral assemblage could be measured already after 48 years of weathering (Fig. 4). Smectite (1.61 nm) became more significant than in the parent material. Furthermore, the amount of interstratified mica–HIV increased. Also mica started to transform—shown by the broader peak at 0.99 nm (with a minor peak at 1.03 nm). In addition, some pedogenic kaolinite (with a *d*(001) at 0.72 nm; see also Caner et al., 2010) seemed to form. This is, however, not fully clear as the *d* (002) reflection of chlorite could interfere at this position.

The clay mineralogy after 58 years of weathering was similar to that of the previously-described soil, except for the slightly broader peak at 1.00 nm. This shows that weathering of mica progressively continues (with the formation of some mixed-layered minerals). An expandable mineral with a *d*-spacing of 1.57 nm in the EG-solvated sample indicated some interstratification of smectite with a high-charged (smectite–vermiculite or smectite–mica) or even low-charged component (smectite–HIS).

Mg-saturated and EG-solvated clay samples from the soil having an age of 78 years exhibited XRD patterns with peaks centred at 2.43, 2.10, 1.67, 1.42, 1.23, 1.00, 0.85 and 0.71 nm (Fig. 4). The peaks at low angles were rather broad and weak. The basal reflections at 2.47 and 1.23 nm were attributed to a regularly-interstratified mica–HIV (or mica–HIS) and/or mica–vermiculite (hydrobiotite). Additionally, the basal reflections at 2.10 and 1.04 nm pointed to a newly-formed, regularly-interstratified mica–HIV with a high proportion of mica. Some smectite was also present (1.67 nm) and was not interstratified anymore.

After 108 years of soil evolution, smectite was even better detectable. Also in this sample, regularly-interstratified mica–HIV (and/or mica vermiculite) having a substantial amount of HIV or vermiculite (with *d*(001) and *d*(002) basal reflections at 2.45 and 1.24 nm) and a component having less HIV or vermiculite (with *d*(001) and *d*(002) basal reflections at 2.12 and 1.08 nm) could be detected. In this older sample, the peak at 1.00 nm increased now substantially after K-saturation which is typical for the presence of vermiculite.

The clay mineral assemblage of the oldest soil (138 years) was similar to that of the previously-described one. Smectite, regularly-interstratified mica–HIV and/or mica–vermiculite, vermiculite, kaolinite, chlorite, an interstratified mica–HIV (or mica–chlorite) having a high proportion of chloritic layers, mica, amphibole and plagioclase were measured. The proportion of smectite and weathered mica (interstratified mica–HIV or mica–vermiculite with a high proportion of mica) steadily increased. Compared to the parent material, more kaolinite could be measured (Fig. 3).

4.2. Na-citrate treatment of the clay fraction

Hydroxy interlayers hinder the collapse of expandable 2:1 phyllosilicates when K-saturated and the expansion of low-charge expandable minerals when EG-solvated (Barnhisel and Bertsch, 1989; Karathanasis, 1988). Citrate treatment was effective in removing the hydroxy interlayers from 2:1 phyllosilicates (Table 3). In all samples, a better resolved and clearer peak near 1.65 nm was now detected (Fig. 5). Consequently, all samples contained to a certain degree hydroxy-interlayered smectite (HIS). The peaks at very low angles (<5° 2θ) and also between 1.00 and 1.40 nm did not shift after the Na-citrate treatment and EG solvation. HIS, therefore, occurs as a peculiar phase and does not seem to be interstratified with mica.

The Na-citrate treatment clearly showed that additional smectitic phases were formed immediately after exposure to weathering. Remarkable changes occurred already between 0 and 48 years of soil evolution. The general trend of the smectitic components showed a steady increase with time.

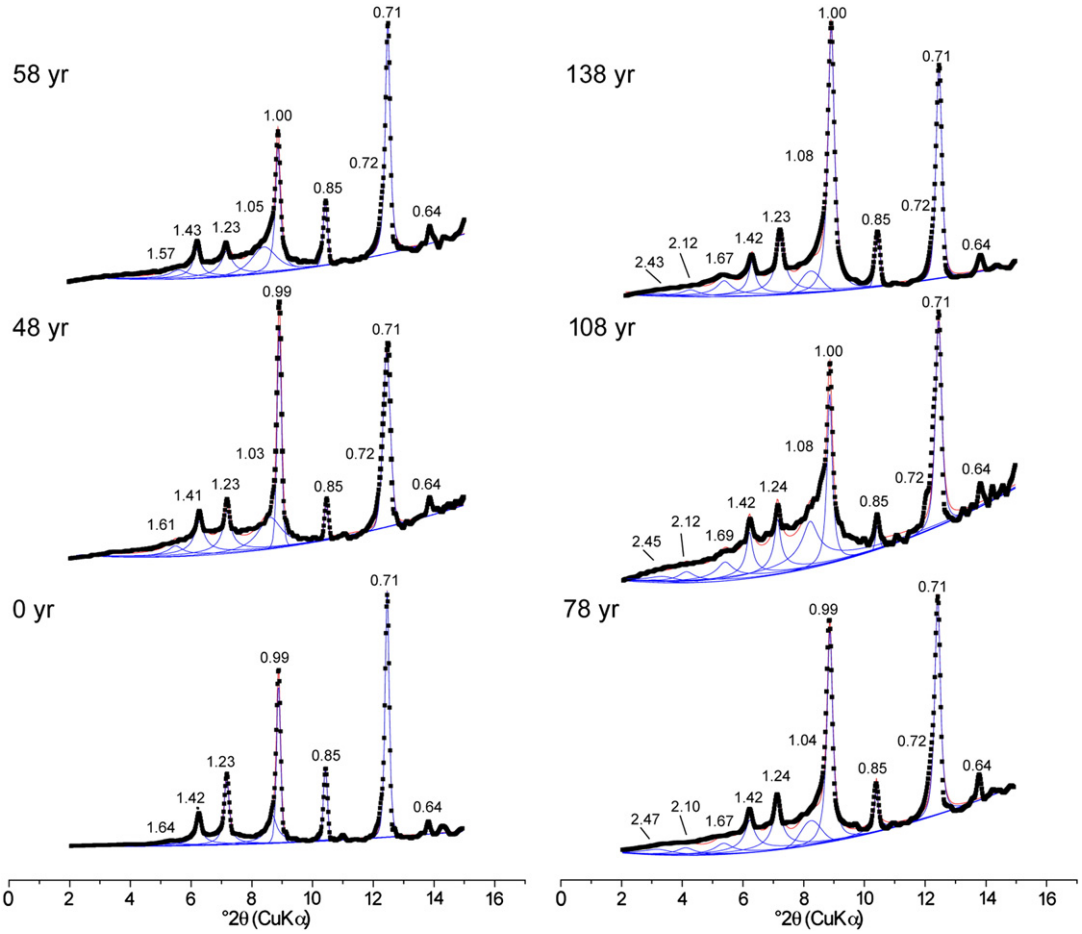

Fig. 4. XRD patterns of the EG-solvated clay fraction from the selected topsoils along the chronosequence. Given are the measured values (squares), modelled elementary curves and the modelled overall curve.

4.3. Trioctahedral and dioctahedral phases

The evaluation of XRD patterns in the d_{060} region of phyllosilicates (58–64° 2θ region) confirmed the presence of both trioctahedral and dioctahedral phases in the parent material (Fig. 6). The XRD pattern fitting enabled the separation of diagnostic peaks.

In general, trioctahedral species, represented by peaks in the range 59–61 °2θ, decreased from the parent material (youngest soil) to the oldest soil and, correspondingly, dioctahedral species (in the range 61–63 °2θ) increased with time. The peaks near 0.1550 and 0.1532 nm were attributed to trioctahedral chlorite and biotite, respectively. In the dioctahedral range, the peak at 0.1519 nm was attributed to Fe-rich dioctahedral phases (Fanning et al., 1989) and the one at 0.1495 nm to kaolinite that was already detected in the parent material. The peak near 0.1506 nm represents dioctahedral phases.

After 78 years, the trioctahedral range already showed a smaller area (Fig. 6). The peak assigned to biotite (0.1536 nm) was smaller than in the parent material. A similar trend was measured for chlorite

Table 3
Clay mineral content (with error range) after standard and Na-citrate treatment.

	Site	Age (yr)	Horizon	Clay phases (%)						
				Smectite	Mica	Chlorite	Vermiculite	HIV	Kaolinite	Mica/HIV
Standard treatment	S1	138	A	6.9 (±1.4)	62.9 (±9.4)	2 (±0.4)	5.4 (±1.1)	0.5 (±0.3)	9.1 (±1.8)	22.1 (±3.3)
	S3	108	A	9.2 (±1.8)	31.4 (±4.7)	1.4 (±0.3)	7.3 (±1.5)	0.9 (±0.3)	4.5 (±0.9)	49.0 (±7.4)
	S6	48	A	7.0 (±1.4)	40.7 (±6.1)	2.9 (±0.6)	8.1 (±1.6)	2 (±0.4)	6.7 (±1.3)	38.1 (±5.7)
	S7	58	A	5.9 (±1.2)	64.4 (±9.7)	3.0 (±0.6)	4.0 (±0.8)	0.1 (±0.3)	6.7 (±1.3)	22.2 (±3.3)
	S8	58	OA	8.3 (±1.7)	45.7 (±6.9)	2.0 (±0.4)	6.8 (±1.4)	0.1 (±0.3)	11.8 (±2.4)	33.9 (±5.1)
	S10	78	A	6.1 (±1.2)	56.0 (±8.4)	4.1 (±0.8)	9.8 (±2.0)	0.0	6.6 (±1.3)	24.0 (±3.6)
	Parent material	0	C[a]	1.7 (±0.4)	59.2 (±8.9)	1.8 (±0.4)	6.3 (±1.3)	0.5 (±0.1)	8.6 (±1.7)	28.6 (±4.3)
Na-citrate treatment	S1	138	A	14.7 (±2.9)	32.1 (±4.8)	4.0 (±0.8)	19.3 (±3.9)	0.9 (±0.3)	9.4 (±1.9)	19.5 (±2.9)
	S3	108	A	14.6 (±2.9)	44.9 (±6.7)	5.9 (±1.2)	7.1 (±1.4)	2.3 (±0.5)	6.8 (±1.4)	17.4 (±2.6)
	S6	48	A	15.8 (±3.2)	46.2 (±6.9)	6.3 (±1.3)	5.8 (±1.2)	3.6 (±0.7)	7.1 (±1.4)	15.2 (±2.3)
	S7	58	A	6.1 (±1.2)	66.0 (±9.9)	1.4 (±0.3)	4.1 (±0.8)	0.6 (±0.3)	9.5 (±1. 9)	10.9 (±1.6)
	S8	58	OA	11.1 (±2.2)	36.9 (±5.5)	2.2 (±0.4)	14.4 (±2.9)	3.1 (±0.6)	11.0 (±2.2)	20.5 (±3.1)
	S10	78	A1	10.7 (±2.2)	46.2 (±6.9)	2.3 (±0.5)	13.6 (±2.7)	2.2 (±0.4)	9.2 (±1.8)	16.0 (±2.4)
	Parent material	0	C	3.2 (±0.6)	62.1 (±9.3)	5.0 (±1.0)	5.8 (±1.2)	2.0 (±0.4)	9.5 (±1.9)	14.9 (±2.2)

[a] Combination of parental material from sites S1, S3, S6, S7, S8, S10 and fresh sediments from the glacier front.

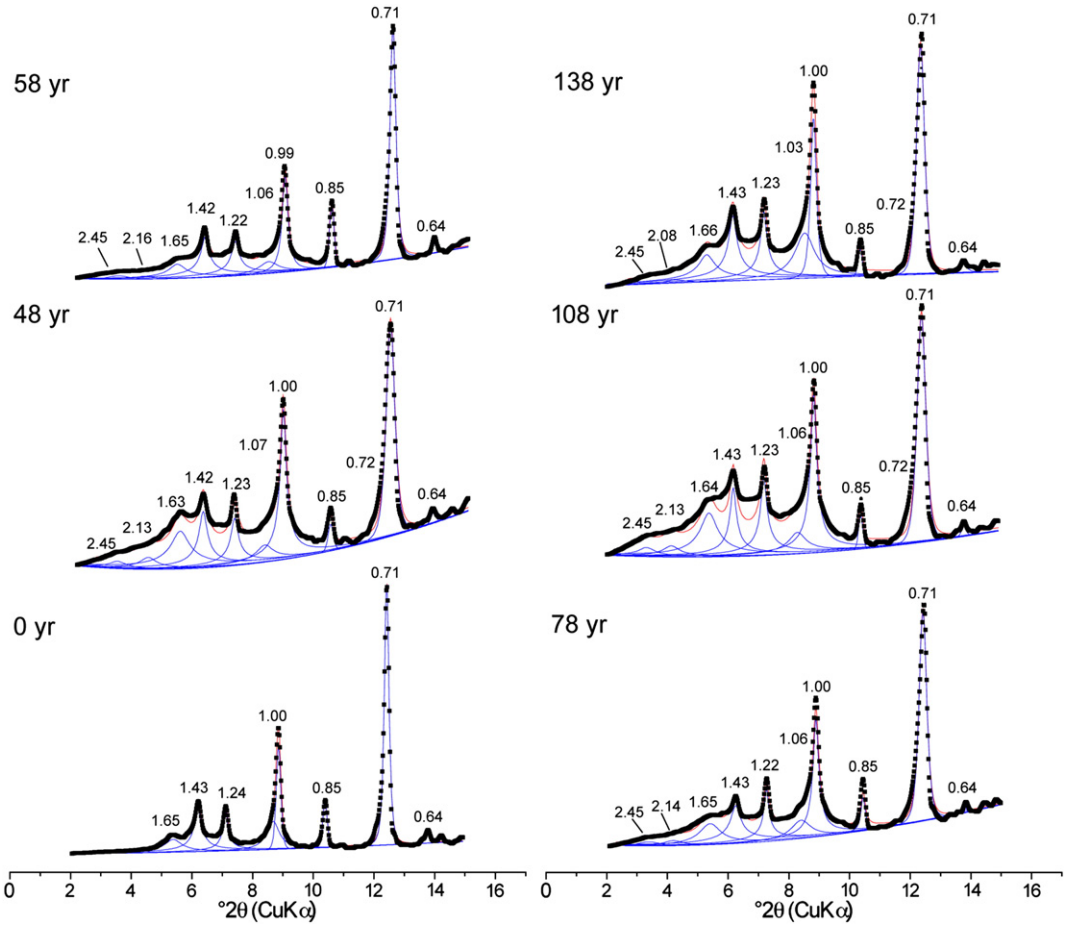

Fig. 5. XRD patterns of the Na-citrate treated and ethylene glycol (EG)-solvated soil clay fractions from selected topsoils along the chronosequence. The XRD curves were smoothed and corrected for Lorentz and polarization factors. *d*-spacings are given in nm. Given are the measured values (squares), modelled elementary curves and the modelled overall curve.

(0.1547 nm). Although not steadily, the contribution of the peak near 0.1495 nm (kaolinite) seemed to increase with time.

The oldest topsoil (t = 138 years) was characterised by a further decrease of the trioctahedral species (Fig. 6). In contrast to that, the dioctahedral range showed a relative increase.

4.4. DRIFT and structural features

FT-IR spectra (OH-bending regions; 600–900 cm^{-1}) of the clay fraction of the parent material (t = 0 year) and oldest topsoil (t = 138 years) are given in Fig. 7. Generally, the bands associated with hydroxyl groups can be discriminated from each other, and band assignment is straightforward. Furthermore, this region is not affected by the presence of residual water molecules (Vantelon et al., 2001). The peak at 652 cm^{-1} was quite pronounced in both soils (parent material and oldest soils). This band is usually attributed to octahedral Fe and Mg in 2:1 sheet silicates (Wilson, 1994). The weak peak at 681 cm^{-1} is attributed to Fe in dioctahedral smectite (Bishop et al., 2002). Near 694 cm^{-1}, the presence of dioctahedral smectite (Madejova and Komadel, 2001; Van der Marel and Beutelspacher, 1976) is confirmed already for the sample with t = 0 year as dioctahedral smectite usually shows values close to c. 700 cm^{-1} (Wilson, 1994). The peak at 748 cm^{-1} was attributed to vermiculite (Wilson, 1994) and was detected in both samples.

The band at 787 cm^{-1}, attributed to δFeMgOH (Vantelon et al., 2001), is less distinct in the older (and more weathered) sample (138 years). The quartz doublet was discernible as well (780 and 800 cm^{-1}; Farmer, 1974). The band at 829 cm^{-1} was assigned to δAlMgOH (Farmer, 1974). At 845 cm^{-1} a weak band attributed to calcite could be observed in the parent material. This peak was not detectable in the oldest topsoil.

Weak Si–O stretching bands, typical for trioctahedral sheet silicates, were detected at 1020 cm^{-1} and were less expressed in the 138 year old sample (Fig. 7b; Farmer, 1974; Madejova and Komadel, 2001; Van der Marel and Beutelspacher, 1976). Similarly, a weak Si–O band at circa 1030 cm^{-1} was found and attributed to newly-forming dioctahedral phases (Fig. 7b; Madejova and Komadel, 2001; Van der Marel and Beutelspacher, 1976).

In the OH-stretching region, additional evidences of mineralogical transformations were detected (Fig. 3). A weak band observed at circa 3618 cm^{-1} in the oldest topsoil was related to Al in dioctahedral structures, probably smectite (Farmer, 1974; Madejova and Komadel, 2001; Van der Marel and Beutelspacher, 1976). Of great interest was the peak near 3694 cm^{-1} that could be assigned to kaolinite. This vibration became more relevant in the older sample (138 years) and is a clear sign of pedogenic kaolinite formation (Wilson, 1994).

4.5. Mean layer-charge estimation

In general, the C18 treatment showed well-developed low charged phyllosilicates with a mean layer-charge value per half unit cell (ξ) ranging from 0.27 to 0.40 in the surface horizons of the investigated soils (Fig. 8).

Low-charged phyllosilicates (with ξ = 0.28 per half unit cell) were detected in the parent material (t = 0 year) and across the selected chronosequence (Fig. 8). High-charged phyllosilicates (ξ > 0.75) were also measured. They were partially attributed to geologically inherited smectite and vermiculite (Arocena et al.,

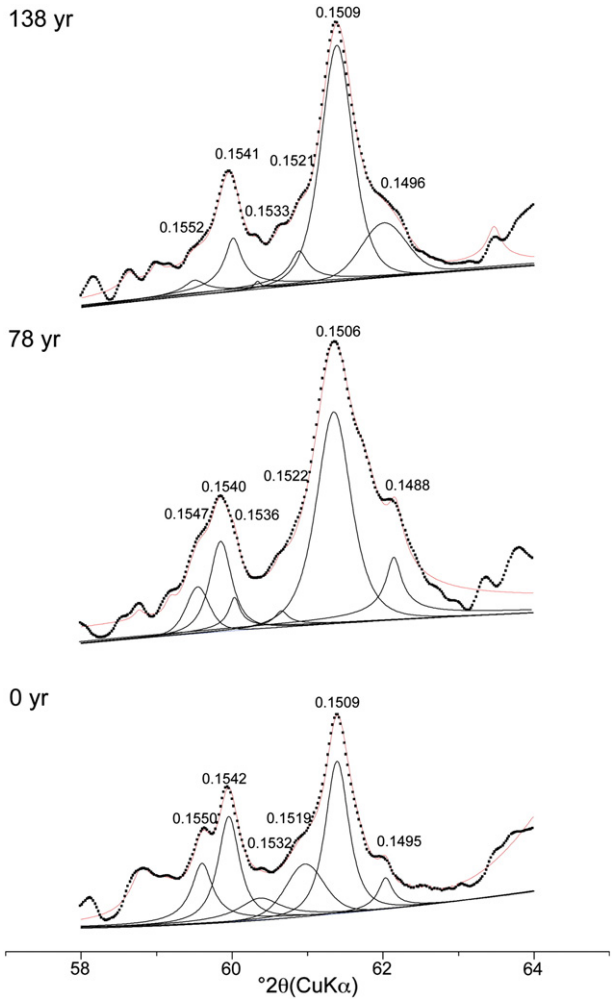

Fig. 6. XRD patterns in the d_{060} region of the soil clays from three investigated sites as a function of time. The peak range between 0.1560 and 0.1530 nm was assigned to trioctahedral and the one between 0.1530 and 0.1480 to dioctahedral phases. Given are the measured values (squares), modelled elementary curves and the modelled overall curve.

1994), respectively. The attribution of the source parent mineral can be performed after a peak splitting procedure. The peak representing low charges ($\xi < 0.6$) could be separated into several smaller peaks. In addition to the very low charge near 0.28, charges in the range of $\xi = 0.34–0.40$ could be detected.

4.6. Silt fraction

The XRD pattern of the fine silt fraction did not reveal major transformation reactions. The peak at 0.99 nm (Fig. 9) shows some weak reflections near 1.02 nm in the oldest soil. This is related to the initial formation of an interstratification within mica. The basal reflection at 1.40 nm seemed to be slightly lower in the oldest sample. This decrease is hypothesised to be due to a weak weathering of chlorite. All other detectable phyllosilicates seemed to be unaffected by the weathering process within the investigated time range.

5. Discussion

Chemical weathering led already within 138 years to traceable formations and transformations of clay-sized phyllosilicates in the investigated proglacial area. An undisturbed and relatively fast soil evolution was measured. A very small amount of smectite was detected already in the parent material. This presence might be due to hydrothermal formation or rock–water interactions that occurred below the glacier (Egli et al., 2001b). Its relative proportion in the soil clay fraction increased over time. Smectitic products could be the result of chlorite, mica and hornblende weathering, or the combination of both (Mirabella and Egli, 2003). Smectite can be taken as a kind of 'tracer-mineral' for weathering intensity in Alpine soils. Egli et al. (2001b, 2003) demonstrated for Swiss alpine regions that smectite and regularly interstratified mica/smectite are end products of chemical weathering of chlorite and mica in strongly acidified soil horizons.

Based on the area proportion and mineral intensity factors for individual minerals (Egli et al., 2003; Kahle et al., 2002), an approximate, relative quantification of the phyllosilicate distribution in the clay fraction was made possible. With time, smectite increased (Fig. 10). Furthermore, the relative concentrations of smectite and vermiculite were negatively correlated to the amount of biotite (Fig. 11). Smectites developed from trioctahedral mica which weathered in a first step to regularly or irregularly interstratified 2:1 clay minerals (hydrobiotite or HIV–mica). Hot citrate treatment allowed the detection of hydroxy-interlayered low-charge expandable minerals (HIS). HIS was mostly a transitory product in the weathering chain of chlorite or mica to smectite transformation (Fig. 8). HIS did not seem to be intercalated with other mineral phases.

Within the investigated chronosequence, a progressive transformation of trioctahedral phases to dioctahedral was discernible in the topsoil. The decrease of trioctahedral phases (mica and chlorite) is therefore related to the increase of dioctahedral phases such as smectite, vermiculite or even kaolinite. Progressive transformation of clay mineral structures led to a decrease of layer charge caused by the substitution of Al^{3+} and Fe^{3+} for Mg^{2+} in the octahedral sheet (Fig. 6; Mirabella and Egli, 2003). The pedogenetic smectites from the surface horizons generally included various interlayer charges that are in agreement with results of Gillot et al. (2001). The heterogeneity of smectites is related to the nature of their precursors. In most cases, the higher the weathering state of the investigated soils, the lower was the layer charge of smectite.

Noteworthy is the behaviour of kaolinite. In the dioctahedral range, the diagnostic peak was already detectable in the parent material. The specific peak area increased with the duration of pedogenesis. This finding is supported by the FT-IR measurements where an increase of the bands typical for kaolinite could be observed. Consequently, active kaolinite formation is already possible within the first decades of pedogenesis.

Minor changes in the layer charge distribution could be also measured with the time span of 138 years. The parent material predominately had charges near $\xi = 0.28$ and >0.75. Low charged clay minerals are usually rather formed during soil formation and weathering. The low charged minerals detected in the parent material either to a kind of weathering that occurred before the material was exposed to atmosphere or to some hydrothermally formed phases (Egli et al., 2001b). With time, it seems that some additional phases developed. Using the layer charges, some smectite transformation mechanisms can be hypothesised (Dreher and Niederbudde, 2000). A part of the newly formed smectite seems to derive from biotite (BDS) and another part from hornblende (HDS) and plagioclase (PDS; Aoudjit et al., 1995; Bétard et al., 2009). Hornblende-derived smectite (HDS) gives rise to a rather low charge (Fig. 8). Comparatively higher charges (i.e. $\xi > 0.4$ per $O_{10}(OH)_2$) are typical for a biotite-derived smectite (BDS; Egli et al., 2003). Soils with highly charged smectites (i.e. $\xi \geq 0.4$), the charge of which is located in the tetrahedrons closely to 100%, have a very high K selectivity (Dreher and Niederbudde, 2000). According to Bétard et al. (2009), weathering of plagioclase produces directly illite and high-charge smectite ('plagioclase-derived smectite' PDS; Fig. 8). Some of the detected smectite in the proglacial area probably is a direct transformation product of plagioclase.

After 48 years, layer charges near $\xi = 0.39$ and $\xi = 0.63$ were detected and attributed to newly-formed phases due to weathering

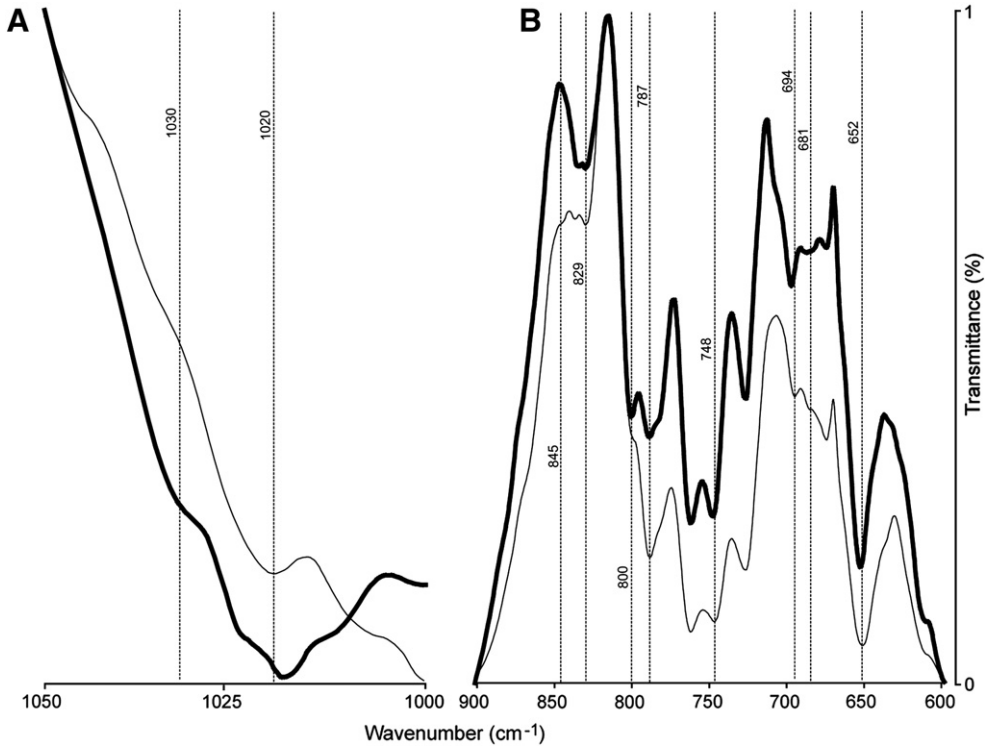

Fig. 7. Comparison of FT-IR spectra in the OH bending (A) and M–O region (B) between t = 0 year (thin line) and t = 138 years (thick line).

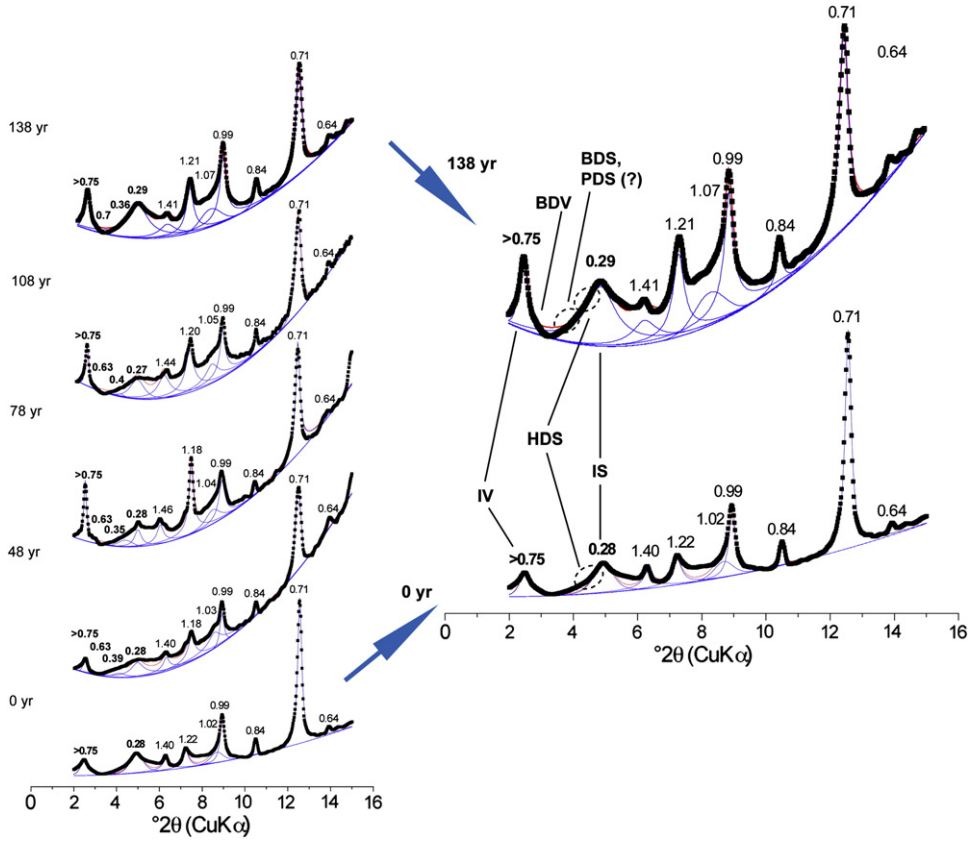

Fig. 8. XRD patterns of soil clays (<2 μm) along the chronosequence. Clays were treated with C18 (18-alkylammonium ion). The XRD-curves were corrected for Lorentz and polarization factors. *d*-spacings are given in nm. The bold numbers indicate the calculated layer charge per half unit cell. BDV = biotite derived vermiculite, HDS = hornblende derived smectite, IS = geologically inherited smectite, IV = inherited vermiculite, BDS = pedogenic biotite berived smectite, PDS = plagioclase derived smectite. Given are the measured values (squares), modelled elementary curves and the modelled overall curve.

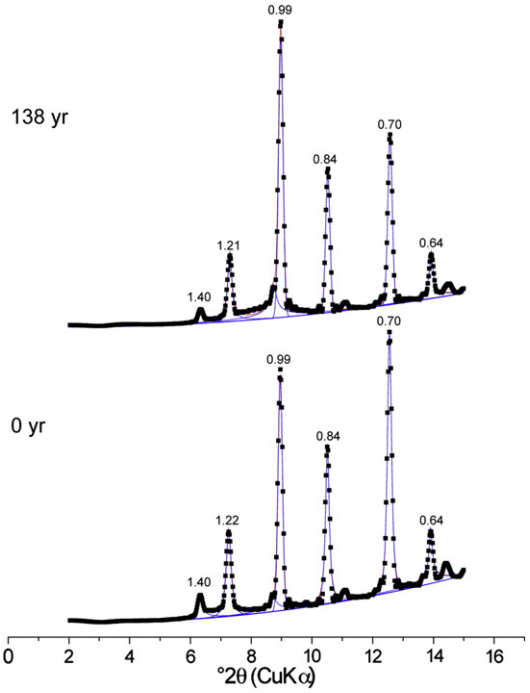

Fig. 9. XRD patterns of EG-solvated silt fractions (32–2 μm) from t = 0 year and t = 138 year topsoil. The XRD curves were smoothed and corrected for Lorentz and polarization factors. *d* spacings are given in nm. Given are the measured values (squares), modelled elementary curves and the modelled overall curve.

(Arocena et al., 1994). The layer charge ξ = 0.39 is a typical value for a pedogenic HDS, while ξ = 0.63 rather corresponds to a BDV (biotite-derived vermiculite) or probably to a BDS (Dreher and Niederbudde, 2000). This phenomenon was observed in all investigated topsoils, where newly-formed phases were detected. In general, geologically inherited smectite had a charge between ξ = 0.27 and 0.28 and biotite (or vermiculite) always ξ > 0.75. Pedogenic HDS usually showed a ξ of approximately 0.34, while BDV or BDS was detected with a charge of ξ = 0.63 (BDV, probably also BDS) or 0.40 (BDS). Higher values for smectite are typical for the initial stages of smectite formation in the soil and tend to decrease as a function of weathering (Mirabella and Egli, 2003).

Clay minerals in soils and weathered rocks are usually interpreted as secondary phyllosilicates derived from the transformation of primary rock-forming minerals with similar properties (e.g. mica) or as direct products of hydrothermal alteration of feldspar (i.e. sericite). Bétard et al. (2009) and also Aoudjit et al. (1995) were able

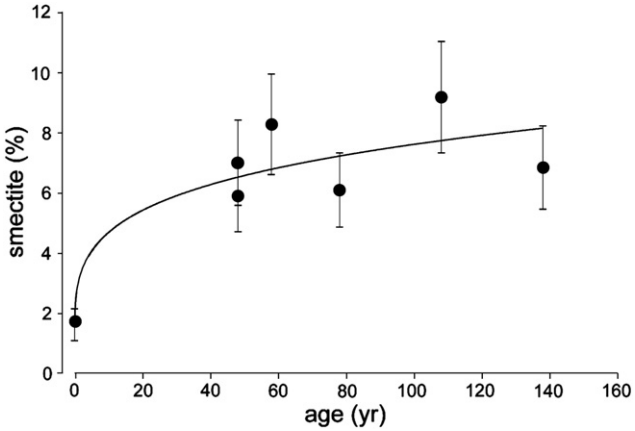

Fig. 10. Smectite content in the clay fraction along the chronosequence. Statistical significance (p) is <0.05.

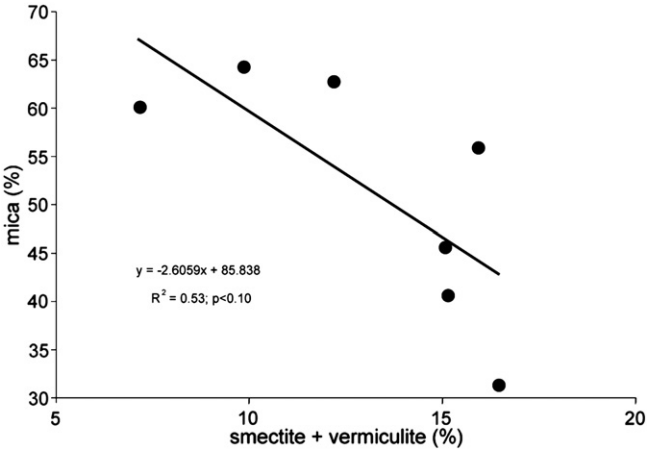

Fig. 11. Correlation between the sum of smectite and vermiculite and the mica content (clay fraction). Symbols: circles for topsoils, square for parent material. Statistical significance (p) is <0.10.

to show that the neoformation of clays inside plagioclase crystals occur after their partial dissolution in the weathering zone.

Mineralogical transformations were clearly linked to the grain size and consequently to the surface area and reactivity. Investigations of the 32–2 μm fraction revealed only relatively small variations within a time span of 140 years. The initial formation of an interstratified mica–vermiculite (or mica–HIV) phase is evidenced by a weak broadening of the 1.00 nm peak.

Data on clay-mineral formation in Alpine soils over a very short time span are scarce. We showed that mineral formation and transformation mechanisms are fast and consequently also detectable within a time span of <150 years. Smectite and kaolinite formation starts within the first decades. This finding is in agreement with the results of Caner et al. (2010). These authors investigated the soil evolution at the Oléron Island and evidenced a smectite formation (due to the weathering of illite) within <188 years. Weathering reactions and smectite formation were driven by the production of complexing organic acids during the decomposition of the pine-needle litter. These induced a rapid acidification and subsequently clay-mineral transformation in the sandy, poorly buffered parent material.

The investigated sites are on relatively stable landscape surfaces where erosion is insignificant compared with the rates of weathering advance. In such landscapes, when soils are young and rich in nutrients, weathering is also controlled by biological processes. Over short timescales, the impact of living organisms is quite apparent: rock weathering, soil formation and erosion, slope stability and river dynamics are directly influenced by biotic processes that mediate chemical reactions, dilate soil, disrupt the ground surface and add strength with a weave of roots (Dietrich and Perron, 2006). Brantley et al. (2011) hypothesise that on landscapes experiencing little erosion, biology drives weathering during initial succession, whereas weathering drives biology over the long term. This most probably applies also to the Morteratsch proglacial area and is the subject of ongoing investigations.

6. Conclusions

The clay mineral formation along a 0–150 year high Alpine chronosequence was studied. We made the following, principle findings:

- Within a relatively short period of time (<150 years), phyllosilicate transformations could be measured in the high Alpine proglacial area
- The mineral transformations were predominately restricted to the clay phase. Some minor transformations, i.e. the formation of a

mica–HIV (or mica–vermiculite) phase having a low proportion of HIV or vermiculite, could be measured in the fine silt fraction.
- With time, smectite and mixed-layered minerals (such as mica–HIV or mica–vermiculite) formed at the expense of biotite.
- Probably different sources contributed to the formation of smectite formation (biotite and probably also hornblende and plagioclase).
- HIS was formed as a transitory product of mica transformation.
- Active formation of kaolinite starts with the first decades of weathering.
- As a consequence of these transformations, the a) layer charge distribution changed over time with the formation of some new low- and high-charged phases and b) dioctahedral species increased at the expense of trioctahedral ones.

Recently deglaciated areas and cryic environments seem to be highly reactive. Using these new results and those of Egli et al. (2003) and Mavris et al. (2010), no humped function (soil production function; according to the concept of Gilbert (1877)) of the weathering intensity could be observed. Weathering intensity was high since the very beginning of soil formation and no retarding effects could be observed in the investigated environmental settings.

Acknowledgements

This research was supported by the Swiss National Foundation (SNF), project grant n. 200021-117568. We would like to thank B. Kägi and M. Hilf for the help in the laboratory.

References

Anderson, R.S., 2002. Modeling the tor-dotted crests, bedrock edges, and parabolic profiles of high alpine surfaces of the Wind River Range, Wyoming. Geomorphology 46, 35–58.
Anderson, S.P., Drever, J.I., Frost, C.D., Holden, P., 2000. Chemical weathering in the foreland of a retreating glacier. Geochimica et Cosmochimica Acta 64, 1173–1189.
Aoudjit, H., Robert, M., Elsass, F., Curmi, P., 1995. Detailed study of smectite genesis in granite saprolites by analytical electron microscopy. Clay Minerals 30, 135–148.
Arn, K., Hosein, R., Föllmi, K.B., Steinmann, P., Aubert, D., Kramers, J., 2003. Strontium isotope systematics in two glaciated crystalline catchments: Rhone and Oberaar glaciers (Swiss Alps). Swiss Bulletin of Mineralogy and Petrology 83, 273–283.
Arocena, J.M., Pawluk, S., Dudas, M.J., 1994. Layer charge of expandable 2:1 phyllosilicates in selected parent materials of some Canadian soils. Canadian Journal of Soil Science 74, 291–299.
Barnhisel, R.I., Bertsch, P.M., 1989. Chlorite and hydroxy-interlayered vermiculite and smectite, In: Dixon, J.B., Weed, S.B. (Eds.), Minerals in Soil Environments, 2nd ed. Soil Science Society of America, SSSA Book Series, 1, pp. 729–788. Madison, WI, USA.
Bétard, F., Caner, L., Gunnell, Y., Bourgeon, G., 2009. Illite neoformation in plagioclase during weathering: evidence from semi-arid Northeast Brazil. Geoderma 152, 53–62.
Bishop, J., Madejova, J., Komadel, P., Fröschl, H., 2002. The influence of structural Fe, Al and Mg of the infrared OH bands in spectra of dioctahedral smectites. Clay Minerals 37, 607–616.
Brantley, S.L., Megonigal, J.P., Scatena, F.N., Balogh-Brunstad, Z., Barnes, R.T., Bruns, M.A., Van Cappellen, P., Dontsova, K., Hartnett, H.E., Hartshorn, A.S., Heimsath, A., Herndon, E., Jin, L., Keller, C.K., Leake, J.R., McDowell, W.H., Meinzer, F.C., Mozdzer, T.J., Petsch, S., Pett-Ridge, J., Pregitzer, K.S., Raymond, P.A., Riebe, C.S., Shumaker, K., Sutton-grier, A., Walter, R., Yoo, K., 2011. Twelve testable hypotheses on the geobiology of weathering. Geobiology. doi:10.1111/j.1472-4669.2010.00264.x.
Büchi, H., 1987. Geologie und Petrographie der Bernina IX. Das Gebiet zwischen Pontresina und dem Morteratschgletscher. Unpubliziert Diplomarbeit Universität Zürich.
Büchi, H., 1994. Der variskische Magmatismus in der östlichen Bernina (Graubünden, Schweiz). Schweizerische Mineralogische und Petrographische Mitteilungen 74, 359–371.
Burga, C., 1999. Vegetation development on the glacier forefield Morteratsch (Switzerland). Applied Vegetation Science 2, 17–24.
Burga, C.A., Krüsi, B., Egli, M., Wernli, M., Elsener, S., Ziefle, M., Mavris, C., 2010. Plant succession and soil development on the foreland of the Morteratsch glacier (Pontresina, Switzerland): straight forward or chaotic? Flora 205, 561–576.
Caner, L., Joussein, E., Salvador-Blanes, S., Hubert, F., Schlicht, J.F., Duigou, N., 2010. Short-time clay-mineral evolution in a soil chronosequence in Oleron Island (France). Journal of Plant Nutrition and Soil Science 173, 591–600.
Conen, F., Yakutin, M.V., Zumbrunn, T., Leifeld, J., 2007. Organic carbon and microbial biomass in two soil development chronosequences following glacial retreat. European Journal of Soil Science 58, 758–762.
Cox, N.J., 1980. On the relationship between bedrock lowering and regolith thickness. Earth Surface Processes 5, 271–274.
D'Amico, C., Innocenti, F., Sassi, F. P., 1998. Magmatismo e Metamorfismo. Ed. UTET, Torino.
Dietrich, W.E., Perron, J.T., 2006. The search for a topographic signature of life. Nature 439, 411–418.
Dreher, P., Niederbudde, E.A., 2000. Characterization of expandable layer silicates in humic–ferralic cambisols (umbrept) derived from biotite and hornblende. Journal of Plant Nutrition Soil Science 163, 447–453.
Dümig, A., Smittenberg, R., Kögel-Knabner, I., 2011. Concurrent evolution of organic and mineral components during initial soil development after retreat of the Damma glacier, Switzerland. Geoderma 163, 83–94.
EDI (Eidgenössisches Departement des Innern), 1992. Hydrologischer Atlas der Schweiz (HADES). Landeshydrologie und -geologie. EDMZ, Bern.
Egli, M., Mirabella, A., Fitze, P., 2001a. Weathering and evolution of soils formed on granitic, glacial deposits: results from chronosequences of Swiss alpine environments. Catena 45, 19–47.
Egli, M., Mirabella, A., Fitze, P., 2001b. Clay mineral formation in soils of two different chronosequences in the Swiss Alps. Geoderma 104, 145–175.
Egli, M., Mirabella, A., Fitze, P., 2003. Formation rates of smectites derived from two Holocene chronosequences in the Swiss Alps. Geoderma 117, 81–98.
Egli, M., Mavris, C., Mirabella, A., Giaccai, D., Kägi, B., Haeberli, W., 2010. Soil organic matter formation along a chronosequence in the Morteratsch proglacial area (Upper Engadine, Switzerland). Catena 82, 61–69.
Ezzaïm, A., Turpault, M.-P., Ranger, J., 1999. Quantification of weathering processes in an acid brown soil developed from tuff (Beaujolais, France) Part II. Soil formation. Geoderma 87, 155–177.
Fanning, D.S., Keramidas, V.Z., El-Desoky, M.A., 1989. Micas, In: Dixon, J.B., Weed, S.B. (Eds.), Minerals in Soil Environment, 2nd Ed. Soil Science Society of America, Madison, WI, USA, pp. 551–634.
Farmer, V.C., 1974. Layer silicates. In: Farmer, V.C. (Ed.), Infrared Spectra of Minerals, Monograph, 4. Mineralogical Society, London, pp. 331–363.
Favilli, F., Egli, M., Brandova, D., Ivy-Ochs, S., Kubik, P., Cherubini, P., Mirabella, A., Sartori, G., Giaccai, D., Haeberli, W., 2009. Combined use of relative and absolute dating techniques for detecting signals of Alpine landscape evolution during the late Pleistocene and early Holocene. Geomorphology 112, 48–66.
Föllmi, K.B., Arn, K., Hosein, R., Adatte, T., Steinmann, P., 2009a. Biogeochemical weathering in sedimentary chronosequences of the Rhône and Oberaar Glaciers (Swiss Alps): rates and mechanisms of biotite weathering. Geoderma 151, 270–281.
Föllmi, K.B., Hosein, R., Arn, K., Steinmann, P., 2009b. Weathering and the mobility of phosphorus in the catchments and foefields of the Rhône and Oberaar glaciers, central Switzerland: implications for the global phosphorus cycle on glacial–interglacial timescales. Geochimica et Cosmochimica Acta 73, 2252–2282.
Gibbs, M.T., Kump, L.R., 1994. Global chemical erosion during the last glacial maximum and the present: sensitivity to changes in lithology and hydrology. Paleoceanography 9, 529–543.
Gilbert, G.K., 1877. Report on the Geology of the Henry Mountains. U.S. Geographical and Geological Survey of the Rocky Mountain Region, Washington, D.C.
Gillot, F., Righi, D., Räisänen, M.L., 2001. Layer-charge evaluation of expandable clays from a chronosequence of podzols in Finland using an alkylammonium method. Clay Minerals 36, 571–584.
Gjems, O., 1967. Studies on clay minerals and clay mineral formation in soil profiles in Scandinavia. Norske Skogfersøksvesen 81, 301–415.
Gustafsson, J.P., Bhhattacharya, P., Bain, D.C., Fraser, A.R., McHardy, W.J., 1995. Podzolisation mechanisms and the synthesis of imogolite in northern Scandinavia. Geoderma 66, 167–184.
Heimsath, A.M., Dietrich, W.E., Nishiizumi, K., Finkel, R.C., 1997. The soil production function and landscape equilibrium. Nature 388, 358–361.
Hosein, R., Arn, K., Steinmann, P., Adatte, T., Föllmi, K.B., 2004. Carbonate and silicate weathering in two presently glaciated, crystalline catchments in the Swiss Alps. Geochimica et Cosmochimica Acta 68, 1021–1033.
Humphreys, G.S., Wilkinson, M.T., 2007. The soil production function: a brief history and its rediscovery. Geoderma 139, 73–78.
IUSS Working Group WRB, 2006. World Reference Base for Soil Resources, World Soil Resources Reports No. 103 2nd edition. FAO (Food and Agriculture Organisation of the United Nations), Rome.
Jenny, H., 1980. The Soil Resource. Origin and Behavior. Ecological Studies, 37. Springer-Verlag, New York.
Kahle, M., Kleber, M., Jahn, R., 2002. Review of XRD-based quantitative analyses of clay minerals in soils: the suitability of mineral intensity factors. Geoderma 109, 191–205.
Karathanasis, A.D., 1988. Compositional and solubility relationships between aluminum-hydroxy interlayered soil-smectites and vermiculites. Soil Science Society of America Journal 52, 1500–1508.
Lanson, B., 1997. Decomposition of experimental X-ray diffraction patterns (profile fitting): a convenient way to study clay minerals. Clays and Clay Mineralogy 45 (2), 132–146.
Laves, D., Jahn, G., 1972. Zur quantitativen röntgenographischen Bodenton-Mineralanalyse. Archiv für Acker-, Pflanzenbau und Bodenkunde 16, 735–739.
Madejova, J., Komadel, P., 2001. Baseline studies of the clay minerals society source clays: infrared methods. Clays and Clay Minerals 49 (5), 410–432.
Mavris, C., Egli, M., Plötze, M., Blum, J.D., Mirabella, A., Giaccai, D., Haeberli, W., 2010. Initial stages of weathering and soil formation in the Morteratsch proglacial area (Upper Engadine, Switzerland). Geoderma 155, 359–371.
Mirabella, A., Egli, M., 2003. Structural transformations of clay minerals in soils of a climosequence in an Italian Alpine environment. Clays and Clay Minerals 51 (3), 264–278.
Moore, D.M., Reynolds Jr., R.C., 1997. X-Ray Diffraction and the Identification and Analysis of Clay Minerals, 2nd edition. Oxford University Press, New York.
Niederbudde, E.A., Kussmaul, H., 1978. Tonmineraleigenschaften und –Umwandlungen in Parabraunerde-Profilpaaren unter Acker und Wald in Süddeutschland. Geoderma 20, 239–255.
Olis, A.C., Malla, P.B., Douglas, L.A., 1990. The rapid estimating of the layer charges of 2:1 expanding clays from a single alkylammonium ion expansion. Clay Minerals 25, 39–50.

Olsson, M.T., Melkerud, P.-A., 2000. Weathering in three podzolized pedons on glacial deposits in northern Sweden and central Finland. Geoderma 94, 149–161.
Schwertmann, U., Niederbudde, E.A., 1993. Tonmineralbestimmung in Böden. In: Jasmund, K., Lagaly, G. (Eds.), Tonminerale und Tone. Struktur, Eigenschaften, Anwendung und Einsatz in Industrie und Umwelt. Steinkopff Verlag, Darmstadt, pp. 255–265.
Tamura, T., 1958. Identification of clay minerals from acid soils. Journal of Soil Science 9, 141–147.
Trommsdorff, V., Dietrich, V., 1999. Grundzüge der Erdwissenschaften. vdf-Verlag, 6. Auflage, Zürich, Switzerland.
Turpault, M.-P., Righi, D., Utérano, C., 2008. Clay minerals: precise markers of the spatial and temporal variability of the biogeochemical soil environment. Geoderma 147 (3–4), 108–115.
Van der Marel, H.W., Beutelspacher, H., 1976. Atlas of Infrared Spectroscopy of Clay Minerals and Their Admixtures. Elsevier Scientific Publishing Company, Amsterdam-Oxford-New York.
Vantelon, D., Pelletier, M., Michot, L.J., Barres, O., Thomas, F., 2001. Fe, Mg and Al distribution in the octahedral sheet of montmorillonites. An infrared study in the OH-bending region. Clay Minerals 36, 369–379.
Wadham, J.L., Cooper, R.J., Tranter, M., Hodgkins, R., 2001. Enhancement of glacial solute fluxes in the proglacial zone of a polythermal glacier. Journal of Glaciology 47, 378–386.
Wilkinson, M.T., Chappell, J., Humphreys, G.S., Fifield, K., Smith, B., Hesse, P.P., 2005. Soil production in heath and forest, Blue Mountains, Australia: influence of lithology and palaeoclimate. Earth Surface Processes and Landforms 30, 923–934.
Wilson, M.J., 1994. Clay Mineralogy: Spectroscopic and Chemical Determinative Methods. Chapman & Hall, London.

Geoderma 164 (2011) 11–21

Contents lists available at ScienceDirect

Geoderma

journal homepage: www.elsevier.com/locate/geoderma

Fast but spatially scattered smectite-formation in the proglacial area Morteratsch: An evaluation using GIS

Markus Egli [a,*], Michael Wernli [b], Conradin Burga [a], Christof Kneisel [c], Christian Mavris [a], Giuseppe Valboa [d], Aldo Mirabella [d], Michael Plötze [e], Wilfried Haeberli [a]

[a] Department of Geography, University of Zürich, Winterthurerstrasse 190, 8057 Zürich, Switzerland
[b] Institute of Natural Resource Sciences, Zurich University of Applied Sciences, Grüental, 8820 Wädenswil, Switzerland
[c] Department of Physical Geography, University of Würzburg, Am Hubland, 97074 Würzburg, Germany
[d] Istituto Sperimentale per lo Studio e la Difesa del Suolo, Centro di ricerca per l'agrobiologia e la Pedologia CRA-ABP, Piazza D'Azeglio 30, 50121 Firenze, Italy
[e] Institute for Geotechnical Engineering, ETH Zurich, CH-8093 Zurich, Switzerland

ARTICLE INFO

Article history:
Received 24 November 2010
Received in revised form 8 April 2011
Accepted 1 May 2011
Available online 1 June 2011

Keywords:
Smectite
Proglacial area
Temporal evolution
Topography
Vegetation
Humus form

ABSTRACT

Proglacial areas in the Alps usually cover a time span of deglaciation of about 150 years (time since the end of the 'Little Ice Age' in the 1850s). In these proglacial areas soils have started to develop. Due to the continuous retreat of the Morteratsch glacier (Swiss Alps), the corresponding proglacial area offers a continuous time sequence from 0 to 150 year-old surfaces. Furthermore, an optimal digital dataset about the development of vegetation and soils is available for this area. The soils have been developing on glacial till having a granitoidic character. We investigated the clay mineral assemblage at 35 sites within the glacier forefield. Smectite can be used as a proxy for weathering intensity in these environments. In the proglacial area, the smectite concentration in the topsoil steadily increased with time of weathering; however, this development displayed a strongly scattered trend. The complex interplay of biological, physical, and chemical processes in pedogenesis and clay mineral evolution limits our ability to predict and interpret landscape dynamics. We consequently tried to analyse the role of topographic and vegetation modifications on the smectite content. Sites not or only slightly prone to erosion (flattening slope ridge, steepening slope ridge) or flat morphology promoted the formation of smectite. In addition, the texture of the soil material influenced soil moisture and hence the degree of weathering and the development of vegetation. Although vegetation is not a fully independent factor, because it is interrelated to the surrounding environmental conditions, it seemed to exert its influence on weathering and, consequently, the formation of smectite. Green alder stands and grass heath, where moister soils develop that have a finer texture or where more organic acids are produced, were correlated with a higher smectite content. Humus forms serve as a proxy for the soil biota and soil organic matter composition. At sites having a Eumoder and a higher soil organic matter content, the smectite concentration was elevated. At these sites, the production of chelating compounds or organic acids in the soil is believed to promote the development of smectites via an intermediate stage of hydroxy-interlayered minerals and the subsequent removal of the hydroxide polymers. In this work we have demonstrated that the topographic signature and the effect of vegetation on the formation of smectite and consequent weathering are pervasive. Our results will serve as a basis for further spatio-temporal modelling.

1. Introduction

Weathering in cold regions has often focused on the notion of 'cold'. As a result of this approach, the predominating perception in terms of weathering has been that mechanical processes predominate, with freeze-thaw weathering as the prime agent and that chemical processes are temperature-inhibited, often to the point of non-occurrence. Indeed, many cold regions show similar or even more intense weathering assemblages than those in warmer regions (e.g. Föllmi et al., 2009a,b; Hall et al., 2002). Contrary to popular presentations, several investigations meanwhile document that weathering in cold Alpine regions, including chemical weathering, is not strictly temperature-limited but rather controlled by moisture availability (Egli et al., 2006). Furthermore, the availability of fresh mineral surfaces that are provided by physical erosion determines chemical weathering rates. Glaciers and periods of glaciation may have a significant impact on global weathering, changing the interplay between physical and chemical weathering processes by putting large volumes of dilute meltwaters and fine-grained sediments in contact with each other (Arn et al., 2003; Föllmi et al., 2009a,b). Glaciers are

* Corresponding author. Tel.: +41 44 635 51 14; fax: +41 44 635 68 48.
E-mail address: megli@geo.unizh.ch (M. Egli).

0016-7061/$ – see front matter © 2011 Elsevier B.V. All rights reserved.
doi:10.1016/j.geoderma.2011.05.001

significant agents of physical erosion; for example, the mechanical denudation of glacierised valleys in Alaska, Norway and the Alps is an order of magnitude greater than that in equivalent non-glacierised basins (Föllmi et al., 2009b; Hallet et al., 1996).

Chemical weathering intensities depend mainly on the lithology (e.g. highly reactive minerals such as carbonates and sulphates vs. crystalline rocks), the accumulation of organic matter (Conen et al., 2007), the rate of supply of fresh rock material, the age of exposure, and the character of the hydrological drainage system. In cryic, ice-free environments, chemical weathering can be an active process leading to the formation of clay minerals (e.g. He and Tang, 2008; Simas et al., 2006). In arctic tundra and partially also in Alpine regions, soil formation and weathering processes may be spatially highly patterned. Cryoturbation and other cryogenic processes produce stripes, non-sorted polygons, earth hummocks etc. Cryogenesis is a controlling factor in patterned ground formation resulting in cryoturbated soil profiles, cryostructures and carbon sequestration (Haugland, 2004; Ping et al., 2008; Ugolini, 1986). Frost disturbance interrupts soil-forming processes and produces a time-lag effect of pedogenesis at such sites compared to soils that are not affected by permafrost (Haugland, 2004).

With respect to chemical weathering, several studies have shown that smectitic constituents can be taken as an indicator of weathering intensity in Alpine soils and cold regions (Egli et al., 2001a,b, 2003a,b, 2006; Righi et al., 1999). Investigations of Egli et al. (2001a) have revealed that the greatest changes in soil chemistry of Alpine soils on granitic host material occur within the first 3000–4000 years of soil development. Element leaching rapidly slows down after this period. Extensive mineral weathering usually results in significant losses of chlorite and mica and the corresponding formation of smectite and regularly and irregularly interstratified mica-smectite. Highest weathering and transformation rates of clay minerals should be measured at the initial stage of soil formation (Egli et al., 2003a; Mavris et al., 2010). Similarly, Föllmi et al. (2009a,b) and Hosein et al. (2004) have shown that biotite weathering in young soils was generally much higher than in old soils (11,000 years). Calculated weathering rates of biotite were several orders of magnitude higher than known field weathering rates. This seems to be due to the predominance of fine-grained (<63 μm) particles in glacial sediments that are mechanically disaggregated and preferentially leached.

Proglacial environments are important for the understanding of global CO_2 cycling on glacial/interglacial timescales as they made up a significant amount of the global land surface during the Quaternary due to the advance and retreat of glaciers and ice sheets (Gibbs and Kump, 1994).

Soils in proglacial areas in the Alps are young and have been forming over a time span of about 150 years (the time since the end of the 'Little Ice Age' in the 1850 s; Fitze, 1982). The proglacial areas are in most cases defined as the zone between the present-day glacier and the terminal moraines deposited in the 1850s. The aim of our research was to examine whether changes of the smectite content along a temporal gradient of very young and consequently reactive soils can be determined. Furthermore, our aim was to relate the concentrations and changes of clay minerals not only to the soil-forming factor time but also other extrinsic factors such as topography and vegetation (Jenny, 1941) with the help of geographic digital datasets.

2. Investigation area

The soils studied lie within the proglacial area of Morteratsch in the Upper Engadine (Switzerland). The border of the proglacial area is given by terminal moraines deposited in the 1850s during the 'Little Ice Age' (Figs. 1 and 2). The actual length of this proglacial area is approx. 2 km and has an area of 1.8 km^2. The proglacial area is in a valley that runs N–S. The altitude ranges from 1900 m asl to about 2100 m asl. The backwall of the glacier is formed by the high mountain peaks of the South Raetian Alps such as Piz Bernina (4049 m asl, the highest peak of the Grisons and the Eastern Alps) and Piz Palü (3901 m asl). Alpine glaciers have fluctuated during the last 12,000 years near the terminal moraines formed in the year 1850 indicating more or less similar climatic (having mean annual temperature fluctuations in the range of 1–1.5 °C) and hydrologic conditions within that period. This has been shown by many geomorphologic and climatic studies (cf. Burga and Perret, 1998; Gamper, 1985; Keller, 1994; Magny, 1992; Maisch, 1992; Patzelt, 1977; Renner, 1982). The glacial till in the glacier forefield consists of granitic and gneissic material and was produced through glacial transport within a small area of relatively homogeneous parent material. The lithostratigraphic units are mainly the Bernina- and Stretta-crystalline (Büchi, 1994; Spillmann, 1993). The parent material was greenschist facies overprinted (Trommsdorff and Dietrich, 1999). Present climatic conditions for the Morteratsch site are approx. 0.5 °C mean annual air temperature and approx. 1000–1300 mm mean annual precipitation as calculated by using data from the nearby meteorological stations Samedan and Bernina.

3. Materials and methods

3.1. Digital data basis and procedure

3.1.1. Soil map

The soil map has a scale of 1:10,000 (Egli et al., 2006; Fig. 2). Soil cartography and classification were performed according to the FAL (Swiss soil classification system; Brunner et al., 1997). Soil units were translated into the WRB system (IUSS Working Group, 2006). Soil mapping already includes a certain generalisation as small-scale variations (approx. <100 m^2) could not be considered. The map items included soil type, soil depth (per unit area) relevant for plant growth (= soil volume − skeleton volume − groundwater volume; result is related to depth instead of volume), parent material, vegetation, topography, soil hydrology, terrain form, pH-value, soil organic matter content, soil skeleton (material >2 mm as a whole), gravels and stones (gravelly: predominantly material <5 cm in diameter; stony: predominantly material >5 cm in diameter), granulometry, soil structure and humus form. The soils vary from Lithic Leptosols to Dystric Cambisols according to the World Reference Base for Soil Resources (WRB) soil classification (IUSS Working Group, 2006). In total, 47 soil pits were made and described in detail and used as reference profiles for mapping. The number of profiles varied according to the area of the soil units: 1 for Endogleyic Cambisol, 3 for Dystric Cambisol, 18 for Humi-Skeletic Leptosol (including Ranker), 3 for Haplic Fluvisol Endoskeletic and 22 for Skeletic/Lithic Leptosol. Ten pits (that are related to a botanical monitoring; Burga, 1999) were excavated for the chemical and physical analysis of the soil material.

3.1.2. Vegetation map

The first detailed vegetation map (scale 1:10,000) of the glacier forefield Morteratsch was established by Bäumler (1988). A slightly generalised map on a smaller scale (1:13,700) of the actual vegetation cover (modified and completed after Fischer, 1999) gives an overview of the vegetation pattern in the glacier foreland (Fig. 2). Generally, three plant species groups were distinguished (Burga, 1999): a) pioneer species, starting early in the chronosequence and reaching their optimum in early or medium stages, b) subalpine forest and dwarf-shrub/grass heath species — most of them starting in later stages, c) species occurring mainly in alpine grassland having different distributions and optima along the gradient. Burga (1999) established ten permanent plots within the glacier foreland to monitor the vegetation dynamics of deglaciated areas. With the help of the vegetation cover of permanent plots and the time since ice retreat (chronosequence 1857–1997), a generalised model of primary plant succession could be established (Burga et al., 2010).

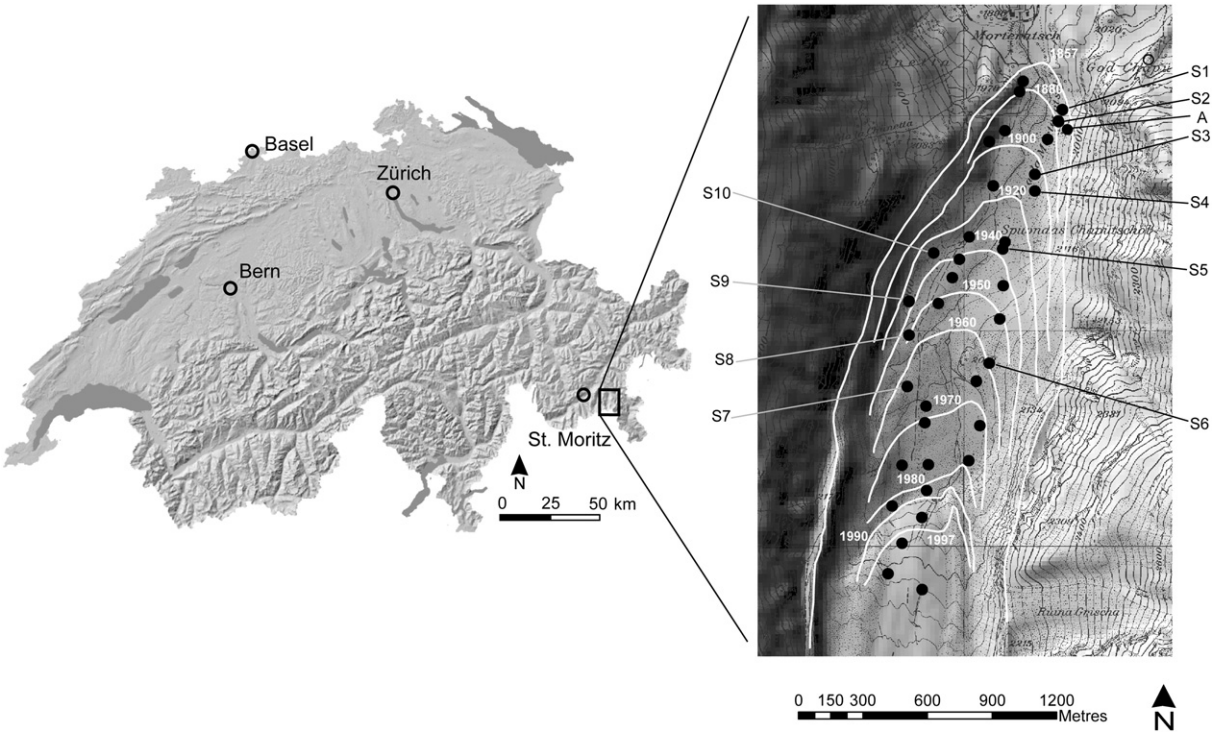

Fig. 1. Location of the Morteratsch proglacial area with isochrones of glacier retreat and position of the topsoil sampling sites (clay mineralogy). Eleven sites were analysed in detail regarding soil chemistry and mineralogy (S1–10, A; Mavris et al., 2010). At the other 24 sites, only the mineralogical composition was measured.

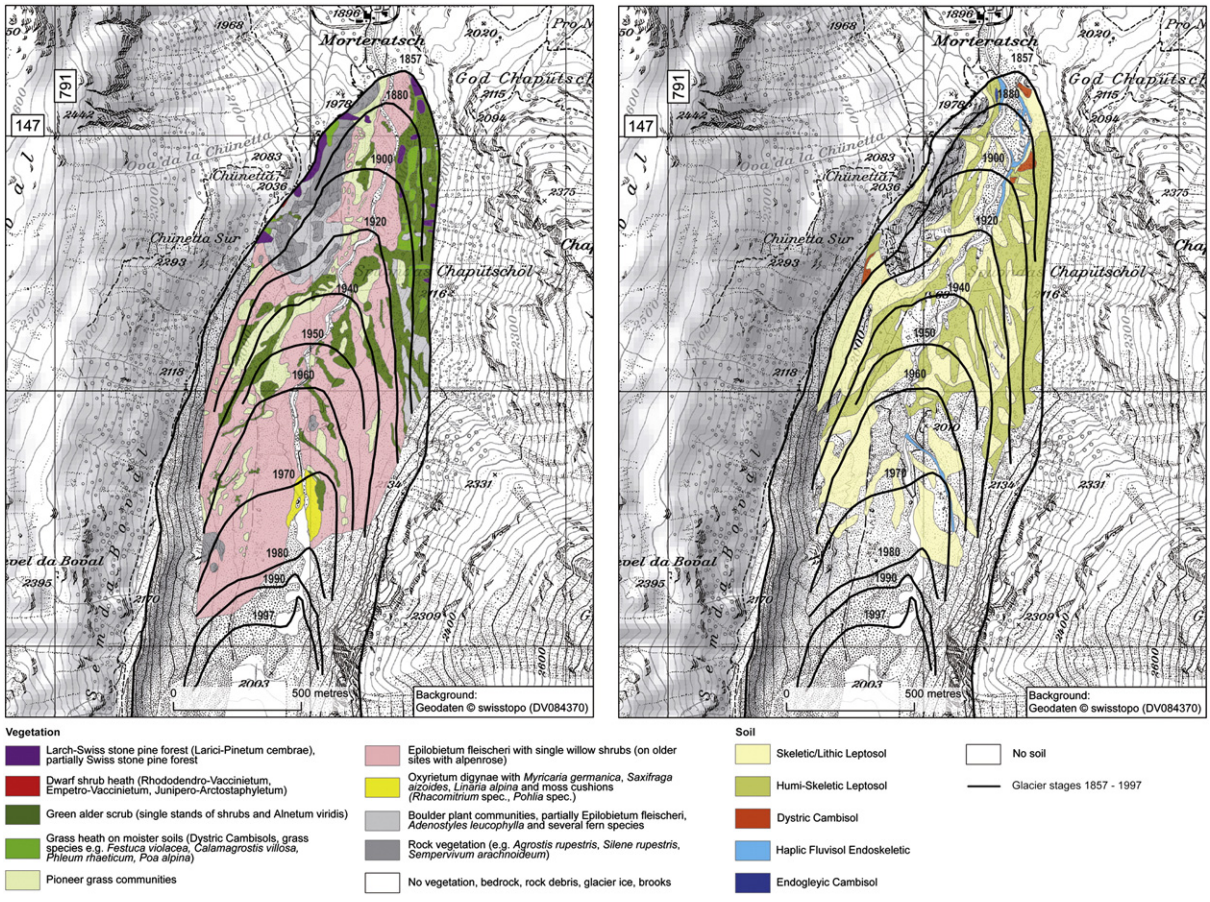

Fig. 2. Spatial distribution of the soil and vegetation units in the proglacial area.

3.2. Soil sampling and mineral analyses

With respect to the clay mineralogy, surface soil samples (topsoils) were collected from 35 soil pits distributed over the whole proglacial area (Fig. 1) forming a soil chronosequence ranging from 0 to 150 years. For each sample, approximately 1–2 kg of material was collected. Eleven of these sites were analysed in detail for both soil chemistry and mineralogy (Mavris et al., 2010). At the other 24 sites, only the mineralogical composition was measured in detail. Soil chemical data of additional 10 soil pits (cf. Mavris et al., 2010) also served as a basis for the soil map (see above), For the GIS analyses (see below) soil acidity, texture, soil organic matter, soil thickness and humus form were retrieved from the soil map.

The soil clay fraction (<2 μm) of all 35 sites was obtained after destruction of organic matter with dilute and Na-acetate buffered H_2O_2 (pH 5) by dispersion with Calgon and sedimentation in water (Jackson, 1956). Oriented specimens on glass slides were analysed by X-ray diffraction using Cu-*K*α radiation (3-kW Rigaku D/MAX III C diffractometer, equipped with a horizontal goniometer and a graphite monochromator) from 2 to 15°2θ with steps of 0.02°2θ at 2 s/step. The following treatments were performed: Mg saturation, ethylene glycol solvation (EG) and K saturation. The K-saturated samples were, after XRD measurement at room temperature, heated for 2 h at 335 and 550 °C.

When chlorite was present, the presence of kaolinite was checked with FT-IR (Brooker Optics, Tensor 27) analysis (OH-stretching region near 3695 cm^{-1}) on powder samples (3% ground soil material, 97% KBr) heated at 80 °C for ≥2 h. Digitised X-ray data were smoothed and corrected for Lorentz and polarisation factors (Moore and Reynolds, 1997). Diffraction patterns were smoothed by a Fourier transform function and fitted by the Origin™ PFM program using the Pearson VII algorithm. Background values were calculated by means of a non-linear function (polynomial 2nd order function; Lanson, 1997).

The semi-quantitative estimation of phyllosilicate concentration was performed by the combination of the areas of the ethylene glycol solvated, the Mg-saturated, the K-saturated and the heated (335 °C and 550 °C) samples. On the basis of the obtained integrals, an estimate of clay minerals composition was performed. The sum of the areas between 2 and 15°2θ, which were attributed to HIV (hydroxy interlayered vermiculites), smectite, vermiculite, mica, chlorite and kaolinite, were normalised to 100%. Although the (semi-)quantification of clay minerals in soils is plagued by manifold problems (Kahle et al., 2002), the applied and standardised (sample preparation, treatments, measurement and calculation) procedure enabled the assessment of the variability of clay mineral assemblage amongst the sites.

3.3. Area statistics

Area calculations (proportion of different soil types between two isochrones and in relation to either time, topographic or vegetational features) and statistics (regression analyses) were performed using ArcGIS 9.3 (ESRI) with modules programmed in Visual Basic for Applications (VBA). Input data sets were the digital soil and vegetation maps, the glacial states (Burga, 1999) and the digital elevation model (raster of 20 m) within the proglacial area. The calculations were done raster based (GRID, 20 m resolution).

The landscape forms (Tables 1 and 2), slope (Table 3) angle and exposure were related to the clay mineral composition. The different exposures were defined as follows: north (315–45°N), south (135–225°N), east (45–135°N) and west (225–315°N). Furthermore (and similar to a previous work; Egli et al., 2006), the exposures were simplified to north and south with north-facing defined as >270–90°N and south-facing as >90–270°N. Relative area calculations refer to the area between two isochrones of deglaciation (Figs. 1 and 2). In total, 11 different glacial states (with corresponding isochrones) could be distinguished (Burga, 1999).

Table 1
Description of landscape forms derived from the digital elevation model.

Landscape form	Landscape code	Landscape form: perpendicular to slope (planform curvature)	Landscape form: direction of slope (profile curvature)
Depressions	10	Concave	Concave
Foot of the slope, flattening slope	20	Planar	Concave
Flattening slope ridge	30	Convex	Concave
Valley shape	40	Concave	Planar
Flat slope	50	Planar	Planar
Steepening slope ridge	60	Convex	Planar
Steepening valley	70	Concave	Convex
Steepening slope	80	Planar	Convex
Ridges	90	Convex	Convex

Table 2
Reclassification of landscape forms (in terms of theoretical gains and losses of material).

Landscape form	Code	Landscape code (see Table 1)
Accumulation	12	10 + 20
Slight erosion possible	36	30 + 60
Erosion	89	80 + 90
Flat slope (accumulation and erosion)	50	50
Valley form	47	40 + 70

Following the suggestions of Winkler (2000), we used a standard error based on the standard deviation in a 95% confidence interval to get statistically significant differences between the data populations:

$$x \pm 1.96 \times \sqrt{(\sigma / \sqrt{n})} \quad (1)$$

where x is the arithmetic mean, σ the standard deviation and n corresponds to the number of measurements.

The clay minerals data distribution (whole dataset as well as dataset of individual classes; see the Results Section) was checked for normal distribution using a Shapiro–Wilk test (SigmaPlot 11.0). Almost all datasets (whole datasets as well as datasets within the individual classes) were not significantly different from a normal distribution. This justifies the above-stated approach of using the standard error and confidence interval.

4. Results

4.1. Vegetation and soil development

The different vegetation units of the proglacial area are given in Table 4. Primary plant succession of the pro-glacial area with its predominantly siliceous parent material starts with the pioneer plant communities Oxyrietum digynae and Epilobietum fleischeri and ends

Table 3
Classification of the slope.

Class	Slope (°)
1	0–3
2	3–6
3	6–9
4	9–14
5	14–19
6	19–27
7	27–37

Table 4
Vegetation units of the proglacial area Morteratsch.

ID	Vegetation type	Description
0	No vegetation, bedrock, rock debris, glacier ice, brooks	No vegetation, bedrock, rock debris, glacier ice, brooks
1	Oxyrietum digynae with Myricaria germanica, Saxifraga aizoides, Linaria alpina and moss cushions (Rhacomitrium spec., Pohlia spec.)	*Oxyria digyna*, *Linaria alpina*, *Saxifraga bryoides*, *Cerastium uniflorum*, *Cardamine resedifolia*, *Poa alpina*, *P. nemoralis*
2	Pioneer grass communities	Geo montani-Nardetum and *Poion alpinae*
3	Epilobietum fleischeri with single willow shrubs and Alpenrose	*Epilobietum fleischeri* with single willow shrubs and Alpenrose
4	Green alder scrub (Alnetum viridis)	*Alnus viridis* and tall perennial herbs, *Salix spec.*, *Poa spec.*, *Deschampsia caespitosa*, *Avenella flexuosa*, *Nardus stricta*, *Festuca spec.*, *Phleum rhaeticum*, *Anthoxanthum alpinum*, *Calamagrostis villosa*
5	Grass heath on moister soils	grass species e.g. *Festuca violacea*, *Calamagrostis villosa*, *Phleum rhaeticum*, *Poa alpina*
6	Boulder plant communities, partially Epilobietum fleischeri	*Epilobium fleischeri*, *Adenostyles leucophylla*, *Rumex scutatus*, *Dryopteris spec.*, *Athyrium spec.*, *Gymnocarpium dryopteris*, *Polystichum lonchitis*
7	Rock vegetation	*Agrostis rupestris*, *Silene rupestris*, *Sempervivum arachnoideum*
9	Larch-Swiss stone pine forest (Larici-Pinetum cembrae), partially Swiss stone pine forest	*Pinus cembra*, *Larix decidua*, *Rhododendron ferrugineum*, *Luzula sylvatica*, *Calamagrostis villosa*, *Vaccinium spec.*, *Clematis alpina*, *Homogyne alpina*, *Oxalis acetosella*, *Avenella flexuosa*
12	Dwarf shrub heath	Rhododendro-Vaccinietum, Empetro-Vaccinietum, Junipero-Arctostaphyletum

with the larch/Swiss stone pine forest (Larici-Pinetum cembrae) after substantially more than 150 years. The first plants, i.e. *Epilobium fleischeri*, *Oxyria digyna*, *Linaria alpina*, *Saxifraga aizoides*, *Rumex scutatus*, appear about 7 years after deglaciation and reach greater cover-abundance values (about 5–25%) after about 27 years. The first species of the short-living Oxyrietum digynae appears approx. 10 years after deglaciation and disappears approx. 30 years later. The first small larch trees, the first shrubs of willows and green alder and the first dwarf-shrubs (e.g. the rust-leaved alpenrose) are found on areas that have been ice-free for about 12 to 15 years (Fig. 2). The establishment of *Larici-Pinetum cembrae* takes place after about 77 years. Surprisingly, lichens such as *Stereocaulon* cf. *dactylophyllum* need about 15–20 years to establish their first populations (Burga et al., 2010).

The dominant soil units (some sites do not have a soil) in the proglacial area are Haplic Fluvisols Endoskeletic, Skeletic or Lithic Leptosols, Humi-skeletic Leptosols (Fig. 2), including some sites with Ranker (IUSS Working Group, 2006), that have a weak B horizon and Dystric and Endogleyic Cambisols (endoskeletic). The young soils that are close to the glacier showed almost no morphologic signs of chemical weathering and alteration products. They were usually characterised by a very thin and often discontinuous humus layer (Fig. 2). The oldest soils (150 years) often had a spatially continuous layer (O or A horizon) with organic matter and some signs of weathering-product formation (formation of Fe- and Al-oxyhydroxides, start of clay mineral formation/transformation) and, thus, a weakly developed B horizon (data shown in Table 2 of Mavris et al., 2010).

4.2. Smectite formation

To give an impression of the clay development in the proglacial area, the X-ray diffraction patterns of a soil clay material in direct proximity to the glacier and a surface soil sample having an age of 140 years are compared (Fig. 3). The XRD pattern of the material that was very recently exposed to weathering (t = 0) showed distinct and sharp reflections at 1.42, 1.23, 0.99 and 0.71 nm. Furthermore a very weak peak near 1.64 nm could be observed after ethylene glycol (EG) solvation. The peak at 0.85 nm can be attributed to amphibole and the

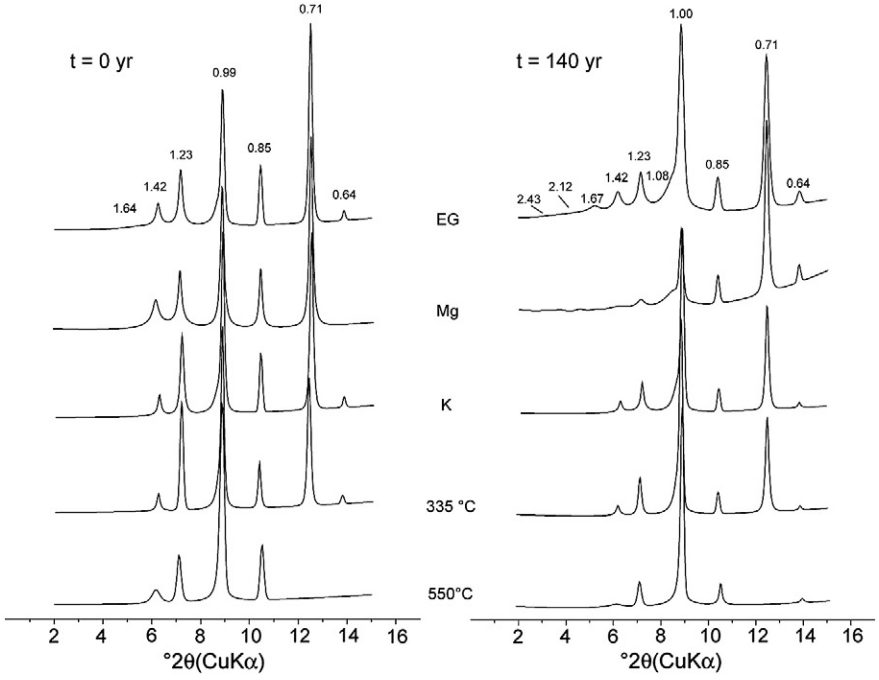

Fig. 3. XRD patterns of soil clays (<2 μm) of the soil material close to the glacier front (having an age of 0 years) and the surface horizon of a soil having an age of 140 years. The XRD-curves were smoothed and corrected for Lorentz and polarisation factors. *d*-spacings are given in nm. EG = ethylene glycol solvation, Mg = Mg-saturation, K = K-saturation and corresponding heating treatments.

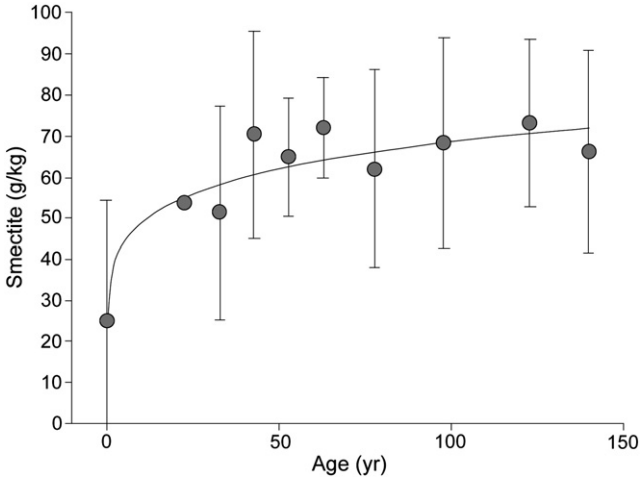

Fig. 4. Temporal evolution of the smectite content (mean values and standard error per time zone; no standard error is given if $n \leq 2$) in the clay fraction.

one at 0.64 nm to plagioclase. Together with the other diagnostic treatments (K-saturation, heating at 335 °C and 550 °C), the clay minerals mica, chlorite, interstratified mica-HIV and traces of an expandable mineral (smectite) could be discerned. After 140 years, the XRD pattern of the clay fraction slightly changes. The peak at 1.67 nm (smectite) after EG solvation is more pronounced. Furthermore, a broadening of the 1.00 nm peak (with another peak near 1.08 nm) could be detected showing that mica is weathering. All other clay phyllosilicates were also detected. It seems that the concentration of chlorite also decreased slightly (Fig. 3; heating at 550 °C).

In principle, a significant ($p = 0.033$) trend could be observed along the investigated chronosequence (Fig. 4): the content of smectite increased with increasing exposure age of the substrate. Traces of smectite could already be detected in the parent material. The variability of the smectite concentration along this sequence was, however, considerable.

Mineral weathering started immediately at the beginning of soil formation and resulted in a significant loss of mica and a corresponding formation of smectite (Fig. 5). Chlorite also exhibits a decreasing (but statistically not significant) tendency when compared to smectite. Although the soils were very young and the concentration of smectite was rather low, measurable changes occurred within a very short period of time.

4.3. Effect of topographic and vegetational features on smectite formation

The patterned distribution of the soils (especially at their earliest stage) suggests that the soil-forming conditions were not identical everywhere. On a larger scale, the mineralogy and chemistry of the parent material in the proglacial area can be considered to be more or less constant. In this case, the parent material can, thus, be supposed to have a negligible influence as pedogenic factor (Jenny, 1941) in the differentiation of the soils across the selected sites. Also climate does not vary greatly in the area of interest and can therefore be considered a negligible factor.

The vegetation seemed to influence the development of smectite and other phyllosilicates (Fig. 6). The lowest smectite content was measured on sites without vegetation. A measureable, but statistically insignificant, increase in the smectite content was evident over the entire range from the pioneer grass communities to the Epilobietum fleischeri having single willow shrubs and alpenrose and finally to the green alder scrub (Alnetum viridis). Rock vegetation and boulder plant communities resulted in low smectite concentrations. The number of observations (smectite) in these units was, however, very

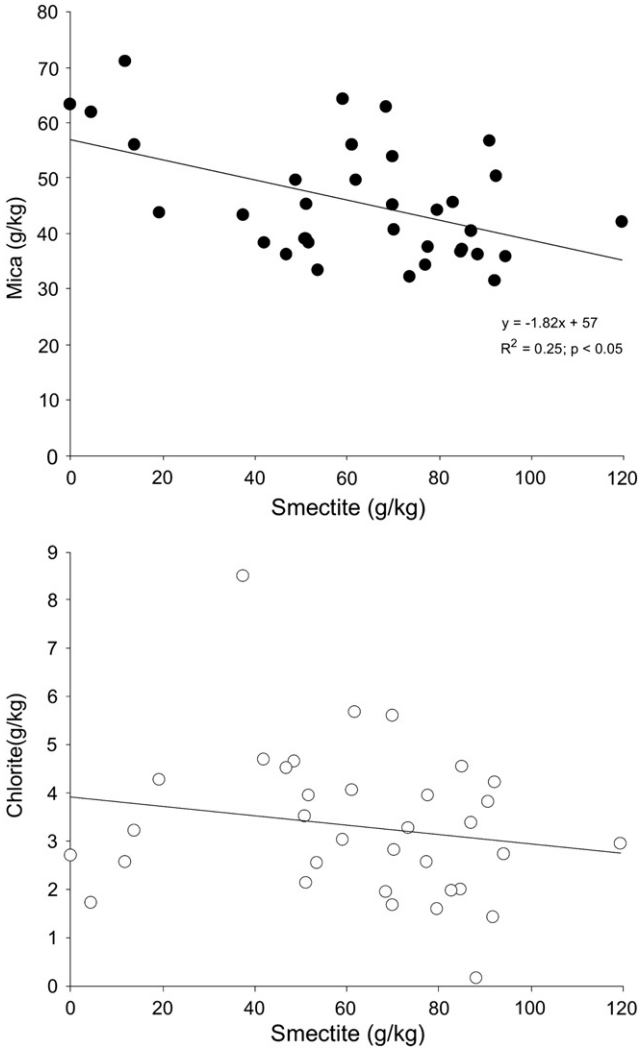

Fig. 5. Relationship between the smectite content and the mica and chlorite content, respectively. For both minerals (mica and chlorite) a trend is observable. The regression equation is given for mica, because only here the correlation is significant.

low. Similar to the green alder scrub, grass heath on moister soils seemed to promote smectite formation. But also here, the number of observations ($n \leq 2$) was too low for reasonable statistics. The smectite content was not measured in areas having the vegetation type 9 and 12 (Table 4).

Higher smectite content correlated with a higher OM content, while for chlorite and mica an opposite trend could be observed. Consequently, the amount of soil organic matter (OM) significantly influenced the clay mineral assemblage (Fig. 7). Not only soil organic matter per se exerted an influence on smectite: also the humus form significantly determined the formation of smectite (Fig. 7). Eumoder seemed to enhance the smectite formation compared to initial moder or no clear humus structures. Transitional weathering products, such as mica-HIV, also seem to be influenced by the humus form (although not significantly).

The concentration of smectite at north-facing (as well as west- and east-facing) sites was slightly higher than at south-facing sites (Fig. 8). For chlorite, an opposite trend (which would make sense in terms of weathering) was measured. If a subdivision of the exposure is undertaken only into north- (>270–90°N) and south-facing (>90–270°N) sites, the differences are less obvious (data not shown). A slightly lower smectite content and a higher chlorite content at south-facing sites can still be measured.

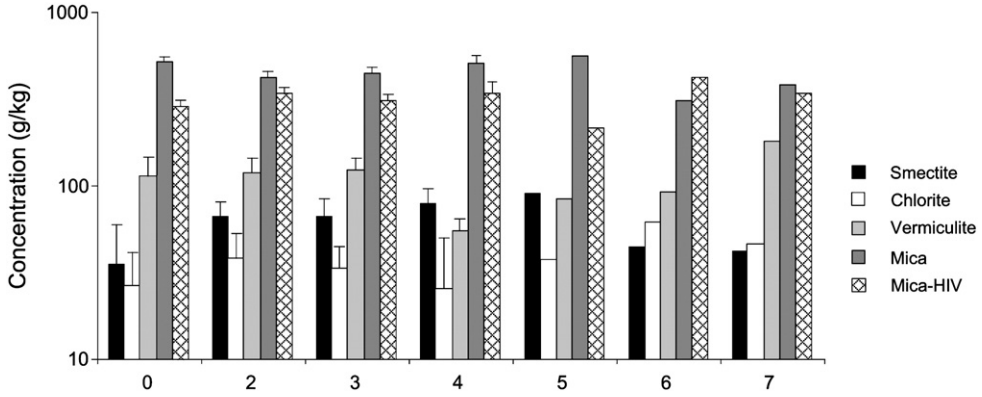

Fig. 6. Mean concentration (±standard error) of the phyllosilicates in the clay fraction as a function of the vegetation. 0 = no vegetation; 2 = pioneer grass communities; 3 = *Epilobietum fleischeri* with single willow shrubs and Alpenrose; 4 = green alder scrub (*Alnetum viridis*); 5 = grass heath on moister soils (Dystric Cambisols, grass species e.g. *Festuca violacea*, *Calamagrostis villosa*, *Phleum rhaeticum*, *Poa alpina*); 6 = Boulder plant communities, partially *E. fleischeri*, *Adenostyles leucophylla* and several fern species; 7 = rock vegetation (e.g. *Agrostis rupestris*, *Silene rupestris*, *Sempervivum arachnoideum*). No standard error was calculated with n ≤ 2.

The form of the landscape should also influence soil formation (see Egli et al., 2006). As shown in Fig. 8, it can be supposed that the clay mineral assemblage was to a certain degree determined by the landform. Sites having a high susceptibility to erosion showed higher mica and the lowest smectite concentrations.

The influence of the slope angle on the clay mineral assemblage is low. There is a tendency (but barely significant) to higher smectite and mica-HIV contents with decreasing slope angle (Fig. 8).

Physical properties of the soil material were correlated to the clay mineral assemblage. Sites having a finer texture (loamy sand; Fig. 9) showed a higher smectite content than sites having a sandy or gravelly texture. With time, soil thickness also increased due to weathering, unless a high erosion activity was present. The amount of smectite increased as the thickness of the soil increased (Fig. 9).

5. Discussion

Proglacial environments and areas having thawing permafrost are important for the understanding of global CO_2 cycling on glacial/interglacial timescales as they made up a significant amount of the global land surface during the Quaternary due to the advance and retreat of glaciers and ice sheets (Gibbs and Kump, 1994; Keller et al., 2007). These areas are often zones of high geochemical reactivity due to the availability of freshly ground reactive material or almost unaltered rock fragments, high water:rock ratios and contact times, high permeability and constant supply of dilute waters to percolate through the deposits (Föllmi et al., 2009a,b). Chemical weathering is ultimately coupled to mineral formation and transformation processes. The weathering of silicates and formation or transformation of minerals theoretically depend on mineral reactivity, the supply of minerals, water, acid reactants, ligands and the Arrhenius rate law (Lasaga et al., 1994; West et al., 2005).

Soil development proceeded quickly in the proglacial area. Within 150 years, significant soil formation and clay mineral transformations took place. As hypothesised by Egli et al. (2003a), the transformation rate of mica (and probably chlorite) at the beginning of soil formation is particularly high. The formation of smectite is predominantly due to the transformation of precursor products such as mica (Fig. 5), chlorite (Carnicelli et al., 1997; Egli et al., 2001a,b; Righi et al., 1993) or, to a lesser extent, amphiboles (Dreher and Niederbudde, 2000; Mavris et al., 2010). With time, the smectite content in the clay fraction continuously increased at the expense of mica and, secondarily, chlorite (Fig. 5). This increase was, however, highly scattered. Apart from the above-mentioned transformation processes, patterned structures may be associated with abrupt thresholds that either enhance or stop/hinder soil formation and mineral transformation. This might be due to several causes such as microclimatic conditions, micro-relief (both parameters were not any of into account in this investigation), deposition of physically inhomogeneous parent material (sites with a more fine-grained deposit close to rock debris) and probably also to brief periglacial activity (cf. Egli et al., 2006; Haugland, 2004).

Besides the factor time, topographic characteristics, vegetational features and probably physical characteristics of the parent material may consequently also be responsible for the variability of smectite formation along the chronosequence. According to the paradigm of Jenny (1941), the factor vegetation is not a fully independent one. The smectite content that can be taken as an indicator of weathering intensity (Egli et al., 2003a,b) could also be related to factors other than only time: other influences on the spatial pattern of smectite could be the vegetation distribution, soil organic matter, humus forms, exposure, relief forms and grain size.

Egli et al. (2006) showed that weathering differed between south- and north-facing sites with north-facing sites having the higher weathering intensity. Usually, north-facing sites are hypothesised to have moister soils that give rise to a more intense weathering regime. Our results indicate that the exposure probably also has some effects on the clay mineralogy (Fig. 8). The results of Roering et al. (2010) suggest a significant biological role in sculpting landscapes and driving weathering and physical conversion of bedrock to soil. The properties of the substratum such as the texture of the parent material, the distribution of moisture and the availability of nutrients are essential factors for the establishment of the vegetation (Burga, 1999). Small-scale factors such as the texture determine plant growth and, in a further step, weathering and soil evolution (Burga et al., 2010). A higher content of smectite was found in soils having the finest texture in the proglacial area (sandy loam). A finer texture also retains more water and makes it available for weathering reactions. Green alder stands and grass heath on moister soils were correlated to the presence of Humi-skeletic Leptosols (the most developed soils in the proglacial area) and consequently to a higher content of smectite. Once vegetation is established, it influences weathering processes by releasing organic ligands and acids that promote dissolution and transformation reactions (Caner et al., 2010). Grass heath is known to be an important source of organic acids (Matzner and Ulrich, 1980) that finally may promote the formation of smectite. Furthermore, grass heath is found at rather moist sites. The higher availability of water finally also promotes dissolution and transformation reactions. In contrast, rock vegetation and boulder plant communities develop on a strongly gravelly (diameter < 5 cm; 20–30 vol.%) and strongly

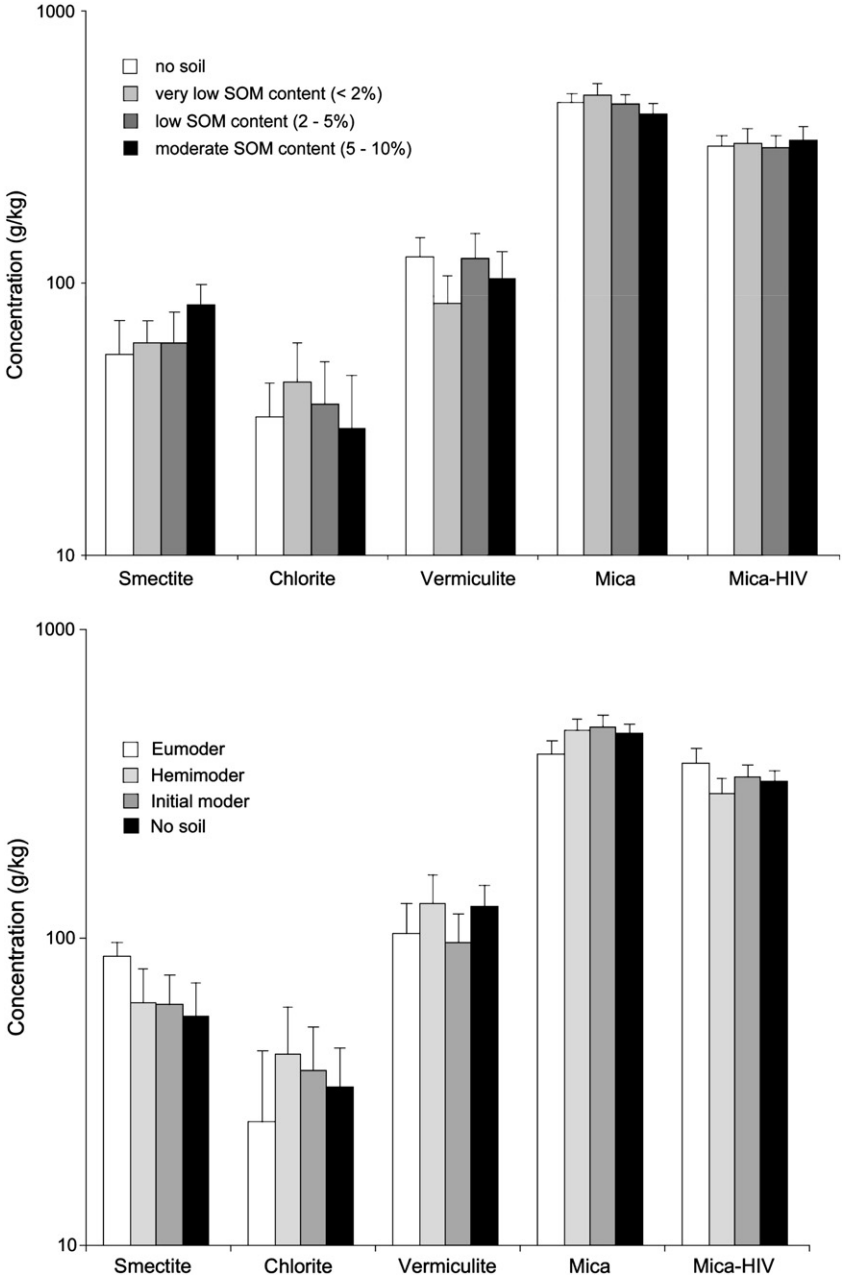

Fig. 7. Mean concentration (±standard error) of the phyllosilicates in the clay fraction as a function of soil organic matter concentration (SOM) and the humus form.

stony (diameter>5 cm; 20–30% vol.%) substrate (Burga et al., 2010). The predominance of gravel and stones in the composition of the material leads to low smectite concentrations.

Humus forms and soil organic matter closely relate to the vegetation, the soil biota and climate. This interrelationship is furthermore based on the fact that humus forms result from the activity of soil organisms and, at the same time, act as habitat for them (Lalanne et al., 2008). The composition of plant litter greatly influences microbial degradation and, therefore, also SOM stability (Williams and Gray, 1974; Zunino et al., 1982). Humification is related to the preferential oxidation of plant polysaccharides, the selective preservation of more recalcitrant organic compounds such as lignin and phenolic structures and to the incorporation of organic compounds of microbial origin (Rosa et al., 2005; Zech et al., 1997). The humus forms serve as a proxy for the soil biota (macro- and microbiology) and soil organic matter composition. The morphological properties of humus forms are known to correlate with soil biodiversity and thus with the decomposition rate of organic material as a result of soil biological activity (Broll, 1998; Klinka et al., 1990; Ponge et al., 2002; Sartori et al., 2005). The highest accumulation of soil organic matter in the proglacial area, the highest acidity and the highest production of organic ligands must be expected in the humus form Eumoder (Zanella et al., 2009). Eluviation of chemical elements was highest at the sites having a Eumoder where the highest amount of smectite was also measured. Organic ligands enhanced weathering (leaching of elements) and promoted the formation of low charge expandable minerals (smectites; Egli et al., 2008a). The Eumoder humus form, representing acidic conditions and conditions where organic ligands are formed, is a transition from a Hemimoder to a Dysmoder (Green et al., 1993; Zanella et al., 2009).

Clay minerals and other weathering products contribute to the stabilisation of soil organic matter. As shown by Denef and Six (2004), Egli et al. (2008b) and other authors, the type of clay minerals can affect the macroaggregate formation and stabilisation (and

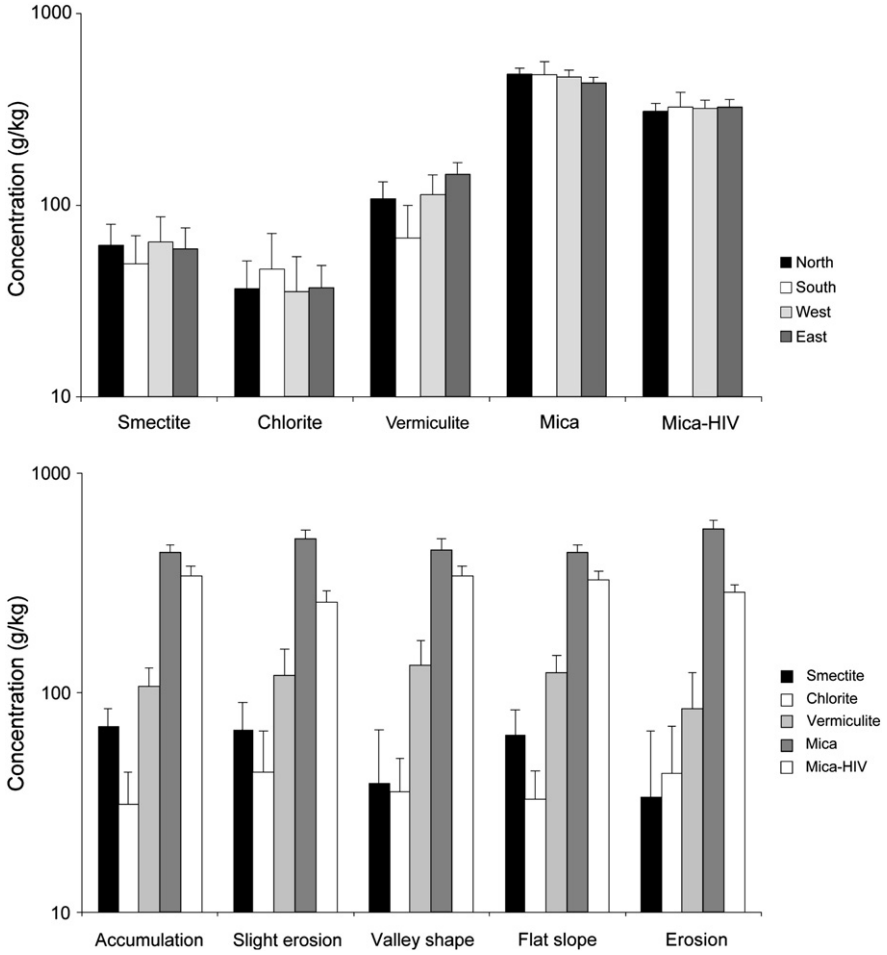

Fig. 8. Mean concentration (±standard error) of the phyllosilicates in the clay fraction as a function of exposure and landform (see also Table 1).

consequently organic C). This may be coupled to feedback regarding the formation of clay minerals.

High precipitation rates and the production of chelating compounds in the soil are believed to accelerate the formation of smectites (that in these environments are the weathering end-products of the phyllosilicates mica or chlorite) through the intermediate stage of hydroxy-interlayered minerals and the subsequent removal of the hydroxide polymers (Carnicelli et al., 1997; Egli et al., 2003b; Malcolm et al., 1969; Righi et al., 1999; Senkayi et al., 1981).

According to Anderson et al. (2000), silicate-weathering reactions are substantial only after vegetation cover is established. In proglacial areas, however, fresh mineral surfaces are provided by physical erosion of the parent material by the glacier. Freshly-ground material is very reactive and gives rise to high chemical weathering and mineral transformation rates (Föllmi et al., 2009a,b). Geochemical and physical controls of weathering fluxes are interrelated (Anderson et al., 2007; Heimsath et al., 2001; Riebe et al., 2004). Jin et al. (2010) found that chemical weathering was higher in upslope areas and slowed down in the valley floor. This seems also to be true, at least partially, for our investigation area. Smectite concentrations were highest in areas having a potentially slight erosion activity and on flat slopes. Lowest concentrations were measured in the valley floor. Sites on a flat slope (with an assumed more-or-less balanced in- and output of surface material), sites having a low susceptibility to erosion and sites having a high susceptibility to accumulating surface material showed the most advanced weathering stages with the highest smectite concentrations (Fig. 8). Our findings also agree well with the rather large-scale, 'macroscopic' investigations. Egli et al. (2006) found that better-developed and thicker soils were found at sites having a tendency to accumulate (such as depressions and at the foot of the slopes) as well as on concave slopes or flat slopes. At some sites, furthermore, fluvial erosion was a mechanism causing lower smectite content in the valley floor of the Morteratsch proglacial area. Although high erosion rates are coupled with high chemical weathering rates (Anderson et al., 2007; Heimsath et al., 2001; Jin et al., 2010; Riebe et al., 2004), this does not necessarily mean that highly weathered soils and consequently a high amount of smectite are always encountered at such sites. In fact, weathering products (newly formed or transformed mineral species) might be eroded and, consequently, weakly weathered or freshly-ground primary minerals may accumulate.

6. Conclusion

We studied the scattered formation of smectite along a chronosequence having a time span of 150 years. The following were the principal findings:

- Smectite was actively formed in the proglacial area but it exhibited a strongly scattered trend. Elevated smectite contents were found at sites having a thicker soil.
- Topography pertains to the configurations of the landscape and refers to inclination, concavity or convexity and (north- and south-) exposure. Sites showing slight erosion (flattening slope ridge, steepening slope ridge) or flat slopes had the highest smectite content. Sites having high erosion rates and valley floors (where either accumulation or erosion may occur due to fluvial processes) exhibited a lower smectite amount.

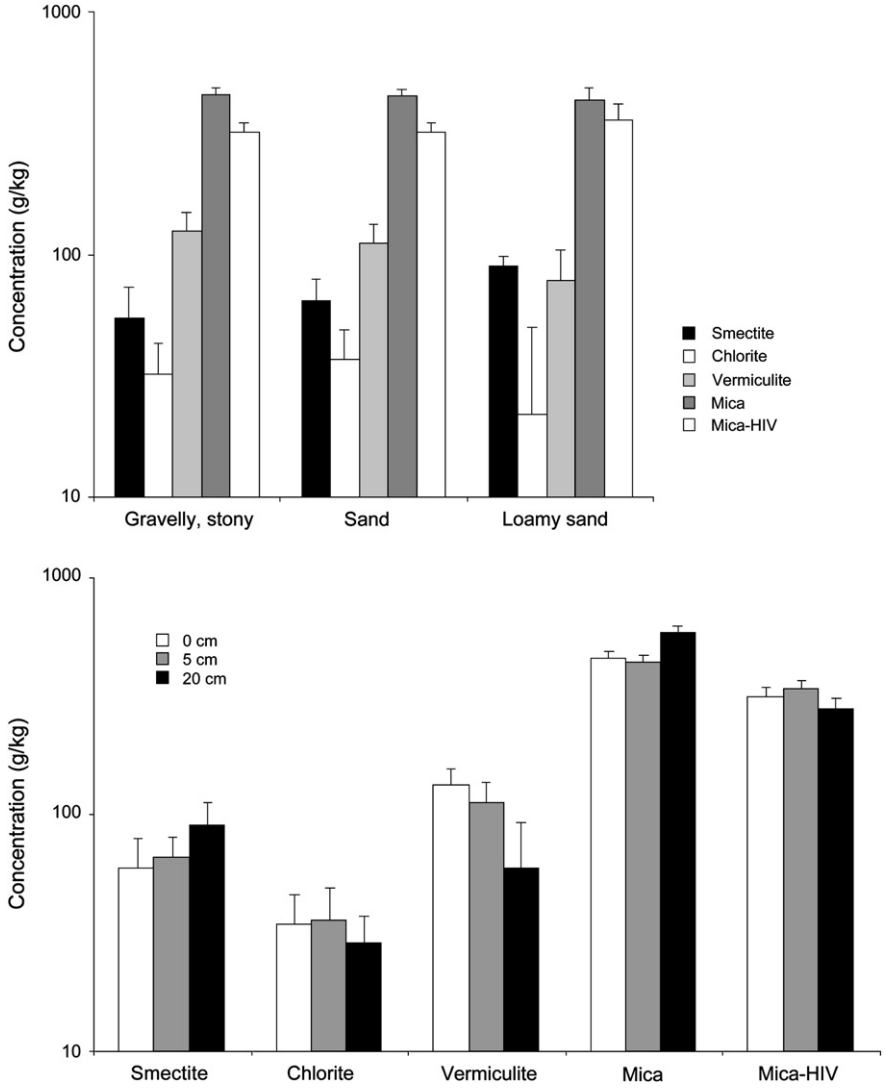

Fig. 9. Phyllosilicate concentrations as a function of the texture and soil thickness.

- The texture of the soil material influenced weathering and development of vegetation. A higher content of smectite was found in the finest-textured material of the proglacial area (sandy loam).
- Vegetation cannot be considered as a fully independent factor as it is interrelated to the surrounding conditions. Higher contents of smectite were related to green alder stands and grass heath where moister soils (having in most cases also a finer texture) could be encountered. Green alders need a better-developed soil where they actively contribute to enhanced pedogenesis by stabilising the surface. Grass heath needs a moist environment and contributes to weathering through the release of organic acids.
- Humus forms served as a proxy for the soil biota and soil organic matter composition. The production of chelating organic ligands and acidity was highest at sites having a Eumoder. At these sites, the smectite content was elevated. High percolation rates and the production of chelating compounds in the soil are believed to promote the development of smectites from mica and chlorite.

Acknowledgements

This research was supported by the Swiss National Foundation (SNF), project grant n. 200021–117568. We would like to thank B. Kägi for the support in the laboratory. We are, furthermore, indebted to Dr. Brice Mourier and an unknown reviewer for their helpful comments on an earlier version of the manuscript.

References

Anderson, S.P., Drever, J.I., Frost, C.D., Holden, P., 2000. Chemical weathering in the foreland of a retreating glacier. Geochimica et Cosmochimica Acta 64, 1173–1189.
Anderson, S.P., von Blanckenburg, F., White, A.F., 2007. Physical and chemical controls on the critical zone. Elements 3, 315–319.
Arn, K., Hosein, R., Föllmi, K.B., Steinmann, P., Aubert, D., Kramers, J., 2003. Strontium isotope systematics in two glaciated crystalline catchments: Rhone and Oberaar glaciers (Swiss Alps). Swiss Bulletin of Mineralogy and Petrology 83, 273–283.
Bäumler, E. 1988. Untersuchungen zur Besiedlungsdynamik und Populationsbiologie einiger Pionierpflanzen im Morteratschgletschervorfeld. Doctoral Thesis, University of Basel.
Broll, G., 1998. Diversity of soil organisms in alpine and arctic soils in Europe. Review and reasearch needs. Pirineos 151-152, 43–72.
Brunner, J., Jäggli, F., Nievergelt, J., Peyer, K., 1997. Kartieren und Beurteilen von Landwirtschaftsböden, 24. Schriftenreihe der FAL (Eidgenössische Forschungsanstalt für Agrarökologie und Landbau), Zürich-Reckenholz.
Büchi, H., 1994. Der variskische Magmatismmus in der östlichen Bernina (Graubünden, Schweiz). Schweizerische Mineralogische und Petrographische Mitteilungen 74, 359–371.
Burga, C., 1999. Vegetation development on the glacier forefield Morteratsch (Switzerland). Applied Vegetation Science 2, 17–24.
Burga, C., Perret, R., 1998. Vegetation und Klima der Schweiz seit dem jüngeren Eiszeitalter. Ott Verlag, Thun.
Burga, C.A., Krüsi, B., Egli, M., Wernli, M., Elsener, S., Ziefle, M., Mavris, C., 2010. Plant succession and soil development on the foreland of the Morteratsch glacier (Pontresina, Switzerland): Straight forward or chaotic? Flora 205, 561–576.

Caner, L., Joussein, E., Salvador-Blanes, S., Hubert, F., Schlicht, J.F., Duigou, N., 2010. Short-time clay-mineral evolution in a soil chronosequence in Oleron Island (France). Journal of Plant Nutrition and Soil Science 173, 591–600.
Carnicelli, S., Mirabella, A., Cecchini, G., Sanesi, G., 1997. Weathering of chlorite to a low-charge expandable mineral in a Spodosol on the Apennine mountains, Italy. Clays and Clay Minerals 45, 28–41.
Conen, F., Yakutin, M.V., Zumbrunn, T., Leifeld, J., 2007. Organic carbon and microbial biomass in two soil development chronosequences following glacial retreat. European Journal of Soil Science 58, 758–762.
Denef, K., Six, J., 2004. Clay mineralogy determines the importance of biological versus abiotic processes for macroaggregate formation and stabilization. European Journal of Soil Science 56, 469–479.
Dreher, P., Niederbudde, E.-A., 2000. Characterization of expandable layer silicates in humic-ferralic cambisols (Umbrept) derived from biotite and hornblende. Journal of Plant Nutrition and Soil Science 163, 447–453.
Egli, M., Mirabella, A., Fitze, P., 2001a. Clay mineral formation in soils of two different chronosequences in the Swiss Alps. Geoderma 104, 145–175.
Egli, M., Mirabella, A., Fitze, P., 2001b. Weathering and evolution of soils formed on granitic, glacial deposits: results from chronosequences of Swiss alpine environments. Catena 45, 19–47.
Egli, M., Mirabella, A., Fitze, P., 2003a. Formation rates of smectites derived from two Holocene chronosequences in the Swiss Alps. Geoderma 117, 81–98.
Egli, M., Mirabella, A., Sartori, G., Fitze, P., 2003b. Weathering rates as a function of climate: results from a climosequence of the Val Genova (Trentino, Italian Alps). Geoderma 111, 99–121.
Egli, M., Wernli, M., Kneisel, C., Haeberli, W., 2006. Melting glaciers and soil development in the proglacial area Morteratsch (Swiss Alps): I Soil type chronosequence. Arctic, Antarctic, and Alpine Research 38, 499–509.
Egli, M., Mirabella, A., Sartori, G., 2008a. The role of climate and vegetation in weathering and clay mineral formation in late Quaternary soils of the Swiss and Italian Alps. Geomorphology 102, 307–324.
Egli, M., Merkli, C., Sartori, G., Mirabella, A., Plötze, M., 2008b. Weathering, mineralogical evolution and soil organic matter along a Holocene soil toposequence on carbonate-rich materials. Geomorphology 97, 675–696.
Fischer, M. 1999. Waldgrenzökoton und Wiederbewaldungsdynamik im Gebiet des Morteratschgletschers. Unpublished diploma thesis Geographisches Institut der Universität Zürich.
Fitze, P.F., 1982. Zur Relativdatierung von Moränen aus der Sicht der Bodenentwicklung in den kristallinen Zentralalpen. Catena 9, 265–306.
Föllmi, K.B., Arn, K., Hosein, R., Adatte, T., Steinmann, P., 2009a. Biogeochemical weathering in sedimentary chronosequences of the Rhône and Oberaar Glaciers (Swiss Alps): rates and mechanisms of biotite weathering. Geoderma 151, 270–281.
Föllmi, K.B., Hosein, R., Arn, K., Steinmann, P., 2009b. Weathering and the mobility of phosphorus in the catchments and foefields of the Rhône and Oberaar glaciers, central Switzerland: implications for the global phosphorus cycle on glacial-interglacial timescales. Geochimica et Cosmochimica Acta 73, 2252–2282.
Gamper, M., 1985. Morphochronologische Untersuchungen an Solifluktionszungen, Moränen und Schwemmkegeln in den Schweizer Alpen. Schriftenreihe Physische Geographie, 17. Zürich.
Gibbs, M.T., Kump, L.R., 1994. Global chemical erosion during the last glacial maximum and the present: Sensitivity to changes in lithology and hydrology. Paleoceanography 9, 529–543.
Green, R.N., Trowbridge, R.L., Klinka, K., 1993. Towards a Taxonomic Classification of Humus Forms, Forest Science, Monograph 29. Society of American Foresters, Bethesda, MD.
Hall, K., Thorn, C.E., Matsuoka, N., Prick, A., 2002. Weathering in cold regions: some thoughts and perspectives. Progress in Physical Geography 26, 577–603.
Hallet, B., Hunter, L., Bogen, J., 1996. Rates of erosion and sediment evacuation by glaciers: a review of field data and their implications. Global and Planetary Change 12, 213–235.
Haugland, J.E., 2004. Formation of patterned ground and fine-scale soil development within two late Holocene glacial chronosequences: Jotunheimen, Norway. Geomophology 61, 287–301.
He, L., Tang, Y., 2008. Soil development along primary succession sequences on moraines of Hailuogou Glacier, Gongga Mountain, Sichuan, China. Catena 72, 259–269.
Heimsath, A.M., Dietrich, W.E., Nishiizumi, K., Finkel, R.C., 2001. Stochastic processes of soil production and transport: erosion rates, topographic variation and cosmogenic nuclides in the Oregon Coast Range. Earth Surface Processes and Landforms 26, 531–552.
Hosein, R., Arn, K., Steinmann, P., Adatte, T., Föllmi, K.B., 2004. Carbonate and silicate weathering in two presently glaciated, crystalline catchments in the Swiss Alps. Geochimica et Cosmochimica Acta 68, 1021–1033.
IUSS Working Group WRB, 2006. World Reference Base for Soil Resources 2006, World Soil Resources Reports No. 1032nd edition. FAO (Food and Agriculture Organisation of the United Nations), Rome.
Jackson, M.L., 1956. Soil Chemical Analysis. Prentice-Hall, Englewood Cliffs, NJ.
Jenny, H., 1941. Factors of Soil Formation. Mc Graw-Hill Book Company, New York.
Jin, L., Ravella, R., Ketchum, B., Biermann, P.R., Heaney, P., White, T., Brantkley, S.I., 2010. Mineral weathering and elemental transport during hillslope evolution at the Susquehanna/Shale Hills Critical Zone Observatory. Geochimica et Cosmochimica Acta 74, 3669–3691.
Kahle, M., Kleber, M., Jahn, R., 2002. Review of XRD-based quantitative analyses of clay minerals in soils: the suitability of mineral intensity factors. Geoderma 109, 191–205.
Keller, O., 1994. Entstehung und Entwicklung des Bodensees - Ein geologischer Lebenslauf. In: Maurer, H. (Ed.), Umweltwandel am Bodensee. UVK Fachverlag für Wissenschaft und Studium GmbH, St. Gallen, pp. 33–92.
Keller, K., Blum, J.D., Kling, G.W., 2007. Geochemistry of soils and streams on surfaces of varying ages in Arctic Alaska. Arctic, Antarctic and Alpine Research 39, 84–98.
Klinka, K., Wang, Q., Carter, R.E., 1990. Relationships among humus forms, forest floor nutrient properties, and understorey vegetation. Forest Science 36, 564–581.
Lalanne, A., Bardat, J., Lalanne-Amara, F., Gautrot, T., Ponge, J.-F., 2008. Opposite responses of vascular plant and moss communities to changes in humus forms, as expressed by the Humus Index. Journal of Vegetable Science 19, 645–652.
Lanson, B., 1997. Decomposition of experimental X-ray diffraction patterns (profile fitting): a convenient way to study clay minerals. Clays and Clay Minerals 45, 132–146.
Lasaga, A.C., Soler, J.M., Ganor, J., Burch, T.E., Nagy, K.L., 1994. Chemical weathering rate laws and global geochemical cycles. Geochimica et Cosmochimica Acta 58, 2361–2386.
Magny, M., 1992. Holocene lake-level fluctuations in Jura and the northern subalpine ranges, France. Regional pattern and climatic implications. Boreas 21, 319–334.
Maisch, M., 1992. Die Gletscher Graubündens: Rekonstruktion und Auswertung der Gletscher und deren Veränderung sit dem Hochstand von 1850 im Gebiet der östlichen Schweizer Alpen (Bündnerland und angrenzende Regionen). Schriftenreihe Physische Geographie, 32. Universität Zürich-Irchel.
Malcolm, R.L., Nettleton, W.D., McCracken, R.J., 1969. Pedogenic formation of montmorillonite from a 2:1–2:2 intergrade clay mineral. Clays and Clay Minerals 16, 405–414.
Matzner, E., Ulrich, B., 1980. The transfer of chemical elements within a heath-ecosystem (Calluna vulgaris) in Northwest Germany. Zeitschrift für Pflanzenernährung und Boden kunde 143, 666–678.
Mavris, C., Egli, M., Plötze, M., Blum, J., Mirabella, A., Giaccai, D., Haeberli, W., 2010. Initial stages of weathering and soil formation in the Morteratsch proglacial area (Upper Engadine, Switzerland). Geoderma 155, 359–371.
Moore, D.M., Reynolds, R.C., 1997. X-ray Diffraction and the Identification and Analysis of Clay Minerals, 2nd ed. Oxford University Press, New York.
Patzelt, G., 1977. Der zeitliche Ablauf und das Ausmass postglazialer Kimaschwankungen in den Alpen. In: Frenzel, B. (Ed.), Dendrochronologie und postglaziale Klimaschwankungen in Europa, 13. Erdwiss. Forschung, Wiesbaden, pp. 248–259.
Ping, C.L., Michaelson, G.J., Kimble, J.M., Romanovsky, V.E., Shur, Y.L., Swanson, D.K., Walker, D.A., 2008. Cryogenesis and soil formation along a bioclimate gradient in Arctic North America. Journal of Geophysical Research — Biogeosciences 113 (G03S12), 1–14.
Ponge, J.-F., Chevalier, R., Loussot, P., 2002. Humus index: an integrated tool for the assessment of forest floor and topsoil properties. Soil Science Society of America Journal 66, 1996–2001.
Renner, F., 1982. Beiträge zur Gletschergeschichte des Gotthardgebbietes und dendroklimatologische Analysen an fossilen Hölzern. Schriftenreihe Physische Geographie, 8. Zürich.
Riebe, C.S., Kirchner, J.W., Finkel, R.C., 2004. Erosional and climatic effects on long-term chemical weathering rates in granitic landscapes spanning diverse climate regimes. Earth and Planetary Science Letters 224, 547–562.
Righi, D., Petit, S., Bouchet, A., 1993. Characterization of hydroxy-interlayered vermiculite and illite-smectite interstratified minerals from the weathering of chlorite in a Cryorthod. Clays and Clay Minerals 41, 484–495.
Righi, D., Huber, K., Keller, C., 1999. Clay formation and podzol development from postglacial moraines in Switzerland. Clay Minerals 34, 319–332.
Roering, J.J., Marshall, J., Booth, A.M., Mort, M., Jin, Q., 2010. Evidence for biotic controls on topography and soil production. Earth and Planetary Science Letters 298, 183–190.
Rosa, A.H., Simões, M.L., de Oliviera, L.C., Rocha, J.C., Neto, L.M., Milori, D.M.B.P., 2005. Multimethod study of the degree of humification of humic substances extracted from different tropical soil profiles in Brazil's Amazonian region. Geoderma 127, 1–10.
Sartori, G., Mancabelli, A., Corradini, F., Wolf, U., 2005. Atlante dei suoli del Parco Adamello-Brenta. Suoli e paesaggi. Monografie Museo Tridentino di Scienze Naturali II, 239.
Senkayi, A.L., Dixon, J.B., Hossner, L.R., 1981. Transformation of chlorite to smectite through regularly interstratified intermediates. Soil Science Society of America Journal 45, 650–656.
Simas, F.N.B., Schaefer, C.E.G.R., Melo, V.F., Guerra, M.B.B., Saunders, M., Gilkes, R.J., 2006. Clay-sized minerals in permafrost-affected soils (Cryosols) from King George Island, Antarctica. Clays and Clay Minerals 54, 721–736.
Spillmann, P., 1993: Die Geologie des penninisch-ostalpinen Grenzbereichs im südlichen Berninagebirge. Ph.D. thesis ETH Zürich, Switzerland.
Trommsdorff, V., Dietrich, V., 1999: Grundzüge der Erdwissenschaften. vdf-Verlag, 6. Auflage, Zürich, Switzerland.
Ugolini, F.C., 1986. Pedogenetic zonation in the well-drained soils of the arctic regions. Quaternary Research 26, 100–120.
West, A.J., Galy, A., Bickle, M., 2005. Tectonic and climatic controls on silicate weathering. Earth and Planetary Science Letters 235, 211–228.
Williams, S.T., Gray, T.R.G., 1974. Decomposition of litter on the soil surface. In: Dickinson, C.H., Pugh, G.J.F. (Eds.), Biology of Plant Litter Decomposition, Vol. 2. Academic Press, London, pp. 611–632.
Winkler, S., 2000. The little ice age maximum in the Southern Alps, New Zealand: preliminary results at Mueller Glacier. The Holocene 10, 643–647.
Zanella, A., Jabiol, B., Ponge, J.-F., Sartori, G., De Waal, R., Van Delfi, B., Graefe, U., Cools, N., Katzensteiner, K., Hager, H., English, M., Brethes, A., 2009. Toward a European humus forms reference base. Studi Trentini di Scienze Naturali 85, 145–151.
Zech, W., Senesi, N., Guggenbergger, G., Kaiser, K., Lehmann, J., Miano, T.M., Miltner, A., Schrotz, G., 1997. Factors controlling humification and mineralization of soil organic matter in the tropics. Geoderma 79, 117–161.
Zunino, H., Borie, F., Aguilera, S., Martin, J.P., Haider, K., 1982. Decomposition of ^{14}C-labeled glucose, plant and microbial products and phenols in volcanic ash-derived soils of Chile. Soil Biology and Biochemistry 14, 37–43.

Sedimentary Geology xxx (2012) xxx–xxx

Contents lists available at SciVerse ScienceDirect

Sedimentary Geology

journal homepage: www.elsevier.com/locate/sedgeo

Weathering and mineralogical evolution in a high Alpine soil chronosequence: A combined approach using SEM–EDX, cathodoluminescence and Nomarski DIC microscopy

Christian Mavris [a,*], Jens Götze [b], Michael Plötze [c], Markus Egli [a]

[a] Department of Geography, University of Zurich, Winterthurerstrasse 190, CH-8057 Zürich, Switzerland
[b] TU Bergakademie Freiberg, Institute of Mineralogy, Brennhausgasse 14, D-09596 Freiberg, Germany
[c] ETH Zurich, Institute for Geotechnical Engineering, Zurich, CH-8093, Switzerland

ARTICLE INFO

Article history:
Received 2 May 2011
Received in revised form 21 March 2012
Accepted 16 April 2012
Available online xxxx

Keywords:
Cathodoluminescence
Nomarski DIC microscopy
SEM–EDX
Weathering
Quartz
Apatite

ABSTRACT

Physical and chemical weathering of primary minerals of granitic till in the proglacial area of Morteratsch (Switzerland) was investigated using cathodoluminescence (CL), Nomarski differential interference contrast (DIC) microscopy and scanning electron microscope (SEM–EDX). The investigated time-span ranges from 0 to 140 years of sediment exposure. For the very early stage of weathering or soil formation only little information is available. The main aim of our investigation was consequently to see whether weathering of primary minerals can be detected in such a short time-span using for the first time for soils well-established methods as CL and Nomarski DIC microscopy in geo- and material science such. For that purpose, the fine earth fraction (<2 mm) of topsoil samples was investigated. Some physical weathering had taken place within 140 years. The delamination of biotite seems to increase with time. SEM and CL analyses also demonstrate early weathering of quartz by evidencing edge pits and structural bonds – such as Si – O – Si in quartz – that start to break and to transform into free radicals. K-feldspar and plagioclase contain Fe. When using Fe^{3+} as reference point (680–700 nm) to standardise the CL spectra, the Al – O^- – Al defects of K-feldspar exhibit a relative decrease with time; this was not the case for plagioclase. The CL measurements showed that the investigated apatite contained REE (rare earth elements) in the crystal structure. However, none of the other techniques (DIC, SEM–EDX) was helpful in detecting any specific weathering features for apatite. In the time span of 140 years, epidote weathering was evidenced using XRD in a previous investigation and here using DIC microscopy (morphologic changes). Several mineral changes could be traced within a very short weathering sequence using the applied techniques. These changes include physical (e.g. biotite), chemical or crystal structure (K-feldspar, biotite) features. Such an analytical combination is promising, therefore, for the detection of chemical, physical and mineralogical characteristics and changes in very young glacial sediments.

1. Introduction

Due to global warming, glaciers retreat and new areas are exposed to weathering. Glaciers and discontinuous permafrost in these ecosystems react sensitively to atmospheric warming because the year-round temperature of their surrounding is not greatly below their melting point (Haeberli and Beniston, 1998). The abrasive action of active ice masses produces sediments (i.e. moraines), which tend to weather as a function of their exposure time. In the chemical sense, soil development is roughly synonymous with weathering. Elemental and mineralogical compositions of soils evolve due to complex feedbacks among geochemical and geomorphic processes within and at the boundaries of the soil layer. Geochemical processes involve dissolution, leaching, precipitation and colloidal translocation (Yoo and Mudd, 2008), whereas geomorphic processes include the conversion of parent material to soil materials and the colluvial transport of the soil materials.

It is often assumed that weathering mechanisms in cold regions are slow due to the low temperatures. The proglacial area is, however, a potential zone of a) high geochemical reactivity due to the availability of freshly-ground reactive material (subglacially derived), b) high water-to-rock ratios and contact times, c) high permeability, and d) a constant supply of dilute waters (meltwaters and rain/snowmelt) percolating through the deposits. All these factors should favour chemical weathering. There is no agreement about the velocity of reaction in proglacial areas. Anderson et al. (1997, 2000) concluded from their measurements that silicate weathering reactions in proglacial areas may be important only after a vegetation cover is established. In contrast, Wadham et al. (2001), Egli et al. (2003) and Hosein et al. (2004) suggest that glacially derived material is

* Corresponding author. Tel.: +41 44 635 51 14; fax: +41 44 635 638 48.
E-mail address: christian.mavris@geo.uzh.ch (C. Mavris).

0037-0738/$ – see front matter © 2012 Elsevier B.V. All rights reserved.
doi:10.1016/j.sedgeo.2012.04.008

subjected to intense chemical weathering, starting immediately after deposition in the proglacial zone and subsequently continuing for thousands of years after glacier retreat.

Hosein et al. (2004) and Föllmi et al. (2009a,b) measured high weathering rates in proglacial areas in the Alps (10^{-15} to 10^{-13} mol biotite m^{-2} s^{-1} for a 140–270 year-old exposed proglacial area). Biotite weathering in young soils was generally much higher than in old soils. The calculated weathering rates of biotite were several orders of magnitude higher than known field weathering rates (e.g., Swoboda-Colberg and Drever, 1993; Murphy et al., 1998). This seems to be related to the predominance of fine-grained particles (<63 μm) in glacial sediment that are mechanically disaggregated and preferentially leached.

In general, the availability of data about weathering rates and alteration of primary rock-forming minerals in young and cold areas is scarce. The detection of changes is often limited by the choice of techniques. The combination of transmitted-light cathodoluminescence (CL), Nomarski DIC (Differential Interference Contrast) microscopy and scanning electron microscopy (SEM–EDX) can give important insights into the chemical composition and crystal arrangement of minerals (i.e. point defects, cationic changes, etc.). Most materials have distinct luminescence properties that allow a rapid identification of phase distribution and transformation. Nomarski DIC microscopy is an optically-based technique first documented by Nomarski and Weill (1951) and Nomarski (1955). It allows the observation of micromorphological features in natural materials and/or metal alloys, and has been applied in reflected light microscopy in metallurgy and petrographic research (e.g. Pearce et al., 1987; Keevil and Walker, 1992). Despite a relatively straightforward preparation of the samples and the high amount of information that can be retrieved by the combination of CL and Nomarski DIC, their coupled application is rare (Götze and Siedel, 2004, 2007). Transmitted-light CL microscopy is a technique applied to building materials (Michalski et al., 2002; Götze and Siedel, 2007; Götze, 2009), archaeology (Lapuente et al., 2000; Götze and Siedel, 2004) and geosciences (e.g. Götze and Zimmerle, 2000; Götze et al., 2000; 2004; Richter et al., 2003).

The aim of this study is to trace mineralogical and crystallographic changes in soils that have developed across a recently exposed granitic till. For that purpose, the proglacial area of the Morteratsch glacier was selected. The combination of preferential weathering patterns and elemental depletion (for the main structure modifier elements) for primary mineral phases were taken into account.

For this purpose, CL and Nomarski DIC microscopy – well-known analytical techniques in material science but not applied so far for soil studies – analyses were performed in combination with SEM–EDX. An additional aim was consequently to test the power and suitability of these techniques for studying short-term and initial weathering processes in young soils.

2. Study area

The proglacial area of Morteratsch is located in Upper Engadine, SE Switzerland (Fig. 1). The valley runs in N–S direction and the current length of the exposed area is approx. 3 km. The glacier has been continuously retreating without re-advancements since the 1850s (end of the Little Ice Age; Burga, 1999). The altitude of the investigated proglacial valley ranges from 1900 m asl to approx. 2150 m asl, with no abrupt stacks and slopes along its main axis.

Geologically, the glacial till consists of granitic material. The morainic material was produced through glacial transport within a small area of relatively homogeneous parent material (Mavris et al., 2010, 2011). The proglacial area of Morteratsch is set in the Lower Austroalpine Bernina Nappe, which is mainly composed of plutonic rocks, such as granodiorites, diorites, syenites and alkaligranites. Rarely, accessory rocks such as dolomites, gabbros and serpentines are reported (Büchi, 1994). In the investigated area, these rock types were not observed (Mavris et al., 2010, 2011). The rock units underwent greenschist facies metamorphism during the High Alpine orogenesis (Oligocene–Eocene; Trommsdorff and Dietrich, 1999). This event caused the saussuritisation of primary rock-forming plagioclases into albite, epidote and calcite (D'Amico et al., 1998).

The vegetation cover of the Morteratsch proglacial area has been studied by Burga (1999). The first flowering plants colonising the young deglaciated surfaces are scattered individuals of *Epilobium fleischeri* and *Linaria alpina* that appear after about 7 years. First plants of the community *Oxyrietum digynae* appear after c. 12 years and disappear after c. 27 years. The establishment of *Larici-Pinetum cembrae* forests takes place after about 77 years on sites where the soil is more intensely weathered (Burga, 1999). The soils are weakly developed and are mostly Lithic Leptosols (IUSS Working Group WRB, 2006; Table 1). Present climatic conditions for the Morteratsch site are 0.5 °C mean annual temperature and 1000–1300 mm mean annual precipitation.

3. Material and methods

3.1. Soil sampling and preparation

Soil samples were collected from 10 soil pits distributed over the whole proglacial area (Fig. 1). This procedure resulted in the collection of a soil chronosequence of surfaces ranging from 0 (starting from the glacier front or unweathered parent material) to 140 years old. Soil profiles were excavated down to the C horizon (Table 1). For each horizon, 1–2 kg of material was collected. The parent material (t = 0 year) is the unweathered glacial sediment that can be found either at the glacier front or below the soils (C horizon). The unweathered parent material used for the optical investigations was collected at the bottom of the excavated profiles or glacial front (n = 7 C horizon samples were considered). The soil and parent material samples were oven-dried and sieved to 2 mm (Department of Geography, University of Zurich, Switzerland). An aliquot of the fine earth sample (<2 mm) was washed with de-ionised water and, when present, the suspended organic fraction (<1 g/cm^3) was removed by floating. These samples were used for the preparation of thin sections. Fine earth samples (material with a diameter<2 mm) were dispersed with an ultrasonic disperser, then embedded in polyester resin and cut to a thickness of c. 30 μm in order to ensure a good transparency of the sample. Thin sections were then polished and carbon coated. The grain size of the investigated minerals was in the range of 10 to 800 μm.

In total, >20 grains were analysed using the Nomarski DIC microscopy or SEM–EDX.

3.2. SEM–EDX

The fine-earth fraction of n = 4 topsoil samples and n = 1 parent material were analysed using scanning electron microscopy (SEM) and energy-dispersive spectroscopy (EDS). The analysis was performed using a Dual Beam Quanta 200 3D FEI coupled with EDX, with Dual BSD detector and W emitter operating at an accelerating voltage of 20 kV. The EDS detector is equipped with an ultra-thin window allowing detection of mineral elements and carbon. EDS provided the elemental composition of the solid phases and helped to identify them (point analyses and elemental maps). Investigations were performed on both thin sections (carbon coated) and loose granular samples (uncoated) at the Institute for Building Materials (ETH Zurich, Switzerland).

3.3. Cathodoluminescence

Luminescence is a common phenomenon in inorganic and organic compounds, resulting from an emission transition of anions, molecules

Please cite this article as: Mavris, C., et al., Weathering and mineralogical evolution in a high Alpine soil chronosequence: A combined approach using SEM–EDX, cathodoluminescence and Nomarski DIC microscopy, Sediment. Geol. (2012), doi:10.1016/j.sedgeo.2012.04.008

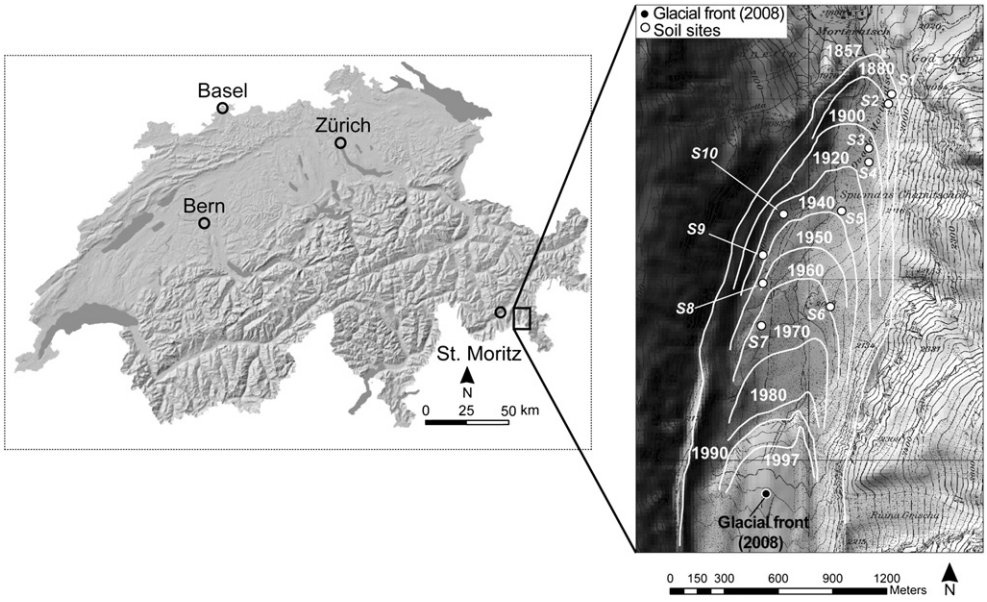

Fig. 1. Overview of the investigated area with the monitored sites in the proglacial area. The isochrones are according to Burga (1999).

or a crystal from an excited electronic state to a ground or other state having less energy (Götze, 2009). In the present study, n = 4 topsoils and n = 1 parent material were investigated. CL measurements were carried out at the Institute of Mineralogy of the TU Bergakademie Freiberg (Germany) using a hot cathode CL microscope HC1-LM (Neuser et al., 1995). The system was operated at 14 kV accelerating voltage and a current density of about 10 μA/mm^2. Luminescence images were taken on-line during CL operations using a Peltier-cooled digital video camera (KAPPA 961-1138 CF 20 DXC). CL spectra were recorded in the wavelength range 320 to 900 nm using an Acton Research SP-2356 digital triple-grating spectrograph with a Princeton Pixi 256B Spec 10 CCD detector that was attached to the CL microscope by a silica-glass fibre guide. CL spectra were measured under standardised conditions (wavelength calibration by a Hg-halogen lamp, spot width 30 μm, measuring time 1–5 s).

Spectral data evaluation was performed considering the relative intensity (counts/s) of the luminescence emission from each sample. The CL spectra depend on the crystal orientation (Barbarand and Pagel, 2001; Finch et al., 2003). Therefore, a comparison of the same mineral type in different samples must be done carefully if the orientation is not the same. Because we were analysing soil systems, a similar orientation of the investigated minerals (in a time series) could not be achieved. A quantitative analysis of weathering in the considered time-span was therefore not possible. To have, however, a semi-

Table 1
Properties of the monitored soil sites. Grain sizes: sand (2000–63 μm), silt (63–2 μm) and clay (<2 μm).

Site/soil	Soil age (years)	Horizons	Depth (cm)	Skeleton (wt.%)	Sand (g/kg)	Silt (g/kg)	Clay (g/kg)	pH ($CaCl_2$)
S1/Humi-Skeletic Leptosol	138	O	0–6	41	n.m.	n.m.	n.m.	4.60
		A	6–9	50	777	184	39	4.80
		BC	9–14	53	830	158	12	4.70
		C	14–30	40	757	222	21	4.60
S2/Humi-Skeletic Leptosol	128	A	0–10	64	754	204	42	4.85
		AC	10–40	68	695	272	33	4.90
S3/Humi-Skeletic Leptosol	108	A	0–3	54	667	265	68	5.10
		AC	3–15	70	677	281	42	4.50
S4/Humi-Skeletic Leptosol	98	A	0–1	55	n.m.	n.m.	n.m.	5.30
		AC	1–5	51	939	61	15	5.20
		C	5–30	70	931	57	12	5.20
S5/Humi-Skeletic Leptosol	68	A1	0–1	7	n.m.	n.m.	n.m.	4.85
		A2	1–4	1	530	432	38	4.55
		C1	4–9	36	573	387	40	4.65
		C2	9–20	64	570	372	58	4.60
S6/Skeletic Leptosol	48	A	0–2.5	64	n.m.	n.m.	n.m.	4.80
		C	2.5–25	68	852	129	19	5.00
S7/Skeletic Leptosol	48	A	0–4	26	n.m.	n.m.	n.m.	6.10
		C1	4–11	37	823	146	31	5.20
		C2	11–34	67	747	211	42	5.10
S8/Skeletic Leptosol	58	OA	0–12	63	n.m.	n.m.	n.m.	4.60
		C	12–33	48	712	220	68	4.40
S9/Humi-Skeletic Leptosol	73	O	0–3	44	n.m.	n.m.	n.m.	5.15
		AC	3–10	65	785	175	40	4.40
		C	10–36	58	832	133	35	4.65
S10/Humi-Skeletic Leptosol	78	A1	0–2	49	n.m.	n.m.	n.m.	4.70
		A2	2–10	68	818	143	39	4.50
		AC	10–25	84	733	219	48	4.80

n.m. = not measured

Please cite this article as: Mavris, C., et al., Weathering and mineralogical evolution in a high Alpine soil chronosequence: A combined approach using SEM–EDX, cathodoluminescence and Nomarski DIC microscopy, Sediment. Geol. (2012), doi:10.1016/j.sedgeo.2012.04.008

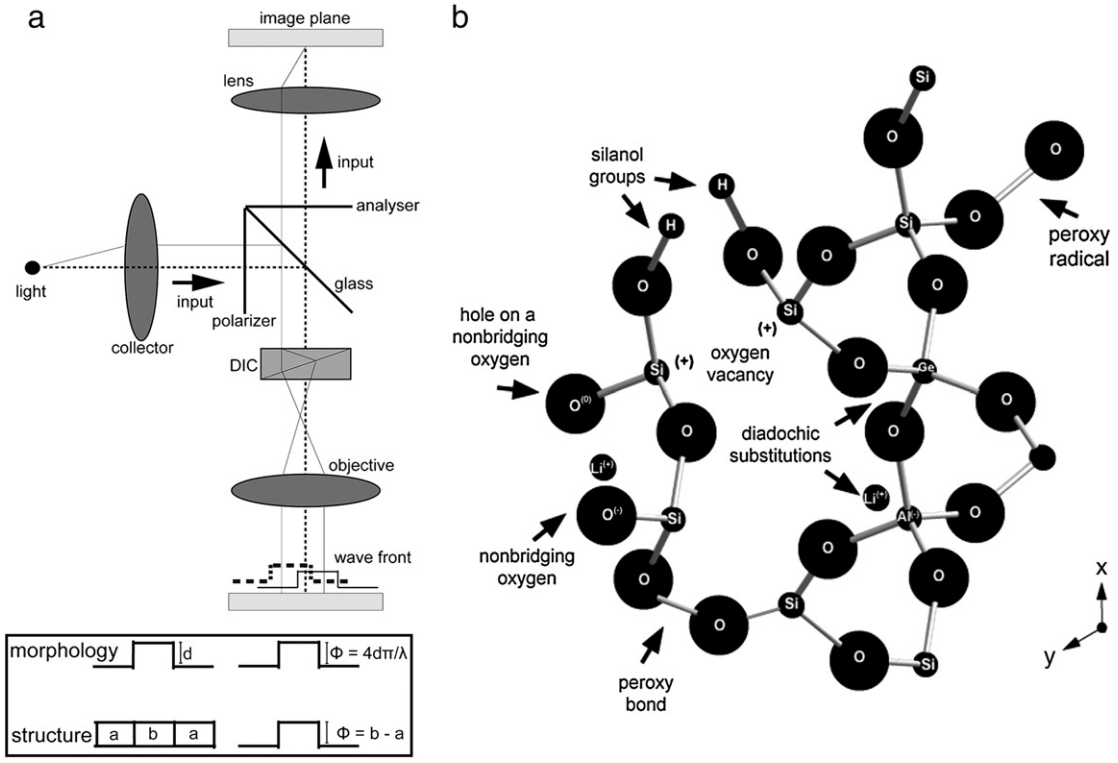

Fig. 2. Schematic sketch (modified after Götze, 2009) showing: a) simplified structure of quartz with some typical features detectable using cathodoluminescence (modified after Götze et al., 2001) and b) Nomarski DIC microscopy. Optical diagram with the structure of the DIC microscope; bottom: the phase difference (Φ) is explained by geometric (step height 'd') and physical factors (difference in the material specific phase shift 'a' and 'b').

quantitative indication for K-feldspar and plagioclase, peaks in the CL spectra were normalised to the Fe peak of the minerals in the parent material and in the soil of interest.

3.4. Nomarski DIC microscopy

Nomarski DIC microscopy is a modern technique applied in material science to visualise different phases and/or to image the surface relief of samples (Fig. 2). In the present study, n = 4 topsoils and n = 1 parent material were investigated. The polarisation objectives used have a magnification/numerical aperture of 20×/0.50, 40×/0.75 and 50×/0.80 with specific DIC prisms for transmitted and reflected light studies (Götze, 2009). The microscope was coupled with a digital video camera. The investigations and observations were carried out at the Institute of Mineralogy of the TU Bergakademie Freiberg (Germany).

3.5. Total element analysis

Element pools in the soil (Ca, Mg, Na, K, Si, Fe, Al, Ti, and Mn) were determined by a total dissolution method for the parental material (average of n = 7 C horizons) and the topsoils having an age > 100 - years (n = 4; Table 2). Oven-dried samples were dissolved using a mixture of HF, HCl, HNO_3, and H_3BO_3 (Hossner, 1996) in a microwave oven and at a pressure of c. 25 bar in a closed system. Concentrations were determined by an AAanalyst 600 Perkin Elmer Atomic Absorption Spectrometer (AAS) at the Department of Geography, University of Zurich (Switzerland).

4. Results

The soil mineralogy of the Morteratsch proglacial area has a predominantly silicatic character due to the granitoid parent rock (Mavris et al., 2010, 2011 and Table 2). In the parent material the most abundant phases detected were quartz, K-feldspar and Na-rich plagioclase followed by Fe-rich mica (biotite) and epidote. Apatite was also detected. Furthermore, accessory phases such as pyrite, titanite and ilmenite were detected, but were not the object of this study. Secondary phases due to weathering were almost undetectable. The total concentration of elements remains stable with exposure time (Table 2). The variability is predominantly due to some inhomogeneities of the glacial sediment.

Table 2
Total chemical analysis of the > 100 year topsoils (n = 4) and the parent material (n = 7) with standard deviation (SD).

	Al (g/kg)	Si (g/kg)	Ti (g/kg)	Ca (g/kg)	Mg (g/kg)	K (g/kg)	Na (g/kg)	Fe (g/kg)	Mn (g/kg)
Parent material	76.8	310.2	8.00	17.2	9.53	28.7	26.8	22.5	0.58
SD	6.5	27.4	2.38	6.4	3.20	4.1	3.87	6.9	0.16
Topsoils (age > 100 years)	65.0	330.4	5.90	27.3	7.32	28.1	25.3	29.1	0.62
SD	5.8	24.0	2.25	22.3	2.77	2.4	2.6	16.1	0.14

Please cite this article as: Mavris, C., et al., Weathering and mineralogical evolution in a high Alpine soil chronosequence: A combined approach using SEM–EDX, cathodoluminescence and Nomarski DIC microscopy, Sediment. Geol. (2012), doi:10.1016/j.sedgeo.2012.04.008

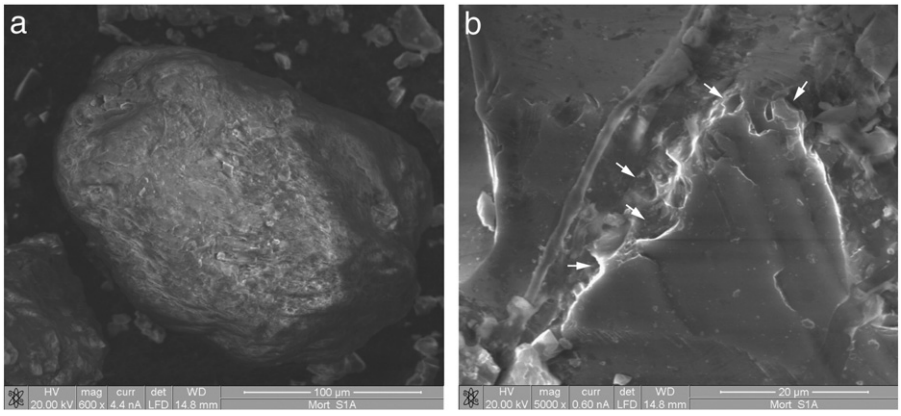

Fig. 3. SEM micrographs with a) quartz grain from the 140 year old topsoil and b) surface morphology showing an early chemical corrosion of quartz. The arrows point to distinct surface dissolution pits.

The morphology of the minerals is characterised by smooth surfaces and sharp angles — typical for a low weathering degree and limited transport (see Figs. 3 and 4). The amount of rounded grains is low, which is common for morainic material having a minimal chemical leaching and limited transport.

4.1. Quartz

4.1.1. SEM–EDX

Quartz grains of the parent material have sharp edges and conchoidal surfaces, typical for short glacial transport. Quartz from the 140 year old soil features a much more uneven surface. The degree of roundness of the grains is higher, and at high magnifications weak traces of chemical corrosion could be detected (Fig. 3). Elemental mapping of quartz grains did not give any evidence of chemical changes following 140 years of weathering, because, apart Si or O, all other elements were below the detection limit of EDS.

4.1.2. CL

The luminescence for the investigated quartz grains was homogeneously dark brown-blue. Primary internal structures (e.g. growth zoning) were usually not observed in the quartz crystals (Fig. 4). CL spectra of quartz indicated some structural changes. The observed broad CL bands of quartz at 450 nm and 650 nm are typical for granitoid–pegmatitic quartz (Richter et al., 2003). The first band represents a defect due to an oxygen vacancy (Stevens Kalceff and Phillips, 1995). The second band is caused by 'nonbridging oxygen hole centres' (NBOHC) (Götze et al., 2001; Fig. 2). A detailed observation of the quartz spectrum of the fresh sediment revealed a small contribution at 620 nm. This is attributed to Si-OH (silanol groups) and becomes hindered by the broad 'NBOHC' band with time (Stevens Kalceff and Phillips, 1995; Fig. 5). In addition, a pronounced band was detected at 710 nm for the quartz of the parent material. This band most likely indicates a substitutional incorporation of Fe^{3+} into the quartz lattice as observed in other silicate structures. This would be typical for the alkali-metasomatic alteration (fenitisation) of the granite (Götze et al., 2001).

4.1.3. Nomarski DIC microscopy

This technique revealed a quite homogeneous morphology for quartz. The rare fractures detected along the surface of the crystals showed that only – if ever – a slight corrosive pre-exposure occurred. In the oldest soil, no clear weathering features were observed.

4.2. Feldspar

4.2.1. SEM–EDX

K-feldspar and Na-plagioclase display similar chemical stability with respect to weathering (Allen and Hajek, 1989). Morphologically, we were not able to clearly distinguish the two phases using SEM. In the parent material, the grains appeared to be coarsely-shaped, with sharp, regular cleavage edges, indicating short transport and mechanical abrasion. Across the grain surfaces, a diffuse roughness was observed in both parent material and topsoil samples.

4.2.2. CL

The luminescence of K-feldspar showed a blue-violet colour (Fig. 4). Plagioclase showed green luminescence, slightly fading as a function of time. The heterogeneous distribution of CL colours in feldspar minerals indicates weathering/alteration already in the initial rock material. In the CL spectra two emission bands could be observed (Fig. 5). The band at c. 460 nm, whose intensity decreases with soil age, is related to $Al-O^{-}-Al$ defects (e.g. Marfunin, 1979). The band at c. 680 nm is generated by Fe^{3+} impurities in Al lattice positions (Götze et al., 1999).

4.2.3. Nomarski DIC microscopy

Na-plagioclase and K-feldspar exhibited similar features (Fig. 6). Using parallel and crossed Nicols polarised light, the grains revealed surfaces having distinctive, cross-cutting preferential cleavage fissures. Already in the glacial till, two sets of weathering surfaces were distinguishable (Fig. 6). The first one (red arrow) is observed at the outer part of the grain from where the fissures started to penetrate and propagate randomly into the inner part of the mineral grain. The second one (black arrow) developed along parallel sets of cleavage surfaces.

4.3. Biotite

4.3.1. SEM–EDX

Biotite occurs as layered aggregates with some typical perfect basal cleavages (Fig. 7). In both the parent material and topsoil mechanical deformation and delamination of the layers due to glacial abrasive activity were observed. Furthermore, Ti-containing minerals (titanite?) and feldspar were detected among the mica-layers (Fig. 8). SEM–EDX did not evidence a development of secondary phases. In the surface layer and along fissures of the biotite platelets, K appeared depleted compared to Fe due to leaching processes (Fig. 8).

Please cite this article as: Mavris, C., et al., Weathering and mineralogical evolution in a high Alpine soil chronosequence: A combined approach using SEM–EDX, cathodoluminescence and Nomarski DIC microscopy, Sediment. Geol. (2012), doi:10.1016/j.sedgeo.2012.04.008

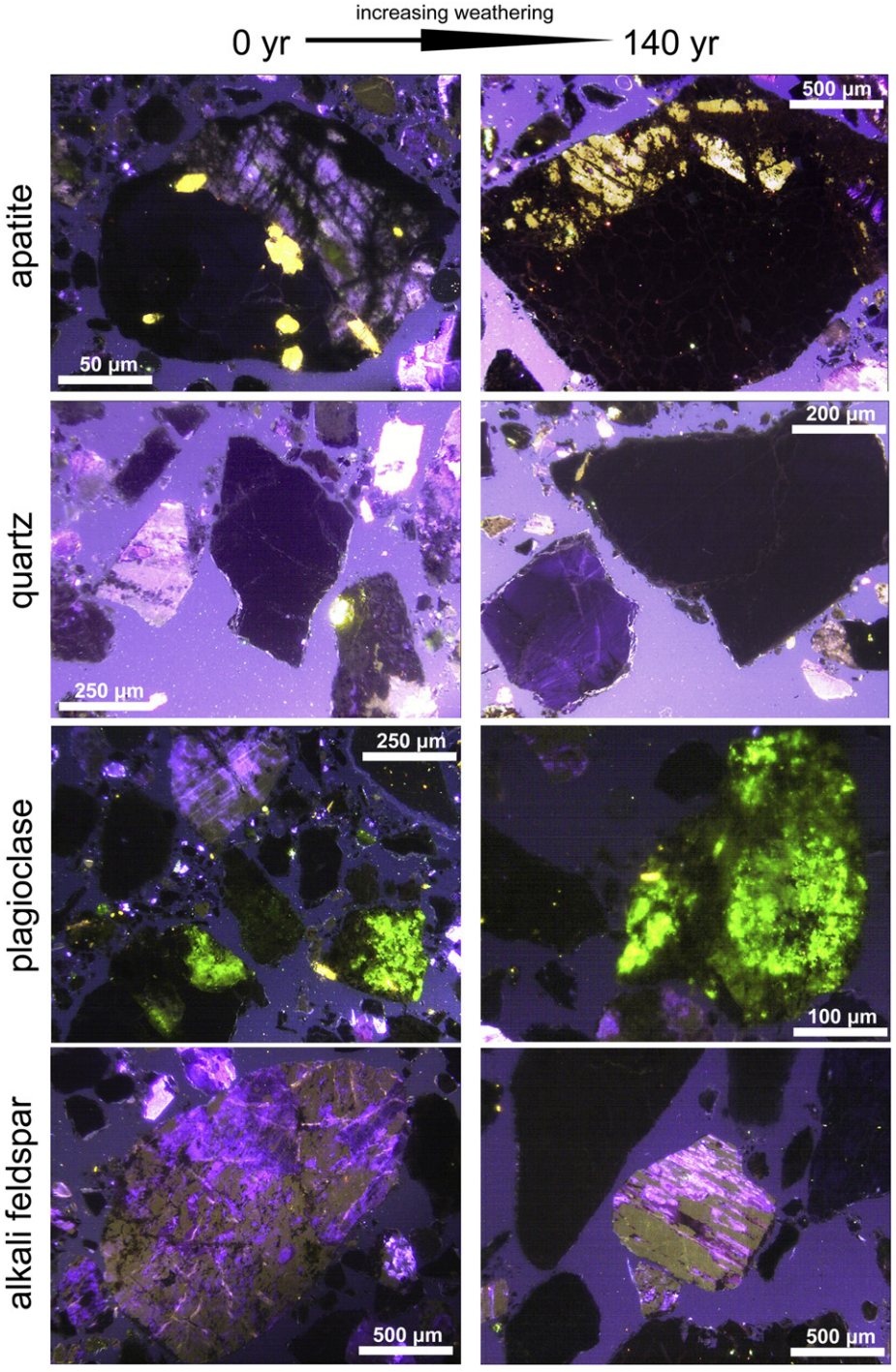

Fig. 4. Cathodoluminescence micrographs of apatite, quartz, plagioclase and alkali feldspar of the parent material (0 year) and 140 year old topsoil. *Apatite*: yellow luminescing crystals due to the activation of Mn^{2+}; *quartz*: blue-brown CL; *plagioclase*: green luminescing areas with strongly emitting Mn^{2+} peak; *alkali feldspar*: violet emitting grains, related to both Al – O^{-} – Al defects and Fe^{3+} in Al-sites. (For interpretation of the references to colour in this figure legend, the reader is referred to the web version of this article.)

4.3.2. CL

Biotite shows a very weak CL intensity because of the quenching by structural iron. Therefore, neither images nor CL spectra were obtained.

4.3.3. Nomarski DIC microscopy

Within the weathering sequence, an increasing delamination of biotite with time could be observed. Using the Nomarski technique and SEM, larger spaces between the mica layers were detectable in the older samples (Fig. 7). As a consequence of the delamination process of mica, a much higher surface area became available for chemical weathering. However, the presence of structurally weaker phases, i.e. newly-formed clay minerals, could not be detected within the biotite platelets. This confirms physical – rather than chemical – alteration of biotite.

4.4. Apatite (accessory phase)

4.4.1. SEM–EDX

In the glacial till, apatite was detected as sporadically occurring, euhedral crystals having a size of up to 30 µm. Despite a rather low resistance to weathering in soil profiles having low pH (Allen

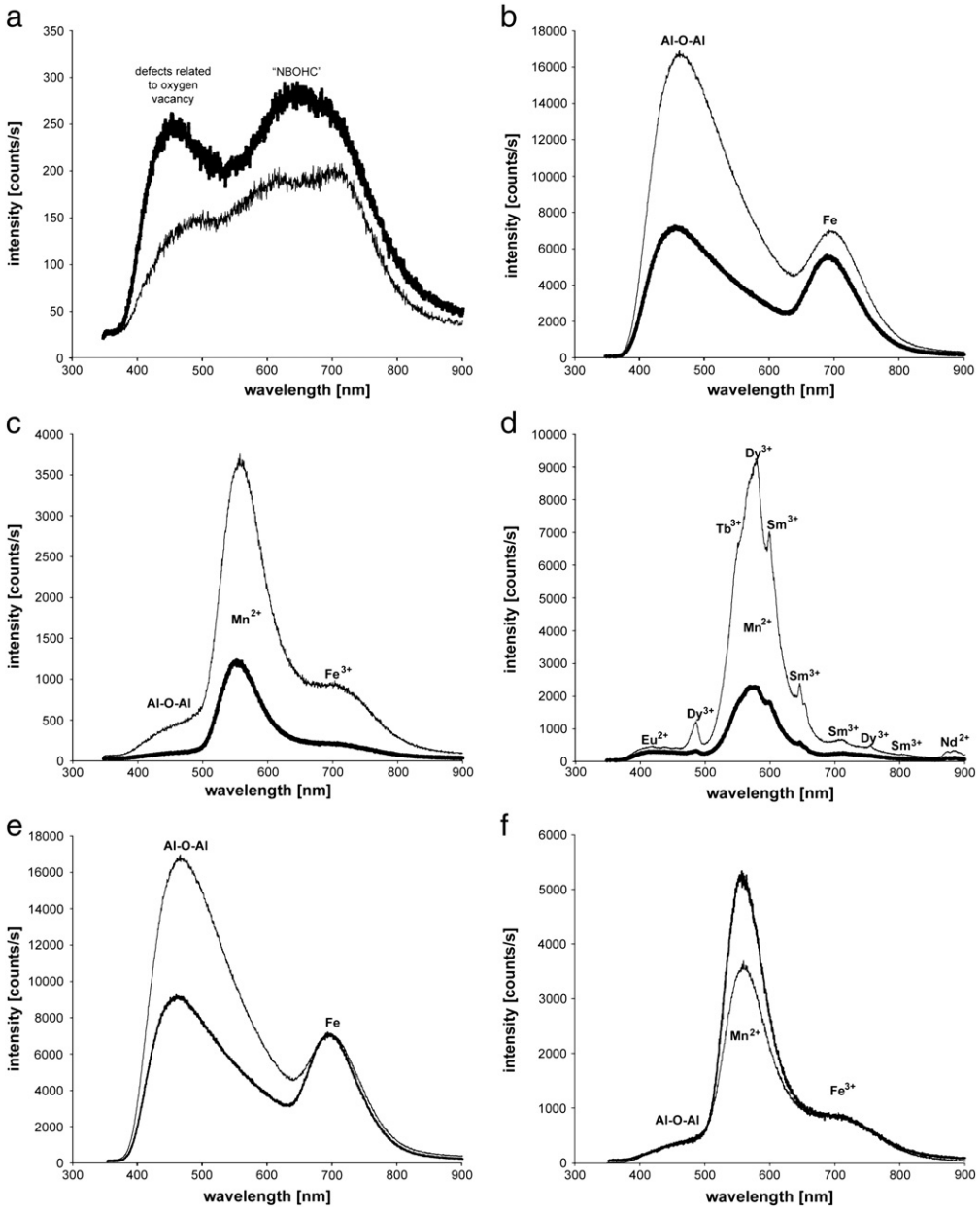

Fig. 5. Cathodoluminescence emission spectra of a) quartz, b) alkali feldspar, c) plagioclase and d) apatite. The bold line denotes the 140 year topsoil and the thin line the parent material. The spectra e (alkali feldspar) and f (plagioclase) are normalised to the Fe-spectrum of the parent material.

and Hajek, 1989; Taunton et al., 2000), it was still possible to find apatite crystallites in the oldest topsoil. The EDX measurements did not evidence any significant chemical change in the considered timespan.

4.4.2. CL

Apatite was observed having a strong yellow luminescence emission but did not feature any rim (or growing) structures in the crystal, reflecting a homogeneous composition of apatite (Fig. 4). The CL emission spectra of apatite evidenced sharp emission lines of REE together with a strong Mn^{2+} band at c. 560 nm (Mariano, 1988). A strong enrichment in Ce^{3+}, Nd^{3+}, Sm^{3+} and Eu^{2+} is typical for apatite originating from alkaline magmatic complexes (Zhang et al., 1985; Fleischer and Altschuler, 1986; Mariano, 1988; Boudreau and Kruger, 1990; Kempe and Götze, 2002).

4.4.3. Nomarski DIC microscopy

The detected apatite particles were too small (i.e. <30 μm) to be properly analysed from a morphological point of view.

4.5. Epidote

4.5.1. SEM–EDX

Epidote occurs mainly as elongated crystals having a size of >50 μm (Fig. 9). In the glacial till, no pre-exposure weathering traces were detected on the epidote crystals. EDX revealed two varieties, a common Fe-rich and a sporadically-occurring REE-bearing epidote (data not shown; see also Mavris et al., 2010). The occurrence of the REE-bearing phases correlates with the dismantlement of pegmatite veins (cf. Büchi, 1994). Epidote did not show any distinct chemical or mechanical weathering alterations in the oldest topsoil.

Please cite this article as: Mavris, C., et al., Weathering and mineralogical evolution in a high Alpine soil chronosequence: A combined approach using SEM–EDX, cathodoluminescence and Nomarski DIC microscopy, Sediment. Geol. (2012), doi:10.1016/j.sedgeo.2012.04.008

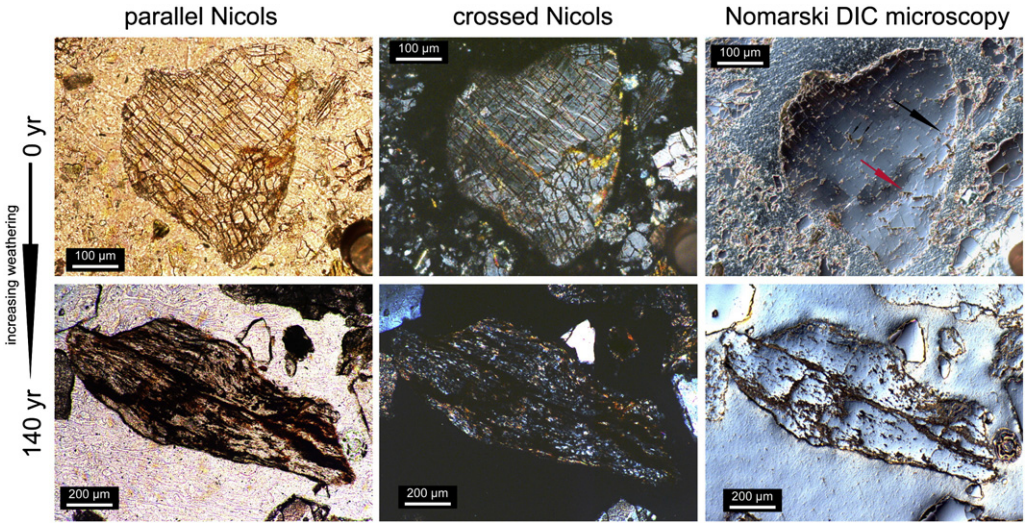

Fig. 6. Plagioclase from the parent material (0 year) and the 140 year old topsoil. In the parent material, two sets of weathering patterns are underlined: geologically inherited (along cleavage surfaces; red arrows), and pedogenic (mostly on the outer surface of the grains; black arrow). The image shows the grains in thin section in parallel and crossed Nicols transmitted (polarised) light. (For interpretation of the references to colour in this figure legend, the reader is referred to the web version of this article.)

4.5.2. CL

Epidote featured a very weak (dark green) luminescence glow. The needle structure of the small crystals, coupled with the strong interfering luminescence of the hosting feldspar did not allow spectral CL measurement of epidote.

4.5.3. Nomarski DIC microscopy

In contrast to SEM–EDX, a distinct epidote alteration was traceable (Fig. 9). Epidote appeared to have a physically and chemically affected crystal structure when compared to the associated (surrounding) phases. The differential interference contrast evidenced this feature where epidote was associated to tectosilicate-structured phases. Neither secondary clay minerals nor oxyhydroxides were observed on the surface of epidote.

5. Discussion

The collapse of structure bonds is paramount for the transformation of primary tectosilicatic structure into secondary phases (e.g. smectite; Aoudjit et al., 1995). Physical weathering processes (such as freeze-thawing cycles) tend to weaken mineral crystal structures such as large cation-bond tectosilicatic crystal lattices and thus facilitate a further step of elemental leaching by circulating waters (e.g. Hall et al., 2002). The chemical and mineralogical structure of

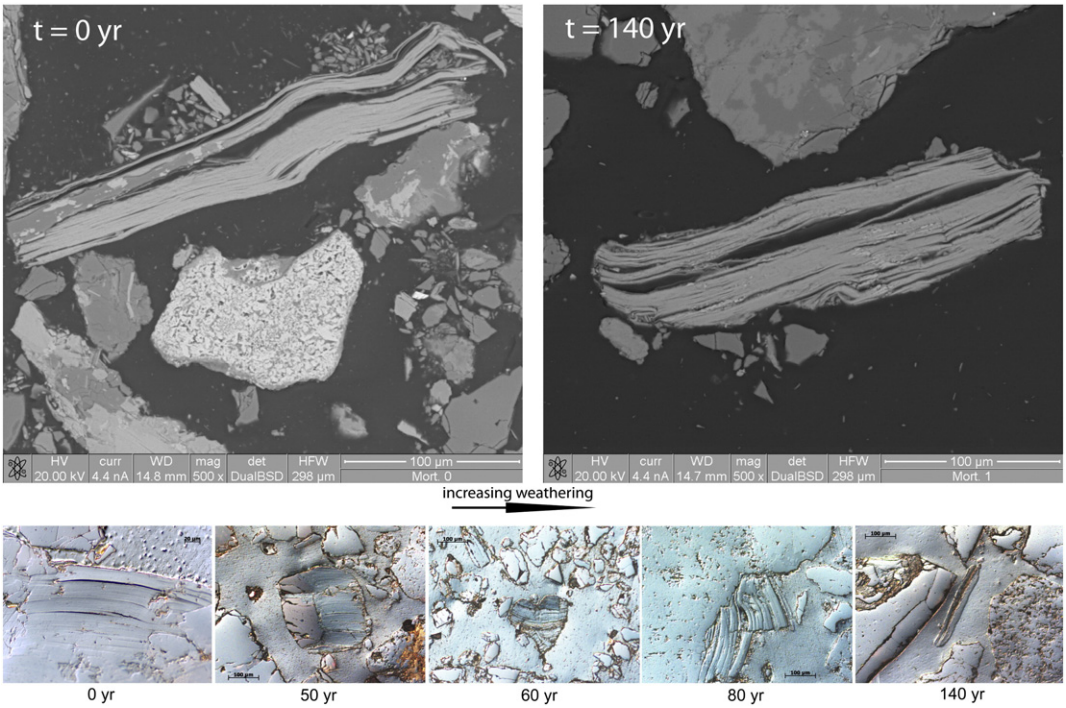

Fig. 7. (*Above*) Delamination of biotite crystallites in the parent material (t = 0 year) and in the oldest topsoil (t = 140 years) observed using SEM; (*below*) biotite delamination as a function of the time documented using Nomarski DIC microscopy.

Please cite this article as: Mavris, C., et al., Weathering and mineralogical evolution in a high Alpine soil chronosequence: A combined approach using SEM–EDX, cathodoluminescence and Nomarski DIC microscopy, Sediment. Geol. (2012), doi:10.1016/j.sedgeo.2012.04.008

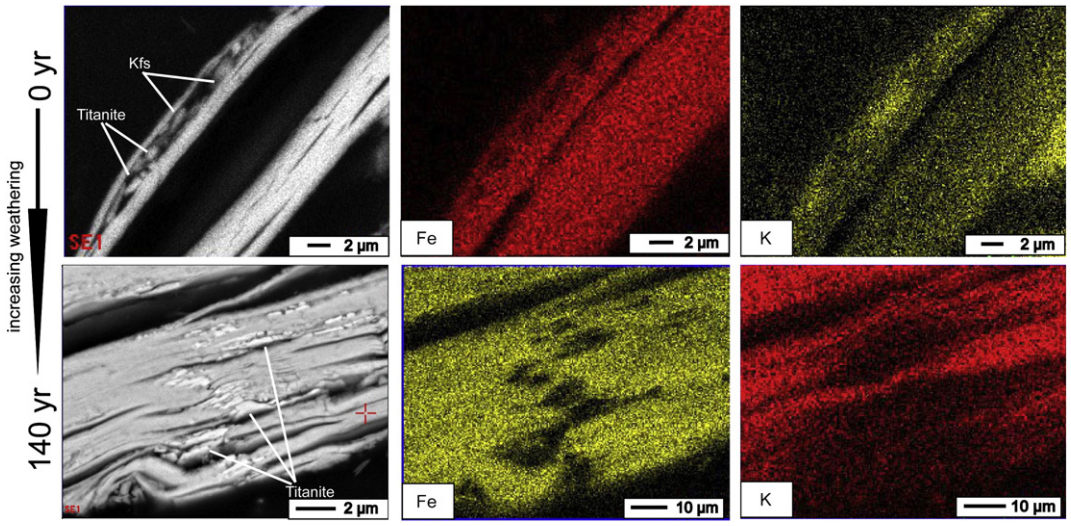

Fig. 8. Elemental mapping (SEM–EDX) of K and Fe in biotite of the parent material and the oldest soil.

minerals, such as the Fe(II) content, oxygen sharing (the resistance of a primary mineral to weathering increases the degree of sharing of oxygen between adjacent Si tetrahedra in the crystal lattice), lattice distortion etc. strongly determine weathering stability (Curtis, 1976).

In the investigated till, it appears that structural bonds – such as Si – O – Si in quartz – start to break and to transform into free radicals at very early stages of weathering (Figs. 3 and 5). This process was also shown in controlled dissolution experiments using quartz (Bennett et al., 1988). The surface of quartz in aqueous solutions consists entirely of species derived from the hydrolysis and hydroxylation of broken ═Si – O – Si═ and the subsequent protonation and deprotonation of these sites (Furrer and Stumm, 1986; Brady and Walther, 1990). CL spectroscopy was a helpful tool to detect such nano-scale features (Fig. 5). The increase of both oxygen vacancy and 'NBOHC' bands is the direct consequence of the bond disintegration and a subsequent leaching of Si (or other accessory impurities present, if any).

In both, the parent material and the oldest soil of the glacier forefield, the presence of apatite could be verified. Apatite, the main source of inorganic P in the Morteratsch proglacial area, neither displays significant chemical and structural changes nor specific dissolution patterns, even after 140 years of weathering. This is in contrast to the findings of Föllmi et al. (2009b). Their observations of the progressive change in surface morphology of whole apatite grains, the systematic shift in the composition of P phases from detrital to iron-bound and organic P and estimations of the weathering rate of detrital P in the moraine samples indicated that apatite is biogeochemically actively weathered in the proglacial areas of the Rhône and Oberaar glaciers. That we do not observe such a trend in the proglacier area of Morteratsch might be due to a different chemical composition of the apatite or the low number of observations. The CL measurements seem to indicate a weathering of REE in the investigated apatite; however, due to technical constraints, a definitive conclusion is not possible.

The amount of epidote decreased as a function of time (see Mavris et al., 2010). Apparently, the sorosilicate structure of epidote undergoes a leaching of major cations (predominantly Ca^{2+}), thus featuring a chemically-changed crystal lattice (Fig. 9). However, an extended X-ray absorption fine structure (EXAFS) spectroscopy study on Fe in the Damma glacier forefield showed that the Fe

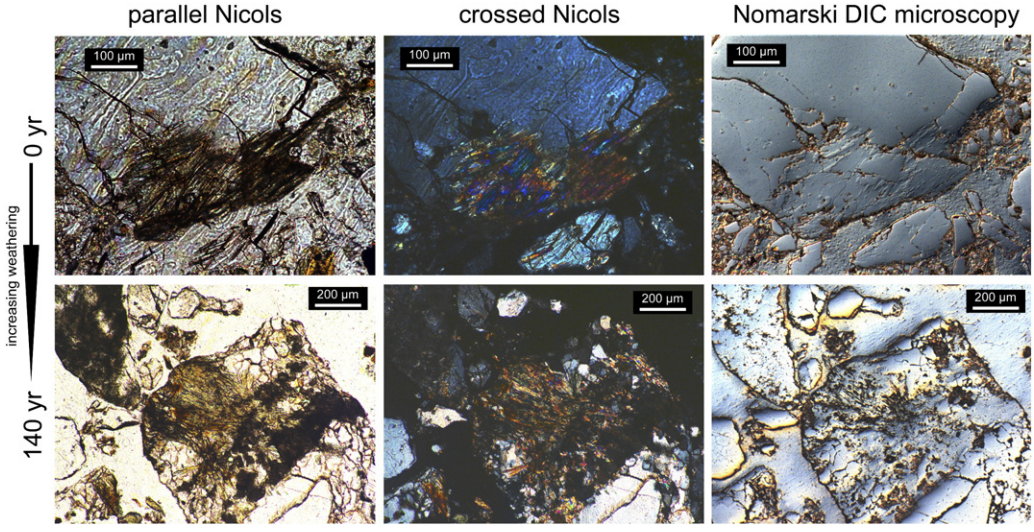

Fig. 9. Micrographs of epidote from the parent material (0 year) and the oldest topsoil aged (140 years). The image shows the grains in thin section in parallel and crossed Nicols transmitted (polarised) light.

Please cite this article as: Mavris, C., et al., Weathering and mineralogical evolution in a high Alpine soil chronosequence: A combined approach using SEM–EDX, cathodoluminescence and Nomarski DIC microscopy, Sediment. Geol. (2012), doi:10.1016/j.sedgeo.2012.04.008

fraction within epidote remained constant over the chronosequence (of c. 150 years), indicating a rather low Fe weathering rate of epidote (Kiczka-Cyriac, 2010).

Within the 140 years of weathering the Al – O$^-$ – Al bonds of K-feldspar seemed to decrease (Fig. 5) which might be due to a weakening of the crystal structure. Compared to Fe, less Al structural bonds are present in the mineral structure. These structural changes were also confirmed by the Nomarski DIC microscopy (Fig. 6). This reveals remarkable chemical variations most often on the grain surface and at a lattice level. The standardised CL spectra of plagioclase were overwhelmingly overlapping (Fig. 5f) and, consequently, no major changes could be observed. Finch et al. (2003) reported about a (structurally) ordered plagioclase. The peak ratios after CL excitation/stimulation changed up to 34.3% with the different crystallographic directions of the plagioclase. One way to detect the effective change of specific bonds in a time series is the normalisation (ratio) of the band of interest to an 'inert' compound (such as Fe^{3+} in oxic environments). If this ratio varies between two samples more than 34.3%, a real crystallographic change is more likely. If we assume that such a change as a function of orientation is also valid for the plagioclase in the Morteratsch area then no changes can be measured after 140 years because the peak ratio changes remain below this value. The Al – O$^-$ – Al/Fe (460/680 nm) ratio is for 0 year (parent material) = 0.51 and for 140 years = 0.48. The change in the Al – O$^-$ – Al/Fe ratio of K-feldspar, however, between 0 year (2.43) and 140 years (1.24) is much higher than one would expect from a spectra-change of the same mineral with varying orientation (according to Finch et al., 2003). Consequently, a part of the Al – O$^-$ – Al decrease in the K-feldspar (Fig. 5e, f) must be attributed to weathering (and not only to a change in orientation of the mineral).

Both chemical and physical transformations – namely, elemental depletion of K over Fe, and increased delamination over time – confirmed biotite weathering in the proglacial sediments (Figs. 7 and 8). As observed by other authors, biotite typically expands with time, delaminates and contributes to an increase in porosity of the weathered rock (Meunier et al., 2007; Graham et al., 2010; Rossi and Graham, 2010; Caner, 2011). The opening of fissures in mineral grains and the increase in porosity finally give rise to accelerated alteration rates (chemical weathering; Meunier et al., 2007). Fast weathering rates, not only of biotite, can usually be observed at the beginning of soil formation when fresh and reactive surfaces are available (Egli et al., 2003; Mavris et al., 2011). With time, these rates often decrease (Brantley and Mellott, 2000; Kump et al., 2000; Peters, 2009) due to the progressive occlusion of pores by secondary minerals and a decreased chemical potential in the alteration product (Caner, 2011).

The combined CL/Nomarski DIC/ESEM observations of the Morteratsch sediments are based on only a small number of observations. Consequently, our findings cannot be conclusive and, in particular, more CL measurements on individual minerals are required.

The total elemental concentration in the investigated topsoils reveals that the loss of structure-modifying cations within the investigated time span of 140 years is not yet high enough to give rise to a chemical trend along the proglacial area (Table 2). However, on the much smaller atomic and mineral structural scale weathering features can be detected using a combination of CL, Nomarski and SEM–EDX techniques.

6. Conclusions

Active chemical and physical weathering in a high Alpine chronosequence of recently exposed, granitic sediments could be documented. We have the following main findings:

- Biotite shows distinct mechanical weathering due to delamination of layers within the observed time-span of 140 years.
- Although the bulk chemistry of the soils did not change over time, K-feldspar and Na-plagioclase showed some chemical transformations with respect to Al (K-feldspar) and Mn (plagioclase). SEM–EDX analyses indicated a loss of K in biotite.
- Apatite seemed to be resistant to weathering.
- Epidote, however, shows clear weathering features (such as physical structure disintegration) after 140 years.

The combined use of chemical, mineralogical and spectroscopic analyses proved to be a useful approach in deciphering weathering patterns even at the atomic bond scale (crystal structures). CL and Nomarski DIC have a great potential in detecting and analysing chemical, physical and mineral structural changes due to weathering also in soils. Such an approach should in future enable a qualitative and semi-quantitative estimation of lattice position losses in primary and accessory minerals.

Acknowledgements

This research was supported by the Swiss National Foundation (SNF) project grant no. 200021-117568 and the SIMP fellowship 2009 (SIMP, Italian Society for Mineralogy and Petrology, Italy). We would like to thank G. Peschke and F. Favilli for the help during field-work and in the laboratory. We are furthermore indebted to Dr. Carita Augustsson, Dr. Sergio Andò and the editorial staff of Sedimentary Geology for the fruitful comments to a previous version of the manuscript.

References

Allen, B.L., Hajek, B.F., 1989. Mineral occurrence in soil environments. In: Dixon, J.B., Weed, S.B. (Eds.), Minerals in Soil Environments: SSSA Book Series, 1, pp. 199–278.
Anderson, S.P., Drever, J.I., Humphrey, N.F., 1997. Chemical weathering in glacial environments. Geology 25, 399–402.
Anderson, S.P., Drever, J.I., Frost, C.D., Holden, P., 2000. Chemical weathering in the foreland of a retreating glacier. Geochimica et Cosmochimica Acta 64, 1173–1189.
Aoudjit, H., Robert, M., Elsass, F., Curmi, P., 1995. Detailed study of smectite genesis in granite saprolites by analytical electron microscopy. Clay Minerals 30, 135–148.
Barbarand, J., Pagel, M., 2001. Cathodoluminescence study of apatite crystals. American Mineralogist 86, 473–484.
Bennett, P.C., Siegeld, I., Melcerm, E., Bassett, J.P., 1988. The dissolution of quartz in dilute aqueous solutions of organic acids at 25 °C. Geochimica et Cosmochimica Acta 52, 1521–1530.
Boudreau, A.E., Kruger, F.J., 1990. Variation in the composition of apatite through the Merensky cyclic unit in the Western Bushveld Complex. Economic Geology 85, 737–745.
Brady, P.V., Walther, J.V., 1990. Quartz dissolution at low temperature. Chemical Geology 82, 253–264.
Brantley, S.L., Mellott, N., 2000. Surface area and porosity of primary silicate minerals. American Mineralogist 85, 1767–1783.
Büchi, H., 1994. Der variskische Magmatismus in der östlichen Bernina (Graubünden, Schweiz). Schweizerische Mineralogische und Petrographische Mitteilungen 74, 359–371.
Burga, C., 1999. Vegetation development on the glacier forefield Morteratsch (Switzerland). Applied Vegetation Science 2, 17–24.
Caner, L., 2011. Phyllosilicates des sols: de l'altération à la quantification. Habilitation, University of Poitiers, France.
Curtis, C.D., 1976. Stability of minerals in surface weathering reactions: a general thermochemical approach. Earth Surface Processes 1, 63–70.
D'Amico, C., Innocenti, F., Sassi, F. P., 1998. Magmatismo e Metamorfismo. Ed. UTET, Torino.
Egli, M., Mirabella, A., Fitze, P., 2003. Formation rates of smectites derived from two Holocene chronosequences in the Swiss Alps. Geoderma 117, 81–98.
Finch, A.A., Hole, D.E., Townsend, P.D., 2003. Orientation dependence of luminescence in plagioclase. Physics and Chemistry of Minerals 30, 373–381.
Fleischer, M., Altschuler, Z.S., 1986. The lanthanides and yttrium in minerals of the apatite group: an analysis of the available data. Neues Jahrbuch für Mineralogie Monatshefte 10, 467–480.
Föllmi, K.B., Arn, K., Hosein, R., Adatte, T., Steinmann, P., 2009a. Biogeochemical weathering in sedimentary chronosequences of the Rhône and Oberaar Glaciers (Swiss Alps): rates and mechanisms of biotite weathering. Geoderma 151, 270–281.
Föllmi, K.B., Hosein, R., Arn, K., Steinmann, P., 2009b. Weathering and the mobility of phosphorus in the catchments and forefields of the Rhône and Oberaar glaciers, central Switzerland: implications for the global phosphorus cycle on glacial–interglacial timescales. Geochimica et Cosmochimica Acta 73, 2252–2282.
Furrer, G., Stumm, W., 1986. The coordination chemistry of weathering: I. Dissolution kinetics of δ-Al_2O_3, and BeO. Geochimica et Cosmochimica Acta 50, 1847–1860.
Götze, J., 2009. Application of Nomarski DIC and cathodoluminescence (CL) microscopy to building material. Material Characterization 60, 594–602.

Please cite this article as: Mavris, C., et al., Weathering and mineralogical evolution in a high Alpine soil chronosequence: A combined approach using SEM–EDX, cathodoluminescence and Nomarski DIC microscopy, Sediment. Geol. (2012), doi:10.1016/j.sedgeo.2012.04.008

Götze, J., Siedel, H., 2004. Microscopic scale characterization of ancient building sandstones from Saxony (Germany). Material Characterization 53, 209–222.
Götze, J., Siedel, H., 2007. A complex investigation of building sandstones from Saxony (Germany). Material Characterization 58, 1082–1094.
Götze, J., Zimmerle, W., 2000. Quartz and silica as guide to provenance in sediments and sedimentary rocks. Contributions to Sedimentary Geology 12, 1–91.
Götze, J., Habermann, D., Neuser, R.D., Richter, D.K., 1999. High-resolution spectrometric analysis of rare earth elements-activated cathodoluminescence in feldspar minerals. Chemical Geology 153, 81–91.
Götze, J., Krbetschek, M.R., Habermann, D., Wolf, D., 2000. High-resolution cathodoluminescence studies of feldspar minerals. In: Pagel, M., Barbin, V., Blanc, P., Ohnenstetter, D. (Eds.), Cathodoluminescence in Geosciences. Springer, Berlin, pp. 245–270.
Götze, J., Plötze, M., Habermann, D., 2001. Origin, spectral characteristics and practical applications of the cathodoluminescence (CL) of quartz — a review. Mineralogy and Petrology 71, 225–250.
Götze, J., Plötze, M., Graupner, T., Hallbauer, D.K., Bray, C.J., 2004. Trace element incorporation into quartz: a combined study by ICP-MS, electron spin resonance, cathodoluminescence, capillary ion analysis, and gas chromatography. Geochimica et Cosmochimica Acta 68, 3741–3759.
Graham, R.C., Rossi, A.M., Hubbert, K.R., 2010. Rock to regolith conversion: producing hospitable substrates for terrestrial ecosystems. GSA Today 20, 4–9.
Haeberli, W., Beniston, M., 1998. Climate change and its impacts on glaciers and permafrost in the Alps. Ambio 27, 258–265.
Hall, K., Thorn, C.E., Matsuoka, N., Prick, A., 2002. Weathering in cold regions: some thoughts and perspectives. Progress in Physical Geography 26, 577–603.
Hosein, R., Arn, K., Steinmann, P., Adatte, T., Föllmi, K.B., 2004. Carbonate and silicate weathering in two presently glaciated, crystalline catchments in the Swiss Alps. Geochimica et Cosmochimica Acta 68, 1021–1033.
Hossner, C.R., 1996. Dissolution for total elemental analysis. In: Sparks, D.L. (Ed.), Methods of Soil Analysis, Part 3, Chemical Methods. Soil Science Society of America Inc. and American Society of Agronomy Inc., Madison, WI, pp. 49–64.
IUSS Working Group WRB, 2006. World reference base for soil resources 2006, World Soil Resources Reports No. 103, FAO, 2nd edition. Food and Agriculture Organisation of the United Nations, Rome.
Keevil, C.W., Walker, J., 1992. Nomarski DIC microscopy and image analysis of biofilms. Binary Computational Microbiology 4, 93–95.
Kempe, U., Götze, J., 2002. Cathodoluminescence (CL) behaviour and crystal chemistry of apatite from rare-metal deposits. Mineralogical Magazine 66, 151–172.
Kiczka-Cyriac, M., 2010. Iron isotope fractionation mechanisms of silicate weathering and iron cycling by plants. Ph.D. thesis, ETH Zurich.
Kump, L.R., Brantley, S.L., Arthur, M.A., 2000. Chemical weathering, atmospheric CO_2, and climate. Annual Review of Earth and Planetary Sciences 28, 611–617.
Lapuente, M.P., Turi, B., Blanc, P., 2000. Marbles from Roman Hispania: stable isotope and cathodoluminescence characterization. Applied Geochemistry 15, 1469–1493.
Marfunin, A.S., 1979. Spectroscopy, Luminescence and Radiation Centers in Minerals. Springer-Verlag, Berlin.
Mariano, A.N., 1988. Some further geological applications of cathodoluminescence. In: Marshall, D.J. (Ed.), Cathodoluminescence of Geological Materials. Unwin Hyman, Boston, USA, pp. 94–123.
Mavris, C., Egli, M., Plötze, M., Blum, J.D., Mirabella, A., Giaccai, D., Haeberli, W., 2010. Initial stages of weathering and soil formation in the Morteratsch proglacial area (Upper Engadine, Switzerland). Geoderma 155, 359–371.
Mavris, C., Plötze, M., Mirabella, A., Giaccai, D., Valboa, G., Egli, M., 2011. Clay mineral evolution along a soil chronosequence in an Alpine proglacial area. Geoderma 165, 106–117.
Meunier, A., Sardini, P., Robinet, J.C., Prêt, D., 2007. The petrography of weathering processes. Facts and outlooks. Clay Minerals 42, 415–435.
Michalski, S.T., Götze, J., Siedel, H., Magnus, M., Heimann, R.B., 2002. Investigations into provenance and properties of ancient building sandstones of the Zittau/Görlitz region (Upper Lusatia, Eastern Saxony, Germany). In: Siegesmund, S., Vollbrecht, A., Weiss, T. (Eds.), Natural Stone, Weathering Phenomena, Conservation Strategies and Case Studies. : Special Publications, vol. 205. Geological Society, London, pp. 281–295.
Murphy, S.F., Brantley, S.L., Blum, A.E., White, A.F., Dong, H., 1998. Chemical weathering in a tropical watershed, Luquillo Mountains. Puerto Rico: II. Rate and mechanism of biotite weathering. Geochimica et Cosmochimica Acta 62, 227–243.
Neuser, R.D., Bruhn, F., Gätze, F., Haberman, J., Richter, D.K., 1995. Kathodolumineszenz: Methodik und Anwendung. Zentralblatt für Geologie und Paläontologie Teil 1, 287–306.
Nomarski, G., 1955. Microinterféromètre differentiell a ondes polarisées. Journal de Le Physique et Le Radium 16, 9–13.
Nomarski, G., Weill, A.R., 1951. Sur l'observation des figures de croissance des cristaux par les methods interférentielles à deux ondes. Société française de Minéralogie et de Cristallographie Bulletin 77, 840–868.
Pearce, T.H., Russell, J.K., Wolfson, I., 1987. Laser-interference and Nomarski interference imaging of zoning profiles in plagioclase phenocrysts from the May 18, 1980, eruption of Mount St. Helens, Washington. American Mineralogist 72, 1131–1143.
Peters, C.A., 2009. Accessibilities of reactive minerals in consolidated sedimentary rock: an imaging study of three sandstones. Chemical Geology 265, 198–208.
Richter, D.K., Götte, T., Götze, J., Neuser, R.D., 2003. Progress in application of cathodoluminescence (CL) in sedimentary petrology. Mineralogy and Petrology 79, 127–166.
Rossi, A.M., Graham, R.C., 2010. Weathering and porosity formation in subsoil granitic clasts, Bishop Creek Moraines, California. Soil Science Society of America Journal 74, 172–185.
Stevens Kalceff, M.A., Phillips, M.R., 1995. Cathodoluminescence microcharacterization of the defect structure of quartz. Physical Review 52, 3122–3135.
Swoboda-Colberg, N.G., Drever, J.I., 1993. Mineral dissolution rates in plot-scale field and laboratory experiments. Chemical Geology 105, 51–69.
Taunton, A.E., Welch, S.A., Banfield, J.F., 2000. Microbial control on phosphate and lanthanide distributions during granite weathering and soil formation. Chemical Geology 169, 371–382.
Trommsdorff, V., Dietrich, V., 1999. Grundzüge der Erdwissenschaften, 6th edition. vdf-Verlag, Zürich, Switzerland.
Wadham, J.L., Cooper, R.J., Tranter, M., Hodgkins, R., 2001. Enhancement of glacial solute fluxes in the proglacial zone of a polythermal glacier. Journal of Glaciology 47, 378–386.
Yoo, K., Mudd, S.M., 2008. Toward process-based modelling of geochemical soil formation across diverse landforms: a new mathematical framework. Geoderma 146, 248–260.
Zhang, S., Wang, L., Yang, W., 1985. Use of REE analysis in apatite to distinguish petrological and mineralogical series of granitic rocks. Geochimica 1, 45–57.

Please cite this article as: Mavris, C., et al., Weathering and mineralogical evolution in a high Alpine soil chronosequence: A combined approach using SEM–EDX, cathodoluminescence and Nomarski DIC microscopy, Sediment. Geol. (2012), doi:10.1016/j.sedgeo.2012.04.008